

Efficient numerical treatment of the fractional Laplacian in three dimensions

Von der Universität Bayreuth
zur Erlangung des Grades eines
Doktors der Naturwissenschaften (Dr. rer. nat.)
genehmigte Abhandlung

von
Bernd Feist
aus Brand bei Marktredwitz

1. Gutachter: Prof. Dr. Mario Bebendorf
2. Gutachter: Prof. Dr. Sergej Rjasanow

Tag der Einreichung: 21. April 2023
Tag des Kolloquiums: 28. Juli 2023

Abstract

English abstract

Partial differential equations play an important role in many applications. Therefore it is of enormous significance to provide algorithms and methods to solve them numerically in a reasonable time. One operator that has gained importance in recent years is the fractional Laplacian. The dissertation is dedicated to the goal of providing tools to handle finite element problems in three dimensions involving the fractional Laplacian in a numerically efficient way.

The fractional Laplacian belongs to the class of elliptic operators and is, as the name suggests, closely related to the Laplace operator. The major difference between the two is that the fractional Laplacian is a non-local operator and this results in some fundamental differences between the properties of both. The most important difference for us is the stiffness matrix. This poses two enormous challenges from a numerical point of view. On the one hand, the stiffness matrix is densely populated in contrast to the Laplace operator and on the other hand the calculation of the entries can be very complex and expensive. The reason for this is that in the worst case the entries consist of a sum of five- and six-dimensional integrals, which are singular if the support of the linear basis functions overlap. Therefore, a main contribution of this work is to develop efficient quadrature and cubature formulas for the singular integrals, and another is to derive suitable approximation methods for the stiffness matrix.

For the first part we adapt the Duffy transformation to the needs of the fractional Laplacian in three dimensions. A total of seven different singularity cases have to be investigated individually. In order to make the numerical integration efficient, the integration error is adapted to the error of the finite element solution. Thus, we develop new quadrature formulas for an efficient calculation of the entries. In addition, we also present efficient cubature formulas based on these error estimates, which are based on an adaptation of the Duffy transformation. For the second problem, we choose to use hierarchical matrices (\mathcal{H} -matrices) and prove that this method is also efficient for the fractional Laplacian. \mathcal{H} -matrices offer the advantage that the effort for constructing the approximation and performing the matrix-vector-multiplication is only quasi-linear instead of quadratic. Moreover, we also present a new, kernel-independent method to construct uniform \mathcal{H} - and \mathcal{H}^2 -matrix approximations for nonlocal operators. The presented method is based on an adaptation of the cross approximation. Finally, the efficiency of the methods and procedures presented here is tested by means of numerical examples.

Deutsche Kurzzusammenfassung

Partielle Differentialgleichungen spielen in vielen Anwendungen eine wichtige Rolle. Deshalb ist es von enormer Bedeutung Algorithmen und Methoden bereitzustellen, um diese in annehmbarer Zeit numerisch zu lösen. Ein Operator, der in den letzten Jahren an Bedeutung gewonnen hat, ist der fraktionale Laplace Operator. Die vorliegende Dissertation ist dem Ziel gewidmet, Werkzeuge bereit zu stellen, um finite Elemente Probleme im dreidimensionalen Raum, die den fraktionalen Laplace involvieren, numerisch effizient zu handhaben.

Der fraktionale Laplace gehört zur Klasse der elliptischen Operatoren und ist, wie der Name vermuten lässt, eng mit dem Laplace Operator verwandt. Der gravierende Unterschied zwischen den beiden ist allerdings, dass der fraktionale Laplace ein nicht-lokaler Operator ist, wodurch sich teilweise fundamentale Unterschiede zwischen den Eigenschaften der beiden Operatoren ergeben. Der für uns wichtigste Unterschied ist die Steifigkeitsmatrix. Diese stellt uns aus numerischer Sicht vor zwei signifikante Probleme. Zum einem ist die Steifigkeitsmatrix im Unterschied zum Laplace Operator dicht besetzt und zum anderen kann sich die Berechnung der Einträge als höchst zeitaufwendig und komplex erweisen. Der Grund dafür ist, dass die Einträge im schlimmsten Fall aus einer Summe von fünf- und sechsdimensionalen Integralen bestehen, die auch noch singular sind, wenn sich die Träger der linearen Basisfunktionen überschneiden. Der Hauptteil der Arbeit besteht darin, zum einem effiziente Quadratur- und auch Kubaturformeln für die singulären Integrale zu entwickeln und zum anderen geeignete Approximationsmethoden für die Steifigkeitsmatrix herzuleiten.

Für den ersten Teil haben wir die Duffy Transformation auf die Bedürfnisse des fraktionalen Laplaces im dreidimensionalen Raum adaptiert. Dazu müssen insgesamt sieben verschiedene Singularitätsfälle einzeln untersucht werden. Um die numerische Integration effizient zu gestalten, wird der Integrationsfehler an den Fehler der finite Elemente Lösung angepasst. Dadurch ergeben sich neue Quadraturformeln für eine effiziente Berechnung der Einträge. Zusätzlich stellen wir auf Basis dieser Fehlerabschätzungen auch effiziente Kubaturformel vor, die auf einer Anpassung der Duffy Transformation basieren. Für die zweite Problematik entscheiden wir uns für den Einsatz von hierarchischen Matrizen (\mathcal{H} -Matrizen) und beweisen, dass diese Methode auch für den fraktionalen Laplace effizient einsetzbar ist. \mathcal{H} -Matrizen bieten die Vorteile, dass der Aufwand für das Aufstellen der Approximation nur quasi-linear ist, ebenso wie der Aufwand für die Matrix-Vektor-Multiplikation. Zusätzlich stellen wir auch eine neue, kern-unabhängige Methode vor, um uniforme \mathcal{H} - und \mathcal{H}^2 -Matrixapproximationen für nicht-lokale Operatoren zu konstruieren. Die vorgestellte Methode basiert auf einer Anpassung der Kreuzapproximation. Zum Abschluss wird die Effizienz der hier vorgestellten Methoden und Verfahren an Hand von numerischen Beispielen getestet.

Contents

1. Introduction	1
2. Fractional Laplacian	5
2.1. Introduction	5
2.2. Singular integral representation	5
2.3. Weak formulation	9
2.4. Finite element approximation	11
3. Duffy transformation	15
3.1. A simple introductory example	15
3.2. Interaction between two tetrahedra	16
3.2.1. Point singularity	17
3.2.2. Singularity along an edge	19
3.2.3. Singularity on a face	22
3.2.4. Two identical tetrahedra	24
3.3. Interaction between a tetrahedron and a panel	25
3.3.1. Point singularity	26
3.3.2. Singularity along an edge	27
3.3.3. Singularity on a face	27
3.4. Summary	29
4. Error estimates for the integrals	30
4.1. Derivative free error estimates	30
4.2. Preparation	30
4.2.1. Analyticity of the integrands	30
4.2.2. Error estimates for the integrands	35
4.2.3. Error estimates for the integrals	40
4.3. Rules for the number of Gauss points	40
5. Improved Duffy transformation	42
5.1. Interaction between two tetrahedra	43
5.1.1. Point singularity	43
5.1.2. Singularity along an edge	44
5.1.3. Singularity on a face	46
5.1.4. Two identical tetrahedra	48
5.2. Interaction between a tetrahedron and a panel	49
5.2.1. Point singularity	49
5.2.2. Singularity along an edge	50
5.2.3. Singularity on a face	51
5.3. Summary	52
6. \mathcal{H}-matrix approximation of the stiffness matrix	53
6.1. A short introduction to \mathcal{H} -matrices	53

Contents

6.2. Degenerate kernel approximation	54
6.2.1. Interpolation on tensor product grids	57
6.2.2. Cross approximation	59
6.3. The adaptive cross approximation	61
6.3.1. The algorithm	61
6.3.2. Error estimation	62
7. \mathcal{H}-Approximation of the inverse of the stiffness matrix	64
7.1. Idea of the proof	64
7.2. Approximation of the discretized inverse operator	66
7.3. Degenerate kernel approximation	67
7.3.1. Caccioppoli inequality	67
7.3.2. Construction of the approximation space	72
7.3.3. Approximation result	75
8. Uniform \mathcal{H}-matrices and \mathcal{H}^2-matrices	77
8.1. Interpolants and quadrature rules	77
8.1.1. Harmonic interpolants	78
8.1.2. s -harmonic interpolants	81
8.2. Exponential error estimates for multivariate interpolation	84
8.3. Uniform \mathcal{H} -matrix	87
8.4. \mathcal{H}^2 -matrix	89
9. Numerical results	92
9.1. Singular integrals	92
9.2. Fractional diffusion process on a unit ball	95
9.3. Fractional diffusion process on an ellipse	99
10. Conclusion	103
10.1. Summary	103
10.2. Outlook	104
A. Appendix: Duffy Transformation	105
A.1. Interaction between two tetrahedra	105
A.1.1. Singularity on a face	105
A.1.2. Two identical tetrahedra	112
A.2. Interaction between a tetrahedron and a panel	120
A.2.1. Point singularity	120
A.2.2. Singularity along an edge	121
A.2.3. Singularity on a face	122
List of Figures	126
List of Tables	127

Contents

References	128
Publications	134

1. Introduction

Partial differential equations and their numerical solutions play a significant role in applications. One operator that has received more attention in recent years is the fractional Laplacian, e.g. in the modeling of cardiac electrical propagation [23], in fractional quantum mechanics [66, 67], in the modeling of anomalous diffusion [26, 85], in fluid mechanics [32, 33], and in stochastic processes [17, 59, 63] as so called Lévy processes.

The fractional Laplacian belongs to the family of elliptic operators and has close connections to the Laplace operator; see [58, 65, 80]. However, in contrast to the Laplace operator, the fractional Laplacian is a non-local operator, which causes quite some differences and issues. For example the mean value property of the fractional Laplacian is also a non-local property and the corresponding stiffness matrix is dense; see [1, 2, 3, 4, 22, 58, 65]. As a consequence, especially the computation of the entries of the stiffness matrix and its efficient approximation are of utmost importance to be able to solve the applications numerically in reasonable time. For the two-dimensional case these two issues are already resolved in [1, 2, 3, 4, 75]. However, the computation of the entries of the stiffness matrix is strongly dependent on the dimension of the problem.

The aims of this work are to introduce the fractional Laplacian and its theoretical framework, and to present an efficient numerical treatment for the finite element method (FEM) approach of this operator in three dimensions. In contrast to [4], which used the fast multipole method introduced by Greengard and Rokhlin (see [28, 48, 49, 74]), we employ \mathcal{H} -matrices (see [13, 18, 51]) to approximate the stiffness matrix. While in a SIAM News article [30] the multipole method has been named to be one of the top 10 algorithms of the 20th century, the issue is that it relies on explicit kernel expansions, which on the one hand allows to tailor the expansion tightly to the respective problem, but on the other hand requires its own analytic apparatus including a-priori error estimates for each kernel. In order to overcome this technical difficulty, kernel-independent generalizations were introduced; see [81]. While these keep the analytic point of view, \mathcal{H} - and \mathcal{H}^2 -matrices (see [50, 53, 55]) generalize the method as much as possible by an algebraic perspective. In addition to the n -body problem, these methods can be applied to general elliptic boundary value problems either in its differential or its integral representation; see [13, 51]. Furthermore, approximate replacements of usual matrix operations such as addition, multiplication, and inversion can be carried out with logarithmic-linear complexity, which allows to construct preconditioners in a fairly automatic way.

This dissertation is divided into ten chapters, the introduction being the first one. The second chapter is devoted to the introduction of the fractional Laplacian and the main problem, the finite element approximation of the operator. One way to define the *fractional Laplacian* is as an integral operator, i.e.

$$(-\Delta)^s u(x) := c_{d,s} \text{ f.p.} \int_{\mathbb{R}^d} \frac{u(x) - u(y)}{|x - y|^{d+2s}} dy, \quad c_{d,s} := \frac{2^{2s} \Gamma(s + d/2)}{\pi^{d/2} \Gamma(1 - s)}.$$

Here, $s \in (0, 1)$ is called the order of the fractional Laplacian, Γ is the Gamma function, and f.p. denotes the finite part of the integral of a function singular at $x \in \mathbb{R}^d$; see [2, 22, 58, 80]. Following the work of [22, 24, 58, 65, 73] we present known results such as the fundamental solution, the s -mean value property, the Poisson kernel for balls and the Green's function. These results are the counterparts of the classical results for the Laplace operator; see [40, 46]. In Section 2.3 we concentrate on the weak formulation of the fractional Laplacian. For this purpose, appropriate Sobolev spaces are introduced

1. Introduction

(see [2, 3, 4, 70, 80]) and we illustrate how the computational domain can be reduced to a finite domain. This is necessary since due its non-local nature the fractional Laplacian is defined by an integral over the whole \mathbb{R}^d . The last part of Section 2 describes main problem, the finite element approximation of the fractional Laplacian, and we state some error estimates for the finite element solution.

In Chapter 3 the foundation for the computation of the entries is laid. Depending on the support of the linear basis function used for the FEM approach, the entries of the stiffness matrix consists of five- and six-dimensional integrals. If the support of the linear basis functions overlap, the integrals become singular and a singularity treatment is necessary to compute these entries. In two dimensions ($d = 2$) this issue is handled in [3, 4, 75]. By extending the ideas of [36, 75] to our three-dimensional cases, we introduce an adapted version of the Duffy transformation to the interaction between two tetrahedra and between a tetrahedron and a panel to lift the arising singularities. In total, this leads to seven different singularity cases which have to be treated separately. In contrast to [29], where quadrature rules for the interaction between d -dimensional simplices are presented, our approach allows a higher reduction of the dimension of the integrals that need to be treated numerically. In [29], $(2d - 1)$ -dimensional integrals have to be computed numerically, whereas our method guarantees that only in the worst case we have to compute five-dimensional integrals. In most cases, a lower-dimensional numerical integration is sufficient. In Section 3.4 we give a quick summary over each case, including the costs of the singularity removal and the number of integrals which have to be computed numerically.

Since all singularities are lifted, Chapter 4 illustrates how the resulting integrals can be computed efficiently. By applying the results [4, 75], error estimates for the integrals are provided and we derive a rule to choose the number of Gauss points per dimension in order to satisfy the error estimates for the finite element solution presented in Chapter 2.

In Chapter 5 we introduce an improved Duffy transformation. In contrast to Chapter 3, we illustrate that the nonlinear transformation which lifts the singularity does not have to map the integration domain to the six-dimensional unit cube, but it can also map the integration domain to a combination of suitable reference elements and still lift the singularity. The idea of this approach is that we can use symmetric cubature rules (see [86]) instead of a tensor Gauss quadrature approach in order to reduce the costs of the numeric integration. Additionally, we obtain some geometrical insight of what happens with the starting geometry after the Duffy transformation.

Since we developed efficient tools to compute the entries of the stiffness matrix, Chapter 6 deals with the issue of an efficient approximation of the stiffness matrix itself. Since the stiffness matrix is a dense matrix, it is too costly to compute the whole matrix for larger problems. Therefore, we give an introduction on the well known concept of \mathcal{H} -matrices; see [13, 18, 51]. \mathcal{H} -matrices are an effective way to approximate stiffness matrices of elliptic operators, since the setting up of the matrix only requires $\mathcal{O}(N \log(N))$ steps and the matrix-vector multiplication only requires $\mathcal{O}(N \log(N))$ steps, where N is the size of the discretized system. In addition to this, we also provide two known methods by which an \mathcal{H} -matrix can be computed: a degenerate kernel approximation and the adaptive cross approximation, the ACA. As a major contribution in this chapter, we prove that the stiffness matrix of the fractional Laplacian can also be approximated by an \mathcal{H} -matrix.

Besides the efficient approximation of the stiffness matrix, preconditioners also play a crucial role in FEM. This also holds true for the fractional Laplacian, since the condition number of the stiffness matrix scales like $\mathcal{O}(h^{-2s})$, where h is the discretization size of the geometry; see [4]. It is well-known

1. Introduction

that for a large class of elliptic problems the inverse of the stiffness matrix can be approximated by an \mathcal{H} -matrix and can be used as a preconditioner; see [13, 42, 43, 44, 45]. Chapter 7 is dedicated to this topic. In [60], it is already proven that the inverse of stiffness can also be efficiently approximated by an \mathcal{H} -matrix. In contrast to this approach, we do not want use the Caffarelli-Silvestre extension of the fractional Laplacian (see [25, 80]), but the integral form of the operator and the weak formulation of the problem. Therefore we are not required to Beppo-Levi spaces, which makes our approach easier accessible to a wide audience. The aim of this chapter is to apply and adapt these ideas to the case of the fractional Laplacian. While we were able to prove that the inverse can be approximated with an \mathcal{H} -matrix, using this approach it is still an open question if the approximation can be done efficiently, i.e. the approximation error decays exponentially w.r.t. the rank of the approximation. Additionally, we can prove a local Caccioppoli inequality for the fractional Laplacian.

Chapter 8 is dedicated to uniform \mathcal{H} -matrices and \mathcal{H}^2 -matrices. Both are specializations of standard \mathcal{H} -matrices; see [50, 53, 55]. \mathcal{H}^2 -matrix approximations cannot be constructed without taking into account the analytic background. For instance, the construction of suitable cluster bases is a crucial task. In order to guarantee as much universality of the method as possible, polynomial spaces are frequently used; see [19]. While this choice is quite convenient due to special properties of polynomials, it is usually not the most efficient approach. To see why, keep in mind that the three-dimensional approach based on spherical harmonics [28] requires $k = \mathcal{O}(p^2)$ terms in a truncated expansion with precision of order p . The number of polynomial terms for the same order of precision requires $k = \mathcal{O}(p^3)$ terms. In the special case of surface problems, an isogeometric approach exploiting surface information and a suitable parameterization can also yield a behavior of $k = \mathcal{O}(p^2)$; see [57]. The number of terms k required to achieve a prescribed accuracy is crucial for the overall efficiency of the method. In addition to its dependence on the kernel, this number also depends on the underlying geometry (local patches of the geometry may have a smaller dimension). Additionally, a-priori error estimates usually lead to an overestimation of k . It is therefore helpful to find k in an automatic way, i.e. by an adaptive procedure. Such a method has already been introduced in Section 6.3, the ACA [12]. In Section 8.1 we generalize the cross approximation method to the kernel-independent construction of uniform \mathcal{H} -matrices and \mathcal{H}^2 -matrices for matrices $A \in \mathbb{R}^{N \times N}$ with entries of the form

$$a_{ij} = \int_{\Omega} \int_{\Omega} |x - y|^{-\alpha} \varphi_i(x) \varphi_j(y) \, dy \, dx, \quad i = 1, \dots, N, \, j = 1, \dots, N.$$

Here, φ_i and φ_j denote linear basis functions and $\alpha > 0$. The next two sections are dedicated to uniform \mathcal{H} -matrices and \mathcal{H}^2 -matrices, respectively. Each matrix type is introduced and we state error estimates for the approximation with the method introduced in Section 8.1. Additionally, in Section 8.3 a new algorithm for efficient precomputations is derived.

After the theory chapters, we turn to numerical tests and exemplify the theoretical results from the previous chapters numerically. For this purpose, Chapter 9 is divided into three sections. The first section deals with the efficient calculation of the entries of the stiffness matrix, i.e. with the results from Chapters 3 to 5. On two selected singularity cases, we verify that the two Duffy transformations lift the singularity and that the errors behave according to the estimates presented in Chapter 4. In addition, the two different Duffy transformations are compared with each other in terms of accuracy and effort. In Section 9.2 the dense stiffness matrix is compared to its \mathcal{H} -matrix approximation and we test the efficiency of the \mathcal{H} -matrix approximation of the inverse of the stiffness matrix. The last example covers the theory of Chapter 8. Using a fractional diffusion process, the three methods

1. Introduction

to approximate the stiffness matrix, the standard \mathcal{H} -matrix approximation, the uniform \mathcal{H} -matrix approximation, and the \mathcal{H}^2 -matrix approximation, are compared with each other. This takes into account the amount of memory required, the time required to set up the matrix, and the time required to solve the system of linear equations.

In the last chapter of the dissertation we give a short summary. In doing so, we take the opportunity to address what could still be improved to make the processes even more efficient.

2. Fractional Laplacian

2.1. Introduction

For the fractional Laplacian a lot of different representations and approaches exist. The operator can be defined by an extension problem (see [25, 80]), a heat semi-group approach (see [80]) or as a singular integral (see [2, 22]) to name a few of them. In order to get an overview, we recommend [64, 69, 80]. Here, we prefer the representation as a singular integral for two reasons. The first one is that this definition gives an easy access to the standard FEM framework; see e.g. [2, 3, 4]. The second reason is that we gain access to important features of elliptic operators, such as the mean value property, fundamental solution, Green's function and Poisson operators, which are the keystones for the classic theory for the Laplace operator; see e.g. [40, 46, 52]. These properties are a good way to develop a feeling for the fractional Laplacian and to work out similarities and differences with the Laplace operator. The link between these two is the potential theory, mainly the Riesz potentials; see e.g. [65, 73]. In this chapter we summarize known results for the fractional Laplacian from the literature based on [22, 58].

2.2. Singular integral representation

Let $d \in \mathbb{N}$ and $\Omega \subset \mathbb{R}^d$ be a Lipschitz domain. We consider the fractional Poisson problem

$$\begin{aligned} (-\Delta)^s u &= f && \text{in } \Omega, \\ u &= 0 && \text{in } \mathbb{R}^d \setminus \Omega, \end{aligned} \tag{1}$$

where the *fractional Laplacian* (see [80]) is defined as

$$(-\Delta)^s u(x) := c_{d,s} \text{ f.p.} \int_{\mathbb{R}^d} \frac{u(x) - u(y)}{|x - y|^{d+2s}} dy, \quad c_{d,s} := \frac{2^{2s} \Gamma(s + d/2)}{\pi^{d/2} \Gamma(1 - s)}. \tag{2}$$

Here, $s \in (0, 1)$ is called the order of the fractional Laplacian and Γ is the Gamma function. Notice that for smooth functions vanishing at infinity the integral in (2) is absolutely convergent for $0 < s < 1/2$; see [80]. For $1/2 \leq s < 1$ the integral has to be understood in a regularized sense; see [80]. Here, f.p. denotes the finite part of the integral of a function singular at $x \in \mathbb{R}^d$. For the fractional Laplacian this means that for any $\delta > 0$

$$\begin{aligned} (-\Delta)^s u(x) &= c_{d,s} \lim_{\varepsilon \rightarrow 0} \int_{\mathbb{R}^d \setminus B_\varepsilon(x)} \frac{u(x) - u(y)}{|x - y|^{d+2s}} dy \\ &= c_{d,s} \int_{\mathbb{R}^d} \frac{u(x) - u(y) - \nabla u(x)^T (x - y) \chi_{|x-y| < \delta}(y)}{|x - y|^{d+2s}} dy, \end{aligned} \tag{3}$$

where χ denotes the characteristic function. It is well-known, see e.g. [22, 80], that (2) is well defined for functions $u \in L_s^1(\mathbb{R}^d) \cap C^{0, 2s+\varepsilon}(\Omega)$ for $s < 1/2$ and $u \in L_s^1(\mathbb{R}^d) \cap C^{1, 2s+\varepsilon-1}(\Omega)$ for $s \geq 1/2$ and for all $\varepsilon > 0$. Note,

$$L_s^1(\mathbb{R}^d) := \left\{ u \in L_{\text{loc}}^1(\mathbb{R}^d) : \int_{\mathbb{R}^d} \frac{|u(x)|}{1 + |x|^{d+2s}} dx < \infty \right\}$$

2. Fractional Laplacian

is a weighted L^1 space, equipped naturally with the norm

$$\|u\|_{L_s^1(\mathbb{R}^d)} := \int_{\mathbb{R}^d} \frac{|u(x)|}{1 + |x|^{d+2s}} \, dx.$$

For the sake of brevity, we write $C^{2s+\varepsilon}(\Omega)$ to denote both $C^{0,2s+\varepsilon}(\Omega)$ for $s < 1/2$ and $C^{1,2s+\varepsilon-1}(\Omega)$ for $s \geq 1/2$.

As mentioned before, the Laplace operator and the fractional Laplacian have quite some similarities, namely a fundamental solution, a Green's function, a Poisson operator and a mean value property. All of these properties will be introduced regarding the fractional Laplacian. It is well-known, see e.g. [65], that the fundamental solution of the Laplace operator is the kernel of the *Newton potential* and the Newton potential is a special *Riesz potential*, namely the Riesz potential of the order 2. Here, the *fundamental solution* F of the fractional Laplacian,

$$F(x) := a_{d,s} |x|^{-d+2s} \quad \text{for } x \in \mathbb{R}^d \setminus \{0\} \quad \text{and} \quad a_{d,s} = \frac{\Gamma(d/2 - s)}{2^{2s} \pi^{d/2} \Gamma(s)},$$

is up to a constant factor the kernel to the Riesz potential of the order $2s$; see [65]. The corresponding properties are summarized in the following theorem; see [22, 80].

Theorem 1. F is a solution to

$$(-\Delta)^s F = \delta_0$$

in the distributional sense, where δ_0 is the Dirac Delta distribution evaluated at zero.

Let $f \in C_0^{2s+\varepsilon}(\mathbb{R}^d)$ and let u be defined as

$$u(x) := (-\Delta)^{-s} f(x) := \int_{\mathbb{R}^d} F(x-y) f(y) \, dy.$$

Then $u \in L_s^1(\mathbb{R}^d)$ and in the distributional sense

$$(-\Delta)^s u = f.$$

Moreover, $u \in C^{2s+\varepsilon}(\mathbb{R}^d)$ and point-wise in \mathbb{R}^d

$$(-\Delta)^s u(x) = f(x). \tag{4}$$

Notice that $(-\Delta)^{-s}$ is the inverse operator to the fractional Laplacian in (4). Analogous to the harmonic functions we define the s -harmonic functions.

Definition 1. Let $D \subset \mathbb{R}^d$. A function u satisfying $(-\Delta)^s u = 0$ in D is called s -harmonic in D . If u satisfies $(-\Delta)^s u = 0$ in \mathbb{R}^d , u is called s -harmonic.

Next we introduce the *Poisson kernel* for balls; see [22, 58].

Definition 2. Let $r > 0$ and $\xi \in \mathbb{R}^d$. For $x \in B_r(\xi)$ and $y \in \mathbb{R}^d \setminus \overline{B_r(\xi)}$, the *Poisson kernel* $P_{\xi,r}$ is defined by

$$P_{\xi,r}(x,y) := a_{d,s} \frac{(r^2 - |x - \xi|^2)^s}{(|y - \xi|^2 - r^2)^s} |y - x|^{-d-2s}, \quad a_{d,s} := \pi^{-d/2-1} \Gamma(d/2) \sin(\pi s). \tag{5}$$

2. Fractional Laplacian

In contrast to the Laplace operator, for the fractional Laplacian a function, which lives on the complement of the ball $B_r(\xi)$, is needed to construct an s -harmonic function inside the ball $B_r(\xi)$; see [22, 58].

Theorem 2. *Let $r > 0$, $g \in L^s_1(\mathbb{R}^d) \cap C(\mathbb{R}^d)$ and let*

$$\mathcal{P}_{\xi,r}g(x) := \begin{cases} \int_{\mathbb{R}^d} P_{\xi,r}(y,x) g(y) dy, & \text{if } x \in B_r(\xi), \\ g(x), & \text{if } x \in \mathbb{R}^d \setminus B_r(\xi). \end{cases}$$

Then $\mathcal{P}_{\xi,r}g$ is the unique point-wise continuous solution of the problem

$$\begin{aligned} (-\Delta)^s u &= 0 & \text{in } B_r(\xi), \\ u &= g & \text{in } \mathbb{R}^d \setminus B_r(\xi). \end{aligned}$$

Remark. *There also exists an Poisson operator, which constructs s -harmonic functions outside a ball; see [65].*

Using the Poisson kernel and the fundamental solution, the *Green's function* G for balls can be introduced; see [22].

Lemma 1. *Let $r > 0$ and $\xi \in \mathbb{R}^d$. For any $x, z \in B_r(\xi)$ and $x \neq z$, the function G is defined by*

$$G(x, z) := F(x - z) - \int_{\mathbb{R}^d \setminus B_r(\xi)} F(z - y) P_{\xi,r}(y, x) dy.$$

Remark. *This principle can also be applied to more complicated domains. For more details; see [65].*

Similar to the Laplace operator, the Green function can be used to construct solutions to fractional Poisson problems.

Theorem 3. *Let $r > 0$, $\xi \in \mathbb{R}^d$, $f \in C^{2s+\varepsilon}(B_r(\xi)) \cap C(\overline{B_r(\xi)})$ with $\varepsilon > 0$ and let*

$$u(x) := \begin{cases} \int_{B_r(\xi)} f(y) G(x, y) dy & \text{if } x \in B_r(\xi), \\ 0 & \text{if } x \in \mathbb{R}^d \setminus B_r(\xi). \end{cases}$$

Then u is the unique point-wise continuous solution of the problem (1)

$$\begin{aligned} (-\Delta)^s u &= f & \text{in } B_r(\xi), \\ u &= 0 & \text{in } \mathbb{R}^d \setminus B_r(\xi). \end{aligned}$$

As the final property of the four, we present the *s -mean value property*; see [22].

Definition 3. *Let $D \subset \mathbb{R}^d$ be a domain. A function $u \in L^1_s(\mathbb{R}^d) \cap C(D)$ satisfies the s -mean value property in D , if for all closed balls $\overline{B_r(x)} \subset D$ it holds that*

$$u(x) = \mathcal{M}_s(x, u, r), \quad \mathcal{M}_s(x, u, r) := a_s \int_{\mathbb{R}^d \setminus B_r(x)} \frac{r^{2s}}{(|y-x|^2 - r^2)^s} \frac{u(y)}{|y-x|^d} dy,$$

where $a_s := \pi^{-d/2-1} \Gamma(d/2) \sin(\pi s)$.

2. Fractional Laplacian

Since the s -mean value property is defined by a convolution, it can alternatively be required only that $u \in L^2(\mathbb{R}^d)$ and that the integral exists for all closed balls $\overline{B_\varepsilon(x)} \subset D$; see [58]. Following the work of [58], we want to present three interesting properties of functions satisfying the s -mean value property. First, we start with the uniqueness of such a function.

Lemma 2. *Let u and v satisfy the s -mean value property in a domain D . If $u(x) = v(x)$ in D , then $u(x) = v(x)$ a.e. in \mathbb{R}^d .*

Moreover, we can show a direct connection between a harmonic function and a function satisfying the s -mean value property. Each function being harmonic in \mathbb{R}^d satisfies also the s -mean value property there; see [58].

Lemma 3. *If u is harmonic in the usual sense in \mathbb{R}^d , then u satisfies the s -mean value property in \mathbb{R}^d .*

Notice, this statement does not apply if \mathbb{R}^d is replaced by a domain $D \subset \mathbb{R}^d$. This is because the s -mean value property demands information about u throughout \mathbb{R}^d , whereas this does not apply to harmonic functions in D .

Furthermore, the Poisson kernel can be used as an alternative representation of functions satisfying the s -mean value property; see [58].

Lemma 4. *Let u satisfy the s -mean value property in a domain $D \subset \mathbb{R}^d$. For each open ball $B_r(\xi)$ contained with its closure in D ,*

$$u(x) = \mathcal{P}_{\xi,r}u(x)$$

in $B_r(\xi)$ and u is analytic in D .

As it can be seen, a function satisfying the s -mean value property is a smooth function. These three lemmas are important keystones to prove the equivalence between the s -mean value property and s -harmonicity.

Theorem 4. *Let D be a domain in \mathbb{R}^d and $u \in L^1_s(\mathbb{R}^d) \cap C^{2s+\varepsilon}(D)$ with $\varepsilon > 0$. Then u satisfies the s -mean value property in D if and only if u is s -harmonic in D .*

Proof. Let D be a domain in \mathbb{R}^d and let $u \in C(D)$ be a Lebesgue measurable function in \mathbb{R}^d . By using the Lemmas 2 to 4 it is shown in [58, Theorem 2] that u satisfies the s -mean value property if and only if $(-\Delta)^s u$ exists in D and $(-\Delta)^s u(x) = 0$ in D . The existence of the operator can be guaranteed by $u \in L^1_s(\mathbb{R}^d) \cap C^{2s+\varepsilon}(D)$; see [22, 80]. \square

Remark. *Note that the function space*

$$\tilde{L}^2(\Omega) := \{u \in L^2(\mathbb{R}^d) : u = 0 \text{ a.e. in } \mathbb{R}^d \setminus \Omega\} \subset L^1_s(\mathbb{R}^d). \quad (6)$$

The inclusion can be easily seen by applying the Cauchy-Schwarz inequality:

$$\|u\|_{L^1_s(\mathbb{R}^d)} \leq |\Omega|^{1/2} \|u\|_{L^2(\Omega)}.$$

To finish this introduction to the fractional Laplacian, we show the point-wise limits for s ; see [80].

2. Fractional Laplacian

Theorem 5. *Let $x \in \mathbb{R}^d$ and $0 < \alpha < 1$. If $u \in C^2(B_2(x)) \cap L^\infty(\mathbb{R}^d)$ then*

$$\lim_{s \rightarrow 1^-} (-\Delta)^s u(x) = -\Delta u(x).$$

If $u \in C^\alpha(B_2(x)) \cap L^1_0(\mathbb{R}^d)$ then

$$\lim_{s \rightarrow 0^+} (-\Delta)^s u(x) = u(x).$$

2.3. Weak formulation

Let $\Omega \subset \mathbb{R}^d$ be a Lipschitz domain. Again, we consider the fractional Poisson problem

$$\begin{aligned} (-\Delta)^s u &= f & \text{in } \Omega, \\ u &= 0 & \text{in } \mathbb{R}^d \setminus \Omega. \end{aligned} \tag{7}$$

Now, the solution of problem (7) is searched for in Sobolev spaces

$$H^s(\Omega) = \{v \in L^2(\Omega) : |v|_{H^s(\Omega)} < \infty\},$$

where

$$|v|_{H^s(\Omega)}^2 = \int_{\Omega} \int_{\Omega} \frac{|v(x) - v(y)|^2}{|x - y|^{d+2s}} dx dy$$

is the *Slobodeckij seminorm*. The space $H^s(\Omega)$ is a Hilbert space, equipped with the norm

$$\|v\|_{H^s(\Omega)} = \|v\|_{L^2(\Omega)} + |v|_{H^s(\Omega)}.$$

Zero trace spaces $H^s_0(\Omega)$ can be defined as the closure of $C^\infty_0(\Omega)$ w.r.t. this norm.

Due to the non-local nature of the fractional Laplacian, we need to define the Hilbert space

$$\tilde{H}^s(\Omega) := \{u \in H^s(\mathbb{R}^d) : u = 0 \text{ in } \mathbb{R}^d \setminus \Omega\},$$

which can be equipped with the norm

$$\|u\|_{\tilde{H}^s(\Omega)} = |u|_{H^s(\mathbb{R}^d)}.$$

$\tilde{H}^s(\Omega)$ is the closure of $C^\infty_0(\Omega)$ in $H^s(\mathbb{R}^d)$; see [70]. It is known (see [3]) that $\tilde{H}^s(\Omega)$ coincides with $H^s_0(\Omega)$ for $s \neq 1/2$, and for $s = 1/2$ it holds that $\tilde{H}^{1/2}(\Omega) \subset H^{1/2}_0(\Omega)$. Negative order spaces $H^{-s}(\Omega)$ can be defined as the dual space of $\tilde{H}^s(\Omega)$.

With this notation we can reformulate (7) in a weak form: given $f \in H^r(\Omega)$ with $r \geq -s$ find $u \in \tilde{H}^s(\Omega)$ satisfying

$$a(u, v) = \langle f, v \rangle_\Omega, \quad v \in \tilde{H}^s(\Omega), \tag{8}$$

where

$$a(u, v) = c_{d,s} \int_{\mathbb{R}^d} \int_{\mathbb{R}^d} \frac{u(x) - u(y)}{|x - y|^{d+2s}} v(x) dy dx.$$

2. Fractional Laplacian

and $\langle \cdot, \cdot \rangle_\Omega$ denotes the duality pairing. Due to symmetry and the support of u and v , we observe that

$$a(u, v) = \frac{c_{d,s}}{2} \int_{\mathbb{R}^d} \int_{\mathbb{R}^d} \frac{[u(x) - u(y)][v(x) - v(y)]}{|x - y|^{d+2s}} dy dx \quad (9a)$$

$$= \frac{c_{d,s}}{2} \int_{\Omega} \int_{\Omega} \frac{[u(x) - u(y)][v(x) - v(y)]}{|x - y|^{d+2s}} dy dx + c_{d,s} \int_{\Omega} \int_{\mathbb{R}^d \setminus \Omega} \frac{u(x)v(x)}{|x - y|^{d+2s}} dy dx. \quad (9b)$$

$$= \frac{c_{d,s}}{2} \int_{\Omega} \int_{\Omega} \frac{[u(x) - u(y)][v(x) - v(y)]}{|x - y|^{d+2s}} dy dx + \frac{c_{d,s}}{2s} \int_{\Omega} u(x)v(x) \int_{\partial\Omega} \frac{(x - y)^T n_y}{|x - y|^{d+2s}} ds_y dx,$$

where n_y is the inward normal vector w.r.t. $\partial\Omega$. The last step is due to applying the Gauss theorem to $|x - y|^{-d-2s}$. The following lemma together with the well known Lax-Milgram theorem shows that the variational problem (8) is uniquely solvable. Furthermore, it shows that a can be defined for a larger set of functions. In the following we use the expression for

$$\kappa_{d,s}(\varepsilon) := \int_{\mathbb{R}^d \setminus B_\varepsilon(0)} |x|^{-d-2s} dx = \omega_d \int_\varepsilon^\infty r^{d-1-d-2s} dr = \frac{\omega_d}{2s} \varepsilon^{-2s},$$

where ω_d denotes the surface area of the unit ball in \mathbb{R}^d .

Lemma 5. *The bilinear form $a : \tilde{H}^s(\Omega) \times \tilde{H}^s(\Omega) \rightarrow \mathbb{R}$ is symmetric, coercive and continuous. $a(u, v)$ is defined for $u \in L^2(\mathbb{R}^d) \cap H^s(\hat{K})$ and $v \in \tilde{H}^s(K)$, where $K \subset \hat{K} \subset \mathbb{R}^d$ such that K is bounded and $\text{dist}(K, \partial\hat{K}) > 0$.*

Proof. The symmetry is obvious and the coercivity and the continuity follow (see (9a)) from

$$a(v, v) = \frac{c_{d,s}}{2} |v|_{H^s(\mathbb{R}^d)}^2 = \frac{c_{d,s}}{2} \|v\|_{\tilde{H}^s(\Omega)}^2.$$

For the second part of the assertion, observe similar to (9b)

$$\begin{aligned} a(u, v) &= \frac{c_{d,s}}{2} \int_{\hat{K}} \int_{\hat{K}} \frac{[u(x) - u(y)][v(x) - v(y)]}{|x - y|^{d+2s}} dy dx + c_{d,s} \int_{\hat{K}} \int_{\mathbb{R}^d \setminus \hat{K}} \frac{[u(x) - u(y)]v(x)}{|x - y|^{d+2s}} dy dx \\ &\leq \frac{c_{d,s}}{2} |u|_{H^s(\hat{K})}^2 |v|_{H^s(\hat{K})}^2 + c_{d,s} \int_K v(x) \int_{\mathbb{R}^d \setminus \hat{K}} \frac{u(x) - u(y)}{|x - y|^{d+2s}} dy dx. \end{aligned}$$

Setting $\delta := \text{dist}(K, \partial\hat{K}) > 0$, the latter integral can be estimated as

$$\begin{aligned} &\int_K v(x) \int_{\mathbb{R}^d \setminus \hat{K}} \frac{u(x) - u(y)}{|x - y|^{d+2s}} dy dx \\ &= \int_K u(x)v(x) \int_{\mathbb{R}^d \setminus \hat{K}} \frac{1}{|x - y|^{d+2s}} dy dx - \int_K v(x) \int_{\mathbb{R}^d \setminus \hat{K}} \frac{u(y)}{|x - y|^{d+2s}} dy dx \\ &\leq \kappa_{d,s}(\delta) \|u\|_{L^2(K)} \|v\|_{L^2(K)} + \int_K |v(x)| \int_{\mathbb{R}^d \setminus B_\delta(x)} \frac{|u(y)|}{|x - y|^{d+2s}} dy dx \end{aligned}$$

2. Fractional Laplacian

and

$$\begin{aligned}
\int_K |v(x)| \int_{\mathbb{R}^d \setminus B_\delta(x)} \frac{|u(y)|}{|x-y|^{d+2s}} dy dx &\leq \|u\|_{L^2(\mathbb{R}^d)} \int_K |v(x)| \left(\int_{\mathbb{R}^d \setminus B_\delta(x)} \frac{1}{|x-y|^{2(d+2s)}} dy \right)^{1/2} dx \\
&\leq \sqrt{\kappa_{d,d/2+2s}(\delta)} \|u\|_{L^2(\mathbb{R}^d)} \int_K |v(x)| dx \\
&\leq \sqrt{|K| \kappa_{d,d/2+2s}(\delta)} \|u\|_{L^2(\mathbb{R}^d)} \|v\|_{L^2(K)}.
\end{aligned}$$

□

Additionally to the uniqueness of the solution, there exists also a regularity result relative to the smoothness of the boundary of Ω ; see [1].

Theorem 6. *Let $u \in \tilde{H}^s(\Omega)$ be the solution of (8) and $\varepsilon > 0$. If $\partial\Omega$ is of C^∞ class, then $u \in H^{s+1/2-\varepsilon}(\Omega)$.*

As one can see, we can not expect regularity as in the Laplace case, where $u \in H^2(\Omega)$ if $\partial\Omega$ is of C^2 class or if Ω is a convex polygon and $f \in L^2(\Omega)$; see [39]. Actually, there exists a well know example for this, see e.g. [2, 4],

$$\begin{aligned}
(-\Delta)^s u &= 1 && \text{in } B_1(0), \\
u &= 0 && \text{in } \mathbb{R}^d \setminus B_1(0),
\end{aligned} \tag{10}$$

which will be used later on for the numerical tests, too. The peculiarity is that the analytical solution u of this problem is only in $H^{s+1/2-\varepsilon}(B_1(0))$ for any $\varepsilon > 0$,

$$u(x) = \frac{2^{-2s}}{\Gamma(1+s)^2} (1 - |x|^2)^s,$$

although both the right-hand side and the boundary of the ball $B_1(0)$ are smooth. Similar regularity results are known w.r.t. the right-hand side f ; see [2].

Theorem 7. *Let $0 < s < 1/2$ and $\varepsilon > 0$. If $f \in C^{1/2-s}(\Omega)$ for some $\beta > 0$, then the solution u of (8) belongs to $H^{s+1/2-\varepsilon}(\Omega)$.*

Let $1/2 < s < 1$ and $\varepsilon > 0$. If $f \in C^\beta(\Omega)$ for some $\beta > 0$, then the solution u of (8) belongs to $H^{s+1/2-\varepsilon}(\Omega)$.

2.4. Finite element approximation

Henceforth, let Ω be a polygon. As we have seen in the last section, the fractional Poisson problem

$$\begin{aligned}
(-\Delta)^s u &= f && \text{in } \Omega, \\
u &= 0 && \text{in } \mathbb{R}^d \setminus \Omega,
\end{aligned}$$

can be reformulated in the weak form: find $u \in \tilde{H}^s(\Omega)$ satisfying

$$a(u, v) = \langle f, v \rangle_\Omega, \quad v \in \tilde{H}^s(\Omega). \tag{11}$$

2. Fractional Laplacian

We use a Galerkin approach to discretize the problem with piecewise linear basis functions; see [21]. Let the set $\{\varphi_1, \dots, \varphi_N\}$ denote the basis of the space of piecewise linear functions $V(\mathcal{T}) \subset \tilde{H}^s(\Omega)$, where \mathcal{T} is a regular partition of Ω into M tetrahedra and N inner points. \mathcal{P} is the set of panels, being the faces of the tetrahedra of \mathcal{T} . Additionally, we impose three assumptions for the discretization. The first one is that the tetrahedra are quasi-uniform, i.e. there exist constants $c_1, c_2 > 0$ with

$$c_1 h_{t_1} \leq h_{t_2} \leq c_2 h_{t_1} \quad (12)$$

for all $t_1, t_2 \in \mathcal{T}$, where h_t is defined as the diameter of the tetrahedron t . The second assumption is that the elements of the discretization, the panels and the tetrahedra, do not degenerate, i.e. both the interior angles and the solid angles of the tetrahedra are bounded below independently of h_t by the angle $\theta_{\mathcal{T}} > 0$:

$$\theta_t > \theta_{\mathcal{T}} \quad \text{for all } t \in \mathcal{T}, \quad (13)$$

where θ_t is the minimal interior angle of the tetrahedron t . Since each element of \mathcal{P} is a face of a tetrahedron in \mathcal{T} , the interior angles of the panels are also bounded below by $\theta_{\mathcal{T}}$.

Last, we assume that only a bounded number of supports of the linear basis functions overlap; i.e. there is a number $\nu \in \mathbb{N}$ such that for each $i \in \{1, \dots, N\}$

$$\max_{x \in \text{int supp } \varphi_i} |\{j \in \{1, \dots, N\} : x \in \text{int supp } \varphi_j\}| \leq \nu. \quad (14)$$

Moreover, we introduce h as the mean of all diameters, i.e.

$$h := \frac{1}{|\mathcal{T}|} \sum_{t \in \mathcal{T}} h_t. \quad (15)$$

Then (12) is also valid for h , i.e.

$$c_1 h \leq h_t \leq c_2 h \quad (16)$$

for all $t \in \mathcal{T}$. Now we are interested in the solution u_h of the discrete problem (11):

$$a(u_h, v_h) = \langle f, v_h \rangle_{\Omega}, \quad v_h \in V_h := V(\mathcal{T}) \subset \tilde{H}^s(\Omega).$$

Since we use a conforming discretization V_h of $\tilde{H}^s(\Omega)$, the Lax-Milgram theorem still guarantees the existence and uniqueness of the Galerkin approximation u_h . The Galerkin method yields the discrete fractional Poisson problem $Au_N = g$ with $A \in \mathbb{R}^{N \times N}$, $g, u_N \in \mathbb{R}^N$ having the entries

$$\begin{aligned} a_{ij} &= \frac{c_{d,s}}{2} \int_{\Omega} \int_{\Omega} \frac{[\varphi_i(x) - \varphi_i(y)][\varphi_j(x) - \varphi_j(y)]}{|x - y|^{d+2s}} dx dy \\ &\quad + \frac{c_{d,s}}{2s} \int_{\Omega} \varphi_i(x) \varphi_j(x) \int_{\partial\Omega} \frac{(x - y)^T n_y}{|x - y|^{d+2s}} ds_y dx, \quad i, j = 1, \dots, N, \\ g_i &= \langle f, \varphi_i \rangle_{\Omega}, \quad i = 1, \dots, N. \end{aligned}$$

By using the compact support of the linear basis functions, the expression for a_{ij} can be simplified to

$$\begin{aligned} a_{ij} &= \frac{c_{d,s}}{2} \int_{\Omega_{ij}} \int_{\Omega_{ij}} \frac{[\varphi_i(x) - \varphi_i(y)][\varphi_j(x) - \varphi_j(y)]}{|x - y|^{d+2s}} dx dy \\ &\quad + \frac{c_{d,s}}{2s} \int_{\Omega_{ij}} \varphi_i(x) \varphi_j(x) \int_{\partial\Omega_{ij}} \frac{(x - y)^T n_y}{|x - y|^{d+2s}} ds_y dx \end{aligned} \quad (17)$$

2. Fractional Laplacian

where $\Omega_{ij} := \text{supp } \varphi_i \cup \text{supp } \varphi_j$. If the supports of the basis functions φ_i and φ_j are disjoint, the computation of the entry a_{ij} simplifies to

$$a_{ij} = -c_{d,s} \int_{\text{supp } \varphi_i} \int_{\text{supp } \varphi_j} \frac{\varphi_i(x) \varphi_j(y)}{|x-y|^{d+2s}} dx dy. \quad (18)$$

Besides the stiffness matrix A , we introduce two other $N \times N$ matrices

$$A = \mathcal{J}^*(-\Delta)^s \mathcal{J}, \quad B = \mathcal{J}^*(-\Delta)^{-s} \mathcal{J}, \quad \text{and} \quad M = \mathcal{J}^* \mathcal{J}. \quad (19)$$

B is the Galerkin discretization of the inverse of $(-\Delta)^s$ and M is the mass matrix. Here, \mathcal{J} is the natural bijection $\mathcal{J} : \mathbb{R}^n \rightarrow V_h$ defined by

$$\mathcal{J}x = \sum_{i=1}^N x_i \varphi_i,$$

and $\mathcal{J}^* : V_h' \rightarrow \mathbb{R}^n$ is defined by

$$(\mathcal{J}^* \varphi, x)_h = (\varphi, \mathcal{J}x)_{L^2} \quad \text{for all } x \in \mathbb{R}^n, \varphi \in V_h',$$

where $(x, y)_h := h^d x^T y$ denotes the (naturally scaled) Euclidian inner product; see [13]. According to [52], under the assumptions (12) to (16) there are constants $0 < c_{\mathcal{J},1} < c_{\mathcal{J},2}$ independent of h and d such that

$$c_{\mathcal{J},1} \|x\|_h \leq \|\mathcal{J}x\|_{L^2(\Omega)} \leq c_{\mathcal{J},2} \|x\|_h \quad \text{for all } x \in \mathbb{R}^d. \quad (20)$$

For the Galerkin approximation u_h , error estimates exist; see [2].

Theorem 8. *If the family of triangulations \mathcal{T}_h satisfies (12) and (13), and $u \in H^l(\Omega)$, for $0 < s \leq 1/2 < l < 1$ or $1/2 < s < 1 < l < 2$, then*

$$\|u - u_h\|_{\tilde{H}^s(\Omega)} \leq C(s, d) h^{l-s} |u|_{H^l(\Omega)}. \quad (21)$$

In particular, by applying regularity estimates for u in terms of the data f , the solution satisfies

$$\|u - u_h\|_{\tilde{H}^s(\Omega)} \leq \begin{cases} C(s) h^{1/2} |\log h| \|f\|_{C^{1/2-s}(\Omega)} & \text{if } 0 < s < 1/2, \\ C(s) h^{1/2} |\log h| \|f\|_{L^\infty(\Omega)} & \text{if } s = 1/2, \\ \frac{C(s,\beta)}{2s-1} h^{1/2} \sqrt{|\log h|} \|f\|_{C^\beta(\Omega)} & \text{if } 1/2 < s < 1, \beta > 0. \end{cases}$$

By using a standard Aubin-Nitsche argument [39], we obtain estimates in $L^2(\Omega)$; see [20].

Theorem 9. *If the family of triangulations \mathcal{T}_h satisfies (12) and (13), and, for $\varepsilon > 0$, $u \in H^{s+1/2-\varepsilon}(\Omega)$, then*

$$\|u - u_h\|_{L^2(\Omega)} \leq \begin{cases} C(s, \varepsilon) h^{1/2+s-\varepsilon} |u|_{H^{s+1/2-s}(\Omega)} & \text{if } 0 < s < 1/2, \\ C(s, \varepsilon) h^{1-2\varepsilon} |u|_{H^{s+1/2-\varepsilon}(\Omega)} & \text{if } 1/2 \leq s < 1. \end{cases}$$

Remark. *For $s > 1/2$ the assumption (12) can be replaced by the assumption of so called locally quasi-uniform meshes, which enables the use of graded meshes; see [2].*

2. Fractional Laplacian

These results naturally assume that the stiffness matrix A can be calculated exactly. However, looking at (17) it seems that this is not possible. Even in the simplest case (see (18)) we are not able to calculate the six-dimensional integrals analytically. Therefore, we have to rely on numerical integration. Additionally, the integrals may even become singular if the supports of the linear basis functions have a nonempty intersection. In the next section, we derive a method to lift these singularities and we provide estimates in dependence of the discretization parameter h indicating which quadrature rule must be used to guarantee the error estimate (21).

3. Duffy transformation

The Duffy transformation is a well-known method for singularity lifting of singular integrals. In his original work M. Duffy [36] described how to lift point singularities at one corner of a three-dimensional pyramid. For this purpose the integration domain was transformed to the unit cube and the singularity was lifted by the Jacobi determinant of the nonlinear transformation. This is done in a similar way to spherical coordinates.

Based on this idea, Sauter and Schwab [75] have investigated singularities that can arise from the interaction of triangles, such as a point singularity when the triangles touch at a corner, or a singularity along a common edge of these triangles. Such problems occur in the context of the boundary element method (BEM) for elliptic operators; see [78].

Here, their theory and the Duffy transformation are adapted to the requirements of the fractional Laplacian in three dimensions, i.e. to the integrals in (17):

$$I_{t_1, t_2} := \int_{t_1} \int_{t_2} k_1(x, y) dy dx := \int_{t_1} \int_{t_2} \frac{[\varphi_i(x) - \varphi_i(y)] [\varphi_j(x) - \varphi_j(y)]}{|x - y|^{3+2s}} dy dx, \quad (22)$$

$$I_{t, \tau} := \int_t \int_{\tau} k_2(x, y) ds_y dx := \int_t \varphi_i(x) \varphi_j(x) \int_{\tau} \frac{(y - x)^T n_{\tau}(y)}{|x - y|^{3+2s}} ds_y dx, \quad (23)$$

where $t, t_1, t_2 \in \mathcal{T}$, $\tau \in \mathcal{P}$ and n_{τ} is the normal vector w.r.t. the panel τ . As we can see in (22) and (23), we have to study the cases of the interaction of two tetrahedra and of a tetrahedron and a triangle, respectively. This results in a total of seven singularity cases, which must be considered individually. However, the procedures for each case share common principles.

3.1. A simple introductory example

To understand the basic idea, we present an adapted version of the basic problem of [36],

$$I_p = \int_p f(\omega) d\omega,$$

where $p := \{\omega \in \mathbb{R}^4 : 0 \leq \omega_4 \leq \omega_1, 0 \leq \omega_3 \leq \omega_2, 0 \leq \omega_2 \leq \omega_1 \text{ and } 0 \leq \omega_1 \leq 1\}$, and where $f(\omega) = |\omega|^{-2}$ is a function with a point singularity at $(0, 0, 0, 0)^T$. Then we have

$$I_p = \int_0^1 \int_0^{\omega_1} \int_0^{\omega_2} \int_0^{\omega_1} \frac{1}{\omega_1^2 + \omega_2^2 + \omega_3^2 + \omega_4^2} d\omega_4 d\omega_3 d\omega_2 d\omega_1.$$

Obviously, the singularity can be lifted with spherical coordinates. However, the integration domain is not well suited for this approach. Surprisingly, the simple nonlinear transformation,

$$\xi := \omega_1, \quad \eta_1 := \omega_2/\omega_1, \quad \eta_2 := \omega_3/\omega_2, \quad \eta_3 := \omega_4/\omega_1,$$

is also sufficient to lift the singularity. First, we study the Jacobi determinant $\det \mathcal{J}(\xi, \eta) = \xi^3 \eta_1$ of the nonlinear transformation. Second, we consider the integration domain

$$\left\{ \begin{array}{l} 0 \leq \omega_1 \leq 1 \\ 0 \leq \omega_2 \leq \omega_1 \\ 0 \leq \omega_3 \leq \omega_2 \\ 0 \leq \omega_4 \leq \omega_1 \end{array} \right\} \Leftrightarrow \left\{ \begin{array}{l} 0 \leq \xi \leq 1 \\ 0 \leq \xi \eta_1 \leq \xi \\ 0 \leq \xi \eta_1 \eta_2 \leq \xi \eta_1 \\ 0 \leq \xi \eta_3 \leq \xi \end{array} \right\} \Leftrightarrow \left\{ \begin{array}{l} 0 \leq \xi \leq 1 \\ 0 \leq \eta_1 \leq 1 \\ 0 \leq \eta_2 \leq 1 \\ 0 \leq \eta_3 \leq 1 \end{array} \right\} \quad (24)$$

3. Duffy transformation

and then the complete integral

$$\begin{aligned} I_p &= \int_0^1 \int_0^1 \int_0^1 \int_0^1 \frac{\xi^3 \eta_1}{\xi^2 + (\xi \eta_1)^2 + (\xi \eta_1 \eta_2)^2 + (\xi \eta_3)^2} d\eta_3 d\eta_2 d\eta_1 d\xi \\ &= \frac{1}{2} \int_0^1 \int_0^1 \int_0^1 \frac{\eta_1}{1 + \eta_1^2 + (\eta_1 \eta_2)^2 + \eta_3^2} d\eta_3 d\eta_2 d\eta_1. \end{aligned}$$

The decisive factor is the structure of the integration domain, which induces an ordering of the variables, i.e.

$$0 \leq \omega_3 \leq \omega_2 \leq \omega_1 \leq 1 \quad \text{and} \quad 0 \leq \omega_4 \leq \omega_1 \leq 1. \quad (25)$$

This order is used by the nonlinear transformation to lift the singularity in two steps, which is similar to using spherical coordinates, where ξ takes the role of the radius. First, ξ is factored out of the fraction, which is clearly not singular anymore, and second, the determinant of the Jacobi matrix is used to lift the remaining singularity w.r.t. ξ .

In order to apply this technique to our problems, we need to understand more about the ordering of the variables, which is of crucial importance in the removal of the singularity. As it can be seen in (25), the ordering leads to two inequality chains. To be more precise it leads to one inequality chain, which splits up after at least one common variable (in this case ω_1). We call such an inequality chain a forking inequality chain. In this situation, after the application of the nonlinear transformation, ξ can be factored out of the denominator, which is crucial for lifting the singularity. Therefore, we have to make sure that all variables can be described with a forking inequality chain. To ensure such a forking chain, it may be necessary to split up the integration domain.

3.2. Interaction between two tetrahedra

First, we consider (22), i.e. how two tetrahedra interact with each other. Here, we have to distinguish four different cases: the tetrahedra can have a common point, a common edge, a common face or can be identical. In order to describe the resulting singularity types, the geometry will be shifted to the reference element, the unit tetrahedron

$$\tilde{t} := \{\tilde{x} \in \mathbb{R}^3 : 0 \leq \tilde{x}_3 \leq 1 - \tilde{x}_1 - \tilde{x}_2, \quad 0 \leq \tilde{x}_2 \leq 1 - \tilde{x}_1, \quad 0 \leq \tilde{x}_1 \leq 1\}.$$

For this we need the linear mapping $\chi_t : \tilde{t} \rightarrow t$,

$$\chi_t(\tilde{x}) = M_t \tilde{x} + a_t, \quad (26)$$

where $M_t := [b_t - a_t, c_t - a_t, d_t - a_t] \in \mathbb{R}^{3 \times 3}$ and a_t, b_t, c_t and d_t denote the corners of the tetrahedron t . Note that this specific unit tetrahedron is chosen due to Chapter 5. Using the transformation theorem, we get for (22)

$$I_{t_1, t_2} = \int_{\tilde{t}} \int_{\tilde{t}} k_1(\chi_{t_1}(\tilde{x}), \chi_{t_2}(\tilde{y})) |M_{t_1}| |M_{t_2}| d\tilde{y} d\tilde{x} =: \int_{\tilde{t}} \int_{\tilde{t}} \tilde{k}_1(\tilde{x}, \tilde{y}) d\tilde{y} d\tilde{x}, \quad (27)$$

where $|M_\star| := |\det M_\star|$ for $\star \in \{t_1, t_2\}$. Additionally, let the linear basis functions φ_i be defined in the following way,

$$\varphi_i(x) := \alpha_i^T \begin{pmatrix} x \\ 1 \end{pmatrix} = \alpha_{i,1:3}^T x + \alpha_{i,4}, \quad \alpha_i \in \mathbb{R}^4,$$

3. Duffy transformation

where $\alpha_{i,1:3} := (\alpha_{i,1}, \alpha_{i,2}, \alpha_{i,3})^T$. Additionally, we denote by e_1, e_2 and e_3 the first, the second, and the third canonical unit vector in \mathbb{R}^3 .

3.2.1. Point singularity

First, we consider the simplest case, that the two tetrahedra have a common corner point. Without loss of generality the mappings χ_{t_1} and χ_{t_2} are chosen in such a way that $a_{t_1} = a_{t_2}$. This implies that the integrand \tilde{k}_1 is singular for $\tilde{x} = 0 = \tilde{y}$. By considering the integration domain as a set of inequalities and rewriting them,

$$\left\{ \begin{array}{l} 0 \leq \tilde{x}_1 \leq 1 \\ 0 \leq \tilde{x}_2 \leq 1 - \tilde{x}_1 \\ 0 \leq \tilde{x}_3 \leq 1 - \tilde{x}_1 - \tilde{x}_2 \\ 0 \leq \tilde{y}_1 \leq 1 \\ 0 \leq \tilde{y}_2 \leq 1 - \tilde{y}_1 \\ 0 \leq \tilde{y}_3 \leq 1 - \tilde{y}_1 - \tilde{y}_2 \end{array} \right\} \Leftrightarrow \left\{ \begin{array}{l} 0 \leq \tilde{x}_1 \leq 1 \\ \tilde{x}_1 \leq \tilde{x}_1 + \tilde{x}_2 \leq 1 \\ \tilde{x}_1 + \tilde{x}_2 \leq \tilde{x}_1 + \tilde{x}_2 + \tilde{x}_3 \leq 1 \\ 0 \leq \tilde{y}_1 \leq 1 \\ \tilde{y}_1 \leq \tilde{y}_1 + \tilde{y}_2 \leq 1 \\ \tilde{y}_1 + \tilde{y}_2 \leq \tilde{y}_1 + \tilde{y}_2 + \tilde{y}_3 \leq 1 \end{array} \right\},$$

We see that the variables form two disjoint inequality chains:

$$0 \leq \tilde{x}_1 \leq \tilde{x}_1 + \tilde{x}_2 \leq \tilde{x}_1 + \tilde{x}_2 + \tilde{x}_3 \leq 1 \quad \text{and} \quad 0 \leq \tilde{y}_1 \leq \tilde{y}_1 + \tilde{y}_2 \leq \tilde{y}_1 + \tilde{y}_2 + \tilde{y}_3 \leq 1.$$

However, as the initial example (25) has shown, a forking inequality chain is needed to lift the singularity. Therefore, we connect the two chains with each other by introducing an artificial dependence on the first chain link:

$$\tilde{y}_1 + \tilde{y}_2 + \tilde{y}_3 \leq \tilde{x}_1 + \tilde{x}_2 + \tilde{x}_3 \leq 1 \quad \text{and} \quad \tilde{x}_1 + \tilde{x}_2 + \tilde{x}_3 \leq \tilde{y}_1 + \tilde{y}_2 + \tilde{y}_3 \leq 1.$$

From the geometric point of view, this means that the integration domain must be split up:

$$\left\{ \begin{array}{l} 0 \leq \tilde{x}_1 \leq 1 \\ \tilde{x}_1 \leq \tilde{x}_1 + \tilde{x}_2 \leq 1 \\ \tilde{x}_1 + \tilde{x}_2 \leq \tilde{x}_1 + \tilde{x}_2 + \tilde{x}_3 \leq 1 \\ 0 \leq \tilde{y}_1 \leq 1 \\ \tilde{y}_1 \leq \tilde{y}_1 + \tilde{y}_2 \leq 1 \\ \tilde{y}_1 + \tilde{y}_2 \leq \tilde{y}_1 + \tilde{y}_2 + \tilde{y}_3 \leq \|\tilde{x}\|_1 \end{array} \right\} \cup \left\{ \begin{array}{l} 0 \leq \tilde{y}_1 \leq 1 \\ \tilde{y}_1 \leq \tilde{y}_1 + \tilde{y}_2 \leq 1 \\ \tilde{y}_1 + \tilde{y}_2 \leq \tilde{y}_1 + \tilde{y}_2 + \tilde{y}_3 \leq 1 \\ 0 \leq \tilde{x}_1 \leq 1 \\ \tilde{x}_1 \leq \tilde{x}_1 + \tilde{x}_2 \leq 1 \\ \tilde{x}_1 + \tilde{x}_2 \leq \tilde{x}_1 + \tilde{x}_2 + \tilde{x}_3 \leq \|\tilde{y}\|_1 \end{array} \right\}. \quad (28)$$

Notice that $\tilde{x}_i, \tilde{y}_i \geq 0$ for $i = 1, 2, 3$. As a consequence, we obtain the desired forking inequality chain for each of the two domains. For the first domain it reads

$$0 \leq \tilde{y}_1 \leq \tilde{y}_1 + \tilde{y}_2 \leq \tilde{y}_1 + \tilde{y}_2 + \tilde{y}_3 \leq \tilde{x}_1 + \tilde{x}_2 + \tilde{x}_3 \leq 1 \quad \text{and} \quad 0 \leq \tilde{x}_1 \leq \tilde{x}_1 + \tilde{x}_2 \leq \tilde{x}_1 + \tilde{x}_2 + \tilde{x}_3 \leq 1$$

and for the second domain

$$0 \leq \tilde{x}_1 \leq \tilde{x}_1 + \tilde{x}_2 \leq \tilde{x}_1 + \tilde{x}_2 + \tilde{x}_3 \leq \tilde{y}_1 + \tilde{y}_2 + \tilde{y}_3 \leq 1 \quad \text{and} \quad 0 \leq \tilde{y}_1 \leq \tilde{y}_1 + \tilde{y}_2 \leq \tilde{y}_1 + \tilde{y}_2 + \tilde{y}_3 \leq 1.$$

Similar to the introductory example, these inequality chains are used to introduce a set of new variables $\omega \in \mathbb{R}^6$ for each domain. By interchanging the order of integration we see for both domains:

3. Duffy transformation

- domain I:

$$\omega_1 := \tilde{x}_1 + \tilde{x}_2 + \tilde{x}_3, \omega_2 := \tilde{x}_1 + \tilde{x}_2, \omega_3 := \tilde{x}_1, \omega_4 := \tilde{y}_1 + \tilde{y}_2 + \tilde{y}_3, \omega_5 := \tilde{y}_1 + \tilde{y}_2, \omega_6 := \tilde{y}_1,$$

$$\int_0^1 \int_0^{\omega_1} \int_0^{\omega_2} \int_0^{\omega_1} \int_0^{\omega_4} \int_0^{\omega_5} \tilde{k}_1 \left(\begin{bmatrix} \omega_3 \\ \omega_2 - \omega_3 \\ \omega_1 - \omega_2 \end{bmatrix}, \begin{bmatrix} \omega_6 \\ \omega_5 - \omega_6 \\ \omega_4 - \omega_5 \end{bmatrix} \right) d\omega.$$

- domain II:

$$\omega_1 := \tilde{y}_1 + \tilde{y}_2 + \tilde{y}_3, \omega_2 := \tilde{y}_1 + \tilde{y}_2, \omega_3 := \tilde{y}_1, \omega_4 := \tilde{x}_1 + \tilde{x}_2 + \tilde{x}_3, \omega_5 := \tilde{x}_1 + \tilde{x}_2, \omega_6 := \tilde{x}_1,$$

$$\int_0^1 \int_0^{\omega_1} \int_0^{\omega_2} \int_0^{\omega_1} \int_0^{\omega_4} \int_0^{\omega_5} \tilde{k}_1 \left(\begin{bmatrix} \omega_6 \\ \omega_5 - \omega_6 \\ \omega_4 - \omega_5 \end{bmatrix}, \begin{bmatrix} \omega_3 \\ \omega_2 - \omega_3 \\ \omega_1 - \omega_2 \end{bmatrix} \right) d\omega.$$

Finally, each domain can be mapped onto the six-dimensional unit cube:

$$\xi := \omega_1, \eta_1 := \omega_2/\omega_1, \eta_2 := \omega_3/\omega_2, \eta_3 := \omega_4/\omega_1, \eta_4 := \omega_5/\omega_4, \eta_5 := \omega_6/\omega_5,$$

where again $\det \mathcal{J}(\xi, \eta) = \xi^5 \eta_1 \eta_3^2 \eta_4 = \xi^5 \det \mathcal{J}(\eta)$, denotes the Jacobi determinant of the nonlinear transformation. The transformation of the integration domain works analogously to (24). All in all this leads to

$$I_{t_1, t_2} = \int_{[0,1]^5} \int_{[0,1]^5} [\tilde{k}_1(\mathcal{D}_1(\xi, \eta)) + \tilde{k}_1(\mathcal{D}_2(\xi, \eta))] \det \mathcal{J}(\xi, \eta) d\eta d\xi,$$

where

$$\mathcal{D}_m(\xi, \eta) := (\mathcal{D}_m^1(\xi, \eta), \mathcal{D}_m^2(\xi, \eta)) = (\xi \mathcal{D}_m^1(\eta), \xi \mathcal{D}_m^2(\eta)) = \xi \mathcal{D}_m(\eta), \quad m = 1, 2, \quad (29)$$

with

$$\mathcal{D}_1(\eta) := \left(\begin{bmatrix} \eta_1 \eta_2 \\ \eta_1(1 - \eta_2) \\ (1 - \eta_1) \end{bmatrix}, \begin{bmatrix} \eta_3 \eta_4 \eta_5 \\ \eta_3 \eta_4(1 - \eta_5) \\ \eta_3(1 - \eta_4) \end{bmatrix} \right) \quad \text{and} \quad \mathcal{D}_2(\eta) := \left(\begin{bmatrix} \eta_3 \eta_4 \eta_5 \\ \eta_3 \eta_4(1 - \eta_5) \\ \eta_3(1 - \eta_4) \end{bmatrix}, \begin{bmatrix} \eta_1 \eta_2 \\ \eta_1(1 - \eta_2) \\ 1 - \eta_1 \end{bmatrix} \right)$$

is the Duffy transformation for the m -th sub-domain. To see that ξ can also be factored out of

$$\tilde{k}_1(\tilde{x}, \tilde{y}) = \frac{[\varphi_i(x) - \varphi_i(y)][\varphi_j(x) - \varphi_j(y)]}{|x - y|^{d+2s}} |M_{t_1}| |M_{t_2}|,$$

where $x = \chi_{t_1}(\tilde{x})$ and $y = \chi_{t_2}(\tilde{y})$, let us first investigate the denominator. Due to the choice of χ_{t_1} and χ_{t_2} ,

$$|x - y|^{-d-2s} = |\chi_{t_1}(\tilde{x}) - \chi_{t_2}(\tilde{y})|^{-d-2s} = \xi^{-d-2s} |M_{t_1} \mathcal{D}_m^1(\eta) - M_{t_2} \mathcal{D}_m^2(\eta)|^{-d-2s}, \quad m = 1, 2. \quad (30)$$

However, the examination of the product of the linear basis functions φ_i, φ_j is more complicated due to the interaction between the linear basis functions and the tetrahedra. Depending on the choice of the tetrahedra, terms in the product $[\varphi_i(x) - \varphi_i(y)][\varphi_j(x) - \varphi_j(y)]$ of the differences can vanish.

3. Duffy transformation

There exists three different cases: a term vanishes in both, in one, and in none of the factors. First, we consider the case that no term vanishes. This happens if and only if $t_1, t_2 \subset \text{supp } \varphi_i \cap \text{supp } \varphi_j$. In this case, we obtain

$$\varphi_\star(x) - \varphi_\star(y) = \alpha_{\star,1:3}^T (M_{t_1} \tilde{x} - M_{t_2} \tilde{y}) = \xi \alpha_{\star,1:3}^T (M_{t_1} \mathcal{D}_m^1(\eta) - M_{t_2} \mathcal{D}_m^2(\eta)) \quad (31)$$

for $m = 1, 2$ and for $\star = i, j$. This implies that ξ can be factored out of the difference. For the second case, we only have to investigate the factor which contains the vanishing term, because the other factor can be treated in the same way as (31). Without loss of generality, we assume that $t_2 \not\subset \text{supp } \varphi_i$ and $t_1, t_2 \subset \text{supp } \varphi_j$. Moreover, we know that $a_{t_1} = a_{t_2} \in t_2$, which implies that $\varphi_i(a_{t_1}) = 0$ and that

$$\varphi_i(x) = \varphi_i(\chi_{t_1}(\tilde{x})) = \alpha_{i,1:3}^T M_{t_1} \tilde{x} + \varphi_i(a_{t_1}) = \alpha_{i,1:3}^T M_{t_1} \tilde{x} = \xi \alpha_{i,1:3}^T M_{t_1} \mathcal{D}_m^1(\eta) \quad (32)$$

for $m = 1, 2$. The last case happens if and only if $\text{supp } \varphi_i \cap \text{supp } \varphi_j = a_{t_1}$. Then the ideas used in (32) can be applied twice.

By combining the results of (30), (31), and (32), it is shown that ξ can be factored out of \tilde{k}_1 ,

$$I_{t_1, t_2} = \frac{1}{5 - 2s} \int_{[0,1]^5} \tilde{k}_{1,V}(\eta) d\eta, \quad \tilde{k}_{1,V}(\eta) := [\tilde{k}_1(\mathcal{D}_1(\eta)) + \tilde{k}_1(\mathcal{D}_2(\eta))] \det \mathcal{J}(\eta). \quad (33)$$

Since the integral relative to ξ can be integrated analytically, only a five-dimensional integral has to be integrated numerically. The regularity of the remaining integrand will be proved in Lemma 8.

Since the number of regions increases with the degree of singularity, we introduce a new notation to exploit the symmetry of \mathcal{D}_m . Let \mathcal{D}_m be a transformation as mentioned above,

$$\mathcal{D}_m(\xi, \eta) = (\mathcal{D}_m^1(\xi, \eta), \mathcal{D}_m^2(\xi, \eta)) \quad \text{and} \quad \mathcal{D}_m(\eta) = (\mathcal{D}_m^1(\eta), \mathcal{D}_m^2(\eta)),$$

then we define \mathcal{D}_m^T as

$$\mathcal{D}_m^T(\xi, \eta) := (\mathcal{D}_m^2(\xi, \eta), \mathcal{D}_m^1(\xi, \eta)) \quad \text{and} \quad \mathcal{D}_m^T(\eta) := (\mathcal{D}_m^2(\eta), \mathcal{D}_m^1(\eta)).$$

3.2.2. Singularity along an edge

For the next case, we assume that the tetrahedra t_1 and t_2 have a common edge. Without loss of generality the mappings χ_{t_1} and χ_{t_2} are chosen in such a way that $a_{t_1} = a_{t_2}$ and $b_{t_1} = b_{t_2}$. This leads to $\chi_{t_1}(\kappa e_1) = \chi_{t_2}(\kappa e_1)$ for all $\kappa \in [0, 1]$. Therefore, \tilde{k}_1 is singular if and only if $\tilde{x}_1 = \tilde{y}_1$ and if the remaining variables are zero. We can exploit this to make the emerging inequalities more compact by first performing a linear transformation, $\hat{x}_1 := 1 - \tilde{x}_1$ and $\hat{y}_1 := 1 - \tilde{y}_1$, since the integrand is still singular if and only if $\hat{x}_1 = \hat{y}_1$. For the sake of simplicity we denote \hat{x}_1 and \hat{y}_1 again by \tilde{x}_1 and \tilde{y}_1 , respectively. This leads to

$$I_{t_1, t_2} = \int_0^1 \int_0^{\tilde{x}_1} \int_0^{\tilde{x}_1 - \tilde{x}_2} \int_0^1 \int_0^{\tilde{y}_1} \int_0^{\tilde{y}_1 - \tilde{y}_2} \tilde{k}_1 \left(\begin{bmatrix} 1 - \tilde{x}_1 \\ \tilde{x}_2 \\ \tilde{x}_3 \end{bmatrix}, \begin{bmatrix} 1 - \tilde{y}_1 \\ \tilde{y}_2 \\ \tilde{y}_3 \end{bmatrix} \right) d\tilde{y} d\tilde{x}. \quad (34)$$

3. Duffy transformation

Before introducing the local coordinates, we first split the integration domain and change the integration order in the second domain

$$\left\{ \begin{array}{l} 0 \leq \tilde{x}_1 \leq 1 \\ 0 \leq \tilde{x}_2 \leq \tilde{x}_1 \\ 0 \leq \tilde{x}_3 \leq \tilde{x}_1 - \tilde{x}_2 \\ 0 \leq \tilde{y}_1 \leq \tilde{x}_1 \\ 0 \leq \tilde{y}_2 \leq \tilde{y}_1 \\ 0 \leq \tilde{y}_3 \leq \tilde{y}_1 - \tilde{y}_2 \end{array} \right\} \cup \left\{ \begin{array}{l} 0 \leq \tilde{y}_1 \leq 1 \\ 0 \leq \tilde{y}_2 \leq \tilde{y}_1 \\ 0 \leq \tilde{y}_3 \leq \tilde{y}_1 - \tilde{y}_2 \\ 0 \leq \tilde{x}_1 \leq \tilde{y}_1 \\ 0 \leq \tilde{x}_2 \leq \tilde{x}_1 \\ 0 \leq \tilde{x}_3 \leq \tilde{x}_1 - \tilde{x}_2 \end{array} \right\}. \quad (35)$$

This is basically the same idea as in (28) only used on

$$0 \leq \tilde{x}_1 \leq 1 \quad \text{and} \quad 0 \leq \tilde{y}_1 \leq 1.$$

Next, we introduce local coordinates to describe the singularity along the edge as a five-dimensional point singularity. For the first domain choose $\tilde{z} \in \mathbb{R}^5$ as $\tilde{z}_1 := \tilde{y}_1 - \tilde{x}_1$, $\tilde{z}_i := \tilde{y}_i$, $\tilde{z}_{i+2} := \tilde{x}_i$, $i = 2, 3$, and for the second domain choose $\tilde{z} \in \mathbb{R}^5$ as $\tilde{z}_1 := \tilde{x}_1 - \tilde{y}_1$, $\tilde{z}_i := \tilde{x}_i$, $\tilde{z}_{i+2} := \tilde{y}_i$, $i = 2, 3$. Thus, (35) becomes

$$\left\{ \begin{array}{l} 0 \leq \tilde{x}_1 \leq 1 \\ 0 \leq \tilde{z}_4 \leq \tilde{x}_1 \\ 0 \leq \tilde{z}_5 \leq \tilde{x}_1 - \tilde{z}_4 \\ -\tilde{x}_1 \leq \tilde{z}_1 \leq 0 \\ 0 \leq \tilde{z}_2 \leq \tilde{x}_1 + \tilde{z}_1 \\ 0 \leq \tilde{z}_3 \leq \tilde{x}_1 + \tilde{z}_1 - \tilde{z}_2 \end{array} \right\} \cup \left\{ \begin{array}{l} 0 \leq \tilde{y}_1 \leq 1 \\ 0 \leq \tilde{z}_4 \leq \tilde{y}_1 \\ 0 \leq \tilde{z}_5 \leq \tilde{y}_1 - \tilde{z}_4 \\ -\tilde{y}_1 \leq \tilde{z}_1 \leq 0 \\ 0 \leq \tilde{z}_2 \leq \tilde{y}_1 + \tilde{z}_1 \\ 0 \leq \tilde{z}_3 \leq \tilde{y}_1 + \tilde{z}_1 - \tilde{z}_2 \end{array} \right\}. \quad (36)$$

The advantage of the early split up (35) is that after the introduction of the relative coordinates the singularity is already at the boundary of each domain. The next step is to introduce an ordered set of variables. The first sub-domain yields the following forking inequality chains

$$0 \leq -\tilde{z}_1 \leq -\tilde{z}_1 + \tilde{z}_2 \leq -\tilde{z}_1 + \tilde{z}_2 + \tilde{z}_3 \leq \tilde{x}_1 \leq 1 \quad \text{and} \quad 0 \leq \tilde{z}_4 \leq \tilde{z}_4 + \tilde{z}_5 \leq \tilde{x}_1 \leq 1.$$

The forking inequality chain splits after the first chain link \tilde{x}_1 . However, the set for which \tilde{k}_1 is singular is characterized by $\tilde{z} = 0$. Therefore, we have to divide the sub-domain again to push the splitting one link further. This is done by applying the same ideas as in (28) to obtain

$$-\tilde{z}_1 + \tilde{z}_2 \leq -\tilde{z}_1 + \tilde{z}_2 + \tilde{z}_3 \leq \tilde{z}_4 + \tilde{z}_5 \quad \text{and} \quad \tilde{z}_4 \leq \tilde{z}_4 + \tilde{z}_5 \leq -\tilde{z}_1 + \tilde{z}_2 + \tilde{z}_3.$$

Therefore, the first integration domain can be described by

$$\left\{ \begin{array}{l} 0 \leq \tilde{x}_1 \leq 1 \\ 0 \leq \tilde{z}_4 \leq \tilde{x}_1 \\ 0 \leq \tilde{z}_5 \leq \tilde{x}_1 - \tilde{z}_4 \\ -\tilde{x}_1 \leq \tilde{z}_1 \leq 0 \\ 0 \leq \tilde{z}_2 \leq \tilde{x}_1 + \tilde{z}_1 \\ 0 \leq \tilde{z}_3 \leq \tilde{z}_4 + \tilde{z}_5 + \tilde{z}_1 - \tilde{z}_2 \end{array} \right\} \cup \left\{ \begin{array}{l} 0 \leq \tilde{x}_1 \leq 1 \\ 0 \leq \tilde{z}_4 \leq \tilde{x}_1 \\ 0 \leq \tilde{z}_5 \leq -\tilde{z}_1 + \tilde{z}_2 + \tilde{z}_3 - \tilde{z}_4 \\ -\tilde{x}_1 \leq \tilde{z}_1 \leq 0 \\ 0 \leq \tilde{z}_2 \leq \tilde{x}_1 + \tilde{z}_1 \\ 0 \leq \tilde{z}_3 \leq \tilde{x}_1 + \tilde{z}_1 - \tilde{z}_2 \end{array} \right\}.$$

By introducing a new set of variables $\omega \in \mathbb{R}^6$ representing the forking inequality chains and by interchanging the order of integration, we obtain:

3. Duffy transformation

- domain I a):

$$\omega_1 := \tilde{x}_1, \omega_2 := \tilde{z}_4 + \tilde{z}_5, \omega_3 := \tilde{z}_4, \omega_4 := -\tilde{z}_1 + \tilde{z}_2 + \tilde{z}_3, \omega_5 := -\tilde{z}_1 + \tilde{z}_2, \omega_6 := -\tilde{z}_1,$$

$$\int_0^1 \int_0^{\omega_1} \int_0^{\omega_2} \int_0^{\omega_2} \int_0^{\omega_4} \int_0^{\omega_5} \tilde{k}_1 \left(\begin{bmatrix} 1 - \omega_1 \\ \omega_3 \\ \omega_2 - \omega_3 \end{bmatrix}, \begin{bmatrix} 1 - \omega_1 + \omega_6 \\ \omega_5 - \omega_6 \\ \omega_4 - \omega_5 \end{bmatrix} \right) d\omega$$

- domain I b):

$$\omega_1 := \tilde{x}_1, \omega_2 := -\tilde{z}_1 + \tilde{z}_2 + \tilde{z}_3, \omega_3 := -\tilde{z}_1 + \tilde{z}_2, \omega_4 := -\tilde{z}_1, \omega_5 := \tilde{z}_4 + \tilde{z}_5, \omega_6 := \tilde{z}_4,$$

$$\int_0^1 \int_0^{\omega_1} \int_0^{\omega_2} \int_0^{\omega_3} \int_0^{\omega_2} \int_0^{\omega_5} \tilde{k}_1 \left(\begin{bmatrix} 1 - \omega_1 \\ \omega_6 \\ \omega_5 - \omega_6 \end{bmatrix}, \begin{bmatrix} 1 - \omega_1 + \omega_4 \\ \omega_3 - \omega_4 \\ \omega_2 - \omega_3 \end{bmatrix} \right) d\omega$$

The domains are mapped onto the six-dimensional unit cube. The mapping and the computation of the Jacobian determinants are handled in the same way as in (24):

- domain I a):

$$\xi_1 := \omega_1, \xi_2 := \omega_2/\omega_1, \eta_1 := \omega_3/\omega_2, \eta_2 := \omega_4/\omega_2, \eta_3 := \omega_5/\omega_4, \eta_4 := \omega_6/\omega_5, \\ \det \mathcal{J}_1(\xi, \eta) = \xi_1^5 \xi_2^4 \eta_2^2 \eta_3 =: \det \mathcal{J}(\xi) \det \mathcal{J}_1(\eta)$$

$$\int_{[0,1]^2} \int_{[0,1]^4} \tilde{k}_1 \left(\begin{bmatrix} 1 - \xi_1 \\ \xi_1 \xi_2 \eta_1 \\ \xi_1 \xi_2 (1 - \eta_1) \end{bmatrix}, \begin{bmatrix} 1 - \xi_1 + \xi_1 \xi_2 \eta_2 \eta_3 \eta_4 \\ \xi_1 \xi_2 \eta_2 \eta_3 (1 - \eta_4) \\ \xi_1 \xi_2 \eta_2 (1 - \eta_3) \end{bmatrix} \right) \det \mathcal{J}_1(\xi, \eta) d\eta d\xi$$

- domain I b):

$$\xi_1 := \omega_1, \xi_2 := \omega_2/\omega_1, \eta_1 := \omega_3/\omega_2, \eta_2 := \omega_4/\omega_3, \eta_3 := \omega_5/\omega_2, \eta_4 := \omega_6/\omega_5, \\ \det \mathcal{J}_2(\xi, \eta) = \xi_1^5 \xi_2^4 \eta_1 \eta_3 =: \det \mathcal{J}(\xi) \det \mathcal{J}_2(\eta),$$

$$\int_{[0,1]^2} \int_{[0,1]^4} \tilde{k}_1 \left(\begin{bmatrix} 1 - \xi_1 \\ \xi_1 \xi_2 \eta_3 \eta_4 \\ \xi_1 \xi_2 \eta_3 (1 - \eta_4) \end{bmatrix}, \begin{bmatrix} 1 - \xi_1 + \xi_1 \xi_2 \eta_1 \eta_2 \\ \xi_1 \xi_2 \eta_1 (1 - \eta_2) \\ \xi_1 \xi_2 (1 - \eta_1) \end{bmatrix} \right) \det \mathcal{J}_2(\xi, \eta) d\eta d\xi$$

Using the symmetry between the two sub-domains in (36), the singular integral can be written as

$$I_{t_1, t_2} = \int_{[0,1]^6} \sum_{m=1}^4 \tilde{k}_1(\mathcal{D}_m(\xi, \eta)) \det \mathcal{J}_m(\xi, \eta) d\xi d\eta,$$

where \mathcal{D}_m are again the Duffy transformation of the m -th sub-domain and $\mathcal{D}_3 = \mathcal{D}_1^T$, $\mathcal{D}_4 = \mathcal{D}_2^T$ due to symmetry. If we take a closer look at the \mathcal{D}_m , one can notice these transformations have a structure which can be used to simplify the integrals

$$\begin{aligned} \mathcal{D}_m(\eta, \xi) &= (\mathcal{D}_m^1(\xi, \eta), \mathcal{D}_m^2(\xi, \eta)) = (\xi_1 e_1 + \xi_1 \xi_2 \mathcal{D}_m^1(\eta), \xi_1 e_1 + \xi_1 \xi_2 \mathcal{D}_m^1(\eta)) \\ &= \xi_1 (e_1, e_1) + \xi_1 \xi_2 \mathcal{D}_m(\eta), \end{aligned} \tag{37}$$

3. Duffy transformation

where

$$\mathcal{D}_1(\eta) = \left(\begin{bmatrix} 0 \\ \eta_1 \\ 1 - \eta_1 \end{bmatrix}, \begin{bmatrix} \eta_2 \eta_3 \eta_4 \\ \eta_2 \eta_3 (1 - \eta_4) \\ \eta_2 (1 - \eta_3) \end{bmatrix} \right) \quad \text{and} \quad \mathcal{D}_2(\eta) = \left(\begin{bmatrix} 0 \\ \eta_3 \eta_4 \\ \eta_3 (1 - \eta_4) \end{bmatrix}, \begin{bmatrix} \eta_1 \eta_2 \\ \eta_1 (1 - \eta_2) \\ 1 - \eta_1 \end{bmatrix} \right).$$

Notice that we can almost use the same arguments as in (33) to factor ξ_1 and ξ_2 out of \tilde{k}_1 . In detail, we get for the denominator

$$\begin{aligned} |x - y|^{-d-2s} &= |\chi_{t_1}(\tilde{x}) - \chi_{t_2}(\tilde{y})|^{-d-2s} \\ &= |\xi_1 \xi_2 [M_{t_1} \mathcal{D}_1^m(\eta) - M_{t_2} \mathcal{D}_2^m(\eta)] + \chi_{t_1}([1 - \xi_1] e_1) - \chi_{t_2}([1 - \xi_1] e_1)|^{-d-2s} \\ &= (\xi_1 \xi_2)^{-d-2s} |M_{t_1} \mathcal{D}_1^m(\eta) - M_{t_2} \mathcal{D}_2^m(\eta)|^{-d-2s} \end{aligned}$$

for $m = 1, \dots, 4$, since the remaining difference cancels out to due $\chi_{t_1}(\kappa e_1) = \chi_{t_2}(\kappa e_1)$ for all $\kappa \in [0, 1]$. For the numerator of the integrand, we have again to distinguish between the three cases: a term vanishes in both, in one, and in none of the factors. The last case is analogous to the treatment of the denominator

$$\varphi_i(x) - \varphi_i(y) = \alpha_{i,1:3}^T (M_{t_1} \tilde{x} - M_{t_2} \tilde{y}) = \xi_1 \xi_2 \alpha_{i,1:3}^T (M_{t_1} \mathcal{D}_1^m(\eta) - M_{t_2} \mathcal{D}_2^m(\eta))$$

for $m = 1, \dots, 4$. Without loss of generality one term vanishes if and only if $t_2 \not\subset \text{supp } \varphi_i$ and $t_1, t_2 \subset \text{supp } \varphi_j$,

$$\varphi_i(x) = \alpha_{i,1:3}^T M_{t_1} \tilde{x} + \varphi_i(a_{t_1}) = \xi_1 \xi_2 \alpha_{i,1:3}^T M_{t_1} \mathcal{D}_1^m(\eta) + \varphi_i(\chi_{t_1}([1 - \xi] e_1)) = \xi_1 \xi_2 \alpha_{i,1:3}^T M_{t_1} \mathcal{D}_1^m(\eta)$$

for $m = 1, \dots, 4$. The last step is due to $\chi_{t_1}([1 - \xi] e_1) \subset [a_{t_1}, b_{t_1}]$ and $\varphi_i|_{[a_{t_1}, b_{t_1}]} = 0$, since $t_2 \not\subset \text{supp } \varphi_i$. If in both factors a term vanishes that means without loss of generality that $t_2 \not\subset \text{supp } \varphi_i$ and $t_1 \not\subset \text{supp } \varphi_j$. Applying the ideas of the procedure presented in Section 3.2.1 it is obvious that $\xi_1 \xi_2$ can be factored out. Thus, we obtain

$$I_{t_1, t_2} = \frac{1}{5 - 2s} \frac{1}{4 - 2s} \int_{[0,1]^4} \tilde{k}_{1,E}(\eta) d\eta, \quad \tilde{k}_{1,E}(\eta) := \sum_{m=1}^4 \tilde{k}_1(\mathcal{D}_m(\eta)) \det \mathcal{J}_m(\eta). \quad (38)$$

As one can see, after the Duffy transformation only a four-dimensional integral has to be integrated numerically instead of a six-dimensional one. The regularity of the remaining integrand will be shown in Lemma 8.

3.2.3. Singularity on a face

Let t_1 and t_2 have a common face τ . Without loss of generality the mappings χ_{t_1} and χ_{t_2} are chosen in such a way that $a_{t_1} = a_{t_2}$, $b_{t_1} = b_{t_2}$ and $c_{t_1} = c_{t_2}$. This leads to

$$\chi_{t_1}(\kappa_1 e_1 + \kappa_2 e_2) = \chi_{t_2}(\kappa_1 e_1 + \kappa_2 e_2) \quad \text{for all } \kappa_1, \kappa_2 \in [0, 1].$$

3. Duffy transformation

Therefore, \tilde{k}_1 is singular if $\tilde{x}_i = \tilde{y}_i$ for $i = 1, 2$ and $\tilde{x}_3 = 0 = \tilde{y}_3$. First, we introduce local variables $\tilde{z} \in \mathbb{R}^4$ to describe the singularity as a four-dimensional point singularity, $\tilde{z}_i := \tilde{y}_i - \tilde{x}_i$, $i = 1, 2$, $\tilde{z}_3 := \tilde{y}_3$ and $\tilde{z}_4 := \tilde{x}_3$. Hence, we obtain by starting with (34)

$$I_{t_1, t_2} = \int_0^1 \int_0^{\tilde{x}_1} \int_{-\tilde{x}_1}^{1-\tilde{x}_1} \int_{-\tilde{x}_2}^{\tilde{z}_1+\tilde{x}_1-\tilde{x}_2} \int_0^{\tilde{z}_1-\tilde{z}_2+\tilde{x}_1-\tilde{x}_2} \int_0^{\tilde{x}_1-\tilde{x}_2} \tilde{k}_1 \left(\begin{bmatrix} 1 - \tilde{x}_1 \\ \tilde{x}_2 \\ \tilde{z}_4 \end{bmatrix}, \begin{bmatrix} 1 - \tilde{z}_1 - \tilde{x}_1 \\ \tilde{z}_2 + \tilde{x}_2 \\ \tilde{z}_3 \end{bmatrix} \right) d\tilde{z} d\tilde{x}_{1:2}.$$

Since we want to apply the ideas from the introductory example in Section 3.1, the singularity has to be shifted to the boundary of the integration domain by splitting it up. To simplify this procedure, the order of integration relative to $\tilde{x}_{1:2}$ and \tilde{z} is reversed, which results in

$$\left\{ \begin{array}{l} -1 \leq \tilde{z}_1 \leq 1 \\ \max\{-1, -1 + \tilde{z}_1\} \leq \tilde{z}_2 \leq \min\{1, 1 + \tilde{z}_1\} \\ 0 \leq \tilde{z}_3 \leq \min\{1, 1 + \tilde{z}_1\} + \min\{0, -\tilde{z}_2\} \\ \max\{0, -\tilde{z}_2, -\tilde{z}_1 + \tilde{z}_3, \tilde{z}_2 - \tilde{z}_1 + \tilde{z}_3\} \leq \tilde{x}_1 \leq \min\{1, 1 - \tilde{z}_1\} \\ \max\{0, -\tilde{z}_2\} \leq \tilde{x}_2 \leq \tilde{x}_1 + \min\{0, \tilde{z}_1 - \tilde{z}_2 - \tilde{z}_3\} \\ 0 \leq \tilde{z}_4 \leq \tilde{x}_1 - \tilde{x}_2 \end{array} \right\}. \quad (39)$$

The following procedure is similar to the two singularity cases before. The domain is subdivided to push the point singularity to the boundary. In total, we split the set into nine sub-domains to resolve the min and max constraints. Furthermore, eight of these domains have to be refined again to satisfy a suitable forking inequality chain in the same way as in Section 3.2.2. Here, only the final result after the nonlinear transformation to the six-dimensional unit cube is presented. For a detailed consideration we refer to Appendix A.1.1. In the same sense as in (29) and (37) the nonlinear transformations \mathcal{D}_m for the domains share a common structure which will be used to simplify them:

$$\begin{aligned} \mathcal{D}_m(\xi, \eta) &= (\xi_1 e_1 + \xi_1[1 - \xi_2] e_2 + \xi_1 \xi_2 \xi_3 \mathcal{D}_m^1(\eta), \xi_1 e_1 + \xi_1[1 - \xi_2] e_2 + \xi_1 \xi_2 \xi_3 \mathcal{D}_m^2(\eta)) \\ &= \xi_1 (e_1, e_1) + \xi_1[1 - \xi_2] (e_2, e_2) + \xi_1 \xi_2 \xi_3 \mathcal{D}_m(\eta) \end{aligned} \quad (40)$$

with

$$\begin{aligned} \mathcal{D}_1(\eta) &= \left(\begin{bmatrix} 0 \\ \eta_1 \\ 1 - \eta_1 \end{bmatrix}, \begin{bmatrix} \eta_1 \eta_2 \eta_3 \\ 0 \\ \eta_1 \eta_2 (1 - \eta_3) \end{bmatrix} \right), & \mathcal{D}_2(\eta) &= \left(\begin{bmatrix} 0 \\ \eta_1 \eta_2 \\ \eta_1 (1 - \eta_2) \end{bmatrix}, \begin{bmatrix} -\eta_1 \eta_2 \eta_3 \\ 0 \\ 1 - \eta_1 \eta_2 \eta_3 \end{bmatrix} \right), \\ \mathcal{D}_3(\eta) &= \left(\begin{bmatrix} 0 \\ \eta_1 \eta_2 \\ 1 - \eta_1 \eta_2 \end{bmatrix}, \begin{bmatrix} \eta_1 \eta_2 \eta_3 \\ 0 \\ \eta_1 (1 - \eta_2 \eta_3) \end{bmatrix} \right), & \mathcal{D}_4(\eta) &= \left(\begin{bmatrix} 0 \\ \eta_1 \eta_2 \eta_3 \\ \eta_1 \eta_2 (1 - \eta_3) \end{bmatrix}, \begin{bmatrix} \eta_1 \\ 0 \\ 1 - \eta_1 \end{bmatrix} \right), \\ \mathcal{D}_5(\eta) &= \left(\begin{bmatrix} 0 \\ \eta_1 \eta_2 \eta_3 \\ \eta_1 (1 - \eta_2 \eta_3) \end{bmatrix}, \begin{bmatrix} \eta_1 \eta_2 \\ 0 \\ 1 - \eta_1 \eta_2 \end{bmatrix} \right), & \mathcal{D}_6(\eta) &= \left(\begin{bmatrix} 0 \\ \eta_1 \eta_2 \eta_3 \\ 1 - \eta_1 \eta_2 \eta_3 \end{bmatrix}, \begin{bmatrix} \eta_1 \eta_2 \\ 0 \\ \eta_1 (1 - \eta_2) \end{bmatrix} \right), \\ \mathcal{D}_7(\eta) &= \left(\begin{bmatrix} 0 \\ 0 \\ 1 \end{bmatrix}, \begin{bmatrix} \eta_1 \eta_2 \eta_3 \\ \eta_1 \eta_2 (1 - \eta_3) \\ \eta_1 (1 - \eta_2) \end{bmatrix} \right), & \mathcal{D}_{15}(\eta) &= \left(\begin{bmatrix} \eta_1 \eta_2 \eta_3 \\ \eta_1 \eta_2 (1 - \eta_3) \\ 1 - \eta_1 \eta_2 \end{bmatrix}, \begin{bmatrix} 0 \\ 0 \\ \eta_1 \end{bmatrix} \right), \end{aligned}$$

3. Duffy transformation

where we set $\xi_1 := \omega_1$, $\xi_2 := \omega_2/\omega_1$, $\xi_3 := \omega_3/\omega_2$, $\eta_1 := \omega_4/\omega_3$, $\eta_2 := \omega_5/\omega_4$ and $\eta_3 := \omega_6/\omega_5$. The transformations \mathcal{D}_8 to \mathcal{D}_{14} are the symmetric versions of \mathcal{D}_1 to \mathcal{D}_7 , i.e. $\mathcal{D}_{7+i}(\eta) = \mathcal{D}_i^T(\eta)$ for $i = 1, \dots, 7$. The remaining two are described by

$$\mathcal{D}_{16}(\eta) = \left(\begin{bmatrix} 0 \\ 0 \\ \eta_3 \end{bmatrix}, \begin{bmatrix} -\eta_1\eta_2 \\ \eta_1(1-\eta_2) \\ 1-\eta_1 \end{bmatrix} \right) \quad \text{and} \quad \mathcal{D}_{17}(\eta) = \left(\begin{bmatrix} -\eta_1\eta_2 \\ \eta_1(1-\eta_2) \\ 1-\eta_1 \end{bmatrix}, \begin{bmatrix} 0 \\ 0 \\ \eta_1\eta_3 \end{bmatrix} \right).$$

For these cases the transformation relative to η has to be partially adjusted, i.e. $\eta_3 := \omega_6/\omega_3$ for $m = 16$, and $\eta_2 := \omega_6/\omega_4$ and $\eta_3 := \omega_6/\omega_4$ for $m = 17$. For the corresponding Jacobi determinants, it holds that $\det \mathcal{J}_m(\xi, \eta) = \det \mathcal{J}(\xi) \det \mathcal{J}_m(\eta)$ for $m = 1, \dots, 17$, where $\det \mathcal{J}(\xi) = \xi_1^5 \xi_2^4 \xi_3^3$ and $\det \mathcal{J}_m(\eta) = \eta_1^2 \eta_2$, $m = 1, \dots, 15$. The remaining two cases are $\det \mathcal{J}_{16}(\eta) = \eta_1$ and $\det \mathcal{J}_{17}(\eta) = \eta_1^2$. All in all, the Duffy transformation can now be applied:

$$I_{t_1, t_2} = \prod_{j=0}^2 \frac{1}{5-j-2s} \int_{[0,1]^3} \tilde{k}_{1,F}(\eta) d\eta, \quad \tilde{k}_{1,F}(\eta) := \sum_{m=1}^{17} \tilde{k}_1(\mathcal{D}_m(\eta)) \det \mathcal{J}_m(\eta). \quad (41)$$

Again, we used the linearity of the basis functions and the transformation between the reference tetrahedron and the original tetrahedron to simplify the Duffy transformation. Since the procedure is completely analogous to the case of the singularity along an edge, we omit the details. The only difference is to consider that in the case of a single vanishing term, it holds that $\chi_{t_1}(\kappa_1 e_1 + \kappa_2 e_2) \in \tau$ and $\varphi_i|_\tau = 0$. As one can see, after the Duffy transformation only a three-dimensional integral has to be integrated numerically instead of a six-dimensional one. The regularity of the remaining integrand will be shown in Lemma 8.

3.2.4. Two identical tetrahedra

We now deal with the strongest singularity, i.e. the two tetrahedra coincide. Since t_1 equals t_2 , we drop the index and \tilde{k}_1 is singular if and only if $\tilde{x} = \tilde{y}$. Starting from (34) we introduce local variables $\tilde{z} \in \mathbb{R}^3$, $\tilde{z} := \tilde{y} - \tilde{x}$ to describe the singularity as a three dimensional point singularity, which leads to

$$I_{t,t} = \int_0^1 \int_0^{\tilde{x}_1} \int_0^{\tilde{x}_1 - \tilde{x}_2} \int_{-\tilde{x}_1}^{1-\tilde{x}_1} \int_{-\tilde{x}_2}^{\tilde{z}_1 + \tilde{x}_1 - \tilde{x}_2} \int_{-\tilde{x}_3}^{\tilde{z}_1 - \tilde{z}_2 + \tilde{x}_1 - \tilde{x}_2 - \tilde{x}_3} \tilde{k}_1 \left(\begin{bmatrix} 1 - \tilde{x}_1 \\ \tilde{x}_2 \\ \tilde{x}_3 \end{bmatrix}, \begin{bmatrix} 1 - \tilde{z}_1 - \tilde{x}_1 \\ \tilde{z}_2 + \tilde{x}_2 \\ \tilde{z}_3 + \tilde{x}_3 \end{bmatrix} \right) d\tilde{z} d\tilde{x}.$$

Then the point singularity is moved to the boundary by swapping the integration order and splitting up the integration domain:

$$\left\{ \begin{array}{l} -1 \leq \tilde{z}_1 \leq 1 \\ -1 + \max\{0, \tilde{z}_1\} \leq \tilde{z}_2 \leq 1 + \min\{0, \tilde{z}_1\} \\ -1 + \max\{0, \tilde{z}_1\} + \max\{0, -\tilde{z}_2\} \leq \tilde{z}_3 \leq 1 + \min\{0, \tilde{z}_1\} + \min\{0, -\tilde{z}_2\} \\ \max\{0, -\tilde{z}_1, -\tilde{z}_2, -\tilde{z}_3, \\ -\tilde{z}_2 - \tilde{z}_3, \tilde{z}_2 - \tilde{z}_1, -\tilde{z}_1 + \tilde{z}_3, \tilde{z}_2 - \tilde{z}_1 + \tilde{z}_3\} \leq \tilde{x}_1 \leq 1 + \min\{0, -\tilde{z}_1\} \\ \max\{0, -\tilde{z}_2\} \leq \tilde{x}_2 \leq \tilde{x}_1 + \min\{0, \tilde{z}_1 - \tilde{z}_2, \tilde{z}_1 - \tilde{z}_2 - \tilde{z}_3\} \\ \max\{0, -\tilde{z}_3\} \leq \tilde{x}_3 \leq \tilde{x}_1 - \tilde{x}_2 + \min\{0, \tilde{z}_1 - \tilde{z}_2 - \tilde{z}_3\} \end{array} \right\}.$$

3. Duffy transformation

The split is necessary to make it easier to describe the domain. The detailed preparation of the set can be found in the Appendix A.1.2. All in all, we obtain 18 integration domains each of which satisfies a forking inequality chain. This ultimately leads to

$$\begin{aligned} I_{t,t} &= \int_{[0,1]^4} \int_{[0,1]^2} \sum_{m=1}^{18} \tilde{k}_1(\mathcal{D}_m(\xi, \eta)) \det \mathcal{J}_m(\xi, \eta) d\eta d\xi \\ &= 2 \prod_{l=0}^3 \frac{1}{5-l-2s} \int_{[0,1]^2} \tilde{k}_{1,T}(\eta) d\eta, \quad \tilde{k}_{1,T}(\eta) := \sum_{m=1}^9 \tilde{k}_1(\mathcal{D}_m(\eta)) \det \mathcal{J}_m(\eta), \end{aligned} \quad (42)$$

with $\mathcal{D}_m(\xi, \eta) = \xi_1 \xi_2 \xi_3 \xi_4 \mathcal{D}_m(\eta)$ for $m = 1 \dots, 18$, where

$$\begin{aligned} \mathcal{D}_1(\eta) &= \left(\begin{bmatrix} 0 \\ \eta_1 \\ \eta_1 \end{bmatrix}, \begin{bmatrix} \eta_1 \eta_2 \\ 0 \\ 1 \end{bmatrix} \right), & \mathcal{D}_2(\eta) &= \left(\begin{bmatrix} 0 \\ 1 \\ 0 \end{bmatrix}, \begin{bmatrix} \eta_1 \eta_2 \\ 0 \\ \eta_1(1-\eta_2) \end{bmatrix} \right), & \mathcal{D}_3(\eta) &= \left(\begin{bmatrix} 0 \\ \eta_1 \\ -1 \end{bmatrix}, \begin{bmatrix} \eta_1 \eta_2 \\ 0 \\ -\eta_1 \eta_2 \end{bmatrix} \right), \\ \mathcal{D}_4(\eta) &= \left(\begin{bmatrix} 0 \\ \eta_1 \eta_2 \\ -\eta_1 \eta_2 \end{bmatrix}, \begin{bmatrix} \eta_1 \\ 0 \\ -1 \end{bmatrix} \right), & \mathcal{D}_5(\eta) &= \left(\begin{bmatrix} 0 \\ \eta_1 \eta_2 \\ \eta_1(1-\eta_2) \end{bmatrix}, \begin{bmatrix} 1 \\ 0 \\ 0 \end{bmatrix} \right), & \mathcal{D}_6(\eta) &= \left(\begin{bmatrix} 0 \\ \eta_1 \eta_2 \\ -1 \end{bmatrix}, \begin{bmatrix} \eta_1 \\ 0 \\ -\eta_1 \end{bmatrix} \right), \\ \mathcal{D}_7(\eta) &= \left(\begin{bmatrix} 0 \\ 0 \\ 0 \end{bmatrix}, \begin{bmatrix} \eta_1 \eta_2 \\ \eta_1(1-\eta_2) \\ -1 \end{bmatrix} \right), & \mathcal{D}_8(\eta) &= \left(\begin{bmatrix} 0 \\ 0 \\ -1 \end{bmatrix}, \begin{bmatrix} \eta_1 \eta_2 \\ \eta_1(1-\eta_2) \\ -\eta_1 \end{bmatrix} \right), & \mathcal{D}_9(\eta) &= \left(\begin{bmatrix} 0 \\ 0 \\ \eta_1 \end{bmatrix}, \begin{bmatrix} \eta_2 \\ 1-\eta_2 \\ 0 \end{bmatrix} \right). \end{aligned}$$

For $m = 1, \dots, 8$, we set $\xi_1 := \omega_1$, $\xi_2 := \omega_2/\omega_1$, $\xi_3 := \omega_3/\omega_2$, $\xi_4 := \omega_4/\omega_3$, $\eta_1 := \omega_5/\omega_4$, and $\eta_2 := \omega_6/\omega_5$. The last domain needs an adapted scheme for η , i.e. $\eta_2 := \omega_6/\omega_4$. The Jacobi determinants result in $\det \mathcal{J}_m(\eta) = \eta_1$ for $m = 1, \dots, 8$, and $\det \mathcal{J}_9(\eta) = 1$. The factor 2 in (42) is due to the symmetry. Since $\mathcal{D}_{m+9}(\eta) = \mathcal{D}_m(\eta)^T$ for $m = 1, \dots, 9$ and since t_1 equals t_2 , the corresponding mappings are identical, too. Moreover, the differences of the linear basis functions do not vanish. Therefore, the simplifications of the \mathcal{D}_m and the first step in (42) are easily seen. As one can see, after the Duffy transformation only a two-dimensional integral has to be integrated numerically instead of a six-dimensional one. The regularity of the remaining integrand will be shown in Lemma 8.

3.3. Interaction between a tetrahedron and a panel

The procedure here is similar to the procedure in Section 3.2. The main difference is that the interaction between a tetrahedron t and a panel τ has to be studied. There are three different singularity cases: a common point, a common edge, and the panel τ is a face of the tetrahedron t . Again, to describe the resulting singularity types, t and τ will be mapped to the corresponding reference element. For the panel this the unit panel $\tilde{\tau}$,

$$\tilde{\tau} := \{\tilde{y} \in \mathbb{R}^2 : 0 \leq \tilde{y}_2 \leq 1 - \tilde{y}_1, \quad 0 \leq \tilde{y}_1 \leq 1\}.$$

The transformation will be done by the mapping $\chi_\tau : \tilde{\tau} \rightarrow \tau$,

$$\chi_\tau(\tilde{y}) = M_\tau \tilde{y} + a_\tau, \quad (43)$$

3. Duffy transformation

where $M_\tau := [b_\tau - a_\tau, c_\tau - a_\tau] \in \mathbb{R}^{3 \times 2}$ and a_τ, b_τ and c_τ denote the corners of the panel τ . Then we get for equation (23)

$$I_{t,\tau} = \int_{\tilde{t}} \int_{\tilde{\tau}} k_2(\chi_t(\tilde{x}), \chi_\tau(\tilde{y})) |M_t| |M_\tau| d\tilde{y} d\tilde{x} =: \int_{\tilde{t}} \int_{\tilde{\tau}} \tilde{k}_2(\tilde{x}, \tilde{y}) d\tilde{y} d\tilde{x}, \quad (44)$$

where $|M_t| := |\det M_t|$ and $|M_\tau| := |(b_\tau - a_\tau) \times (c_\tau - a_\tau)|$. Moreover, the canonical unit vectors of \mathbb{R}^2 are denoted by \hat{e}_1 and \hat{e}_2 .

3.3.1. Point singularity

We start with the simplest case that the tetrahedron and the panel have a common vertex. Without loss of generality the linear mappings χ_t and χ_τ are chosen in such a way that $a_t = a_\tau$. Since the procedure is analogous to the procedure in Section 3.2.1, only the result of the Duffy transformation is presented. The remaining procedure is shown in Appendix A.2.1. We obtain two sub-domains and for the integrals this implies that

$$I_{t,\tau} = \int_{[0,1]} \int_{[0,1]^4} \sum_{m=1}^2 \tilde{k}_2(\mathcal{D}_m(\xi, \eta)) \det \mathcal{J}_m(\xi, \eta) d\eta d\xi,$$

where again $\mathcal{D}_m(\xi, \eta) = \xi (\mathcal{D}_m^1(\eta), \mathcal{D}_m^2(\eta)) = \xi \mathcal{D}_m(\eta)$, $m = 1, 2$, is the Duffy transformation for the m -th sub-domain with

$$\mathcal{D}_1(\eta) = \left(\begin{bmatrix} 1 \\ \eta_1 \eta_2 \\ \eta_1(1 - \eta_2) \end{bmatrix}, \begin{bmatrix} \eta_3 \\ \eta_3 \eta_4 \end{bmatrix} \right) \quad \text{and} \quad \mathcal{D}_2(\eta) = \left(\begin{bmatrix} \eta_2 \\ \eta_2 \eta_3 \eta_4 \\ \eta_2 \eta_3 (1 - \eta_4) \end{bmatrix}, \begin{bmatrix} 1 \\ \eta_1 \end{bmatrix} \right),$$

and where $\xi := \omega_1$, $\eta_1 := \omega_2/\omega_1$, $\eta_2 := \omega_3/\omega_2$, $\eta_3 := \omega_4/\omega_1$, and $\eta_4 := \omega_5/\omega_4$ for $m = 1$, and where $\xi := \omega_1$, $\eta_1 := \omega_2/\omega_1$, $\eta_2 := \omega_3/\omega_1$, $\eta_3 := \omega_4/\omega_3$, and $\eta_4 := \omega_5/\omega_4$ for $m = 2$. The Jacobi determinants results in $\det \mathcal{J}_m(\xi, \eta) = \xi^4 \det \mathcal{J}_m(\eta)$ with $\det \mathcal{J}_1(\eta) = \eta_1 \eta_3$ and $\det \mathcal{J}_2(\eta) = \eta_2^2 \eta_3$. This can be seen similar to (29). In contrast to Section 3.2, we now have to consider a different integrand \tilde{k}_2 . It is actually easier to study \tilde{k}_2 because we do not have to distinguish several cases. First, consider the difference of the integration variables

$$x - y = \chi_t(\tilde{x}) - \chi_\tau(\tilde{y}) = M_t \tilde{x} - M_\tau \tilde{y} = \xi (M_t \mathcal{D}_m^1(\eta) - M_\tau \mathcal{D}_m^2(\eta)).$$

For the inner integrand of (44) this means

$$\frac{(x - y)^T n_\tau}{|x - y|^{3+2s}} = \xi^{-2-2s} \frac{(M_t \mathcal{D}_m^1(\eta) - M_\tau \mathcal{D}_m^2(\eta))^T n_\tau}{|M_t \mathcal{D}_m^1(\eta) - M_\tau \mathcal{D}_m^2(\eta)|^{3+2s}}, \quad m = 1, 2.$$

The second part is analogous to the approach in Section 3.2. Since $\tau \subset \partial(\text{supp } \varphi_i \cup \text{supp } \varphi_j)$, it follows without loss of generality that $\varphi_i(a_t) = 0$ and

$$\varphi_i(x) = \alpha_{i,1:3}^T M_t \tilde{x} + \alpha_{i,4} a_t = \alpha_{i,1:3}^T M_t \mathcal{D}_m^2(\xi, \eta) + \varphi_i(a_t) = \xi \alpha_{i,1:3}^T M_t \mathcal{D}_m^2(\eta), \quad m = 1, 2.$$

3. Duffy transformation

By combining these results, we have shown that ξ can be factored out of \tilde{k}_2 :

$$I_{t,\tau} = \frac{1}{4-2s} \int_{[0,1]^4} \tilde{k}_{2,V}(\eta) d\eta, \quad \tilde{k}_{2,V}(\eta) := \sum_{m=1}^2 \tilde{k}_2(\mathcal{D}_m(\eta)) \det \mathcal{J}_m(\eta). \quad (45)$$

Since the integral w.r.t. ξ can be integrated analytically, only a four-dimensional integral has to be integrated numerically. The regularity of the remaining integrand will be proved in Lemma 9.

3.3.2. Singularity along an edge

We consider the case that t and τ share a common edge. Adapting the approach of Section 3.2.2, we obtain four sub-domains:

$$I_{t,\tau} = \int_{[0,1]^5} \sum_{m=1}^4 \tilde{k}_2(\mathcal{D}_m(\xi, \eta)) \det \mathcal{J}_m(\xi, \eta) d\xi d\eta$$

with \mathcal{D}_m being the Duffy-transformations on the corresponding domains and $\det \mathcal{J}_m$ denoting the Jacobi determinant of the m -th sub-domain, $\det \mathcal{J}_m(\xi, \eta) = \xi_1^4 \xi_2^3 \eta_2 =: \det \mathcal{J}(\xi) \det \mathcal{J}_m(\eta)$, $m = 1, 2, 3$, and $\det \mathcal{J}_4(\xi, \eta) = \xi_1^4 \xi_2^3 \eta_1^2 \eta_2 =: \det \mathcal{J}(\xi) \det \mathcal{J}_4(\eta)$. A more detailed approach is presented in Appendix A.2.2. Using the same idea as in (37), we obtain

$$\mathcal{D}_m(\eta, \xi) = (\mathcal{D}_m^1(\xi, \eta), \mathcal{D}_m^2(\xi, \eta)) = (\xi_1 e_1 + \xi_1 \xi_2 \mathcal{D}_m^1(\eta), \xi_1 \hat{e}_1 + \xi_1 \xi_2 \mathcal{D}_m^1(\eta)) =: \xi_1 (e_1, \hat{e}_1) + \xi_1 \xi_2 \mathcal{D}_m(\eta)$$

with

$$\begin{aligned} \mathcal{D}_1(\eta) &= \left(\begin{bmatrix} 0 \\ \eta_1 \\ 1 - \eta_1 \end{bmatrix}, \begin{bmatrix} \eta_2 \eta_3 \\ \eta_2 (1 - \eta_3) \end{bmatrix} \right), & \mathcal{D}_2(\eta) &= \left(\begin{bmatrix} 0 \\ \eta_2 \eta_3 \\ \eta_2 (1 - \eta_3) \end{bmatrix}, \begin{bmatrix} \eta_1 \\ 1 - \eta_1 \end{bmatrix} \right), \\ \mathcal{D}_3(\eta) &= \left(\begin{bmatrix} \eta_2 \eta_3 \\ \eta_2 (1 - \eta_3) \\ 1 - \eta_2 \end{bmatrix}, \begin{bmatrix} 0 \\ \eta_1 \end{bmatrix} \right), & \mathcal{D}_4(\eta) &= \left(\begin{bmatrix} \eta_1 \eta_2 \eta_3 \\ \eta_1 \eta_2 (1 - \eta_3) \\ \eta_1 (1 - \eta_2) \end{bmatrix}, \begin{bmatrix} 0 \\ 1 \end{bmatrix} \right), \end{aligned}$$

where $\xi_1 := \omega_1$, $\xi_2 := \omega_2/\omega_1$, $\eta_1 := \omega_3/\omega_2$, $\eta_2 := \omega_4/\omega_2$, and $\eta_3 := \omega_5/\omega_4$ for $m = 1, 2, 3$. For the last domain only η_2 has to be adjusted to $\eta_2 := \omega_4/\omega_3$. Applying the tricks presented in the previous sections, ξ_1 and ξ_2 can be factored out of \tilde{k}_2 . This results in

$$I_{t,\tau} = \frac{1}{5-2s} \frac{1}{4-2s} \int_{[0,1]^3} \tilde{k}_{2,E}(\eta) d\eta, \quad \tilde{k}_{2,E}(\eta) := \sum_{m=1}^4 \tilde{k}_2(\mathcal{D}_m(\eta)) \det \mathcal{J}_m(\eta). \quad (46)$$

Hence, only a three-dimensional integral has to be integrated numerically. The regularity of the remaining integrand will be proved in Lemma 9.

3.3.3. Singularity on a face

The last case to consider is that the panel is a face of the tetrahedron. Without loss of generality we assume that $a_t = a_\tau$, $b_t = b_\tau$, and $c_t = c_\tau$. This means that $\chi_t(\kappa_1 e_1 + \kappa_2 e_2) = \chi_\tau(\kappa_1 \hat{e}_1 + \kappa_2 \hat{e}_2)$

3. Duffy transformation

for all $\kappa_1, \kappa_2 \in [0, 1]^2$. Again, we outsource the preparation for the nonlinear transformation to Appendix A.2.3. In order to lift the singularity we obtain nine domains:

$$I_{t,\tau} = \int_{[0,1]^5} \sum_{m=1}^9 \tilde{k}_2(\mathcal{D}_m(\xi, \eta)) \det \mathcal{J}_m(\xi, \eta) d\eta d\xi,$$

where we can apply the idea from (40) to

$$\begin{aligned} \mathcal{D}_m(\xi, \eta) &= (\xi_1 e_1 + \xi_1(1 - \xi_2) e_2 + \xi_1 \xi_2 \xi_3 \mathcal{D}_m^1(\eta), \xi_1 \hat{e}_1 + \xi_1(1 - \xi_2) \hat{e}_2 + \xi_1 \xi_2 \xi_3 \mathcal{D}_m^2(\eta)) \\ &= \xi_1 (e_1, \hat{e}_1) + \xi_1(1 - \xi_2) (e_2, \hat{e}_2) + \xi_1 \xi_2 \xi_3 \mathcal{D}_m(\eta) \end{aligned}$$

with

$$\begin{aligned} \mathcal{D}_1(\eta) &= \left(\begin{bmatrix} 0 \\ \eta_1 \\ 1 - \eta_1 \end{bmatrix}, \begin{bmatrix} \eta_1 \eta_2 \\ 0 \end{bmatrix} \right), \quad \mathcal{D}_2(\eta) = \left(\begin{bmatrix} 0 \\ \eta_1 \eta_2 \\ \eta_1(1 - \eta_2) \end{bmatrix}, \begin{bmatrix} 1 \\ 0 \end{bmatrix} \right), \quad \mathcal{D}_3(\eta) = \left(\begin{bmatrix} 0 \\ \eta_1 \eta_2 \\ 1 - \eta_1 \eta_2 \end{bmatrix}, \begin{bmatrix} \eta_1 \\ 0 \end{bmatrix} \right), \\ \mathcal{D}_4(\eta) &= \left(\begin{bmatrix} 0 \\ 0 \\ 1 \end{bmatrix}, \begin{bmatrix} \eta_1 \eta_2 \\ \eta_1(1 - \eta_2) \end{bmatrix} \right), \quad \mathcal{D}_5(\eta) = \left(\begin{bmatrix} \eta_1 \eta_2 \\ \eta_1(1 - \eta_2) \\ 1 - \eta_1 \end{bmatrix}, \begin{bmatrix} 0 \\ 0 \end{bmatrix} \right), \quad \mathcal{D}_6(\eta) = \left(\begin{bmatrix} \eta_1 \\ 0 \\ 1 - \eta_1 \end{bmatrix}, \begin{bmatrix} 0 \\ \eta_1 \eta_2 \end{bmatrix} \right), \\ \mathcal{D}_7(\eta) &= \left(\begin{bmatrix} \eta_1 \eta_2 \\ 0 \\ \eta_1(1 - \eta_2) \end{bmatrix}, \begin{bmatrix} 0 \\ 1 \end{bmatrix} \right), \quad \mathcal{D}_8(\eta) = \left(\begin{bmatrix} \eta_1 \eta_2 \\ 0 \\ 1 - \eta_1 \eta_2 \end{bmatrix}, \begin{bmatrix} 0 \\ \eta_1 \end{bmatrix} \right), \quad \mathcal{D}_9(\eta) = \left(\begin{bmatrix} 0 \\ 0 \\ \eta_2 \end{bmatrix}, \begin{bmatrix} -\eta_1 \\ 1 - \eta_1 \end{bmatrix} \right), \end{aligned}$$

where $\xi_1 := \omega_1$, $\xi_2 := \omega_2/\omega_1$, $\xi_3 := \omega_3/\omega_2$, $\eta_1 := \omega_4/\omega_3$, and $\eta_2 := \omega_5/\omega_4$ for $m = 1, \dots, 8$. For the ninth domain only η_2 has to be adjusted to $\eta_2 := \omega_5/\omega_3$. Hence, the Jacobi determinants result in $\det \mathcal{J}_m(\xi, \eta) = \xi_1^4 \xi_2^3 \xi_3^2 \det \mathcal{J}_m(\eta)$, where $\det \mathcal{J}_m(\eta) = \eta_1$ for $m = 1, \dots, 8$ and $\det \mathcal{J}_9(\eta) = 1$. The integral can be simplified similarly to the case described in Section 3.2.3. This results in

$$I_{t,\tau} = \prod_{j=0}^2 \frac{1}{5 - j - 2s} \int_{[0,1]^2} \tilde{k}_{2,F}(\eta) d\eta, \quad \tilde{k}_{2,F}(\eta) := \sum_{m=1}^9 \tilde{k}_2(\mathcal{D}_m(\eta)) \det \mathcal{J}_m(\eta). \quad (47)$$

Hence, only a two-dimensional integral has to be integrated numerically instead of a five-dimensional one. The regularity of the remaining integrand will be proved in Lemma 9.

3. Duffy transformation

3.4. Summary

In the Sections 3.2 and 3.3 we adapted the Duffy transformation for our purposes, i.e. to lift singular integrals of the type (22) and (23). Table 1 gives an overview over the costs of the Duffy transformation. As it can be seen there, the number of sub-domains increases the stronger the singularity is.

singularity case	point	edge	face	tetrahedron
# sub-domains	2	4	17	9
dim η	5	4	3	2

Table 1: Costs of the Duffy transformation for volume-volume integrals

One must not be deceived by the case where the two tetrahedra are identical, since the number of sub-domains can be halved by exploiting the symmetry. Moreover, Table 1 shows that the dimension of integrals which have to be computed decreases as the singularity becomes stronger. However, this is not a generally valid statement for the Duffy transformation. It holds only in our case, since the structure of the integral (22) is exploited.

The same statements also apply to the volume-surface integrals, as can be seen in Table 2. Note

singularity case	point	edge	face
# sub-domains	2	4	9
dim η	5	4	3

Table 2: Costs of Duffy transformation for volume-surface integrals

that the number of sub-domains between Table 1 and Table 2 differ for the case that the geometries share a common face quite a bit. This is due to the additional dimension in the volume-volume case.

4. Error estimates for the integrals

4.1. Derivative free error estimates

All previous transformations result in integrals over multi-dimensional unit cubes. In the following, we present quadrature rules and the corresponding error estimates. We follow the approach of Sauter and Schwab [75] and use derivative-free estimates, which are based on the work of Davis [35]. By $\mathcal{E}_{a,b}^\rho \subset \mathbb{C}$ we denote the closed ellipse with focal points $a, b \in \mathbb{R}$. Further, $\rho := \bar{a} + \bar{b}$ refers to the sum of the semimajor half-axis $\bar{a} > (b - a)/2$ and the semiminor half-axis \bar{b} . The standard ellipse $\mathcal{E}_{0,1}^\rho$ is abbreviated with \mathcal{E}_ρ . Furthermore, let $k \in \mathbb{N}$ and let $f : [0, 1]^k \rightarrow \mathbb{C}$ be a function. Then we denote by $I[f]$ the integral of f over $[0, 1]^k$ and by $Q^n[f]$ its approximation with a tensor Gauss quadrature of order $n \in \mathbb{N}^k$, i.e., in dimension $i \in \{1, \dots, k\}$ we use a Gaussian quadrature rule with n_i points. Moreover, we define the quadrature error $E^n[f] := |I[f] - Q^n[f]|$.

Theorem 10. *Let $f : [0, 1] \rightarrow \mathbb{C}$ be analytic with an analytic extension f^* to \mathcal{E}_ρ for some $\rho > 1/2$. Then*

$$E^n[f] \leq c(2\rho)^{-2n} \max_{z \in \partial\mathcal{E}_\rho} |f^*(z)|.$$

In order to generalize the previous theorem to a tensor Gauss quadrature, we need the following definition.

Definition 4. *Let $X := [0, 1]^k \subset \mathbb{R}^k$. A function $f : X \rightarrow \mathbb{C}$ is called component-wise analytic if for $i = 1, \dots, k$ there exists $\rho_i > 1/2$ such that for all $x \in X$ the function*

$$f_{i,x} : [0, 1] \rightarrow \mathbb{C}, \quad f_{i,x}(t) := f(x_1, \dots, x_{i-1}, t, x_{i+1}, \dots, x_k),$$

can be extended to an analytic function $f_{i,x}^ : \mathcal{E}_{\rho_i} \rightarrow \mathbb{C}$.*

With this definition we can extend Theorem 10 to the multi-dimensional case.

Theorem 11. *Let $f : [0, 1]^k \rightarrow \mathbb{C}$ be component-wise analytic and let $\rho \in \mathbb{R}^k$ be as in Definition 4. Then the quadrature error with n_i nodes in dimension $i = 1, \dots, k$ satisfies*

$$E^n[f] \leq \sum_{i=1}^k \max_{x \in [0,1]^k} E^{n_i}[f_{i,x}] \leq \sum_{i=1}^k c_i (2\rho_i)^{-2n_i} \max_{x \in [0,1]^k} \max_{z \in \partial\mathcal{E}_{\rho_i}} |f_{i,x}^*(z)|.$$

The constants c_i , $1 \leq i \leq k$, are as in Theorem 10.

The proofs of Theorem 10 and 11 can be found in [75]. Our main goal is to verify the requirements of Theorem 11 for each of the cases in Chapter 3.

4.2. Preparation

4.2.1. Analyticity of the integrands

In order to apply Theorem 11 to our cases (22) and (23), we have to prove that for each singularity case the integrand is component-wise analytic. For this we also need assumptions on the geometry, one for the tetrahedra and one for the panels.

4. Error estimates for the integrals

Assumption 1. *Let us assume that*

1. *For all $t \in \mathcal{T}$ there is $c_A > 0$ and $x_0 \in \bar{t}$ such that $|x - y| \geq c_A (|x - x_0| + |x_0 - y|)$ for all $x \in \Omega \setminus t$ and $y \in t$.*
2. *For all $t_1, t_2 \in \mathcal{T}$ whose intersection consists of a common vertex p , there exists $c_A > 0$ such that $|x - y| \geq c_A (|x - p| + |p - y|)$ for $x \in t_1, y \in t_2$.*
3. *For all $t_1, t_2 \in \mathcal{T}$ with exactly one common edge $E := \bar{t}_1 \cap \bar{t}_2$, there exists $c_A > 0$ and a point $p \in E$ such that $|x - y| \geq c_A (|x - p| + |p - y|)$ for all $x \in t_1, y \in t_2$.*
4. *For all $t_1, t_2 \in \mathcal{T}$ with exactly one common face $F := \bar{t}_1 \cap \bar{t}_2$, there exists $c_A > 0$ and a point $p \in F$ such that $|x - y| \geq c_A (|x - p| + |p - y|)$ for all $x \in t_1, y \in t_2$.*

A similar assumption is made for the combination of tetrahedra in \mathcal{T} and panels in \mathcal{P} .

Assumption 2. *Let us assume that*

1. *For all $t \in \mathcal{T}$ there is $c_A > 0$ and $x_0 \in \bar{t}$ such that $|x - y| \geq c_A (|x - x_0| + |x_0 - y|)$ for all $y \in \tau \subset \mathcal{P} \setminus \bar{t}$ and $x \in t$.*
2. *For all $t \in \mathcal{T}$ and $\tau \in \mathcal{P}$ whose intersection consists of a common vertex p , there is $c_A > 0$ such that $|x - y| \geq c_A (|x - p| + |p - y|)$ for all $x \in t, y \in \tau$.*
3. *For all $t \in \mathcal{T}$ and $\tau \in \mathcal{P}$ with exactly one common edge $E := \bar{t} \cap \bar{\tau}$, there exists $c_A > 0$ and a point $p \in E$ such that $|x - y| \geq c_A (|x - p| + |p - y|)$ for all $x \in t, y \in \tau$.*
4. *For all $t \in \mathcal{T}$ and $\tau \in \mathcal{P}$ with exactly one common face $F := \bar{t} \cap \bar{\tau} = \bar{\tau}$, there is $c_A > 0$ and a point $p \in \bar{\tau}$ such that $|x - y| \geq c_A (|x - p| + |p - y|)$ for all $x \in t, y \in \tau$.*

In addition, we also need information about the scaling behavior of the linear mappings χ_t and χ_τ

Lemma 6. *Let M_τ be as in (43) and let λ_{\max} and λ_{\min} be the largest and the smallest eigenvalue of $M_\tau^T M_\tau$, respectively. Then*

$$c h_\tau^2 \leq \lambda_{\min} \leq \lambda_{\max} \leq 2 h_\tau^2 \quad \text{and} \quad c h_\tau^2 \leq \sqrt{\det M_\tau^T M_\tau} \leq C h_\tau^2$$

with constants $c, C > 0$ that depend only on the minimal interior angle θ_τ of the panel τ .

The proof of Lemma 7 can be found in [75].

Lemma 7. *Let M_t be as in (26) and let λ_{\max} and λ_{\min} be the largest and the smallest eigenvalue of $M_t^T M_t$, respectively. Then*

$$c h_t^2 \leq \lambda_{\min} \leq \lambda_{\max} \leq 3 h_t^2 \quad \text{and} \quad c h_t^3 \leq \sqrt{\det M_t^T M_t} \leq C h_t^3$$

with constants $c, C > 0$ that depend only on the angle θ_t being the minimum of the interior angles and the solid angles of the tetrahedron t .

4. Error estimates for the integrals

Proof. We set $v_1 := b_t - a_t$, $v_2 := c_t - b_t$, and $v_3 := d_t - b_t$ and denote by ρ_t the radius of the insphere of t . The upper bound on the eigenvalues of $M_t^T M_t$ results from the linearity of the scalar product and Young's inequality

$$(M_t \xi, M_t \xi) = \sum_{i,j=1}^3 \xi_i \xi_j (v_i, v_j) \leq 3 \sum_{i=1}^3 \xi_i^2 |v_i|^2 \leq 3 h_t^2 |\xi|^2, \quad \xi \in \mathbb{R}^3.$$

According to [38], for the lower bound it holds that $\lambda_{\min} \geq \rho_t/h_{\bar{t}}$. Using elementary properties of the tetrahedron, the estimates in [72] can be adjusted to our needs as follows:

$$\lambda_{\min} \geq \rho_t h_{\bar{t}}^{-1} = 3h_{\bar{t}}^{-1} \frac{|t|}{|\partial t|} \geq 3h_{\bar{t}}^{-1} \sin^2(\theta_t) \frac{|v_1||v_2||v_3|}{|\partial t|} \geq \tilde{c} \sin^2(\theta_t) h_t.$$

The last step is due to the assumption that the tetrahedra do not degenerate. \square

Since we assumed in (13) that the interior angles and the solid angles of the tetrahedra are bounded below by $\theta_{\mathcal{T}}$, Lemmas 6 and 7 show that there exists a constant $c_{\mathcal{T}} > 0$ such that for each $t \in \mathcal{T}$ and for each $\tau \in \mathcal{P}$ it holds that

$$|M_t x| \geq c_{\mathcal{T}} h_t |x|, \quad x \in \mathbb{R}^3, \quad \text{and} \quad |M_{\tau} y| \geq c_{\mathcal{T}} h_{\tau} |y|, \quad y \in \mathbb{R}^2. \quad (48)$$

4.2.1.1. Tetrahedron and tetrahedron With these assumptions we can prove that the integrands after the Duffy transformation are analytic in the corresponding integration domain. The direct consequence of this is also that the Duffy transformation has lifted the singularity.

Lemma 8. *The integrands $\tilde{k}_{1,V}$ in (33), $\tilde{k}_{1,E}$ in (38), $\tilde{k}_{1,F}$ in (41), and $\tilde{k}_{1,T}$ in (42) are component-wise analytic for $s \in (0, 1)$.*

Proof. Since in the case of the integrand $\tilde{k}_{1,T}$ the two tetrahedra t_1 and t_2 are identical, we drop the index. For each sub-domain, we have to consider three terms: the Jacobi determinant of the Duffy transformation, the product of the linear basis functions and the denominator. The first two can obviously be extended analytically w.r.t. all variables in a complex neighborhood of $[0, 1]^2$ as they are polynomials w.r.t. η . For the denominator we obtain

$$|M_t(\mathcal{D}_m^1(\eta) - \mathcal{D}_m^2(\eta))| \geq c_{\mathcal{T}} h_t |\mathcal{D}_m^1(\eta) - \mathcal{D}_m^2(\eta)| =: c_{\mathcal{T}} h_t \text{dist}_t(\mathcal{D}_m(\eta)), \quad m = 1, \dots, 9, \quad (49)$$

where $c_{\mathcal{T}}$ is defined in (48). Therefore, only the distance has to be studied for each domain:

$$\begin{aligned} \text{dist}_t^2(\mathcal{D}_1(\eta)) &= \eta_1^2(1 + \eta_2^2) + (1 - \eta_1)^2 > 0, & \text{dist}_t^2(\mathcal{D}_2(\eta))^2 &= \eta_1^2 \eta_2^2 + 1 + \eta_1^2(1 - \eta_2)^2 > 0, \\ \text{dist}_t^2(\mathcal{D}_3(\eta)) &= \eta_1^2(1 + \eta_2^2) + (1 - \eta_1 \eta_2)^2 > 0, & \text{dist}_t^2(\mathcal{D}_4(\eta)) &= \eta_1^2(1 + \eta_2^2) + (1 - \eta_1 \eta_2)^2 > 0, \\ \text{dist}_t^2(\mathcal{D}_5(\eta)) &= 1 + \eta_1^2 \eta_2^2 + \eta_1^2(1 - \eta_2)^2 > 0, & \text{dist}_t^2(\mathcal{D}_6(\eta)) &= \eta_1^2(1 + \eta_2^2) + (1 - \eta_1)^2 > 0, \\ \text{dist}_t^2(\mathcal{D}_7(\eta)) &= \eta_1^2 \eta_2^2 + \eta_1^2(1 - \eta_2)^2 + 1 > 0, & \text{dist}_t^2(\mathcal{D}_8(\eta)) &= \eta_1^2 \eta_2^2 + \eta_1^2(1 - \eta_2)^2 + (1 - \eta_1)^2 > 0, \\ \text{dist}_t^2(\mathcal{D}_9(\eta)) &= \eta_1^2 + (1 - \eta_2)^2 + \eta_2^2 > 0. \end{aligned}$$

Notice, due to symmetry it is enough to only consider the first nine sub-domains. Since the denominator has no zeros in $[0, 1]^2$ and consists of analytic functions, the whole integrand $\tilde{k}_{1,T}$ can be analytically extended w.r.t. all variables in a complex neighborhood of $[0, 1]^2$ for $s \in (0, 1)$.

4. Error estimates for the integrals

The main difference for the integrand $\tilde{k}_{1,F}$ is the estimation of the denominator. The intersection between the tetrahedra t_1 and t_2 is a common face $\tau = \bar{t}_1 \cap \bar{t}_2$. Without loss of generality we assume that the parameterizations χ_{t_1} and χ_{t_2} satisfy the relation

$$\chi_{t_1}(\kappa) = \chi_{t_2}(\kappa)$$

with $\kappa := (\kappa_1, \kappa_2, 0)^T$ for all $\kappa_1, \kappa_2 \in [0, 1]$. By Assumption 1, there exists a point p on the common face τ with $p = \chi_{t_1}(\kappa)$, and it holds that

$$\begin{aligned} |\chi_{t_1}(\mathcal{D}_m^1(\eta)) - \chi_{t_2}(\mathcal{D}_m^2(\eta))| &\geq c_A (|M_{t_1}(\mathcal{D}_m^1(\eta) - \kappa)| + |M_{t_2}(\kappa - \mathcal{D}_m^2(\eta))|) \\ &\geq c c_A c_{\mathcal{T}} h \left[\sum_{i=1}^2 (\mathcal{D}_{m,i}^1(\eta) - \kappa_i)^2 + (\kappa_i - \mathcal{D}_{m,i}^2(\eta))^2 + \mathcal{D}_{m,3}^i(\eta)^2 \right]^{1/2} \\ &\geq \frac{c}{2} h \left[\sum_{i=1}^2 (\mathcal{D}_{m,i}^1(\eta) - \mathcal{D}_{m,i}^2(\eta))^2 + \mathcal{D}_{m,3}^i(\eta)^2 \right]^{1/2} \\ &=: \frac{c}{2} h \text{dist}_{\tau}(\mathcal{D}_m(\eta)), \end{aligned}$$

where h and $c_{\mathcal{T}}$ are defined in (15) and (48), respectively. Therefore, only the $\text{dist}_{\tau}(\mathcal{D}_m(\eta))$ has to be studied for each domain. Since the treatment of $\text{dist}_{\tau}(\mathcal{D}_m(\eta))$ is analogous to the treatment of $\text{dist}_t(\mathcal{D}_m(\eta))$, we consider only the first sub-domain:

$$|\text{dist}_{\tau}(\mathcal{D}_1(\eta))|^2 = \eta_1^2(1 + \eta_2^2[\eta_3^2 + (1 - \eta_3)^2]) + (1 - \eta_1)^2 > 0.$$

The remaining sub-domains can be estimated analogously. Since the denominator has no zeros in $[0, 1]^3$ and consists of analytic functions, the whole integrand $\tilde{k}_{1,F}$ can be analytically extended w.r.t. all variables in a complex neighborhood of $[0, 1]^3$ for $s \in (0, 1)$.

Similar arguments apply in the case of the $\tilde{k}_{1,V}$ and $\tilde{k}_{1,E}$. □

4.2.1.2. Tetrahedron and panel In this section the intersection between a tetrahedron and a panel is studied. First, the case that the panel is a face of the tetrahedron is considered.

Lemma 9. *The integrands $\tilde{k}_{2,V}$ in (45), $\tilde{k}_{2,E}$ in (46), and $\tilde{k}_{2,F}$ in (47) are component-wise analytic for $s \in (0, 1)$.*

Proof. For each singularity case, we have to consider for each sub-domain four terms: the Jacobi determinant of the Duffy transformation, the product of the linear basis functions, the nominator and the denominator. The first three can clearly be analytically extended w.r.t. all variables in a complex neighborhood of $[0, 1]^2$ for $s \in (0, 1)$, because they are only polynomial relative to η and polynomials are analytic in \mathbb{C} . Only the denominator has to be considered for each singularity case differently.

The panel τ is a face of the tetrahedron t . Without loss of generality we assume that the parameterizations χ_t and χ_{τ} satisfy the relation

$$\chi_t(\kappa_{1:2,0}) = \chi_{\tau}(\kappa),$$

4. Error estimates for the integrals

with $\kappa_{1:2,0} := (\kappa_1, \kappa_2, 0)^T$ for all $\kappa_1, \kappa_2 \in [0, 1]$ and for all $\kappa \in [0, 1]^2$. By Assumption 2 there exists a point p on $\bar{\tau}$, with $p = \chi_t(\kappa_{1:2,0})$, and it holds

$$\begin{aligned} |\chi_t(\mathcal{D}_m^1(\eta)) - \chi_\tau(\mathcal{D}_m^2(\eta))| &\geq c_A (|M_t(\mathcal{D}_m^1(\eta) - \kappa_{1:2,0})| + |M_\tau(\kappa - \mathcal{D}_m^2(\eta))|) \\ &\geq c c_A c_\mathcal{T} h \left[\sum_{i,j=1}^2 (\mathcal{D}_{m,i}^j(\eta) - \kappa_i)^2 + \mathcal{D}_{m,3}^1(\eta)^2 \right]^{1/2} \\ &\geq \frac{c}{2} h \left[\sum_{i=1}^2 (\mathcal{D}_{m,i}^1(\eta) - \mathcal{D}_{m,i}^2(\eta))^2 + \mathcal{D}_{m,3}^1(\eta)^2 \right]^{1/2} \\ &=: \frac{c}{2} h \text{dist}_F(\mathcal{D}_m(\eta)), \end{aligned}$$

where h and $c_\mathcal{T}$ are defined in (15) and (48), respectively. Therefore, only the $\text{dist}_F(\mathcal{D}_m(\eta))$ has to be studied for each domain:

$$\begin{aligned} |\text{dist}_F(\mathcal{D}_1(\eta))|^2 &= \eta_1^2 (1 + \eta_2^2) + (1 - \eta_1)^2 > 0, \\ |\text{dist}_F(\mathcal{D}_2(\eta))|^2 &= 1 + \eta_1^2 \eta_2^2 + \eta_1^2 (1 - \eta_2)^2 > 0, \\ |\text{dist}_F(\mathcal{D}_3(\eta))|^2 &= \eta_1^2 (1 + \eta_2^2) + (1 - \eta_1 \eta_2)^2 > 0, \\ |\text{dist}_F(\mathcal{D}_4(\eta))|^2 &= \eta_1^2 \eta_2^2 + \eta_1^2 (1 - \eta_2)^2 + 1 > 0, \\ |\text{dist}_F(\mathcal{D}_5(\eta))|^2 &= \eta_1^2 (\eta_2^2 + [1 - \eta_2]^2) + (1 - \eta_1)^2 > 0, \\ |\text{dist}_F(\mathcal{D}_6(\eta))|^2 &= \eta_1^2 (1 + \eta_2^2) + (1 - \eta_1)^2 > 0, \\ |\text{dist}_F(\mathcal{D}_7(\eta))|^2 &= \eta_1^2 \eta_2^2 + \eta_1^2 (1 - \eta_2)^2 + 1 > 0, \\ |\text{dist}_F(\mathcal{D}_8(\eta))|^2 &= \eta_1^2 (1 + \eta_2^2) + (1 - \eta_1 \eta_2)^2 > 0, \\ |\text{dist}_F(\mathcal{D}_9(\eta))|^2 &= \eta_1^2 + (1 - \eta_1)^2 + \eta_2^2 > 0. \end{aligned}$$

Since the denominator has no zeros in $[0, 1]^2$ and consists of analytic functions, the whole integrand can be analytically extended w.r.t. all variables in a complex neighborhood of $[0, 1]^2$ for $s \in (0, 1)$.

For the second singularity case, where the tetrahedron t and the panel τ share a common edge, only the denominator has to be considered. Without loss of generality we assume that the parameterizations χ_t and χ_τ satisfy the relation

$$\chi_t(\kappa e_1) = \chi_\tau(\kappa \hat{e}_1)$$

for all $\kappa \in [0, 1]$. By Assumption 2 there exists a point p on the common edge E , $p = \chi_t(\kappa e_1) \in E$, with

$$\begin{aligned} |\chi_t(\mathcal{D}_m^1(\eta)) - \chi_\tau(\mathcal{D}_m^2(\eta))| &\geq c_A (|M_t(\mathcal{D}_m^1(\eta) - \kappa e_1)| + |M_\tau(\kappa \hat{e}_1 - \mathcal{D}_m^2(\eta))|) \\ &\geq c c_A c_\mathcal{T} h \left[\sum_{j=1}^2 (\mathcal{D}_{m,1}^j(\eta) - \kappa)^2 + \sum_{i=1}^2 \mathcal{D}_{m,2}^i(\eta)^2 + \mathcal{D}_{m,3}^1(\eta)^2 \right]^{1/2} \\ &\geq \frac{c}{2} h [(\mathcal{D}_{m,1}^1(\eta) - \mathcal{D}_{m,1}^2(\eta))^2 + \mathcal{D}_{m,2}^2(\eta)^2 + \mathcal{D}_{m,2}^1(\eta)^2 + \mathcal{D}_{m,3}^1(\eta)^2]^{1/2} \\ &=: \frac{c}{2} h \text{dist}_E(\mathcal{D}_m(\eta)), \end{aligned}$$

4. Error estimates for the integrals

where h and $c_{\mathcal{T}}$ are defined in (15) and (48), respectively. Therefore, only the $\text{dist}_E(\mathcal{D}_m(\eta))$ has to be studied for each domain:

$$\begin{aligned} |\text{dist}_E(\mathcal{D}_1(\eta))|^2 &\geq \eta_1^2 + (1 - \eta_1)^2 > 0, \\ |\text{dist}_E(\mathcal{D}_2(\eta))|^2 &\geq \eta_1^2 + (1 - \eta_1)^2 > 0, \\ |\text{dist}_E(\mathcal{D}_3(\eta))|^2 &\geq \eta_2^2 (\eta_3^2 + [1 - \eta_3]^2) + (1 - \eta_2)^2 > 0, \\ |\text{dist}_E(\mathcal{D}_4(\eta))|^2 &\geq 1 > 0. \end{aligned}$$

Since the denominator has no zeros in $[0, 1]^3$ and consists of analytic functions, the whole integrand can be analytically extended w.r.t. all variables in a complex neighborhood of $[0, 1]^3$ for $s \in (0, 1)$.

Similar arguments apply in the case of $\tilde{k}_{2,V}$. \square

4.2.2. Error estimates for the integrands

Since it was shown in Section 4.2.1 that all regularized integrands are component-wise analytic, the requirements of Theorem 11 are fulfilled. In order to apply it, the sum of the half-axes ρ of the ellipse has to be estimated for each case. Additionally, we need a notation to describe the analytic extension onto the ellipses w.r.t. to the integration domain. We define for $\rho > 0$ and $i \in \{1, \dots, k\}$

$$\mathcal{E}_\rho^{(i)} := [0, 1]^{i-1} \times \mathcal{E}_\rho \times [0, 1]^{k-i} \subset \mathbb{R}^k.$$

4.2.2.1. Tetrahedron and tetrahedron First, we consider the different interactions between two tetrahedra. In contrast to [75], we do not use spherical coordinates to do the estimations, but the Duffy Transformation directly. The next lemma gives the desired error estimation for the case that the two tetrahedra are identical.

Lemma 10. *There exists a constant $\rho > 1/2$ that depends only on $\theta_{\mathcal{T}}$ such that the integrand $\tilde{k}_{1,T}$ in (42) can be analytically extended to $\bigcup_{i=1}^2 \mathcal{E}_\rho^{(i)}$. It holds that*

$$\sup_{\eta \in \mathcal{E}_\rho^{(i)}} |\tilde{k}_{1,T}(\eta)| \leq C h^{3-2s}, \quad i = 1, 2.$$

Proof. Since the two tetrahedra are identical, we drop the index. From Lemma 8 we know that $\tilde{k}_{1,T}$ is analytic in a complex neighborhood of $[0, 1]^2$. Therefore, $\rho > 1/2$ exists such that $\tilde{k}_{1,T}$ can be analytically extended to $\bigcup_{i=1}^2 \mathcal{E}_\rho^{(i)}$. We show that the choice of ρ is independent of h . In the proof of Lemma 8, we have seen that the denominator of

$$\tilde{k}_{1,T}(\eta) = \sum_{m=1}^9 \frac{[\alpha_{i,1:3}^T M_t(\mathcal{D}_m^1(\eta) - \mathcal{D}_m^2(\eta))] [\alpha_{j,1:3}^T M_t(\mathcal{D}_m^1(\eta) - \mathcal{D}_m^2(\eta))]}{|h_t^{-1} M_t(\mathcal{D}_m^1(\eta) - \mathcal{D}_m^2(\eta))|^{3+2s}} h_t^{-3-2s} |\det M_t|^2 \det \mathcal{J}_m(\eta).$$

is responsible for the size of the complex neighborhood. Due to Lemma 7 and (48), it holds that

$$|h_t^{-1} M_t x| \geq c_{\mathcal{T}} |x|, \quad x \in \mathbb{R}^3,$$

4. Error estimates for the integrals

where the positive constant $c_{\mathcal{T}}$ does not depend on h_t . By combining this with (49), we obtain

$$|h_t^{-1} M_t(\mathcal{D}_m^1(\eta) - \mathcal{D}_m^2(\eta))| \geq c_{\mathcal{T}} |\mathcal{D}_m^1(\eta) - \mathcal{D}_m^2(\eta)| > 0, \quad \eta \in [0, 1]^2, \quad m = 1, \dots, 9.$$

Since the \mathcal{D}_m do not depend on h_t , it follows that the size of the complex neighborhood is independent of h_t and thus also independent of h ; see (16). This implies that the choice of ρ is independent of h . We continue with the estimation of the integrand. By considering the scaling of the linear mapping χ_t , we obtain

$$|h_t^{-1} M_t x| \leq |x_1| \frac{|b_t - a_t|}{h_t} + |x_2| \frac{|c_t - a_t|}{h_t} + |x_3| \frac{|d_t - a_t|}{h_t} \leq \sqrt{3}|x|.$$

Due to the scaling of $\alpha_{\star,1:3}$ with $\star \in \{i, j\}$, it holds

$$|\alpha_{\star,1:3}^T M_t x| \leq C |x|,$$

where the positive constant C is independent of h . By combining these results, we obtain for $i = 1, 2$ and for $m = 1, \dots, 9$, that

$$\sup_{\eta \in \mathcal{E}_\rho^{(i)}} \left| \frac{[\alpha_{i,1:3}^T M_t(\mathcal{D}_m^1(\eta) - \mathcal{D}_m^2(\eta))] [\alpha_{j,1:3}^T M_t(\mathcal{D}_m^1(\eta) - \mathcal{D}_m^2(\eta))]}{|h_t^{-1} M_t(\mathcal{D}_m^1(\eta) - \mathcal{D}_m^2(\eta))|^{3+2s}} \det \mathcal{J}_m(\eta) \right| \leq \tilde{c}$$

with $\tilde{c} > 0$ independent of h_t . Using Lemma 7, this leads to

$$\sup_{\eta \in \mathcal{E}_\rho^{(i)}} |\tilde{k}_{1,T}(\eta)| \leq \tilde{c} \sum_{m=1}^9 h_t^{-3-2s} |\det M_t|^2 \leq 9C h^{3-2s}, \quad i = 1, 2.$$

□

Next, the case of a singularity along one face is considered.

Lemma 11. *There exists a constant $\rho > 1/2$ that depends only on $\theta_{\mathcal{T}}$ such that the integrand $\tilde{k}_{1,F}$ in (41) can be analytically extended to $\bigcup_{i=1}^3 \mathcal{E}_\rho^{(i)}$. It holds that*

$$\sup_{\eta \in \mathcal{E}_\rho^{(i)}} |\tilde{k}_{1,F}(\eta)| \leq C h^{3-2s}, \quad i = 1, 2, 3.$$

Proof. From Lemma 8 we know that $\tilde{k}_{1,F}$ is analytic in a complex neighborhood of $[0, 1]^3$. Therefore, a constant $\rho > 1/2$ exists such that $\tilde{k}_{1,F}$ can be analytically extended to $\bigcup_{l=1}^3 \mathcal{E}_\rho^{(l)}$. We show that the choice of ρ is independent of h . In the proof of Lemma 8, we have seen that denominator of $\tilde{k}_{1,F}$

$$\tilde{k}_{1,F}(\eta) = \sum_{m=1}^{17} \frac{\beta_{i,j}(\mathcal{D}_m^1(\eta), \mathcal{D}_m^2(\eta))}{|h^{-1} M_{t_1} \mathcal{D}_m^1(\eta) - h^{-1} M_{t_2} \mathcal{D}_m^2(\eta)|^{3+2s}} h^{-3-2s} |\det M_{t_1}| |\det M_{t_2}| \det \mathcal{J}_m(\eta),$$

is responsible for the size of the complex neighborhood. Note that

$$\beta_{i,j}(\mathcal{D}_m^1(\eta), \mathcal{D}_m^2(\eta)) := [\alpha_{i,1:3}^T (M_{t_1} \mathcal{D}_m^1(\eta) - M_{t_2} \mathcal{D}_m^2(\eta))] [\alpha_{j,1:3}^T (M_{t_1} \mathcal{D}_m^1(\eta) - M_{t_2} \mathcal{D}_m^2(\eta))]$$

4. Error estimates for the integrals

and h is defined in (15). Due to Lemma 7, (48) and (16), it holds that

$$|h^{-1}M_{t_i}x| \geq c_{\mathcal{T}} c_2 |x|, \quad x \in \mathbb{R}^3, \quad i = 1, 2,$$

where the positive constants $c_{\mathcal{T}}$ and c_2 does not depend on h_t . By combining this with (49), we obtain

$$|h^{-1}M_{t_i}(\mathcal{D}_m^1(\eta) - \mathcal{D}_m^2(\eta))| \geq c_{\mathcal{T}} c_2 |\mathcal{D}_m^1(\eta) - \mathcal{D}_m^2(\eta)| > 0, \quad \eta \in [0, 1]^2, \quad m = 1, \dots, 9, \quad i = 1, 2.$$

Since the \mathcal{D}_m do not depend on h , it follows that the size of the complex neighborhood is independent of h . This implies that the choice of ρ is independent of h . We continue with the estimation of the integrand. By considering the scaling of the linear mapping χ_t , we obtain

$$|h^{-1}M_{t_i}x| \leq |x_1| \frac{|b_{t_i} - a_{t_i}|}{h} + |x_2| \frac{|c_{t_i} - a_{t_i}|}{h} + |x_3| \frac{|d_{t_i} - a_{t_i}|}{h} \leq \sqrt{3} c_2 |x|, \quad i = 1, 2.$$

Due to the scaling of $\alpha_{\star, 1:3}$ with $\star \in \{i, j\}$, it holds

$$|\alpha_{\star, 1:3}^T M_{t_i}x| \leq C |x|, \quad i = 1, 2,$$

where the positive constant C is independent of h . Notice that the estimation for $\beta_{i,j}$ is more complicated, since the exact structure of $\beta_{i,j}$ depends on the interaction of the tetrahedra t_1 and t_2 and the linear basis functions φ_i and φ_j . Every occurring case, be it one, two or no degenerate difference, can again be traced back to the above estimation. By combining these results, we obtain for $l = 1, 2, 3$ and for $m = 1, \dots, 17$, that

$$\sup_{\eta \in \mathcal{E}_\rho^{(l)}} \left| \frac{\beta_{i,j}(\mathcal{D}_m^1(\eta), \mathcal{D}_m^2(\eta))}{|h^{-1}M_{t_1}\mathcal{D}_m^1(\eta) - h^{-1}M_{t_2}\mathcal{D}_m^2(\eta)|^{3+2s}} \det \mathcal{J}_m(\eta) \right| \leq \tilde{c},$$

with \tilde{c} independent of h . Using Lemma 7, this leads to

$$\sup_{\eta \in \mathcal{E}_\rho^{(i)}} |\tilde{k}_{1,F}(\eta)| \leq \tilde{c} \sum_{m=1}^{17} h^{-3-2s} |\det M_{t_1}| |\det M_{t_2}| \leq 17 C h^{3-2s}, \quad i = 1, 2, 3.$$

□

Now we take a closer look what happens when the singularity is along a corner.

Lemma 12. *There exists a constant $\rho > 1/2$ that depends only on $\theta_{\mathcal{T}}$ such that the integrand $\tilde{k}_{1,E}$ in (38) can be analytically extended to $\bigcup_{i=1}^4 \mathcal{E}_\rho^{(i)}$. It holds that*

$$\sup_{\eta \in \mathcal{E}_\rho^{(i)}} |\tilde{k}_{1,E}(\eta)| \leq C h^{3-2s}, \quad i = 1, \dots, 4.$$

Here, the singularity at a common vertex is studied.

Lemma 13. *There exists a constant $\rho > 1/2$ that depends only on $\theta_{\mathcal{T}}$ such that the integrand $\tilde{k}_{1,V}$ in (33) can be analytically extended to $\bigcup_{i=1}^5 \mathcal{E}_\rho^{(i)}$. It holds that*

$$\sup_{\eta \in \mathcal{E}_\rho^{(i)}} |\tilde{k}_{1,V}(\eta)| \leq C h^{3-2s}, \quad i = 1, \dots, 5.$$

4. Error estimates for the integrals

Since the proofs of Lemmas 10 to 13 are structurally the same, the proofs of Lemma 12 and Lemma 13 are omitted. Finally, the case is investigated in which the tetrahedra have a positive distance

$$d_{t_1, t_2} := \text{dist}(t_1, t_2) := \inf_{(x, y) \in t_1 \times t_2} |x - y| > 0.$$

The transformation

$$\mathcal{D}(\eta) := (\mathcal{D}_1(\eta_{1:3}), \mathcal{D}_2(\eta_{4:6})) = \left(\begin{bmatrix} \eta_1 \\ \eta_1 \eta_2 \\ \eta_1 \eta_2 \eta_3 \end{bmatrix}, \begin{bmatrix} \eta_4 \\ \eta_4 \eta_5 \\ \eta_4 \eta_5 \eta_6 \end{bmatrix} \right), \quad \eta \in \mathbb{R}^6,$$

is analytic and we have $\det \mathcal{J}(\eta) = \eta_1^2 \eta_2 \eta_4^2 \eta_5$. Applying this transformation to (27), we obtain

$$I_{t_1, t_2} = \int_{[0, 1]^6} \tilde{k}_{1, D}(\eta) \, d\eta \tag{50}$$

with

$$\tilde{k}_{1, D}(\eta) := \frac{\beta_{ij}(\mathcal{D}_1(\eta), \mathcal{D}_2(\eta))}{|\chi_{t_1}(\mathcal{D}_1(\eta)) - \chi_{t_2}(\mathcal{D}_2(\eta))|^{3+2s}} |\det M_{t_1}| |\det M_{t_2}| \det \mathcal{J}(\eta)$$

and

$$\beta_{ij}(\mathcal{D}_1(\eta), \mathcal{D}_2(\eta)) := \begin{cases} -\varphi_i(\chi_{t_1}(\mathcal{D}_1(\eta))) \varphi_j(\chi_{t_2}(\mathcal{D}_2(\eta))), & t_1 \in \text{supp } \varphi_i, t_2 \in \text{supp } \varphi_j, \\ -\varphi_j(\chi_{t_1}(\mathcal{D}_1(\eta))) \varphi_i(\chi_{t_2}(\mathcal{D}_2(\eta))), & t_2 \in \text{supp } \varphi_i, t_1 \in \text{supp } \varphi_j. \end{cases}$$

We focus on the almost singular cases, i.e. $d_{t_1, t_2} \approx h$, as only those cause difficulties in the numerical integration.

Lemma 14. *There exists a constant $\rho > 1/2$ that depends only on $\theta_{\mathcal{T}}$ such that $\tilde{k}_{1, D}$ can be analytically extended to $\bigcup_{i=1}^6 \mathcal{E}_\rho^{(i)}$. It holds that*

$$\sup_{\eta \in \mathcal{E}_\rho^{(i)}} |\tilde{k}_{1, D}(\eta)| \leq C h^{3-2s}, \quad i = 1, \dots, 6.$$

We omit the proof of Lemma 14 as it is analogous to the proof of Lemma 10 and Lemma 11.

4.2.2.2. Tetrahedron and panel Next, we consider the interaction between a tetrahedron and a panel. First, the case of a singularity along a common face is considered, i.e. the panel is a face of the tetrahedron.

Lemma 15. *There exists a constant $\rho > 1/2$ that depends only on $\theta_{\mathcal{T}}$ such that the integrand $\tilde{k}_{2, F}$ in (47) can be analytically extended to $\bigcup_{i=1}^2 \mathcal{E}_\rho^{(i)}$. It holds that*

$$\sup_{\eta \in \mathcal{E}_\rho^{(i)}} |\tilde{k}_{2, F}(\eta)| \leq C h^{3-2s}, \quad i = 1, 2.$$

Second, the case of the singularity along an edge is investigated.

4. Error estimates for the integrals

Lemma 16. *There exists a constant $\rho > 1/2$ that depends only on $\theta_{\mathcal{T}}$ such that the integrand $\tilde{k}_{2,E}$ in (46) can be analytically extended to $\bigcup_{i=1}^3 \mathcal{E}_{\rho}^{(i)}$. It holds that*

$$\sup_{\eta \in \mathcal{E}_{\rho}^{(i)}} |\tilde{k}_{2,E}(\eta)| \leq C h^{3-2s}, \quad i = 1, 2, 3.$$

Next, the singularity at a common vertex is studied.

Lemma 17. *There exists a constant $\rho > \frac{1}{2}$ that depends only on $\theta_{\mathcal{T}}$ such that the integrand $\tilde{k}_{2,V}$ in (45) can be analytically extended to $\bigcup_{i=1}^4 \mathcal{E}_{\rho}^{(i)}$. It holds that*

$$\sup_{\eta \in \mathcal{E}_{\rho}^{(i)}} |\tilde{k}_{2,V}(\eta)| \leq C h^{3-2s}, \quad i = 1, \dots, 4.$$

The proofs of Lemmas 15 to 17 are omitted as they are analogous to the proof of Lemma 10. Finally, the case is considered in which the tetrahedron and the panel have a positive distance

$$d_{t,\tau} := \text{dist}(t, \tau) := \inf_{(x,y) \in t \times \tau} |x - y| > 0,$$

The transformation

$$\mathcal{D}(\eta) := (\mathcal{D}_1(\eta_{1:3}), \mathcal{D}_2(\eta_{4:5})) = \left(\begin{bmatrix} \eta_1 \\ \eta_1 \eta_2 \\ \eta_1 \eta_2 \eta_3 \end{bmatrix}, \begin{bmatrix} \eta_4 \\ \eta_4 \eta_5 \end{bmatrix} \right), \quad \eta \in \mathbb{R}^5,$$

is analytic and we have $\det \mathcal{J}(\eta) = \eta_1^2 \eta_2 \eta_4$. Applying this transformation to (44), we obtain

$$I_{t,\tau} := \int_{[0,1]^5} \tilde{k}_{2,D}(\mathcal{D}(\eta)) \, d\eta \tag{51}$$

with

$$k_{2,D}(\mathcal{D}(\eta)) := \varphi_i(\chi_t(\mathcal{D}_1(\eta))) \varphi_j(\chi_t(\mathcal{D}_1(\eta))) \frac{[\chi_t(\mathcal{D}_1(\eta)) - \chi_{\tau}(\mathcal{D}_2(\eta))]^T n}{|\chi_t(\mathcal{D}_1(\eta)) - \chi_{\tau}(\mathcal{D}_2(\eta))|^{3+2s}} |M_t| |M_{\tau}| \det \mathcal{J}(\eta).$$

Notice that $\tau \in \partial(\text{supp}\varphi \cup \text{supp}\varphi)$ and therefore, it holds that $d_{t,\tau} \approx h$.

Lemma 18. *There exists a constant $\rho > 1/2$ that depends only on $\theta_{\mathcal{T}}$ such that the integrand $\tilde{k}_{2,D}$ can be analytically extended to $\bigcup_{i=1}^5 \mathcal{E}_{\rho}^{(i)}$. It holds that*

$$\sup_{\eta \in \mathcal{E}_{\rho}^{(i)}} |\tilde{k}_{2,D}(\eta)| \leq C h^{3-2s}, \quad i = 1, \dots, 5.$$

Since the proof of Lemma 18 is analogous to the proof of Lemma 14, it is omitted.

4. Error estimates for the integrals

4.2.3. Error estimates for the integrals

First, we start with the integrals of type (22).

Theorem 12. *The approximations of the integrals (33), (38), (41), (42), and (50) by means of a tensor Gauss quadrature converge exponentially w.r.t. number of Gauss points n*

$$|E^n[\tilde{k}_{1,\star}]| \leq C h^{3-2s} (2\rho_\star)^{-2n}$$

with $\rho_\star > 1/2$ and $\star \in \{D, V, E, F, T\}$.

Proof. Lemma 8 shows that the requirement of Theorem 11 is fulfilled for all singularity types and Lemma 10 to Lemma 13 give the corresponding estimates for the integrands. Therefore, we can apply Theorem 11 and obtain the desired results.

Since there is a positive distance between the tetrahedra, the integrand $\tilde{k}_{1,D}$ is obviously analytic. Therefore, Theorem 11 can be applied and by combining it with Lemma 14 we obtain the desired estimate. \square

Notice that for the integral (50) we have a worst-case estimation, since we assume that $d_{t_1, t_2} \approx h$. Second, we consider the integrals of type (23).

Theorem 13. *The approximation of the integrals (45), (46), (47), and (51) by means of a tensor Gauss quadrature converge exponentially w.r.t. the number of Gauss points n*

$$|E^n[\tilde{k}_{2,\star}]| \leq C h^{3-2s} (2\rho_\star)^{-2n}$$

with $\rho_\star > 1/2$ and $\star \in \{D, V, E, F\}$.

Proof. First, we consider the singularity cases. Lemma 9 shows that the requirements of Theorem 11 are fulfilled for all singularity types and Lemma 15 to Lemma 17 provides the corresponding estimates. Therefore, we can apply Theorem 11 and obtain the desired results.

For the non-singular case it is obvious that the integrand $\tilde{k}_{2,D}$ is analytic. Therefore, the requirements of Theorem 11 are fulfilled and Lemma 18 provides the corresponding estimates. \square

4.3. Rules for the number of Gauss points

Since we now have error estimates for the numerical integration, it can be investigated how this error proceeds through the bilinear form. This was first done in [4].

Theorem 14. *Let n_1 and n_2 be the quadrature orders used for touching pairs of tetrahedra and tetrahedron and panel, respectively. Denote by a_Q the resulting approximation to the bilinear form a . Then the consistency error due to the quadrature is bounded by*

$$|a(u, v) - a_Q(u, v)| \leq C(E_1 + E_2) \|u\|_{L^2(\Omega)} \|v\|_{L^2(\Omega)}, \quad u, v \in V_h,$$

where

$$E_1 = h^{-3-2s} (2\rho_1)^{-2n_1} \quad \text{and} \quad E_2 = h^{-2-2s} (2\rho_2)^{-2n_2}$$

with constants $\rho_j > 1/2$, $j = 1, 2$.

4. Error estimates for the integrals

Proof. Let $I := \{1, \dots, N\}$. In [4] it was shown that

$$|a(u, v) - a_Q(u, v)| \leq Ch^{-2d} \left[\max_{t_1, t_2 \in \mathcal{T}} \max_{i, j \in I} |E_{i, j}^{t_1, t_2}| + h \max_{t \in \mathcal{T}, \tau \in \mathcal{P}_{\partial\Omega}} \max_{i, j \in I} |E_{i, j}^{t, \tau}| \right] \|u\|_{L^2(\Omega)} \|v\|_{L^2(\Omega)},$$

where $E_{i, j}^{t_1, t_2}$ and $E_{i, j}^{t, \tau}$ denote the integration error between the integrals $a^{t_1, t_2}(\varphi_i, \varphi_j)$ and $a^{t, \tau}(\varphi_i, \varphi_j)$,

$$a^{t_1, t_2}(\varphi_i, \varphi_j) := \int_{t_1} \int_{t_2} \frac{[\varphi_i(x) - \varphi_i(y)][\varphi_j(x) - \varphi_j(y)]}{|x - y|^{d+2s}} dx dy,$$

$$a^{t, \tau}(\varphi_i, \varphi_j) := \int_t \varphi_i(x) \varphi_j(x) \int_{\tau} \frac{(y - x)^T n_{\tau}}{|x - y|^{d+2s}} ds_y dx,$$

and their approximations, respectively. Theorems 12 to 13 give the corresponding error estimates. \square

Since we know how the integration error affects the bilinear form, we can establish rules for the number of Gaussian points per dimension.

Lemma 19. *The choice of Gauss quadrature rules*

$$n_1 \geq \frac{1}{2}(3 + l + s) \frac{|\log(h)|}{\log(2\rho_1)} \quad \text{and} \quad n_2 \geq \frac{1}{2}(2 + l + s) \frac{|\log(h)|}{\log(2\rho_2)}$$

conserves the convergence rate in Theorem 8.

Proof. In [4] it is already shown that

$$\|u - u_h\|_{\tilde{H}^s(\Omega)} \leq C \left(h^{l-s} |u|_{H^l(\Omega)} + (E_1 + E_2) \|\Pi_h u\|_{L^2(\Omega)} \right),$$

where Π_h is the Scott-Zhang interpolation operator; see [31, 76]. The last step is to choose the number of Gauss points in such a way that the errors E_1 and E_2 in Theorem 14 have the same order of magnitude as the other error, i.e. we require $E_1 \leq h^{l-s}$ and $E_2 \leq h^{l-s}$. \square

Lemma 19 shows that the cost to compute a integral scale as $\mathcal{O}(|\log(h)|)$ per dimension. Since we use a tensor Gauss quadrature, these costs apply for each one-dimensional integral. Obviously, this holds only for the singular integrals and for the nearly singular integrals; i.e. $\text{dist}(t_1, t_2) \approx h$, respectively $\text{dist}(t, \tau) \approx h$. The cost for the nonsingular integrals is constant. The integral is called nonsingular if $\text{dist}(t_1, t_2) > 3h$, respectively $\text{dist}(t, \tau) > 3h$. In Table 3, we present an overview over the costs for the numerical integration for each singularity type.

	nearly singular	vertex	edge	face	tetrahedron
integral (22)	$\mathcal{O}(\log^6(h))$	$\mathcal{O}(\log^5(h))$	$\mathcal{O}(\log^4(h))$	$\mathcal{O}(\log^3(h))$	$\mathcal{O}(\log^2(h))$
integral (23)	$\mathcal{O}(\log^5(h))$	$\mathcal{O}(\log^4(h))$	$\mathcal{O}(\log^3(h))$	$\mathcal{O}(\log^2(h))$	–

Table 3: Costs of the numerical integration

An interesting fact which Table 3 provides is that for fine geometries the nearly singular integrals are more expensive to calculate than the strongly singular integrals. However, for coarse discretizations the costs of the Duffy transformation (see Tables 1 and 2) dominate the costs of the numerical integration.

5. Improved Duffy transformation

In this chapter we want to provide a variant of the Duffy transformation which is more adapted and efficient for the numerical computation than the transformation introduced in Chapter 3. In the two previous chapters the main focus was on lifting the singularity and providing error estimates for the approximation of the emerging integrals, including rules on how to efficiently choose the number of Gaussian points per dimension. Therefore, we have always transformed the tetrahedra interacting with each other into a sum of six-dimensional unit cubes. This procedure is necessary for the error estimates, as we have seen in Chapter 4.

From a computational point of view, however, it does not make any sense to convert two tetrahedra t_1 and t_2 , which have a positive distance between each other, into a six-dimensional unit cube, even if the integral is nearly singular, i.e. $\text{dist}(t_1, t_2) \approx h$. To avoid this geometric blow-up, symmetric cubature rules for tetrahedra and triangles are then used instead of the tensor Gaussian quadrature; see [38, 56, 62, 77, 82, 86]. The advantage is that this potentially reduces the total number of evaluation points for the numerical integration. The idea behind this is well-known. Let n be the number of Gaussian points per dimension, then n^3 is the total number of points for the three-dimensional unit cube. Since the volume of the unit tetrahedron is one sixth of the volume of the three-dimensional unit cube, we take a symmetric cubature rule with at least $n^3/6$ points for the numerical integration. Table 4 shows a list of symmetric cubature formulas of different order with the corresponding number of points. As we can see, there is not a rule for every number of points, but the existing rules meet our requirements.

Order	1	2	3	4	5	6	7	8	9	10	11	12	13	14
points	1	4	8	14	14	24	36	46	61	81	109	140	171	236

Table 4: Number of points for the symmetric cubature rules on the unit tetrahedron

The same ideas are applied to the unit panel. Therefore, we choose symmetric cubature rules for the panel with at least $n^2/4$ points. Analogous to Table 4, Table 5 gives an overview of the symmetric cubature formula for the unit panel. Both tables are from [86].

Order	1	2	3	4	5	6	7	8	9	10	11	12	13	14
points	1	3	6	6	7	12	15	16	19	25	28	33	37	46

Table 5: Number of points for the symmetric cubature rules on unit panel

While the nonlinear transformation is necessary to lift the singularity, the transformation does not have to map to a six-dimensional unit cube. This is due to the fact that only $\det \mathcal{J}(\xi)$ is necessary to lift the singularity. The mapping to the unit cube was mainly there to obtain the error estimates. Therefore, there are still degrees of freedom for the nonlinear transformation w.r.t. η . In the following, we exploit these degrees of freedom for each singularity case by transforming the integration domains not to six-dimensional unit cubes, respectively five-dimensional unit cubes, but

5. Improved Duffy transformation

to a combination for reference elements. This approach gives us two benefits. The first one is that the number of evaluation points for the numerical integration is reduced by avoiding unnecessary geometric blowups. The second benefit is that we can provide a geometric interpretation of what happens to the tetrahedra, respectively the tetrahedron and the panel, after the Duffy transformation.

5.1. Interaction between two tetrahedra

5.1.1. Point singularity

First, we consider the case that the two tetrahedra t_1 and t_2 share a common vertex. In Section 3.2.1 we have already studied this case and found that we need to divide the integration domain into two sub-domains to lift the singularity:

- domain I:

$$\int_0^1 \int_0^{\omega_1} \int_0^{\omega_2} \int_0^{\omega_1} \int_0^{\omega_4} \int_0^{\omega_5} \tilde{k}_1 \left(\begin{bmatrix} \omega_3 \\ \omega_2 - \omega_3 \\ \omega_1 - \omega_2 \end{bmatrix}, \begin{bmatrix} \omega_6 \\ \omega_5 - \omega_6 \\ \omega_4 - \omega_5 \end{bmatrix} \right) d\omega.$$

- domain II:

$$\int_0^1 \int_0^{\omega_1} \int_0^{\omega_2} \int_0^{\omega_1} \int_0^{\omega_4} \int_0^{\omega_5} \tilde{k}_1 \left(\begin{bmatrix} \omega_6 \\ \omega_5 - \omega_6 \\ \omega_4 - \omega_5 \end{bmatrix}, \begin{bmatrix} \omega_3 \\ \omega_2 - \omega_3 \\ \omega_1 - \omega_2 \end{bmatrix} \right) d\omega.$$

The next step is to apply a suitable nonlinear transformation that lifts the singularity. To do so, we inspect again the forking inequality chain of domain I:

$$0 \leq \omega_6 \leq \omega_5 \leq \omega_4 \leq \omega_1 \leq 1 \quad \text{and} \quad 0 \leq \omega_3 \leq \omega_2 \leq \omega_1 \leq 1.$$

Since a separation of the variables already exists, we can take advantage of it. Instead of inflating the problem to the six-dimensional unit cube, we transform it back to the appropriate reference elements, the unit tetrahedron \tilde{t} and the unit panel $\tilde{\tau}$:

$$\xi := \omega_1, \quad \eta_1 := 1 - \omega_2/\omega_1, \quad \eta_2 := \omega_3/\omega_1, \quad \eta_3 := 1 - \omega_4/\omega_1, \quad \eta_4 := 1 - \omega_4/\omega_1 - \omega_5/\omega_1, \quad \eta_5 := \omega_6/\omega_1$$

with $\det \mathcal{J}(\xi, \eta) = \xi^5$. First, we show that this transformation maps the integration domain to the reference elements:

$$\left\{ \begin{array}{l} 0 \leq \omega_2 \leq \omega_1 \\ 0 \leq \omega_3 \leq \omega_2 \end{array} \right\} \Leftrightarrow \left\{ \begin{array}{l} 0 \leq \xi(1 - \eta_1) \leq \xi \\ 0 \leq \xi \eta_2 \leq \xi(1 - \eta_1) \end{array} \right\} \Leftrightarrow \left\{ \begin{array}{l} 0 \leq \eta_1 \leq 1 \\ 0 \leq \eta_2 \leq 1 - \eta_1 \end{array} \right\} \quad (52)$$

and

$$\left\{ \begin{array}{l} 0 \leq \omega_4 \leq \omega_1 \\ 0 \leq \omega_5 \leq \omega_4 \\ 0 \leq \omega_6 \leq \omega_5 \end{array} \right\} \Leftrightarrow \left\{ \begin{array}{l} 0 \leq \eta_3 \leq 1 \\ 0 \leq \eta_4 \leq 1 - \eta_3 \\ 0 \leq \eta_5 \leq 1 - \eta_3 - \eta_4 \end{array} \right\}. \quad (53)$$

With this we obtain for the integral:

$$\int_0^1 \int_{\tilde{\tau}} \int_{\tilde{t}} \tilde{k}_1 \left(\begin{bmatrix} \xi \eta_2 \\ \xi(1 - \eta_1 - \eta_2) \\ \xi \eta_1 \end{bmatrix}, \begin{bmatrix} \xi \eta_5 \\ \xi(1 - \eta_3 - \eta_4 - \eta_5) \\ \xi \eta_4 \end{bmatrix} \right) \det \mathcal{J}(\xi, \eta) d\eta d\xi.$$

5. Improved Duffy transformation

The next step is to repeat the process with domain II and then simplify I_{t_1, t_2} by factoring ξ out of \tilde{k}_1 . The ideas for this are basically the same as in Section 3.2.1. This leads to

$$\begin{aligned} I_{t_1, t_2} &= \frac{1}{5 - 2s} \left(\int_{\tilde{\tau}} \int_{\tilde{t}} \tilde{k}_1(\tilde{\mathcal{D}}_1(\eta)) \, d\eta + \int_{\tilde{t}} \int_{\tilde{\tau}} \tilde{k}_1(\tilde{\mathcal{D}}_2(\eta)) \, d\eta \right) \\ &=: I_{t_1, t_2}[\hat{k}_{1, V}^1] + I_{t_1, t_2}[\hat{k}_{1, V}^2] =: I_{t_1, t_2}[\hat{k}_{1, V}] \end{aligned}$$

with

$$\tilde{\mathcal{D}}_1(\eta) := \left(\begin{bmatrix} \eta_2 \\ 1 - \eta_1 - \eta_2 \\ \eta_1 \end{bmatrix}, \begin{bmatrix} \eta_5 \\ 1 - \eta_3 - \eta_4 - \eta_5 \\ \eta_4 \end{bmatrix} \right) \quad \text{and} \quad \tilde{\mathcal{D}}_2(\eta) := \tilde{\mathcal{D}}_1(\eta)^T.$$

Due to definitions of \tilde{t} and $\tilde{\tau}$ we know that each component of $\tilde{\mathcal{D}}_1^1(\eta)$ and $\tilde{\mathcal{D}}_1^2(\eta)$ is non-negative and

$$\|\tilde{\mathcal{D}}_1^1(\eta)\|_1 = 1 \quad \text{and} \quad \|\tilde{\mathcal{D}}_1^2(\eta)\|_1 = 1 - \eta_3 \geq 0.$$

For $\tilde{\mathcal{D}}_2$ this implies that $\tilde{\mathcal{D}}_2 : \tilde{t} \rightarrow \tilde{t}$ and obviously the mapping is linear and continuous. Therefore it holds that $\chi_t(\tilde{\mathcal{D}}_2(\cdot)) : \tilde{t} \rightarrow t$ is also linear and continuous for all $t \in \mathcal{T}$. Let \tilde{F} be the face of \tilde{t} which is described by

$$\tilde{F} := \{x \in \tilde{t} : \|x\|_1 = 1\}.$$

Then $\tilde{\mathcal{D}}_1$ maps the reference tetrahedron to \tilde{F} . By the analog arguments as before, $\chi_t(\tilde{\mathcal{D}}_1(\cdot))$ is linear and continuous, in particular $\chi_{t_1}(\tilde{\mathcal{D}}_1(\cdot)) : \tilde{t} \rightarrow F$, where F is the side of the tetrahedron opposite the corner point a_{t_1} being the common point of the two tetrahedra. If we now put these insights together and exploit the symmetry between $\tilde{\mathcal{D}}_1$ and $\tilde{\mathcal{D}}_2$, we can now explain the Duffy transformation for the point singularity geometrically: Instead of the interaction of the two tetrahedra, we now let each of the two tetrahedra interact individually with the face of the other tetrahedron which is opposite to the common vertex.

5.1.2. Singularity along an edge

The procedure from the previous section can be applied to the singularity case from Section 3.2.2. First, remember the forking inequality chains of the domains I a) and I b) w.r.t. ω :

$$0 \leq \omega_6 \leq \omega_5 \leq \omega_4 \leq \omega_2 \leq \omega_1 \leq 1 \quad \text{and} \quad 0 \leq \omega_3 \leq \omega_2 \leq \omega_1 \leq 1$$

and

$$0 \leq \omega_6 \leq \omega_5 \leq \omega_2 \leq \omega_1 \leq 1 \quad \text{and} \quad 0 \leq \omega_4 \leq \omega_3 \leq \omega_2 \leq \omega_1 \leq 1.$$

Here, we use a nonlinear transformation to map the domains back to suitable reference elements. The transformation is done in the same way as in (52) and (53).

- I a):

$$\xi_1 := \omega_1, \quad \xi_2 := \omega_2/\omega_1, \quad \eta_1 := \omega_3/\omega_2, \quad \eta_2 := 1 - \omega_4/\omega_2, \quad \eta_3 := 1 - \omega_4/\omega_2 - \omega_5/\omega_2, \quad \eta_4 := \omega_6/\omega_2,$$

$$\int_{[0,1]^2} \int_0^1 \int_{\tilde{t}} \tilde{k}_1 \left(\begin{bmatrix} 1 - \xi_1 \\ \xi_1 \xi_2 \eta_1 \\ \xi_1 \xi_2 (1 - \eta_1) \end{bmatrix}, \begin{bmatrix} 1 - \xi_1 + \xi_1 \xi_2 \eta_4 \\ \xi_1 \xi_2 (1 - \eta_2 - \eta_3 - \eta_4) \\ \xi_1 \xi_2 \eta_3 \end{bmatrix} \right) \det \mathcal{J}(\xi, \eta) \, d\eta \, d\xi$$

5. Improved Duffy transformation

• I b):

$$\xi_1 := \omega_1, \quad \xi_2 := \omega_2/\omega_1, \quad \eta_1 := 1 - \omega_3/\omega_2, \quad \eta_2 := \omega_4/\omega_2, \quad \eta_3 := 1 - \omega_5/\omega_2, \quad \eta_4 := \omega_6/\omega_2,$$

$$\int_{[0,1]^2} \int_{\tilde{\tau}} \int_{\tilde{\tau}} \tilde{k}_1 \left(\begin{bmatrix} 1 - \xi_1 & & & \\ \xi_1 \xi_2 \eta_4 & & & \\ \xi_1 \xi_2 (1 - \eta_3 - \eta_4) & & & \end{bmatrix}, \begin{bmatrix} 1 - \xi_1 + \xi_1 \xi_2 \eta_2 & & & \\ \xi_1 \xi_2 (1 - \eta_1 - \eta_2) & & & \\ \xi_1 \xi_2 \eta_1 & & & \end{bmatrix} \right) \det \mathcal{J}(\xi, \eta) \, d\eta \, d\xi$$

In both cases, it holds that $\det \mathcal{J}(\xi, \eta) = \xi_1^5 \xi_2^4$. Using the same ideas and tricks as in Section 3.2.2 to simplify the integrals, we obtain

$$\begin{aligned} I_{t_1, t_2} &= \frac{1}{5 - 2s} \frac{1}{4 - 2s} \left(\int_{[0,1]} \int_{\tilde{t}} \tilde{k}_1(\tilde{\mathcal{D}}_1(\eta)) + \tilde{k}_1(\tilde{\mathcal{D}}_3(\eta)) \, d\eta + \int_{\tilde{\tau}} \int_{\tilde{\tau}} \tilde{k}_1(\tilde{\mathcal{D}}_2(\eta)) + \tilde{k}_1(\tilde{\mathcal{D}}_4(\eta)) \, d\eta \right) \\ &=: \sum_{m=1}^4 I_{t_1, t_2}[\hat{k}_{1,E}^m] =: I_{t_1, t_2}[\hat{k}_{1,E}], \end{aligned}$$

where $\tilde{\mathcal{D}}_m$ is the Duffy transformation of the m -th domain to the reference elements with

$$\tilde{\mathcal{D}}_1 = \left(\begin{bmatrix} 0 \\ \eta_1 \\ 1 - \eta_1 \end{bmatrix}, \begin{bmatrix} \eta_4 \\ 1 - \eta_2 - \eta_3 - \eta_4 \\ \eta_3 \end{bmatrix} \right) \quad \text{and} \quad \tilde{\mathcal{D}}_2 = \left(\begin{bmatrix} 0 \\ \eta_4 \\ 1 - \eta_3 - \eta_4 \end{bmatrix}, \begin{bmatrix} \eta_2 \\ 1 - \eta_1 - \eta_2 \\ \eta_1 \end{bmatrix} \right).$$

The two remaining cases $\tilde{\mathcal{D}}_3$ and $\tilde{\mathcal{D}}_4$ are again due to symmetry

$$\tilde{\mathcal{D}}_3(\eta) := \tilde{\mathcal{D}}_1(\eta)^T \quad \text{and} \quad \tilde{\mathcal{D}}_4(\eta) := \tilde{\mathcal{D}}_2(\eta)^T.$$

First, we consider $\tilde{\mathcal{D}}_1$. Due to definitions of \tilde{t} we know that each component of $\tilde{\mathcal{D}}_1^1(\eta)$ and $\tilde{\mathcal{D}}_1^2(\eta)$ is non-negative and

$$\|\tilde{\mathcal{D}}_1^1(\eta)\|_1 = 1 \quad \text{and} \quad \|\tilde{\mathcal{D}}_1^2(\eta)\|_1 = 1 - \eta_2 \geq 0.$$

For $\tilde{\mathcal{D}}_1^2$ this implies that $\tilde{\mathcal{D}}_1^2 : \tilde{t} \rightarrow \tilde{t}$ and obviously the mapping is linear and continuous. Therefore it holds that $\chi_t(\tilde{\mathcal{D}}_1^2(\cdot)) : \tilde{t} \rightarrow t$ is also linear and continuous for all $t \in \mathcal{T}$. For $\tilde{\mathcal{D}}_1^1$ the situation is a bit more complicated. Let us first interpret $\tilde{\mathcal{D}}_1^1$ as a mapping of the interval $[0, 1]$ to \tilde{t} , i.e. $\tilde{\mathcal{D}}_1^1 : [0, 1] \rightarrow \tilde{t}$. Since $\|\tilde{\mathcal{D}}_1^1(\eta)\|_1 = 1$, $\tilde{\mathcal{D}}_1^1$ maps the interval to the boundary of the tetrahedron. To be more precise, the interval is mapped to the edge between the vertices $(0, 1, 0)^T$ and $(0, 0, 1)^T$. If we now additionally consider the mapping χ_{t_1} , this means that $\chi_{t_1}(\tilde{\mathcal{D}}_1^1(\cdot))$ maps the interval $[0, 1]$ to the edge of the tetrahedron t_1 , which is between the corner points c_{t_1} and d_{t_1} . This edge of the tetrahedron is the edge, which has the biggest distance to the edge where the singularity is located. Therefore, we can interpret the case $\tilde{\mathcal{D}}_1$ as the interaction between the tetrahedron t_2 and the edge $[c_{t_1}, d_{t_1}]$.

Second, we have a look at $\tilde{\mathcal{D}}_2$. The consideration of $\tilde{\mathcal{D}}_2^2$ is analogous to $\tilde{\mathcal{D}}_1^2$ from Section 5.1.1. $\chi_{t_2}(\tilde{\mathcal{D}}_2^2(\cdot))$ maps $\tilde{\tau}$ to the face of the tetrahedron t_2 enclosed by the corner points b_{t_2}, c_{t_2} and d_{t_2} . Since $\|\tilde{\mathcal{D}}_2^1(\eta)\|_1 \leq 1$ and since the first component of $\tilde{\mathcal{D}}_2^1$ is zero, we conclude that $\chi_{t_1}(\tilde{\mathcal{D}}_2^1(\cdot))$ maps the unit panel to the face of the tetrahedron t_1 enclosed by the corner points a_{t_2}, b_{t_2} and c_{t_2} . Since

5. Improved Duffy transformation

the singularity is chosen such that $a_{t_1} = a_{t_2}$ and $b_{t_1} = b_{t_2}$, we can interpret $\tilde{\mathcal{D}}_1$ as the interaction between the faces of the two tetrahedra t_1 and t_2 which have the biggest distance between each other.

Altogether, we can interpret that after the Duffy transformation the interaction of the tetrahedra is decomposed into two interactions and their symmetric counterparts. The first one is the interaction of one tetrahedron with the edge of the other tetrahedron which is opposite to the common edge of both tetrahedra and the second one is that only an edge of each tetrahedron interact with each other. These edges are characterized by the fact that they are the ones that are farthest from each other and are still connected through the edge over which the singularity is defined.

5.1.3. Singularity on a face

For this singularity case it is not always possible to find a geometrical interpretation. The issue is that a clear splitting of the variables on the individual domains is missing. The reason for this is that the forking inequality chains degenerate to one inequality chain, i.e.

$$0 \leq \omega_6 \leq \omega_5 \leq \omega_4 \leq \omega_3 \leq \omega_2 \leq \omega_1 \leq 1.$$

Since there is no split up, we cannot map the integration domain w.r.t. η into two independent reference elements. For the first fifteen domains of the domains we use the following nonlinear transformation:

$$\begin{aligned} \xi_1 &:= \omega_1, & \xi_2 &:= \omega_2/\omega_1, & \xi_3 &:= \omega_3/\omega_2, \\ \eta_1 &:= 1 - \omega_4/\omega_3, & \eta_2 &:= 1 - \omega_4/\omega_3 - \omega_5/\omega_3, & \eta_3 &:= 1 - \omega_4/\omega_3 - \omega_5/\omega_3 - \omega_6/\omega_3, \end{aligned}$$

with $\det \mathcal{J}(\xi, \eta) = \xi_1^5 \xi_2^4 \xi_3^3$. By applying the ideas and tricks from Section 3.2.3, the integrals can be simplified to

$$\prod_{j=0}^2 \frac{1}{5-j-2s} \int_{\tilde{t}} \tilde{k}_1(\tilde{\mathcal{D}}_m(\eta)) \, d\eta,$$

where,

$$\begin{aligned} \tilde{\mathcal{D}}_1(\eta) &:= \left(\begin{bmatrix} 0 \\ 1 - \eta_1 \\ \eta_1 \end{bmatrix}, \begin{bmatrix} 1 - \eta_1 - \eta_2 - \eta_3 \\ 0 \\ \eta_3 \end{bmatrix} \right), & \tilde{\mathcal{D}}_2(\eta) &:= \left(\begin{bmatrix} 0 \\ 1 - \eta_1 - \eta_2 \\ \eta_2 \end{bmatrix}, \begin{bmatrix} 1 - \eta_1 - \eta_2 - \eta_3 \\ 0 \\ \eta_1 + \eta_2 + \eta_3 \end{bmatrix} \right), \\ \tilde{\mathcal{D}}_3(\eta) &:= \left(\begin{bmatrix} 0 \\ 1 - \eta_1 - \eta_2 \\ \eta_1 + \eta_2 \end{bmatrix}, \begin{bmatrix} 1 - \eta_1 - \eta_2 - \eta_3 \\ 0 \\ \eta_2 + \eta_3 \end{bmatrix} \right), & \tilde{\mathcal{D}}_4(\eta) &:= \left(\begin{bmatrix} 0 \\ 1 - \eta_1 - \eta_2 - \eta_3 \\ \eta_3 \end{bmatrix}, \begin{bmatrix} 1 - \eta_1 \\ 0 \\ \eta_1 \end{bmatrix} \right), \\ \tilde{\mathcal{D}}_5(\eta) &:= \left(\begin{bmatrix} 0 \\ 1 - \eta_1 - \eta_2 - \eta_3 \\ \eta_2 + \eta_3 \end{bmatrix}, \begin{bmatrix} 1 - \eta_1 - \eta_2 \\ 0 \\ \eta_1 + \eta_2 \end{bmatrix} \right), & \tilde{\mathcal{D}}_6(\eta) &:= \left(\begin{bmatrix} 0 \\ 1 - \eta_1 - \eta_2 - \eta_3 \\ \eta_1 + \eta_2 + \eta_3 \end{bmatrix}, \begin{bmatrix} 1 - \eta_1 - \eta_2 \\ 0 \\ \eta_2 \end{bmatrix} \right), \\ \tilde{\mathcal{D}}_7(\eta) &:= \left(\begin{bmatrix} 0 \\ 0 \\ 1 \end{bmatrix}, \begin{bmatrix} 1 - \eta_1 - \eta_2 - \eta_3 \\ \eta_3 \\ \eta_2 \end{bmatrix} \right), & \tilde{\mathcal{D}}_{15}(\eta) &:= \left(\begin{bmatrix} 1 - \eta_1 - \eta_2 - \eta_3 \\ \eta_3 \\ \eta_1 + \eta_2 \end{bmatrix}, \begin{bmatrix} 0 \\ 0 \\ 1 - \eta_1 \end{bmatrix} \right). \end{aligned}$$

The seven remaining cases are the symmetrical version of $\tilde{\mathcal{D}}_i, i = 1, \dots, 7$, i.e.

$$\tilde{\mathcal{D}}_{7+i}(\eta) = \tilde{\mathcal{D}}_i^T(\eta) \text{ for } i = 1, \dots, 7.$$

5. Improved Duffy transformation

As it can be clearly seen, on the one hand from the integration domain and on the other hand from the integrand itself, there is no longer a clear separation into two independent domains as in the previous cases, the point singularity and the singularity along a common edge. This is due to the resolution of the min and max conditions; see (39). Because of the fine splitting, the individual sub-domains are so strongly structured that the variables can be arranged into a single inequality chain.

While we can still trace where \mathcal{D}_1^1 and \mathcal{D}_1^2 map the corresponding reference element to, w.r.t. integration there is a dependency here. Thus, $\chi_{t_1}(\mathcal{D}_1^1(\cdot))$ maps the one-dimensional unit interval to the edge between vertices c_{t_1} and d_{t_1} , while $\chi_{t_2}(\mathcal{D}_1^2(\cdot))$ maps the unit tetrahedron to the side of the tetrahedron t_2 enclosed by the vertices a_{t_2}, c_{t_2} and d_{t_2} . The analogous statements and the same nonlinear transformation also apply to most of the remaining sub-domains.

Only the seventh domain and its symmetric version, the fourteenth domain, are the exemption. This is because $\tilde{\mathcal{D}}_7^1$ does not depend on η . With the experience from Sections 5.1.1 and 5.1.2, we quickly observe that from a geometrical point of view the vertex d_{t_1} interacts with the tetrahedron t_2 , respectively the vertex d_{t_2} interacts with the tetrahedron t_1 .

The remaining two cases behave differently, since there are actual forking inequality chains. First, consider the sixteenth domain,

$$0 \leq w_6 \leq \omega_3 \leq \omega_2 \leq \omega_1 \leq 1 \quad \text{and} \quad 0 \leq \omega_5 \leq \omega_4 \leq \omega_3 \leq \omega_2 \leq \omega_1 \leq 1,$$

and adjust the nonlinear transformation to the inequality chain:

$$\xi_1 := \omega_1, \quad \xi_2 := \omega_2/\omega_1, \quad \xi_3 := \omega_3/\omega_2, \quad \eta_1 := 1 - \omega_4/\omega_3, \quad \eta_2 := 1 - \omega_4/w_3 - \omega_5/\omega_3, \quad \eta_3 := w_6/\omega_3,$$

$$\prod_{j=0}^2 \frac{1}{5-j-2s} \int_{\tilde{\tau}} \int_0^1 \tilde{k}_1(\tilde{\mathcal{D}}_{16}(\eta)) d\eta, \quad \tilde{\mathcal{D}}_{16}(\eta) := \left(\begin{bmatrix} 0 \\ 0 \\ \eta_3 \end{bmatrix}, \begin{bmatrix} 1 - \eta_1 - \eta_2 \\ \eta_2 \\ \eta_1 \end{bmatrix} \right),$$

with $\det \mathcal{J}(\xi, \eta) = \xi_1^5 \xi_2^4 \xi_3^3$. This case can be interpreted as the interaction between the edge between the vertices a_{t_1} and d_{t_2} and the face of the tetrahedron t_2 enclosed by the vertices b_{t_2}, c_{t_2} and d_{t_2} .

The last domain is more complicated, since the forking inequality chain splits up after ω_4 :

$$0 \leq \omega_6 \leq \omega_4 \leq \omega_3 \leq \omega_2 \leq w_1 \leq 1 \quad \text{and} \quad 0 \leq \omega_5 \leq \omega_4 \leq \omega_3 \leq \omega_2 \leq w_1 \leq 1$$

Although we can transform the domain to suitable reference elements, the Jacobi determinant is then no longer independent of η , since the splitting happens only after ω_4 :

$$\xi_1 := \omega_1, \quad \xi_2 := \omega_2/\omega_1, \quad \xi_3 := \omega_3/\omega_2, \quad \eta_1 := 1 - \omega_4/\omega_3, \quad \eta_2 := 1 - \omega_4/w_3 - \omega_5/\omega_3, \quad \eta_3 := w_6/\omega_4,$$

$$\prod_{j=0}^2 \frac{1}{5-j-2s} \int_{\tilde{\tau}} \int_0^1 \tilde{k}_1(\tilde{\mathcal{D}}_{17}(\eta)) (1 - \eta_1) d\eta, \quad \tilde{\mathcal{D}}_{17}(\eta) := \left(\begin{bmatrix} 1 - \eta_1 - \eta_2 \\ \eta_2 \\ \eta_1 \end{bmatrix}, \begin{bmatrix} 0 \\ 0 \\ (1 - \eta_1) \eta_3 \end{bmatrix} \right),$$

with $\det \mathcal{J}(\xi, \eta) = \xi_1^5 \xi_2^4 \xi_3^3 (1 - \eta_1)$. In total, we obtain

$$\begin{aligned} I_{t_1, t_2} &= \prod_{j=0}^2 \frac{1}{5-j-2s} \left(\int_{\tilde{\tau}} \sum_{m=1}^{15} \tilde{k}_1(\tilde{\mathcal{D}}_m(\eta)) d\eta + \int_{\tilde{\tau}} \int_0^1 \tilde{k}_1(\tilde{\mathcal{D}}_{16}(\eta)) + k_1(\tilde{\mathcal{D}}_{17}(\eta)) (1 - \eta_1) d\eta \right) \\ &=: \sum_{m=1}^{17} I_{t_1, t_2}[\hat{k}_{1, F}^m] =: I_{t_1, t_2}[\hat{k}_{1, F}]. \end{aligned}$$

5. Improved Duffy transformation

The higher the degree of the singularity, the more complicated it is to make statements about the geometry, since after application of the nonlinear transformation the domains are interdependent.

5.1.4. Two identical tetrahedra

Here, we consider the case where the two tetrahedra are identical and we omit the index. In Section 3.2.4, we have already seen that after the min and max conditions are resolved, the sub-domains are very well structured. By this we mean that almost all domains satisfy a single inequality chain w.r.t. the variables ω . Thus, these sub-domains can also be processed with the same nonlinear transformation:

$$\xi_1 := \omega_1, \quad \xi_2 := \omega_2/\omega_1, \quad \xi_3 := \omega_3/\omega_2, \quad \xi_4 := \omega_4/\omega_3, \quad \eta_1 := 1 - \omega_5/\omega_4, \quad \eta_2 := w_6/\omega_4,$$

$$\prod_{j=0}^3 \frac{1}{5-j-2s} \int_{\tilde{\tau}} \tilde{k}_1(\tilde{\mathcal{D}}_m(\eta)) d\eta,$$

where $\det \mathcal{J}(\xi, \eta) = \xi_1^5 \xi_2^4 \xi_3^3$ and

$$\begin{aligned} \tilde{\mathcal{D}}_1(\eta) &:= \left(\begin{bmatrix} 0 \\ 1 - \eta_1 \\ \eta_1 \end{bmatrix}, \begin{bmatrix} \eta_2 \\ 0 \\ 0 \end{bmatrix} \right), & \tilde{\mathcal{D}}_2(\eta) &:= \left(\begin{bmatrix} 0 \\ 1 \\ 0 \end{bmatrix}, \begin{bmatrix} \eta_2 \\ 0 \\ 1 - \eta_1 - \eta_2 \end{bmatrix} \right), \\ \tilde{\mathcal{D}}_3(\eta) &:= \left(\begin{bmatrix} 0 \\ 1 - \eta_1 \\ -1 \end{bmatrix}, \begin{bmatrix} \eta_2 \\ 0 \\ \eta_2 \end{bmatrix} \right), & \tilde{\mathcal{D}}_4(\eta) &:= \left(\begin{bmatrix} 0 \\ \eta_2 \\ -\eta_2 \end{bmatrix}, \begin{bmatrix} 1 - \eta_1 \\ 0 \\ -1 \end{bmatrix} \right), \\ \tilde{\mathcal{D}}_5(\eta) &:= \left(\begin{bmatrix} 0 \\ \eta_2 \\ 1 - \eta_1 - \eta_2 \end{bmatrix}, \begin{bmatrix} 1 \\ 0 \\ 0 \end{bmatrix} \right), & \tilde{\mathcal{D}}_6(\eta) &:= \left(\begin{bmatrix} 0 \\ \eta_2 \\ 0 \end{bmatrix}, \begin{bmatrix} 1 - \eta_1 \\ 0 \\ \eta_2 \end{bmatrix} \right), \\ \tilde{\mathcal{D}}_7(\eta) &:= \left(\begin{bmatrix} 0 \\ 0 \\ 0 \end{bmatrix}, \begin{bmatrix} \eta_2 \\ 1 - \eta_1 - \eta_2 \\ -1 \end{bmatrix} \right), & \tilde{\mathcal{D}}_8(\eta) &:= \left(\begin{bmatrix} 0 \\ 0 \\ 0 \end{bmatrix}, \begin{bmatrix} \eta_2 \\ 1 - \eta_1 - \eta_2 \\ \eta_1 \end{bmatrix} \right), \end{aligned}$$

and the sub-domains 10 to 17 are again the symmetric versions of the first eight domains, i.e.

$$\tilde{\mathcal{D}}_{m+9}(\eta) = \tilde{\mathcal{D}}_m(\eta)^T, \quad m = 1, \dots, 8.$$

The remaining two sub-domains behave different because there are real forking inequality chains:

$$\xi_1 := \omega_1, \quad \xi_2 := \omega_2/\omega_1, \quad \xi_3 := \omega_3/\omega_2, \quad \xi_4 := \omega_4/\omega_3, \quad \eta_1 := \omega_5/\omega_4, \quad \eta_3 := w_6/\omega_4,$$

$$\prod_{j=0}^3 \frac{1}{5-j-2s} \int_{(0,1)^2} \tilde{k}_1(\tilde{\mathcal{D}}_9(\eta)) + \tilde{k}_1(\tilde{\mathcal{D}}_{18}(\eta)) d\eta, \quad \tilde{\mathcal{D}}_9(\eta) := \left(\begin{bmatrix} 0 \\ 1 - \eta_1 \\ \eta_1 \end{bmatrix}, \begin{bmatrix} \eta_2 \\ 1 - \eta_2 \\ 0 \end{bmatrix} \right)$$

5. Improved Duffy transformation

where $\tilde{\mathcal{D}}_{18}(\eta) := \tilde{\mathcal{D}}_9(\eta)^T$ and $\det \mathcal{J}(\xi, \eta) = \xi_1^5 \xi_2^4 \xi_3^3$. In total, this leads to

$$\begin{aligned} I_{t,t} &= 2 \prod_{j=0}^3 \frac{1}{5-j-2s} \left(\int_{\tilde{\tau}} \sum_{m=1}^8 \tilde{k}_1(\tilde{\mathcal{D}}_m(\eta)) d\eta + \int_{(0,1)^2} \tilde{k}_1(\tilde{\mathcal{D}}_9(\eta)) d\eta \right) \\ &=: \sum_{m=1}^9 I_{t,t}[\hat{k}_{1,T}^m] =: I_{t,t}[\hat{k}_{1,T}]. \end{aligned}$$

Because the domains are so highly structured, a geometric interpretation is not possible for all domains except three: For example consider domain 5, the interaction of the tetrahedron with itself can be interpreted as the interaction of the vertex b_t with the face enclosed by the vertices a_t, c_t and d_t . For domain 8, we see that the vertex a_t interacts with the face opposite to a_t . For domain 9 the Duffy transformation leads to the observation that instead of the tetrahedron the two edges, which run between the vertices c_t and d_t , and b_t and c_t , are treated.

5.2. Interaction between a tetrahedron and a panel

5.2.1. Point singularity

We start with the case that the tetrahedron t and the panel τ have a common vertex. This case has been studied in Section 3.3.1 and a division of the integration domain is necessary in order to lift the singularity. Both domains, I and II, satisfy a suitable forking inequality chain:

$$0 \leq \omega_5 \leq \omega_4 \leq \omega_1 \leq 1 \quad \text{and} \quad 0 \leq \omega_3 \leq \omega_2 \leq \omega_1 \leq 1,$$

and

$$0 \leq \omega_5 \leq \omega_4 \leq \omega_3 \leq \omega_1 \quad \text{and} \quad 0 \leq \omega_2 \leq \omega_1.$$

Similar to Section 5.1.1, a nonlinear transformation is used to map the two domains to matching reference elements:

- domain I:

$$\xi := \omega_1, \quad \eta_1 := 1 - \omega_2/\omega_1, \quad \eta_2 := \omega_3/\omega_1, \quad \eta_3 := 1 - \omega_4/\omega_1, \quad \eta_4 := \omega_5/\omega_1,$$

$$\int_0^1 \int_{\tilde{\tau}} \int_{\tilde{\tau}} \tilde{k}_2 \left(\left(\begin{array}{c} \xi \eta_2 \\ \xi (1 - \eta_1 - \eta_2) \\ \xi \eta_1 \end{array} \right), \left(\begin{array}{c} \xi \eta_4 \\ \xi (1 - \eta_3 - \eta_4) \end{array} \right) \right) \det \mathcal{J}(\xi, \eta) d\eta d\xi.$$

- domain II:

$$\xi := \omega_1, \quad \eta_1 := \omega_2/\omega_1, \quad \eta_2 := 1 - \omega_3/\omega_1, \quad \eta_3 := 1 - \omega_3/\omega_1 - \omega_4/\omega_1, \quad \eta_4 := \omega_5/\omega_1,$$

$$\int_0^1 \int_0^1 \int_{\tilde{\tau}} \tilde{k}_2 \left(\left(\begin{array}{c} \xi \eta_4 \\ \xi (1 - \eta_2 - \eta_3 - \eta_4) \\ \xi \eta_3 \end{array} \right), \left(\begin{array}{c} \xi \eta_1 \\ \xi (1 - \eta_1) \end{array} \right) \right) \det \mathcal{J}(\xi, \eta) d\eta d\xi.$$

5. Improved Duffy transformation

For both cases it holds that $\det \mathcal{J}_1(\xi, \eta) = \xi^4$. Using the tricks and ideas of Section 3.3.1 the integrals can be simplified to

$$I_{t,\tau} = \frac{1}{4-2s} \left(\int_{\tilde{\tau}} \int_{\tilde{\tau}} \tilde{k}_2(\tilde{\mathcal{D}}_1(\eta)) \, d\eta + \int_0^1 \int_{\tilde{t}} \tilde{k}_2(\tilde{\mathcal{D}}_2(\eta)) \, d\eta \right) =: I_{t,\tau}[\hat{k}_{2,V}^1] + I_{t,\tau}[\hat{k}_{2,V}^1] =: I_{t,\tau}[\hat{k}_{2,V}],$$

where

$$\tilde{\mathcal{D}}_1(\eta) := \left(\begin{bmatrix} \eta_2 \\ 1 - \eta_1 - \eta_2 \\ \eta_1 \end{bmatrix}, \begin{bmatrix} \eta_4 \\ 1 - \eta_3 - \eta_4 \end{bmatrix} \right) \quad \text{and} \quad \tilde{\mathcal{D}}_2(\eta) := \left(\begin{bmatrix} \eta_4 \\ 1 - \eta_2 - \eta_3 - \eta_4 \\ \eta_3 \end{bmatrix}, \begin{bmatrix} \eta_1 \\ 1 - \eta_1 \end{bmatrix} \right).$$

Since there is a clear separation of the geometry, we can explain the Duffy transformation geometrically. With the prior knowledge from Section 5.1.1, we see that after the Duffy transformation the interaction between the tetrahedron and the panel is split up into two parts. In the first part the panel interacts with the face of the tetrahedron which is opposed to the common vertex and in the second part the tetrahedron interacts with the edge of the panel opposite the common vertex.

5.2.2. Singularity along an edge

Here, the case is considered that the tetrahedron t and the panel τ share a common edge. According to Section 3.3.2 the integration has to be split up in four sub-domains in order to lift the singularity:

$$I_{t,\tau} = \int_0^1 \int_0^{\omega_1} \int_0^{\omega_2} \int_0^{\omega_2} \int_0^{\omega_4} \sum_{m=1}^3 \tilde{k}_2(\mathcal{Q}_m(\omega)) \, d\omega + \int_0^1 \int_0^{\omega_1} \int_0^{\omega_2} \int_0^{\omega_3} \int_0^{\omega_4} \tilde{k}_2(\mathcal{Q}_4(\omega)) \, d\omega,$$

where

$$\begin{aligned} \mathcal{Q}_1 &:= \left(\begin{bmatrix} 1 - \omega_1 \\ \omega_3 \\ \omega_2 - \omega_3 \end{bmatrix}, \begin{bmatrix} 1 - \omega_1 + \omega_5 \\ \omega_4 - \omega_5 \end{bmatrix} \right), & \mathcal{Q}_2 &:= \left(\begin{bmatrix} 1 - \omega_1 \\ \omega_5 \\ \omega_4 - \omega_5 \end{bmatrix}, \begin{bmatrix} 1 - \omega_1 + \omega_3 \\ \omega_2 - \omega_3 \end{bmatrix} \right), \\ \mathcal{Q}_3 &:= \left(\begin{bmatrix} 1 - \omega_1 + \omega_5 \\ \omega_4 - \omega_5 \\ \omega_2 - \omega_4 \end{bmatrix}, \begin{bmatrix} 1 - \omega_1 \\ \omega_3 \end{bmatrix} \right), & \mathcal{Q}_4 &:= \left(\begin{bmatrix} 1 - \omega_1 + \omega_5 \\ \omega_4 - \omega_5 \\ \omega_3 - \omega_4 \end{bmatrix}, \begin{bmatrix} 1 - \omega_1 \\ \omega_2 \end{bmatrix} \right). \end{aligned}$$

Next, we exploit the structure of the integration domains to map the sub-domains to matching reference elements. For the first three ones this leads to

$$\xi_1 := \omega_1, \quad \xi_2 := \omega_2/\omega_1, \quad \eta_1 := \omega_3/\omega_2, \quad \eta_2 := 1 - \omega_4/\omega_2, \quad \eta_3 := \omega_5/\omega_2,$$

and for the fourth sub-domain, we obtain that

$$\xi_1 := \omega_1, \quad \xi_2 := \omega_2/\omega_1, \quad \eta_1 := 1 - \omega_3/\omega_2, \quad \eta_2 := 1 - \omega_3/\omega_2 - \omega_4/\omega_2, \quad \eta_3 := \omega_5/\omega_2.$$

Note that in each case it holds that $\det \mathcal{J}(\xi, \eta) = \xi_1^4 \xi_2^3$. By applying the same tricks and ideas from Section 3.3.2, $I_{t,\tau}$ simplifies to

$$I_{t,\tau} = \frac{1}{5-2s} \frac{1}{4-2s} \left(\int_{[0,1]} \int_{\tilde{\tau}} \sum_{m=1}^3 \tilde{k}_2(\tilde{\mathcal{D}}_m(\eta)) \, d\eta + \int_{\tilde{t}} \tilde{k}_2(\tilde{\mathcal{D}}_4(\eta)) \, d\eta \right) =: \sum_{m=1}^4 I_{t,\tau}[\hat{k}_{2,E}^m] =: I_{t,\tau}[\hat{k}_{2,E}],$$

5. Improved Duffy transformation

where

$$\begin{aligned}\tilde{\mathcal{D}}_1 &:= \left(\begin{bmatrix} 0 \\ \eta_1 \\ 1 - \eta_1 \end{bmatrix}, \begin{bmatrix} \eta_3 \\ 1 - \eta_2 - \eta_3 \end{bmatrix} \right), & \tilde{\mathcal{D}}_2 &:= \left(\begin{bmatrix} 0 \\ \eta_3 \\ 1 - \eta_2 - \eta_3 \end{bmatrix}, \begin{bmatrix} \eta_1 \\ 1 - \eta_1 \end{bmatrix} \right), \\ \tilde{\mathcal{D}}_3 &:= \left(\begin{bmatrix} \eta_3 \\ 1 - \eta_2 - \eta_3 \\ \eta_2 \end{bmatrix}, \begin{bmatrix} 0 \\ \eta_1 \end{bmatrix} \right), & \tilde{\mathcal{D}}_4 &:= \left(\begin{bmatrix} \eta_3 \\ 1 - \eta_1 - \eta_2 - \eta_3 \\ \eta_2 \end{bmatrix}, \begin{bmatrix} 0 \\ 1 \end{bmatrix} \right).\end{aligned}$$

As it can be seen, due to the forking inequality chains, there is a strict separation of the geometry in each sub-domain, which makes a geometric interpretation of the Duffy transformation possible. With the knowledge from the previous sections, we can quickly see what became of the tetrahedron t and the panel τ . First, consider the first sub-domain. There, the panel τ interacts with edge of t which is between the vertices c_t and d_t . This edge is the edge of t which has the biggest distance to the singularity. For the second sub-domain the interaction of t and τ becomes after the Duffy transformation the interaction between the face of t enclosed by a_t , c_t and d_t , and an edge of τ enclosed by b_τ and c_τ . These two geometries are connected by the edge along which the singularity resides. The case of the third sub-domain can be interpreted as the symmetric version of the case of the second domain. The Duffy transformation resolves the original interaction to the interaction between the face of t described by the vertices b_t , c_t and d_t and the edge of τ which is located between a_τ and b_τ . The last sub-domain is a little special, since after the Duffy transformation the complete tetrahedron t still interacts with a part of the panel τ , to be more precise t interacts with the vertex c_τ .

5.2.3. Singularity on a face

As the last case, we consider that the panel τ is a face of the tetrahedron t . Since this singularity case was already discussed in detail in Section 3.3.3, we provide only a brief summary,

$$I_{t,\tau} = \int_0^1 \int_0^{\omega_1} \int_0^{\omega_2} \int_0^{\omega_3} \int_0^{\omega_4} \sum_{m=1}^8 \tilde{k}_2(\mathcal{Q}_m(\omega)) d\omega + \int_0^1 \int_0^{\omega_1} \int_0^{\omega_2} \int_0^{\omega_3} \int_0^{\omega_3} \tilde{k}_2(\mathcal{Q}_9(\omega)) d\omega,$$

before we apply the nonlinear transformation to suitable reference elements. For the first eight sub-domains we use

$$\xi_1 := \omega_1, \quad \xi_2 := \omega_2/\omega_1, \quad \xi_3 := \omega_3/\omega_2, \quad \eta_1 := 1 - \omega_4/\omega_3, \quad \eta_2 := \omega_5/\omega_3$$

and for the last sub-domain

$$\xi_1 := \omega_1, \quad \xi_2 := \omega_2/\omega_1, \quad \xi_3 := \omega_3/\omega_2, \quad \eta_1 := \omega_4/\omega_3, \quad \eta_2 := \omega_5/\omega_3.$$

In each case it holds that $\det J(\xi, \eta) = \xi_1^4 \xi_2^3 \xi_3^2$. By applying the same tricks as in Section 3.3.3 this leads to

$$I_{t,\tau} = \prod_{j=0}^2 \frac{1}{5 - j - 2s} \left(\int_{\tilde{\tau}} \sum_{m=1}^8 \tilde{k}_2(\tilde{\mathcal{D}}_m(\omega)) d\omega + \int_{[0,1]^2} \tilde{k}_2(\tilde{\mathcal{D}}_9(\omega)) d\omega \right) =: \sum_{m=1}^9 I_{t,\tau}[\hat{k}_{2,F}^m] =: I_{t,\tau}[\hat{k}_{2,F}],$$

5. Improved Duffy transformation

where

$$\begin{aligned}
\tilde{\mathcal{D}}_1(\omega) &= \left(\begin{bmatrix} 0 \\ 1 - \eta_1 \\ \eta_1 \end{bmatrix}, \begin{bmatrix} \eta_2 \\ 0 \end{bmatrix} \right), & \tilde{\mathcal{D}}_2(\omega) &= \left(\begin{bmatrix} 0 \\ \eta_2 \\ 1 - \eta_1 - \eta_2 \end{bmatrix}, \begin{bmatrix} 1 \\ 0 \end{bmatrix} \right), \\
\tilde{\mathcal{D}}_3(\omega) &= \left(\begin{bmatrix} 0 \\ \eta_2 \\ 1 - \eta_2 \end{bmatrix}, \begin{bmatrix} 1 - \eta_1 \\ 0 \end{bmatrix} \right), & \tilde{\mathcal{D}}_4(\omega) &= \left(\begin{bmatrix} 0 \\ 0 \\ 1 \end{bmatrix}, \begin{bmatrix} \eta_2 \\ 1 - \eta_1 - \eta_2 \end{bmatrix} \right), \\
\tilde{\mathcal{D}}_5(\omega) &= \left(\begin{bmatrix} \eta_2 \\ 1 - \eta_1 - \eta_2 \\ \eta_1 \end{bmatrix}, \begin{bmatrix} 0 \\ 0 \end{bmatrix} \right), & \tilde{\mathcal{D}}_6(\omega) &= \left(\begin{bmatrix} 1 - \eta_1 \\ 0 \\ \eta_1 \end{bmatrix}, \begin{bmatrix} 0 \\ \eta_2 \end{bmatrix} \right), \\
\tilde{\mathcal{D}}_7(\omega) &= \left(\begin{bmatrix} \eta_2 \\ 0 \\ 1 - \eta_1 - \eta_2 \end{bmatrix}, \begin{bmatrix} 0 \\ 1 \end{bmatrix} \right), & \tilde{\mathcal{D}}_8(\omega) &= \left(\begin{bmatrix} \eta_2 \\ 0 \\ 1 - \eta_2 \end{bmatrix}, \begin{bmatrix} 0 \\ 1 - \eta_1 \end{bmatrix} \right)
\end{aligned}$$

and $\tilde{\mathcal{D}}_9(\eta)$ coincides with $\mathcal{D}_9(\eta)$ due to the forking inequality chain. Although there is not a strict separation of the domains in all cases, we can interpret all cases geometrically. For example, in the first case, two edges of t interact with each other that are not connected, namely the edges between the vertices c_t and d_t and the edges between the vertices a_t and b_t . The same is true for the remaining cases, either two edges are considered or a face and a vertex. The crucial point is that there is always a spatial separation between the elements.

5.3. Summary

The Sections 5.1 and 5.2 present an alternative approach to the Duffy transformation. Since only the nonlinear transformation w.r.t. η is adjusted, it is quite obvious that the singularities is lifted for each case. Therefore, the resulting integrals are nonsingular, like their counterparts in the Chapter 3. The costs of the transformation itself are also almost the same, i.e. for each singularity case the same number of splittings is necessary to lift the singularity. An overview of the costs can be found in the Tables 1 and 2 in Section 3.4. While the Duffy transformation presented in Chapter 3 is well suited for a standard multi-dimensional integration approach and for the error estimates presented in Chapter 4, the Duffy transformation introduced in this chapter is more adjusted to the numerics. On the one hand this approach reduces the computation time, because less points are used for the numerical integration and on the other hand for almost each singularity case the Jacobi determinant is identical for each sub-domain. This simplifies this complicated process at least a little bit. Moreover, we now have a geometric idea of how the splitting of the geometry can be interpreted.

6. \mathcal{H} -matrix approximation of the stiffness matrix

In the last chapters we dealt with the efficient computation of the entries of the stiffness matrix A ; see (17). Here, we shift the focus from the entries to the matrix itself. This step is very important for the finite element treatment of the fractional Laplacian, since the operator is non-local. The non-locality of the fractional Laplacian results in A being a dense matrix. Since it is too costly to compute and to store every single entry of A , the stiffness matrix is approximated by a *hierarchical matrix*, also called \mathcal{H} -matrix. \mathcal{H} -matrices offer several crucial advantages, such as the storage requirements being reduced from $\mathcal{O}(N^2)$ to $\mathcal{O}(N \log(N))$, the matrix-vector multiplication can be handled with quasi-linear complexity, i.e. $\mathcal{O}(N \log(N))$, and for elliptic operators a coarse \mathcal{H} -matrix approximation of the inverse of the stiffness matrix can be used for preconditioning; see [13, 50, 51, 53].

In this chapter we summarize the results of [13]. First, we give an short introduction to \mathcal{H} -matrices and prove that the stiffness matrix of the fractional Laplacian can be approximated by \mathcal{H} -matrices. Afterwards we present two well known methods to construct an \mathcal{H} -matrix.

6.1. A short introduction to \mathcal{H} -matrices

The aim of this section is to construct \mathcal{H} -matrix approximations to the stiffness matrix A .

First, the set of indices $I \times I$, $I = \{1, \dots, N\}$, is partitioned into sub-blocks $q \times w$, $q, w \subset I$, such that the associated supports

$$X_q := \bigcup_{i \in q} X_i \quad \text{for } q \subset I \quad \text{and} \quad X_i := \text{supp } \varphi_i,$$

satisfy the so-called geometrical admissible condition, i.e. for some parameter $\rho > 0$ it holds that

$$\min\{\text{diam } X_q, \text{diam } X_w\} \leq \rho \text{dist}(X_q, X_w). \quad (54)$$

The usual way of constructing such partitions is based on *cluster trees*; see [13, 53]. A cluster tree T_I for the index set I is a binary tree with root I , where each $q \in T_I$ and its nonempty successors $S_I(t) = \{q', q''\} \subset T_I$ (if they exist) satisfy $q = q' \cup q''$ and $q' \cap q'' = \emptyset$. We refer to $\mathcal{L}(T_I) = \{q \in T_I : S_I(t) = \emptyset\}$ as the leaves of T_I and define

$$T_I^{(\ell)} := \{q \in T_I : \text{dist}(q, I) = \ell\} \subset T_I,$$

where $\text{dist}(q, w)$ is the minimum distance between q and w in T_I . Furthermore,

$$L(T_I) := \max\{\text{dist}(q, I), t \in T_I\} + 1$$

denotes the depth of T_I . For the construction of the cluster trees the principal component analysis (PCA) is recursively used; see [71]. The so-called main direction of the cluster is calculated by the PCA and the cluster is divided into its two sons by the plane perpendicular to the main direction, which contains the center of the cluster. The advantage of this method is that the resulting cluster tree is geometrically balanced, i.e. there exist constants $c_g, c_G > 0$ such that for each level $l = 0, \dots, L(T_I) - 1$

$$\text{diam}(X_q)^d \leq c_g 2^{-l} \quad \text{and} \quad |X_q| \geq 2^{-l}/c_G \quad \text{for all } q \in T_I^{(l)}. \quad (55)$$

6. \mathcal{H} -matrix approximation of the stiffness matrix

Once the cluster tree T_I for the index set I has been computed, a partition P of $I \times I$ can be constructed from it. A block cluster tree $T_{I \times I}$ is a quad-tree with root $I \times I$ satisfying conditions analogous to a cluster tree. It can be constructed from the cluster tree T_I in the following way. Starting from the root $I \times I \in T_{I \times I}$, let the sons of a block $q \times w \in T_{I \times I}$ be $S_{I \times I}(q, w) := \emptyset$ if $q \times w$ satisfies (54) or $\min\{|q|, |w|\} \leq n_{\min}^{\mathcal{H}}$ with a given constant $n_{\min}^{\mathcal{H}} > 0$. In the remaining case, we set $S_{I \times I}(q, w) := S_I(q) \times S_I(w)$. The set of leaves of $T_{I \times I}$ defines a partition P of $I \times I$ and its cardinality $|P|$ is of the order $|I|$; see [13]. As usual, we partition P into admissible and non-admissible blocks

$$P = P_{\text{adm}} \cup P_{\text{nonadm}},$$

where each $q \times w \in P_{\text{adm}}$ satisfies (54) and each $q \times w \in P_{\text{nonadm}}$ is small, i.e. satisfies $\min\{|q|, |w|\} \leq n_{\min}^{\mathcal{H}}$. Additionally, we introduce a new constant

$$c_{sp} := \max_{q \in T_I} |\{w \subset I : q \times w \in T_{I \times I}\}|, \quad (56)$$

which gives an upper limit to the number of blocks $q \times w \in T_{I \times I}$ associated with a given cluster $q \in T_I$. c_{sp} is called sparsity constant. With this \mathcal{H} -matrices can be defined; see [13].

Definition 5. Let $k \in \mathbb{N}$. The set of hierarchical matrices on the block cluster tree $T_{I \times I}$ with admissible partition $P := \mathcal{L}(T_{I \times I})$ and block-wise rank k is defined as

$$\mathcal{H}(T_{I \times I}, k) = \{A \in \mathbb{R}^{N \times N} : \text{rank } A_b \leq k \text{ for all admissible blocks } b \in P\}.$$

For the sake of brevity, elements from $\mathcal{H}(T_{I \times I}, k)$ will often be called \mathcal{H} -matrices.

Notice, that for each $A \in \mathcal{H}(T_{I \times I}, k)$ it holds that $\text{rank } A_b \leq \max\{k, n_{\min}^{\mathcal{H}}\}$ for $b \in P$. The next step is to construct suitable approximations to the admissible blocks of A .

6.2. Degenerate kernel approximation

Let $m, n \in \mathbb{N}$. The set of matrices of at most rank k is denoted by

$$A \in \mathbb{R}_k^{m \times n} := \{A \in \mathbb{R}^{m \times n} : \text{rank } A \leq k\}.$$

According to [13], each rank- k matrix has an outer product form, i.e. there are matrices $U \in \mathbb{R}^{m \times k}$ and $V \in \mathbb{R}^{n \times k}$ such that

$$A = UV^T.$$

A matrix $A \in \mathbb{R}_k^{m \times n}$ is called low-rank matrix, if

$$k(m+n) < mn.$$

This means that any rank- k matrix is a low-rank matrix, if it is cheaper to store all matrix entries of its outer product form than all entries of the matrix itself.

For the \mathcal{H} -matrix approximation of the stiffness matrix, only the admissible blocks have to be approximated. The non-admissible blocks are computed entrywise. Let $b = q \times w$ be an admissible block, therefore $\text{dist}(X_q, X_w) > 0$ and the entries of the stiffness matrix simplify to

$$a_{ij} = -c_{d,s} \int_{X_w} \int_{X_q} \varphi_i(x) K(x, y) \varphi_j(y) dx dy, \quad K(x, y) := |x - y|^{-d-2s},$$

6. \mathcal{H} -matrix approximation of the stiffness matrix

where $i \in q$ and $j \in w$; see (18). The main idea is to use a degenerate kernel approximation of the kernel K to construct a low-rank approximation of the block; see [13].

Definition 6. Let $D_1, D_2 \subset \mathbb{R}^d$ be two domains. A kernel function $\kappa : D_1 \times D_2 \rightarrow \mathbb{R}$ is called degenerate if $k \in \mathbb{N}$ and functions $u_l : D_1 \rightarrow \mathbb{R}$ and $v_l : D_2 \rightarrow \mathbb{R}$, $l = 1, \dots, k$, exist such that

$$\kappa(x, y) = \sum_{l=1}^k u_l(x) v_l(y), \quad x \in D_1, y \in D_2.$$

The number k is called degree of degeneracy.

Replacing K by its degenerate kernel approximation K_k leads to

$$a_{ij}^k = -c_{d,s} \sum_{l=1}^k \int_{X_q} \varphi_i(x) u_l(x) dx \int_{X_w} \varphi_j(y) v_l(y) dy = \sum_{l=1}^k u_i^l v_j^l = u_i^T v_j,$$

where $i \in q$ and $j \in w$. By combining the corresponding u_i , respectively the corresponding v_j of the same set, we obtain the matrices $U \in \mathbb{R}^{|q| \times k}$ and $V \in \mathbb{R}^{|w| \times k}$ with

$$U_{i,:} := u_i \text{ for all } i \in q \quad \text{and} \quad V_{j,:} := v_j \text{ for all } j \in w.$$

Hence, we can expand the degenerate kernel approximation of K to a rank- k approximation of the block itself, which can easily be seen by

$$A_b^k = UV^T.$$

Based on the degenerate kernel approximation K_k , an \mathcal{H} -matrix $A_{\mathcal{H}}$ can be constructed by

$$(A_{\mathcal{H}})_b = \begin{cases} A_b^k, & \text{if } b \text{ is an admissible block} \\ A_b, & \text{if } b \text{ is a non-admissible block} \end{cases}.$$

For the theoretical treatment the linear operators $\Lambda_q : L^2(\Omega) \rightarrow \mathbb{R}^{|q|}$,

$$(\Lambda_q f)_i = \int_{\Omega} f(x) \varphi_i(x) dx, \quad i \in q, \tag{57}$$

are used; see [13]. Since $\text{supp } \Lambda_q = X_q$, we refer to Λ_q as localizers. For admissible blocks $b = q \times w$ it holds for the block A_{qr} of the stiffness matrix that

$$A_{qw} = \Lambda_q \mathcal{A} \Lambda_w^*, \quad (\mathcal{A} f)(y) := \int_{\Omega} K(x, y) f(x) dx,$$

where $\Lambda_w^* : \mathbb{R}^{|w|} \rightarrow L^2(\Omega)$ is the adjoint of $\Lambda_w : L^2(\Omega) \rightarrow \mathbb{R}^{|w|}$ defined by

$$(\Lambda_w^* z, f)_{L^2(\Omega)} = z^T (\Lambda_w f) \quad \text{for all } z \in \mathbb{R}^{|w|}, f \in L^2(\Omega).$$

Additionally, there exists a constant $c_{\Lambda} > 0$, which usually depend on h , the mean diameter of the tetrahedra, such that

$$\|\Lambda_q u\|_2 \leq c_{\Lambda} \|u\|_{L^2(X_q)}, \tag{58}$$

for all $q \in I$ and $u \in L^2(X_q)$. This can easily be seen by using the Cauchy-Schwarz inequality and (57). The following error estimate shows how the error of the degenerate kernel approximation affects the error of the matrix approximation.

6. \mathcal{H} -matrix approximation of the stiffness matrix

Theorem 15. *Let $\varepsilon > 0$ and assume that there exists $k_\varepsilon \in \mathbb{N}$ such that for each admissible block $b = q \times w$ there is a degenerate kernel function $K_{k_\varepsilon}^b$ satisfying*

$$|K(x, y) - K_{k_\varepsilon}^b(x, y)| \leq \varepsilon, \quad x \in X_q, y \in X_w.$$

Then there exists $A_{\mathcal{H}} \in \mathcal{H}(T_{I \times I}, k_\varepsilon)$ such that

$$\|A - A_{\mathcal{H}}\|_2 \leq \varepsilon c_\Lambda^2 \nu |\Omega|,$$

where the constants c_Λ and ν are defined in (58) and (14), respectively.

The proof of Theorem 15 can be found in [13]. In order to use the relative error for the degenerate kernel approximation instead of the absolute error, the geometric admissibility condition (54) has to be made stricter to

$$\max\{\text{diam } X_q, \text{diam } X_w\} \leq \rho \text{dist}(X_q, X_w). \quad (59)$$

Theorem 16. *Let $\varepsilon > 0$ and assume that there exists $k_\varepsilon \in \mathbb{N}$ such that for each admissible block $b = q \times w$ there is a degenerate kernel function $K_{k_\varepsilon}^b$ satisfying*

$$|K(x, y) - K_{k_\varepsilon}^b(x, y)| \leq \varepsilon |K(x, y)|, \quad x \in X_q, y \in X_w.$$

Then there exists $A_{\mathcal{H}} \in \mathcal{H}(T_{I \times I}, k_\varepsilon)$ such that

$$\|A - A_{\mathcal{H}}\|_2 \leq c_{sp} c_{d,s} \nu \omega_d^2 (\rho/2)^{2d} (\rho^{-1} + 2)^{d-2s} c_g^{\frac{d-2s}{d}} (1 - 2^{-\frac{d-2s}{d}})^{-1} \varepsilon,$$

where the constants c_{sp} , $c_{d,s}$, ν and c_g are defined in (56), (2), (14) and (55), respectively, and ω_d denotes the surface area of the unit ball in \mathbb{R}^d .

Proof. Let $b = q \times w \in P$. If b is non-admissible, we set

$$(A_{\mathcal{H}})_b = A_b.$$

Otherwise b satisfies the geometrical admissibility condition (59)

$$\max\{\text{diam } X_q, \text{diam } X_w\} \leq \rho \text{dist}(X_q, X_w) \quad \text{and} \quad \min\{|q|, |w|\} \geq n_{\min}^{\mathcal{H}}.$$

According to the assumptions, there exists a degenerate kernel $K_{k_\varepsilon}^b(x, y) = \sum_{l=1}^{k_\varepsilon} u_l^b(x) v_l^b(y)$ for each admissible block b . Let the functions u_l^b and v_l^b , $l = 1, \dots, k$, be extended to Ω by zero.

We define a linear operator $\Lambda_b^s : L^2(\Omega \times \Omega) \rightarrow \mathbb{R}^{|q| \times |w|}$ by

$$(\Lambda_b^s f)_{ij} := -c_{d,s} \int_{X_q} \int_{X_w} \varphi_i(x) f(x, y) \varphi_j(y) \, dy \, dx.$$

From

$$\begin{aligned} \|\Lambda_b^s f\|_F^2 &= c_{d,s}^2 \sum_{i \in q} \sum_{j \in w} \left\{ \int_{X_q} \left[\int_{X_w} f(x, y) \varphi_j(y) \, dy \right] \varphi_i(x) \, dx \right\}^2 \\ &\leq c_{d,s}^2 \sum_{i \in q} \|\varphi_i\|_{L^2(X_q)}^2 \sum_{j \in w} \left[\int_{X_w} f(x, y) \varphi_j(y) \, dy \right]^2 \\ &\leq c_{d,s}^2 \sum_{i \in q} \|\varphi_i\|_{L^2(\text{supp } \varphi_i)}^2 \sum_{j \in w} \|\varphi_j\|_{L^2(\text{supp } \varphi_j)}^2 \|f\|_{L^2(X_q \times X_w)}^2 \\ &\leq c_{d,s}^2 \nu^2 |X_q| |X_w| \|f\|_{L^2(X_q \times X_w)}^2 \end{aligned}$$

6. \mathcal{H} -matrix approximation of the stiffness matrix

it follows that $\|\Lambda_b^s\|_{F \leftarrow L^2} \leq c_{d,s}^2 \nu^2 |X_q|^{\frac{1}{2}} |X_w|^{\frac{1}{2}}$, where ν is defined (14). We deduce that

$$\|(A - A_{\mathcal{H}})_b\|_F^2 \leq \|\Lambda_b^s\|_{F \leftarrow L^2} \|K - K_{k_b}^b\|_{L^2(X_q \times X_w)}^2 \leq c_{d,s}^2 \nu^2 |X_q| |X_w| \varepsilon^2 \|K\|_{L^2(X_q \times X_w)}^2,$$

which proves $\|(A - A_{\mathcal{H}})_b\|_2 \leq c_{d,s} \nu |X_q|^{\frac{1}{2}} |X_w|^{\frac{1}{2}} \varepsilon \|K\|_{L^2(X_q \times X_w)}$.

Obviously $K(\cdot, \cdot)$ does not belong to $L^2(\Omega \times \Omega)$. In fact it is easily seen that $\|K\|_{L^2(X_q \times X_w)}$ increases, when the sets X_q and X_w approach each other. The construction of X_w , however, ensures

$$\sigma := \text{dist}(X_q, X_w) \geq \rho^{-1} \text{diam } X_w$$

as well as $\rho\sigma \geq \text{diam } X_q$ due to the admissibility condition (59). Therefore

$$|X_q|^{\frac{1}{2}} |X_w|^{\frac{1}{2}} \|K\|_{L^2(X_q \times X_w)} \leq \sigma^{-d-2s} |X_q| |X_w|.$$

Using $|X_w| \leq \omega_d (\text{diam } X_w / 2)^d \leq \omega_d (\rho\sigma / 2)^d$ and $|X_q| \leq \omega_d (\rho\sigma / 2)^d$, we see that

$$|X_q|^{\frac{1}{2}} |X_w|^{\frac{1}{2}} \|K\|_{L^2(X_q \times X_w)} \leq \omega_d^2 \left(\frac{\rho}{2}\right)^{2d} \sigma^{d-2s}.$$

Let q^* and w^* be the fathers of q and w , respectively. Then

$$\rho \text{dist}(X_{q^*}, X_{w^*}) \leq \max\{\text{diam } X_{q^*}, \text{diam } X_{w^*}\}$$

and it follows from [13, (1.22)] that

$$\begin{aligned} \text{dist}(X_q, X_w) &\leq \text{dist}(X_{q^*}, X_{w^*}) + \text{diam } X_{q^*} + \text{diam } X_{w^*} \\ &\leq (\rho^{-1} + 2) \max\{\text{diam } X_{q^*}, \text{diam } X_{w^*}\} \leq (\rho^{-1} + 2) c_g^{1/d} 2^{-l/d}, \end{aligned}$$

where l denotes the level of t in T_I . Hence, we obtain

$$\|(A - A_{\mathcal{H}})_b\|_2 \leq c_{d,s} \nu \omega_d^2 \left(\frac{\rho}{2}\right)^{2d} (\rho^{-1} + 2)^{d-2s} c_g^{\frac{d-2s}{d}} 2^{-\frac{l(d-2s)}{d}} \varepsilon.$$

From the proof of [13, Theorem 2.16] we see that

$$\|A - A_{\mathcal{H}}\|_2 \leq c_{sp} \sum_{l=0}^{L(T_I)} \|(A - A_{\mathcal{H}})_b\|_2 \leq c_{sp} c_{d,s} \nu \omega_d^2 \left(\frac{\rho}{2}\right)^{2d} (\rho^{-1} + 2)^{d-2s} c_g^{\frac{d-2s}{d}} (1 - 2^{-\frac{d-2s}{d}})^{-1} \varepsilon.$$

□

6.2.1. Interpolation on tensor product grids

One way to construct such a degenerate kernel is by polynomial interpolation on tensor product grids; see [13]. First, we consider the univariate case. Let $y_1, \dots, y_p \in [a, b] \subset \mathbb{R}$ be pairwise distinct points and $f \in C([a, b])$. Then we can define the interpolation polynomial $\mathcal{I}_p f \in \Pi_{p-1}$ by

$$\mathcal{I}_p f(y) = \sum_{i=0}^{p-1} f(y_i) L_i(y), \quad L_i(y) := \prod_{j=0, j \neq i}^{p-1} \frac{y - y_j}{y_i - y_j}.$$

6. \mathcal{H} -matrix approximation of the stiffness matrix

Instead of random interpolation nodes, Chebyshev nodes

$$t_j := \frac{a+b}{2} + \frac{b-a}{2} \cos\left(\frac{2j+1}{2p}\pi\right), \quad j = 0, \dots, p-1,$$

are chosen. The advantage is that the Lebesgue constant $\|\mathcal{I}_p\|$ depends only logarithmically on p ,

$$\|\mathcal{I}_p\| := \max\{\|\mathcal{I}_p f\|_{\infty, [a,b]} / \|f\|_{\infty, [a,b]} : f \in C([a,b])\} \leq 1 + \frac{2}{\pi} \log p, \quad (60)$$

which is asymptotically optimal. Additionally, we consider only a specific class of smooth functions; see [13, 51].

Definition 7. A function $\kappa : \Omega \times \mathbb{R}^d \rightarrow \mathbb{R}$ satisfying $\kappa(x, \cdot) \in C^\infty(\mathbb{R}^d \setminus \{x\})$ for all $x \in \Omega$ is called asymptotically smooth in Ω w.r.t. y if constants c and γ can be found such that for all $x \in \Omega$ and all $\alpha \in \mathbb{N}_0^d$

$$|\partial_y^\alpha \kappa(x, y)| \leq c p! \gamma^p \frac{|\kappa(x, y)|}{|x - y|^p} \text{ for all } y \in \mathbb{R}^d \setminus \{x\},$$

where $p = |\alpha|$.

In [13] it is shown that the interpolation error decreases exponentially w.r.t. p .

Lemma 20. Let $D_1, D_2 \subset \mathbb{R}$ such that D_2 is a closed interval and $D_1 \cap D_2 = \emptyset$. Let κ be asymptotically smooth w.r.t. y . Then for all $x \in D_1$ it holds that

$$\|\kappa(x, \cdot) - \mathcal{I}_{y,p} \kappa(x, \cdot)\|_{\infty, D_2} \leq \bar{c} \left(1 + \frac{2 \text{dist}(x, D_2)}{\gamma \text{diam}(D_2)}\right)^{-p} \|\kappa(x, \cdot)\|_{\infty, D_2},$$

with $\bar{c} := 8cp(1 + \log(p)/\pi)(1 + \gamma \text{diam}(D_2)/\text{dist}(x, D_2))$.

The next step is to adapt the one-dimensional interpolation to multivariate functions $f : D_2 \rightarrow \mathbb{R}$ with $D_2 := \prod_{\nu=1}^d [a_\nu, b_\nu] \subset \mathbb{R}^d$. For the interpolation nodes we consider tensor product nodes

$$y_\alpha = (y_{\alpha_1}^{(1)}, \dots, y_{\alpha_d}^{(d)}) \in D_2, \quad \alpha \in \mathbb{N}_0^d, \quad \|\alpha\|_\infty < p,$$

where $y_i^{(\nu)} \in [a_\nu, b_\nu], i = 1, \dots, p-1$, are pairwise distinct for each $\nu = 1, \dots, d$, and tensor product polynomials

$$\mathcal{I}_p f = \mathcal{I}_p^{(1)} \dots \mathcal{I}_p^{(d)} f \in \Pi_{(p-1)d}^d,$$

where $\mathcal{I}_p^{(\nu)} f$ denotes the univariate interpolation operator applied to the ν -th argument of f . Note that $\mathcal{I}_{p,y} \kappa$ is a degenerate kernel of degree $k = p^d$, since

$$\mathcal{I}_{p,y} \kappa(x, y) = \sum_{\|\alpha\|_\infty < p} \kappa(x, t_\alpha) L_\alpha(y),$$

where $L_\alpha(y^{(1)}, \dots, y^{(d)}) := \prod_{\nu=1}^d L_{\alpha_\nu}(y^{(\nu)}) \in \Pi_{(p-1)d}^d$ is the product of univariate Lagrange polynomials L_{α_ν} . Applying Lemma 20 to the tensor product approach leads to the following result; see [13].

6. \mathcal{H} -matrix approximation of the stiffness matrix

Theorem 17. Let $D_1 \subset \mathbb{R}^d$ and $D_2 = \prod_{i=1}^d [a_i, b_i]$ such that

$$\rho \operatorname{dist}(D_1, D_2) \geq \max_{i=1, \dots, d} b_i - a_i,$$

holds for an $\rho > 0$ satisfying $c\gamma\rho < 1$. Let $\kappa(x, y)$ be asymptotically smooth w.r.t. y . Then for all $x \in D_1$ and $y \in D_2$, it holds that

$$|\kappa(x, y) - \mathcal{I}_{y,p}\kappa(x, y)| \leq c_p |\kappa(x, y)|,$$

where

$$c_p := \tilde{c} p \left(1 + \frac{2}{p} \log p\right)^d \left(\frac{\gamma\rho}{2 + \gamma\rho}\right)^p.$$

6.2.2. Cross approximation

Theorem 17 can be used for our purposes, since according to [51], K is asymptotically smooth for each $d \in \mathbb{N}$ and for each $s \in (0, 1)$. However, the interpolation method on tensor grids has two disadvantages. The first one is that for the geometric admissibility condition the original domain X_q is not sufficient, but a bounding box of X_q is needed. The second disadvantage is that the degree of degeneracy k cannot be increased by one, since it holds that $k = p^d$, where p are the number of interpolation points per dimension. This can make the approximation quite expensive especially if small relative errors are to be achieved.

Another method that does not have these disadvantages is the so-called *cross approximation*. The general idea behind this is that for the approximation not an arbitrary function system is used, but a function system consisting of restrictions of κ itself. Thereby, a quasi optimal approximation is achieved; see [13]. The quasi-optimality is to be understood in such a way that up to constants, the quality of the cross approximation of κ is better than the quality of any given function system $\Xi := \{\xi_1, \dots, \xi_k\}$, i.e.

$$E_k \leq c \inf_{\Xi} \sup_{x \in D_1} \inf_{p \in \operatorname{span} \Xi} \|\kappa(x, \cdot) - p\|_{\infty, D_2},$$

where E_k denotes the error associated with the cross approximation with a degree of degeneracy k .

Again, assume that X_q and X_w satisfy (54), then the cross approximation of κ for $k = 1$ is defined as

$$\kappa_1(x, y) := \frac{\kappa(x, y_0) \kappa(x_0, y)}{\kappa(x_0, y_0)}, \quad x \in X_q, y \in X_w,$$

with fixed $x_0 \in X_q$, $y_0 \in X_w$ and it holds that

$$\kappa_1(x_0, y) = \kappa(x_0, y), \quad y \in X_w \quad \text{and} \quad \kappa_1(x, y_0) = \kappa(x, y_0), \quad x \in X_q.$$

Hence, κ_1 interpolates κ on whole domains. This is a huge advantage compared to the first presented method, since in general interpolation achieves exactness only at the interpolation points. The next step is to extend the procedure to a general degree of degeneracy k . For this purpose, we set

$$\kappa(x, [y]_k) = \begin{pmatrix} \kappa(x, y_1) \\ \vdots \\ \kappa(x, y_k) \end{pmatrix} \in \mathbb{R}^k \quad \text{and} \quad \kappa([x]_k, y) = \begin{pmatrix} \kappa(x_1, y) \\ \vdots \\ \kappa(x_k, y) \end{pmatrix} \in \mathbb{R}^k$$

6. \mathcal{H} -matrix approximation of the stiffness matrix

with points $x_l \in X_q$ and $y_l \in X_w$, $l = 1, \dots, k$. The degenerate kernel approximations can be constructed by

$$\kappa_k(x, y) = \kappa(x, [y]_k)^T W_k^{-1} \kappa([x]_k, y),$$

where the $k \times k$ matrix W_k is defined by

$$W_k = \begin{pmatrix} \kappa(x_1, y_1) & \dots & \kappa(x_1, y_k) \\ \vdots & & \vdots \\ \kappa(x_k, y_1) & \dots & \kappa(x_k, y_k) \end{pmatrix}.$$

In [13] sequences $\{\kappa_k\}$ and $\{r_k\}$ for the approximation of κ have been defined by the following rule

$$r_0(x, y) = \kappa(x, y), \quad \kappa_0(x, y) = 0,$$

and for $k = 0, 1, \dots$

$$\begin{aligned} r_{k+1}(x, y) &= r_k(x, y) - \frac{r_k(x, y_{k+1}) r_k(x_{k+1}, y)}{r_k(x_{k+1}, y_{k+1})}, \\ \kappa_{k+1}(x, y) &= \kappa_k(x, y) + \frac{r_k(x, y_{k+1}) r_k(x_{k+1}, y)}{r_k(x_{k+1}, y_{k+1})}, \end{aligned} \tag{61}$$

where x_{k+1} and y_{k+1} are chosen in each step so that $r_k(x_{k+1}, y_{k+1}) \neq 0$.

Additionally, κ can be described by r_k and κ_k in the following way; see [13].

Lemma 21. *For the generate sequences κ_k and r_k , $k \geq 0$, it holds that*

$$\kappa_k(x, y) + r_k(x, y) = \kappa(x, y).$$

With the lemma above and (61) one sees very nicely that the cross approximation preserves its interpolation property:

$$\kappa_k(x_l, y) = \kappa(x_l, y), \quad y \in X_w \quad \text{and} \quad \kappa_k(x, y_l) = \kappa(x, y_l), \quad x \in X_q, \tag{62}$$

for $l = 1, \dots, k$, respectively. Thus κ_k gradually interpolates κ on $X_q \times X_w$. The next theorem shows the earlier mentioned quasi-optimality of the cross approximation; see [13].

Theorem 18. *Assume that in each step we choose x_k so that*

$$|r_{k-1}(x_k, y_k)| \geq |r_{k-1}(x, y_k)| \text{ for all } x \in D_1.$$

Then it holds for any given system $\Xi = \{\xi_1, \dots, \xi_k\}$ of functions that

$$|r_k(x, y)| \leq 2^k (1 + \|\mathcal{I}_k^\Xi\|) \sup_{z \in \{x, x_1, \dots, x_k\}} \inf_{p \in \text{span } \Xi} \|\kappa(z, \cdot) - p\|_{\infty, D_2},$$

where $\|\mathcal{I}_k^\Xi\|$ is the Lebesgue constant defined in (60) w.r.t. Ξ .

Theorem 18 implies that the error of the cross approximation is up to constants smaller than the approximation error associated with any system of functions $\Xi = \{\xi_1, \dots, \xi_k\}$. Thus the error converges exponentially to zero w.r.t. k , since the earlier mentioned approximation by polynomials is an example. Other examples are the approximation by spherical harmonics or the sinc interpolation; see [54, 79]. The only shortcoming of this error estimation is the exponentially growing factor 2^k . As mentioned in [13], this factor is a worst-case estimate, which is hardly observable in practice.

6.3. The adaptive cross approximation

In this section we want to present an algebraic approach to compute a low-rank approximation of an admissible block. Instead of approximating the kernel function, as we have done in Section 6.2, we focus here directly on the matrix entries themselves and use them for the approximation. This will be done by the *adaptive cross approximation* (ACA) algorithm, which will be presented in this section later on; see [12, 13, 14, 16]. This algorithm is based on the cross approximation, which was introduced in Section 6.2. The ACA is capable of creating a low-rank approximation of an admissible block by only using few of the original matrix entries. For this purpose, it is not necessary to set up the entire matrix beforehand. Since the entries are only computed on demand, the rank of the approximation can be chosen adaptively while kernel approximations require an a-priori choice, which is usually too large.

6.3.1. The algorithm

The next steps are now to adapt the cross approximation to the algebraic setting. For this we follow the work of [13]. Let $A_b \in \mathbb{R}^{m \times n}$ be a matrix block of the stiffness matrix A corresponding to an admissible block b . A_b corresponds here to the function K , that we want to approximate. Therefore set $R_0 := A_b$ and find a nonzero pivot in R_k , say (i_k, j_k) , and subtract a scaled outer product of the i_k -th row and the j_k -th column:

$$R_{k+1} := R_k - [(R_k)_{i_k j_k}]^{-1} (R_k)_{1:m, j_k} (R_k)_{i_k, 1:n}, \quad (63)$$

where we use the notations $(R_k)_{i, 1:n}$ and $(R_k)_{1:m, j}$ for the i -th row and the j -th column of R_k , respectively. Notice that (63) is the algebraic version of (61). According to [13], j_k should be chosen the maximum element in modulus of the i_k -th row (see Theorem 18); i.e.

$$|(R_{k-1})_{i_k j_k}| = \max_{j=1, \dots, n} |(R_{k-1})_{i_k j}|.$$

The choice of i_k is more complicated. There are at least three different options; see [11, 13]: a heuristic way, a rigorous way and a geometrical way. The first one is mostly reliable and easy to compute and implement. In contrary to the heuristic way the rigorous way guarantees that the ACA converges. However, it is more costly and more difficult to implement. The last option also guarantees the convergence of the ACA and it is based on the geometrical information behind the cluster corresponding to rows of A_b . This method will be addressed in Section 8.4.

The interesting part of (63) is that the update from R_k to R_{k+1} consists only of the entries in the j_k -th column and the i_k -th row of the R_k . Therefore, it is not necessary to build the whole matrix R_k . Moreover, this shows that it is enough to only compute few of the original entries of A_b . Taking advantage of this, Algorithm 1 is an efficient reformulation of (63); see [13]. Note that the vectors u_k and \tilde{v}_k coincide with $(R_{k-1})_{1:m, j_k}$ and $(R_{k-1})_{i_k, 1:n}^T$, respectively.

The set Z serves for saving the vanishing rows of R_k . If the i_k -th row of R_k is nonzero and hence is used as v_k , it is also added to Z since the i -th row of R_{k+1} will vanish. The matrix $S_k := \sum_{l=1}^k u_l v_l^T$ will be used as an approximation of $A_b = S_k + R_k$. Obviously, the rank of S_k is bounded by k .

Let $\varepsilon > 0$ be given. According to [13], the following condition

$$\|u_{k+1}\|_2 \|v_{k+1}\|_2 \leq \frac{\varepsilon(1-\rho)}{1+\varepsilon} \|S_k\|_F \quad (64)$$

Algorithm 1 Adaptive Cross Approximation (ACA)

```

Let  $k = 1$ ;  $Z = \emptyset$ 
repeat
  find  $i_k$  according to a mentioned method
   $\tilde{v}_k := a_{i_k, 1:n}$ 
  for  $l = 1, \dots, k - 1$  do
     $\tilde{v}_k := \tilde{v}_k - (u_l)_{i_k} v_l$ 
  end for
   $Z := Z \cup \{i_k\}$ 
  if  $\tilde{v}_k$  does not vanish then
     $j_k := \operatorname{argmax}_{j=1, \dots, n} |(\tilde{v}_k)_j|$ 
     $v_k := (\tilde{v}_k)_{j_k}^{-1} \tilde{v}_k$ 
     $u_k := a_{1:m, j_k}$ 
    for  $l = 1, \dots, k - 1$  do
       $u_k := u_k - (v_l)_{j_k} u_l$ 
    end for
     $k := k + 1$ 
  end if
until the stopping criterion (64) is fulfilled or  $Z = \{1, \dots, m\}$ 
    
```

can be used as a stopping criterion on k . Assume that $\|R_{k+1}\|_F \leq \rho \|R_k\|_F$ with ρ from (54), then

$$\|R_k\|_F \leq \|R_{k+1}\|_F + \|u_{k+1} v_{k+1}^T\|_F \leq \rho \|R_k\|_F + \|u_{k+1}\|_2 \|v_{k+1}\|_2.$$

Hence,

$$\|R_k\|_F \leq \frac{1}{1 - \rho} \|u_{k+1}\|_2 \|v_{k+1}\|_2 \leq \frac{\varepsilon}{1 + \varepsilon} \|S_k\|_F \leq \frac{\varepsilon}{1 + \varepsilon} (\|A_b\|_F + \|R_k\|_F).$$

From the previous estimate we obtain $\|R_k\|_F \leq \varepsilon \|A_b\|_F$, i.e., condition (64) guarantees a relative approximation error ε . Hence, the rank required to guarantee a prescribed accuracy can be found adaptively.

The costs of the Algorithm 1 are of the order $|Z|^2(m + n)$, since $\|S_k\|_F^2$ can be computed by

$$\|S_k\|_F^2 = \|UV^T\|_F^2 = \sum_{i,j}^{i,j} (u_i^T u_j) (v_i^T v_j).$$

6.3.2. Error estimation

The next step is to estimate the remainder R_k . According to [13], the entries of R_k will be estimated by the approximation error

$$F_{qw}^\Xi := \max_{j \in w} \inf_{p \in \operatorname{span} \Xi} \|\mathcal{A} \Lambda_j^* - p\|_{\infty, X_q}$$

in an arbitrary system of functions $\Xi := \{\xi_1, \dots, \xi_k\}$ with $\xi_1 = 1$. Note that $\mathcal{A} \Lambda_j^*$ is an asymptotically smooth function due to $\operatorname{supp} \Lambda_j^* = X_j$. The unsolvency of this problem is guaranteed by the choice

6. \mathcal{H} -matrix approximation of the stiffness matrix

of the pivoting rows for the second and third way mentioned in Section 6.3.1; see [11, 13]. If the heuristic approach is chosen the following assumption

$$\det[\Lambda_i \xi_j]_{i,j=1,\dots,k} \neq 0$$

is needed. In Section 6.2 we have presented systems Ξ together with their approximation errors. In the next theorem the approximation error associated with algorithm 1 is estimated; see [13].

Theorem 19. *Let Λ_i be defined as in (57). Then for $i = 1, \dots, m$ and $j = 1, \dots, n$ it holds that*

$$|(R_k)_{ij}| \leq 2^k (1 + \|I_k^\Xi\|) \left(1 + \sum_{l=1}^k |c_l^{(i)}| \right) \|\varphi_i\|_{L^1} F_{qw}^\Xi,$$

where the $c_l^{(i)}$ satisfy for $i = 1, \dots, m$

$$\int_{\Omega} \left(\frac{\varphi_i}{\|\varphi_i\|_{L^1}} - \sum_{l=1}^k c_l^{(i)} \frac{\varphi_l}{\|\varphi_l\|_{L^1}} \right) q = 0 \text{ for all } q \in \text{span } \Xi.$$

Similar to the error estimate of the cross approximation (63), we obtain here again the exponential growing factor 2^k . However, this growth is also known to be rarely observable in practice. One interesting fact is that the Algorithm 1 has a similarity to the LU factorization, where such a so-called growth of entries may also happen; see [47]. According to [13], this can be seen from $R_k = L_k R_{k-1}$, where

$$L_k = \begin{pmatrix} 1 & & & & & \\ & \ddots & & & & \\ & & 0 & & & \\ & & -\frac{(R_{k-1})_{k+1,k}}{(R_{k-1})_{kk}} & 1 & & \\ & & \vdots & & \ddots & \\ & & -\frac{(R_{k-1})_{mk}}{(R_{k-1})_{kk}} & & & 1 \end{pmatrix} \in \mathbb{R}^{m \times m}.$$

L_k differs from a Gauß matrix only in the position (k, k) .

7. \mathcal{H} -Approximation of the inverse of the stiffness matrix

Besides the efficient approximation of the stiffness matrix A , preconditioners are also of great importance for FEM. This is due to the fact that the condition number of the stiffness matrix deteriorates with a finer geometry. For example it is well-known that the condition number of stiffness matrix of the Laplace operator is of the order of h^{-2} , where h is again the mean diameter of the tetrahedra, while the condition number of the stiffness matrix of the fractional Laplacian scales as h^{-2s} ; see [5]. To counteract this problem, preconditioners are used. However, these usually have to be tailored to the problem.

For elliptic problems \mathcal{H} -matrices can be used to overcome this issue, since the inverse of the stiffness matrix A^{-1} can also be approximated by an \mathcal{H} -matrix; see [13]. In contrast to the approximation of A , a coarser approximation of A^{-1} is used as a preconditioner. However, we have to ensure that the costs for the computation of $A_{\mathcal{H}}^{-1} \in \mathcal{H}(T_I \times I, k)$, which are of the order of $\mathcal{O}(k^2 L^2(T_I)|I|)$, remain within limits, i.e. the rank k of the approximation only depends logarithmically on the accuracy of the approximation.

For a big class of elliptic problems this is already done by [13, 42, 43, 44, 45, 60]. Even for the fractional Laplacian this result is already proven in [60]:

Theorem 20. *Let $\rho > 0$ and $\gamma \in (0, 1)$. Let $b = q \times w$ be a bounding box admissible block, i.e. there exists bounding cubes B_{R_q} and B_{R_w} with side length R_q and R_w , respectively, such that $X_q \subset B_{R_q}$, $X_w \subset B_{R_w}$, and*

$$\max\{B_{R_q}, B_{R_w}\} \leq \rho \operatorname{dist}(B_{R_q}, B_{R_w}).$$

Then, for each $\tilde{k} \in \mathbb{N}$, there exist matrices $U_q \in \mathbb{R}^{|q| \times k}$ and $V_w \in \mathbb{R}^{|w| \times k}$ with rank $k \leq C_{\dim}(2 + \rho)^{d+1} \gamma^{-d+1} \tilde{k}^{d+2}$ such that

$$\|(A^{-1})_b - U_q V_w^T\|_2 \leq C_{\text{apx}} N^{\frac{1+d}{d}} \gamma^{\tilde{k}}.$$

The constants C_{\dim} and C_{apx} depend only on d , Ω , the shape regularity of \mathcal{T} , and on s .

In contrary to the approach presented in [60], we do not want use the Caffarelli-Silvestre extension of the fractional Laplacian (see [25, 80]), but the integral form of the operator and the weak formulation of the problem. Thereby, we are not required to Beppo-Levi spaces, which makes our approach easier accessible to a wide audience. We tried to adapt the ideas of [13] to the framework of the fractional Laplacian. However, for our approach the non-locality of the fractional Laplacian hampers an analogous result. While we can prove that A^{-1} can be approximated with \mathcal{H} -matrices, we cannot verify that the approximation is efficient, i.e. the approximation error decays exponentially w.r.t. the rank k . In the following, we first share the idea of the proof and then partial results, like a local Caccioppoli inequality, and explain in detail what issues we faced.

7.1. Idea of the proof

Instead of directly approximating the inverse of the stiffness matrix with an \mathcal{H} -matrix, a detour is taken, since we do not know the exact form of the Green's function. For this purpose it is first shown that A^{-1} can be approximated by $C := M^{-1} B M^{-1}$, where the mass matrix M and the Galerkin discretization of $(-\Delta)^{-s}$, called B , are defined in (19), and then an \mathcal{H} -matrix approximation of each

7. \mathcal{H} -Approximation of the inverse of the stiffness matrix

component of C is performed. Note that the exact product of \mathcal{H} -matrices is again an \mathcal{H} -matrix; see [13]. The procedure is almost identical to the case of the Laplace operator.

First, we represent the finite element solution u_h via the Ritz projection; see [52],

$$P_h = \mathcal{J}A^{-1}\mathcal{J}^*(-\Delta)^s : \tilde{H}^s(\Omega) \rightarrow V_h,$$

which maps the solution $u \in \tilde{H}^s(\Omega)$ of the variational problem (8) to the finite element solution $u_h = P_h u$ of (11). The finite element error is then given by $e_h(u) := \|u - P_h u\|_{L^2(\Omega)}$ and the weakest form of the finite element convergence is described by

$$e_h(u) \leq \varepsilon_h \|f\|_{H^{-s}(\Omega)} \quad \text{for all } u = (-\Delta)^{-s} f, f \in H^{-s}(\Omega), \quad (65)$$

where $\varepsilon_h \rightarrow 0$ as $h \rightarrow 0$. $(-\Delta)^{-s}$ is called the inverse of the fractional Laplacian; see [80]. Second, we can prove the following lemma. The proof is omitted, since it is identical to the original one; see [13].

Lemma 22. *Let $c_{\mathcal{J},1}, c_{\mathcal{J},2}$ and ε_h be quantities from (20) and (65). Then*

$$\|A^{-1} - C\|_2 \leq \frac{c_{\mathcal{J},2}^2}{c_{\mathcal{J},1}^4} \varepsilon_h.$$

The advantage of this detour is that it is already well-known (see [13]) that M^{-1} can be well approximated by an \mathcal{H} -matrix $N_{\mathcal{H}}$, i.e. for any given $\varepsilon_{M^{-1}} > 0$ there is $N_{\mathcal{H}} \in \mathcal{H}(T_{I \times I}, k_{M^{-1}})$ such that

$$\|M^{-1} - N_{\mathcal{H}}\|_2 \leq \varepsilon_{M^{-1}} \|M^{-1}\|_2,$$

where $k_{M^{-1}} \sim |\log \varepsilon_{M^{-1}}|^d$. For B the approach has to be adapted to the fractional Laplacian. The issues we faced here will be treated in detail later on. First, we want to finish the general idea of the proof. To do this, assume that we have a similar result as for M^{-1} , i.e. for any given $\varepsilon_B > 0$ there is $B_{\mathcal{H}} \in \mathcal{H}(T_{I \times I}, k_B)$ such that

$$\|B - B_{\mathcal{H}}\|_2 \leq \varepsilon_B \|B\|_2,$$

where $k_B \sim |\log \varepsilon_B|^d$. By setting $C_{\mathcal{H}} := N_{\mathcal{H}} B_{\mathcal{H}} N_{\mathcal{H}}$, we have an approximation for A^{-1} . As mentioned before, the exact product of \mathcal{H} -matrices is again an \mathcal{H} -matrix belonging to $\mathcal{H}(T_{I \times I}, k_C)$, where $k_C := c \max\{k_{M^{-1}}, k_B\} L^2(T_I)$ and c is a positive constant; see [13]. From this step on, the rest of the proof is identical to the original work. Hence, we obtain

$$\|C - C_{\mathcal{H}}\|_2 \leq c_1(\varepsilon_{M^{-1}} + \varepsilon_B),$$

where c_1 is a positive constants. This leads to

$$\|A^{-1} - C_{\mathcal{H}}\|_2 \leq c_1(\varepsilon_{M^{-1}} + \varepsilon_B) + c_2 \varepsilon_h,$$

where $c_2 := c_{\mathcal{J},1}^{-4} c_{\mathcal{J},2}^2$. Then we adjust the ranks $k_{M^{-1}}$ and k_B ,

$$k_{M^{-1}} \sim |\log \varepsilon_h|^d \quad \text{and} \quad k_B \sim |\log \varepsilon_h|^d,$$

such that

$$\|A^{-1} - C_{\mathcal{H}}\|_2 \leq 3 c_2 \varepsilon_h.$$

This would lead to the desired result as in [13].

7.2. Approximation of the discretized inverse operator

As we have seen in Section 7.1, the basic idea of the proof works also for the fractional Laplace. The issues start with the \mathcal{H} -matrix approximation of B . Since we do not know the exact form of the Green's function G , we first confirm that B can be approximated with an \mathcal{H} -matrix and assume that there exists a suitable degenerate kernel approximation for G .

Theorem 21. *Let D be a bounded $C^{1,1}$ domain. Assume that for any $\varepsilon > 0$ there exists $k_\varepsilon \in \mathbb{N}$ such that for each block $b = q \times w$ satisfying (59) there is a degenerate kernel function $G_{k_\varepsilon}^b$ satisfying*

$$\|G - G_{k_\varepsilon}^b\|_{L^2(X_q \times X_w)} \leq \varepsilon \|G\|_{L^2(X_q \times \hat{X}_w)},$$

where $\hat{X}_w := \{x \in \Omega : 2\rho \operatorname{dist}(x, X_w) \leq \operatorname{diam} X_w\}$. Then there is $B_{\mathcal{H}} \in \mathcal{H}(T_{I \times I}, k_\varepsilon)$ such that

$$\|B - B_{\mathcal{H}}\|_2 \leq c_{sp} c_{\mathcal{J},2}^2 \tilde{c}_G (\rho^{-1} + 2)^{2s} c_g^{\frac{2s}{d}} (1 - 2^{-\frac{2s}{d}})^{-1} \varepsilon,$$

where the constants c_{sp} , $c_{\mathcal{J}}$, c_g and \tilde{c}_G are defined in (56), (20), (55), and (66), respectively.

Proof. For non admissible blocks b , we simply set

$$(B_{\mathcal{H}})_b = B_b = (\mathcal{J}^*(-\Delta)^{-s}\mathcal{J})_b.$$

Next consider the admissible blocks $b = q \times w$. We define the integral operator

$$\mathcal{H}_b \varphi = \int_{\Omega} G_{k_\varepsilon}^b(x, \cdot) \varphi(x) \, dx \quad \text{for } \operatorname{supp} \varphi \in \bar{\Omega}$$

and set $(B_{\mathcal{H}})_b = (\mathcal{J}^* \mathcal{H}_b \mathcal{J})_b$. The rank of $(B_{\mathcal{H}})_b$ is bounded by k_ε ; see [13, Sect. 3.3].

Let $x \in \mathbb{R}^{|w|}$ and $y \in \mathbb{R}^{|q|}$. To see that $(B_{\mathcal{H}})_b$ approximates the block B_b , use the representation of Δ^{-s} (see [27]), and use (20). The estimate

$$\begin{aligned} ((B - B_{\mathcal{H}})_b x, y)_h &= (\mathcal{J}^*((-\Delta)^{-s} - \mathcal{H}_b)\mathcal{J}x, y)_h \\ &= ((-\Delta)^{-s} - \mathcal{H}_b)\mathcal{J}x, \mathcal{J}y)_{L^2} \\ &\leq \|G - G_{k_\varepsilon}^b\|_{L^2(X_q \times X_w)} \|\mathcal{J}x\|_{L^2(X_w)} \|\mathcal{J}y\|_{L^2(X_q)} \\ &\leq \varepsilon c_{\mathcal{J},2}^2 \|G\|_{L^2(X_q \times X_w)} \|x\|_h \|y\|_h \end{aligned}$$

proves $\|(B - B_{\mathcal{H}})_b\|_2 \leq \varepsilon c_{\mathcal{J},2}^2 \|G\|_{L^2(X_q \times X_w)}$.

From [27, Theorem 1.1] we know that G exists and that

$$|G(x, y)| \leq \frac{c_G}{|x - y|^{d-2s}}, \quad x, y \in D, \, x \neq y,$$

if D is a bounded $C^{1,1}$ domain. The positive constant c_G depends only on s and d . It can be seen that $\|G\|_{L^2(X_q \times X_w)}$ may increase when the sets X_q and \hat{X}_w approach each other. The construction of \hat{X}_w , however, ensures

$$\sigma := \operatorname{dist}(X_q, \hat{X}_w) \geq \frac{1}{2} \operatorname{dist}(X_q, X_w) \geq \frac{1}{2\rho} \operatorname{diam} X_q$$

7. \mathcal{H} -Approximation of the inverse of the stiffness matrix

as well as $2\rho\sigma \geq \text{diam } X_q$ due to the admissibility condition (59). Therefore, it holds that

$$\|G\|_{L^2(X_q \times \hat{X}_w)} \leq c_G \sigma^{-d+2s} |X_q|^{\frac{1}{2}} |\hat{X}_w|^{\frac{1}{2}}.$$

Using $|\hat{X}_w| \leq \omega_d (\frac{1}{2} \text{diam } \hat{X}_w)^d \leq \omega_d (\rho + \frac{1}{2})^d \sigma^d$ and $|X_q| \leq \omega_d \rho^d \sigma^d$, where ω_d is the volume of the unit ball in \mathbb{R}^d , we see that

$$\|G\|_{L^2(X_q \times X_w)} \leq \tilde{c}_G \sigma^{2s}, \quad \tilde{c}_G := c_G \omega_d (\rho(\rho + 1/2))^{d/2}. \quad (66)$$

Let q^* and w^* be the fathers of q and w , respectively. Then

$$\rho \text{dist}(X_{q^*}, X_{w^*}) \leq \max\{\text{diam } X_{q^*}, \text{diam } X_{w^*}\}$$

and it follows from [13, (1.22)] that

$$\begin{aligned} \text{dist}(X_q, \hat{X}_w) &\leq \text{dist}(X_q, X_w) \leq \text{dist}(X_{q^*}, X_{w^*}) + \text{diam } X_{q^*} + \text{diam } X_{w^*} \\ &\leq (\rho^{-1} + 2) \max\{\text{diam } X_{q^*}, \text{diam } X_{w^*}\} \leq (\rho^{-1} + 2) c_g^{1/d} 2^{-l/d} \end{aligned}$$

where l denotes the level of t in T_I . We obtain

$$\|(B - B_{\mathcal{H}})_b\|_2 \leq c_{\mathcal{J},2}^2 \tilde{c}_G (\rho^{-1} + 2)^{2s} c_g^{\frac{2s}{d}} 4^{-\frac{ls}{d}} \varepsilon.$$

From the proof of [13, Theorem 2.16] we see that

$$\|B - B_{\mathcal{H}}\|_2 \leq c_{sp} \sum_{l=0}^{L(T_I)} \|(B - B_{\mathcal{H}})_b\|_2 \leq c_{sp} c_{\mathcal{J},2}^2 \tilde{c}_G (\rho^{-1} + 2)^{2s} c_g^{\frac{2s}{d}} (1 - 4^{-\frac{s}{d}})^{-1} \varepsilon.$$

□

7.3. Degenerate kernel approximation

As Theorem 21 indicates the problem is not to find a suitable \mathcal{H} -approximation of B , but to construct a degenerate kernel approximation of the Green's function G . The approaches presented in Section 6.2 can not be applied, because we neither know if G is asymptotically smooth nor can we verify it. However, it is well-known that the Green's function $G(x, \cdot)$ is s -harmonic in $Y \setminus \{B_\varepsilon(x)\}$ with $\varepsilon > 0$. Therefore, the idea is to approximate G via functions satisfying (11).

Following the road map illustrated in [13] for the Laplace case, we need two results: a local Caccioppoli inequality for the fractional Laplacian and suitable approximation space.

7.3.1. Caccioppoli inequality

In order to prove a local Caccioppoli inequality it is necessary to deepen our understanding of s -harmonic functions and how to construct them. One way to construct an s -harmonic function on a sphere $B_\varepsilon(\xi)$ is to use the Poisson operator $\mathcal{P}_{\xi,\varepsilon}$. For functions $u \in L_1^s(\mathbb{R}^d) \cap C(\mathbb{R}^d)$ we have already done this in Theorem 2. According to [58], this assumption can be relaxed to $L^\infty(\mathbb{R}^d)$ functions.

7. \mathcal{H} -Approximation of the inverse of the stiffness matrix

Lemma 23. *Let $u \in L^\infty(\mathbb{R}^d)$. Then $\mathcal{P}_{\xi,\varepsilon}u$ satisfies the s -mean value property in $B_\varepsilon(\xi)$.*

Notice that the condition $u \in L^\infty(\mathbb{R}^d)$ in the previous lemma can be relaxed further on. Remember from (6) that

$$\tilde{L}^2(\Omega) := \{u \in L^2(\mathbb{R}^d) : u = 0 \text{ a.e. in } \mathbb{R}^d \setminus \Omega\} \subset L_1^s(\mathbb{R}^d).$$

Lemma 24. *Let $\delta > \varepsilon > 0$ and $B_\varepsilon(\xi) \subset \Omega$. If $u \in \tilde{L}^2(\Omega) \cap L^\infty(B_\delta(\xi) \setminus B_\varepsilon(\xi))$, then $\mathcal{P}_{\xi,\varepsilon}u$ satisfies the s -mean value property in $B_\varepsilon(\xi)$.*

Proof. In order to show that the integrals are well-defined, we show that $|\mathcal{P}_{\xi,\varepsilon}u(x)| < \infty$ for $x \in B_\varepsilon(\xi)$. With

$$I_1(x) := \int_{\mathbb{R}^d \setminus B_\delta(\xi)} P_{\xi,\varepsilon}(x,y)u(y) \, dy \quad \text{and} \quad I_2(x) := \int_{B_\delta(\xi) \setminus B_\varepsilon(\xi)} P_{\xi,\varepsilon}(x,y)u(y) \, dy,$$

where $P_{\xi,\varepsilon}$ is the Poisson kernel defined in (5), we split the integral to see that

$$|\mathcal{P}_{\xi,\varepsilon}u(x)| \leq |I_1(x)| + |I_2(x)|.$$

Using $\text{dist}(B_\varepsilon(\xi), \partial B_\delta(\xi)) = \delta - \varepsilon > 0$, we obtain

$$|I_1(x)| \leq a_s \frac{\varepsilon^{2s}}{(\delta^2 - \varepsilon^2)^s} (\delta - \varepsilon)^{-d} \int_{\mathbb{R}^d \setminus B_\delta(\xi)} |u(y)| \, dy \leq a_s \varepsilon^s \sqrt{|\Omega|} (\delta - \varepsilon)^{-d-s} \|u\|_{L^2(\Omega)}.$$

For I_2 we exploit the boundedness of u

$$|I_2(x)| \leq \|u\|_{L^\infty(B_\delta(\xi) \setminus B_\varepsilon(\xi))} \int_{\mathbb{R}^d \setminus B_\varepsilon(\xi)} \lambda_{\xi,\varepsilon}(x,y) \, dy = \|u\|_{L^\infty(B_\delta(\xi) \setminus B_\varepsilon(\xi))}.$$

The last step is due to the normalization of the inner integral; see [58, p. 206]. In summary we obtain

$$|\mathcal{P}_{\xi,\varepsilon}u(x)| \leq M \|u\|_{L^2(\mathbb{R}^d)} + \|u\|_{L^\infty(B_\delta(\xi) \setminus B_\varepsilon(\xi))},$$

where $M := a_s \varepsilon^s \sqrt{|\Omega|} (\delta - \varepsilon)^{-d-s}$. In the same way as in Lemma 2 in [58], it can be shown that $\mathcal{P}_{\xi,\varepsilon}u$ satisfies the s -mean value property in $B_\varepsilon(\xi)$. \square

The requirement $u \in L^\infty(B_\delta(\xi) \setminus B_\varepsilon(\xi))$ is not a critical assumption. It can be seen from the following lemma; see [80].

Lemma 25. *Let $u \in \tilde{H}^s(\Omega)$ be a solution to $(-\Delta)^s u = 0$ in D . Then u is locally bounded, i.e. $\|u\|_{L^\infty(K)} \leq c \|u\|_{L^2(\Omega)}$ for all compact $K \subset D$.*

We introduce the set

$$X^s(D) := \{u \in \tilde{H}^s(\Omega) : a(u, \varphi) = 0 \text{ for all } \varphi \in C_0^\infty(D)\} \tag{67}$$

which consists of \tilde{H}^s -functions being s -harmonic in D and vanishing outside Ω .

Lemma 26. *Let $u \in X^s(D)$ and $K \subset D$ be compact, then u is s -harmonic in $\text{int } K$.*

7. \mathcal{H} -Approximation of the inverse of the stiffness matrix

Proof. Let $\overline{B_\varepsilon(z)} \subset \text{int } K$. Then there is $\varepsilon' > \varepsilon$ such that $\overline{B_{\varepsilon'}(z)} \subset \text{int } K$. Since $u \in X^s(D)$, Lemma 25 guarantees that $u \in L^\infty(K)$. By applying Lemma 24 to $B_{\varepsilon'}(z)$, we obtain that $\mathcal{P}_{z,\varepsilon'}u$ satisfies the s -mean value property in $B_{\varepsilon'}(z)$. Therefore, $\mathcal{P}_{z,\varepsilon'}u$ is also s -harmonic in $B_{\varepsilon'}(z)$; see Lemma 4 and Theorem 4. Since the bilinear form a is symmetric, coercive and continuous (see Lemma 5) and since $u = \mathcal{P}_{\xi,\varepsilon'}u$ a.e. in $\mathbb{R}^d \setminus B_{\varepsilon'}(z)$, Lax-Milgram guarantees that $u = \mathcal{P}_{z,\varepsilon'}u$. Therefore, u is s -harmonic in $B_{\varepsilon'}(z)$. Since this holds for all closed balls in $\text{int } K$, it follows that u is s -harmonic in $\text{int } K$. \square

The following lemma shows that locally smooth functions are sufficient to construct globally smooth cut-off functions.

Lemma 27. *Let $\chi \in C^1(\mathbb{R}^d)$ satisfy $0 \leq \chi \leq 1$ with $\|\nabla\chi\|_\infty < \infty$. If $u \in H^s(K)$, where $K = \text{supp } \chi$, then $\chi^2u \in H^s(\mathbb{R}^d)$.*

Proof. $\varphi := \chi^2u \in H^s(K)$ can be seen from

$$\begin{aligned} |\varphi|_{H^s(K)}^2 &= \int_K \int_K \frac{|\chi^2(x)u(x) - \chi^2(y)u(y)|^2}{|x-y|^{d+2s}} dy dx \\ &\leq 2 \int_K \int_K \frac{|\chi(y)|^4 |u(x) - u(y)|^2 + |\chi^2(x) - \chi^2(y)|^2 |u(x)|^2}{|x-y|^{d+2s}} dy dx \\ &\leq 2|u|_{H^s(K)}^2 + 2 \int_K |u(x)|^2 \int_K \frac{|\chi(x) - \chi(y)|^2 |\chi(x) + \chi(y)|^2}{|x-y|^{d+2s}} dy dx \\ &\leq 2|u|_{H^s(K)}^2 + 8 \int_K |u(x)|^2 \int_K \frac{|\chi(x) - \chi(y)|^2}{|x-y|^{d+2s}} dy dx \end{aligned}$$

and the boundedness of the inner integral w.r.t. $x \in K$

$$\begin{aligned} \int_K \frac{|\chi(x) - \chi(y)|^2}{|x-y|^{d+2s}} dy &\leq \|\nabla\chi\|_\infty^2 \int_{B_1(x)} |x-y|^{2-d-2s} dy + \int_{\mathbb{R}^d \setminus B_1(x)} \frac{1}{|x-y|^{d+2s}} dy \\ &\leq \|\nabla\chi\|_\infty^2 \int_0^1 r^{1-2s} dr + \kappa_{d,s}(1) \leq \frac{\|\nabla\chi\|_\infty^2}{2-2s} + \kappa_{d,s}(1). \end{aligned}$$

Since $\varphi = 0$ in $\mathbb{R}^d \setminus K$, $\varphi \in H^s(\mathbb{R}^d)$ follows from

$$\begin{aligned} |\varphi|_{H^s(\mathbb{R}^d)}^2 &= \int_K \int_K \frac{|\varphi(x) - \varphi(y)|^2}{|x-y|^{d+2s}} dy dx + 2 \int_K \int_{\mathbb{R}^d \setminus K} \frac{|\varphi(x)|^2}{|x-y|^{d+2s}} dy dx \\ &= |\varphi|_{H^s(K)}^2 + 2 \int_K |u(x)|^2 \int_{\mathbb{R}^d \setminus K} \frac{|\chi(x)|^4}{|x-y|^{d+2s}} dy dx. \end{aligned}$$

The inner integral is uniformly bounded for $x \in K$

$$\begin{aligned} \int_{\mathbb{R}^d \setminus K} \frac{|\chi(x)|^4}{|x-y|^{d+2s}} dy &\leq \int_{B_1(x)} \frac{|\chi(x) - \chi(y)|^4}{|x-y|^{d+2s}} dy + \int_{\mathbb{R}^d \setminus B_1(x)} \frac{1}{|x-y|^{d+2s}} dy \\ &\leq \|\nabla\chi\|_\infty^4 \int_{B_1(x)} \frac{|x-y|^4}{|x-y|^{d+2s}} dy + \kappa_{d,s}(1) \\ &\leq \|\nabla\chi\|_\infty^4 \int_0^1 r^{3-2s} dr + \kappa_{d,s}(1) \leq \frac{\|\nabla\chi\|_\infty^4}{4-2s} + \kappa_{d,s}(1). \end{aligned}$$

\square

7. \mathcal{H} -Approximation of the inverse of the stiffness matrix

In [34, Prop. 5.1] a Caccioppoli inequality for a group of kernels satisfying certain conditions is introduced. We will use some ideas of his proof and the framework of [13, Lem. 4.18] and customize it to the fractional Laplacian. Notice that the result in [34] is a global Caccioppoli inequality, i.e. it contains the L^2 -norm of u on Ω on the right-hand side, whereas we need the following local variant.

Theorem 22. *Let $\rho > 0$ and let $K \subset D$ be compact satisfying $\text{diam } K \leq \rho \text{dist}(K, \partial D)$. There is a constant $c_{\mathcal{L}} = c_{\mathcal{L}}(d, s, \rho, \text{diam } K) > 0$ such that*

$$|u|_{H^s(K)} \leq \frac{c_{\mathcal{L}}}{\text{dist}^s(K, \partial D)} \|u\|_{L^2(D)}$$

for all $u \in X^s(D)$.

Proof. Let $\chi \in C^1(\mathbb{R}^d)$ satisfy $0 \leq \chi \leq 1$, $\chi = 1$ in K , such that $\|\nabla \chi\|_{\infty} \leq 2/\sigma$, where $\sigma := \text{dist}(K, \partial K')$ and $K' := \text{supp } \chi \subset D$ satisfies

$$\frac{1}{4} \leq \frac{\sigma}{\text{dist}(K, \partial D)} \leq \frac{1}{2}.$$

The definition (67) of $X^s(D)$ implies $u \in H^s(K')$. Furthermore, Lemma 27 shows that $\varphi := \chi^2 u \in H^s(\mathbb{R}^d)$ and $\varphi = 0$ in $\mathbb{R}^d \setminus D$. Hence, φ may be used as a test function in (9) due to the dense embedding of $C_0^\infty(D)$ in $\tilde{H}^s(D)$. With $a(u, \varphi) = 0$ we obtain that

$$\underbrace{\int_{\Omega} \int_{\Omega} \frac{[u(x) - u(y)][\varphi(x) - \varphi(y)]}{|x - y|^{d+2s}} dy dx}_{=: I} = -2 \underbrace{\int_{\Omega} \int_{\mathbb{R}^d \setminus D} \frac{u(x) \varphi(x)}{|x - y|^{d+2s}} dy dx}_{=: J} + 2 \int_{\Omega} \int_{\Omega \setminus D} \frac{u(x) \varphi(x)}{|x - y|^{d+2s}} dy dx.$$

Due to $\varphi = 0$ in $\Omega \setminus D$, the first integral reads

$$I = \underbrace{\int_D \int_D \frac{[u(x) - u(y)][\varphi(x) - \varphi(y)]}{|x - y|^{d+2s}} dy dx}_{=: I_1} - 2 \underbrace{\int_{\Omega \setminus D} \int_D \frac{u(x) \varphi(y)}{|x - y|^{d+2s}} dy dx}_{=: I_2} + 2 \int_{\Omega} \int_{\Omega \setminus D} \frac{u(x) \varphi(x)}{|x - y|^{d+2s}} dy dx.$$

Hence, we obtain $I_1 = 2(I_2 - J)$. Notice that

$$\begin{aligned} [u(x) - u(y)][\varphi(x) - \varphi(y)] &= \chi^2(x)u^2(x) - [\chi^2(x) + \chi^2(y)]u(x)u(y) + \chi^2(y)u^2(y) \\ &= |\chi(x)u(x) - \chi(y)u(y)|^2 - |\chi(x) - \chi(y)|^2 u(x)u(y) \end{aligned}$$

and, therefore,

$$I_1 \geq \int_{K'} \int_{K'} \frac{|\chi(x)u(x) - \chi(y)u(y)|^2}{|x - y|^{d+2s}} dy dx - \int_D \int_D \frac{|\chi(x) - \chi(y)|^2 |u(x)||u(y)|}{|x - y|^{d+2s}} dy dx.$$

By Young's inequality and by exploiting the symmetry we obtain that

$$\int_D \int_D \frac{|\chi(x) - \chi(y)|^2 |u(x)||u(y)|}{|x - y|^{d+2s}} dy dx \leq \int_D |u(x)|^2 \int_D \frac{|\chi(x) - \chi(y)|^2}{|x - y|^{d+2s}} dy dx.$$

7. \mathcal{H} -Approximation of the inverse of the stiffness matrix

The next step splits the inner integral relative to $x \in D$

$$\int_D \frac{|\chi(x) - \chi(y)|^2}{|x - y|^{d+2s}} dy \leq \int_{D \setminus B_\sigma(x)} \frac{|\chi(x) - \chi(y)|^2}{|x - y|^{d+2s}} dy + \int_{B_\sigma(x)} \frac{|\chi(x) - \chi(y)|^2}{|x - y|^{d+2s}} dy.$$

The first integral is not singular. Using $0 \leq \chi \leq 1$, we have

$$\int_{D \setminus B_\sigma(x)} \frac{|\chi(x) - \chi(y)|^2}{|x - y|^{d+2s}} dy \leq \int_{\mathbb{R}^d \setminus B_\sigma(x)} |x - y|^{-d-2s} dy = \kappa_{d,s}(\sigma) = \frac{\omega_d}{2s} \sigma^{-2s}.$$

For the second integral we use $|\chi(x) - \chi(y)| \leq \|\nabla \chi\|_\infty |x - y| \leq \frac{2}{\sigma} |x - y|$ and obtain

$$\int_{B_\sigma(x)} \frac{|\chi(x) - \chi(y)|^2}{|x - y|^{d+2s}} dy \leq \frac{4}{\sigma^2} \int_{B_\sigma(x)} |x - y|^{2-d-2s} dy = \frac{4\omega_d}{\sigma^2} \int_0^\sigma r^{1-2s} dr = \frac{2\omega_d}{1-s} \sigma^{-2s}.$$

In summary, this leads to

$$I_1 \geq |\chi u|_{H^s(K')}^2 - c \sigma^{-2s} \|u\|_{L^2(D)}^2.$$

Next, we investigate the integral

$$\begin{aligned} I_2 - J &= \int_{K'} \varphi(y) \int_{\mathbb{R}^d \setminus D} \frac{u(x) - u(y)}{|x - y|^{d+2s}} dx dy \\ &= \int_{K'} \varphi(y) \int_{\mathbb{R}^d \setminus \hat{K}} \frac{u(x) - u(y)}{|x - y|^{d+2s}} dx dy - \int_{K'} \varphi(y) \int_{D \setminus \hat{K}} \frac{u(x) - u(y)}{|x - y|^{d+2s}} dx dy =: I_3 - I_4, \end{aligned}$$

where $\hat{K} := \{x \in \mathbb{R}^d : \text{dist}(x, K') < \tilde{\sigma}\} \subset D$ and $\tilde{\sigma} := \sigma/2$. Due to the construction of \hat{K} , there exists a compact set \tilde{K} with $\hat{K} \subset \tilde{K} \subset D$. According to Lemma 26, u is s -harmonic in \tilde{K} . Using the s -harmonicity we obtain for I_3 that

$$I_3 = - \int_{K'} \varphi(y) \int_{\mathbb{R}^d \setminus \hat{K}} \frac{u(y) - u(x)}{|y - x|^{d+2s}} dx dy + c_{d,s}^{-1} \int_{K'} \varphi(y) (-\Delta)^s u(y) dy$$

and distinguish for now between two cases. First, we consider $s < 1/2$:

$$I_3 = \int_{K'} \varphi(y) \int_{\hat{K} \setminus B_{\tilde{\sigma}}(y)} \frac{u(y) - u(x)}{|y - x|^{d+2s}} dx dy + \int_{K'} \varphi(y) \int_{B_{\tilde{\sigma}}(y)} \frac{u(y) - u(x)}{|y - x|^{d+2s}} dx dy.$$

For the first integral we obtain using $|\varphi(y)[u(x) - u(y)]| \leq 3[u^2(x) + u^2(y)]$ that

$$\begin{aligned} \int_{K'} \varphi(y) \int_{\hat{K} \setminus B_{\tilde{\sigma}}(y)} \frac{u(y) - u(x)}{|y - x|^{d+2s}} dx dy &\leq 3 \int_{K'} \int_{\hat{K} \setminus B_{\tilde{\sigma}}(y)} \frac{u^2(y) + u^2(x)}{|y - x|^{d+2s}} dx dy \\ &\leq 3\kappa_{d,s}(\tilde{\sigma}) \|u\|_{L^2(D)}^2 + 3 \frac{|K'|}{\tilde{\sigma}^{d+2s}} \|u\|_{L^2(D)}^2 \leq C \sigma^{-2s} \|u\|_{L^2(D)}^2, \end{aligned}$$

where we have used

$$\begin{aligned} |K'| &\leq \omega_d (\text{diam } K')^d \leq \omega_d (\text{diam } K + \sigma)^d \leq \omega_d [\rho \text{dist}(K, \partial D) + \sigma]^d \\ &\leq \omega_d (4\rho + 1)^d \sigma^d = 2^d \omega_d (4\rho + 1)^d \tilde{\sigma}^d. \end{aligned}$$

7. \mathcal{H} -Approximation of the inverse of the stiffness matrix

Due to its singularity, the second integral in I_3 has to be investigated in more detail. According to Lemma 4, u is analytic in \hat{K} . Hence, we obtain for $0 < s < 1/2$ that

$$\int_{K'} \varphi(y) \int_{B_{\tilde{\sigma}}(y)} \frac{u(y) - u(x)}{|y - x|^{d+2s}} dx dy \leq C_a \omega_d \int_{K'} |\varphi(y)| \int_0^{\tilde{\sigma}} r^{-2s} dr dy \leq \tilde{C} \sigma^{-2s} \|u\|_{L^2(D)}.$$

For the second case, $s \geq 1/2$, we use (3) and choose $\delta = \tilde{\sigma}$:

$$I_3 = \int_{K'} \varphi(y) \int_{\hat{K} \setminus B_{\tilde{\sigma}}(y)} \frac{u(y) - u(x)}{|y - x|^{d+2s}} dx dy + \int_{K'} \varphi(y) \int_{B_{\tilde{\sigma}}(y)} \frac{u(y) - u(x) - \nabla u(y)^T (y - x)}{|y - x|^{d+2s}} dx dy.$$

The first integral in I_3 is for both cases, $s < 1/2$ and $s \geq 1/2$, identical and is handled in the same way. For the second one, we use again that u is an analytic function in \hat{K} :

$$\int_{K'} \varphi(y) \int_{B_{\tilde{\sigma}}(y)} \frac{u(y) - u(x) - \nabla u(y)^T (y - x)}{|y - x|^{d+2s}} dx dy \leq C_a \omega_d \int_{K'} |\varphi(y)| \int_0^{\tilde{\sigma}} r^{1-2s} dr dy \leq \tilde{C} \sigma^{-2s} \|u\|_{L^2(D)}.$$

We now deal with I_4 by using $B_{\tilde{\sigma}}(y) \subset \hat{K}$ for $y \in K'$ and the same ideas as above

$$\begin{aligned} I_4 &\leq 3 \int_{K'} \int_{D \setminus B_{\tilde{\sigma}}(y)} \frac{u^2(y) + u^2(x)}{|y - x|^{d+2s}} dx dy \\ &\leq 3\kappa_{d,s}(\tilde{\sigma}) \|u\|_{L^2(D)}^2 + 3 \frac{|K'|}{\tilde{\sigma}^{d+2s}} \|u\|_{L^2(D)}^2 \leq C \sigma^{-2s} \|u\|_{L^2(D)}^2. \end{aligned}$$

From $I_1 = 2(I_2 - J)$ we finally obtain that

$$\|u\|_{H^s(K)}^2 \leq |\chi u|_{H^s(K')}^2 \leq 2(I_2 - J) + c \sigma^{-2s} \|u\|_{L^2(D)}^2 \leq \tilde{c} \sigma^{-2s} \|u\|_{L^2(D)}^2 \leq \frac{4^{2s} \tilde{c}}{\text{dist}^{2s}(K, \partial D)} \|u\|_{L^2(D)}^2.$$

□

7.3.2. Construction of the approximation space

Adapting the approach of [13], the next step is to construct an approximation space V being a finite dimensional subspace of $X^s(D)$. However, $X^s(D)$ has to be a closed subspace of $L^2(\mathbb{R}^d)$ for this approach. Unfortunately, we are unable to verify it.

To overcome this issue, we introduce, motivated by Lemma 5, the set

$$X_{\text{loc}}^s(D) := \{u \in \tilde{L}^2(\Omega) \cap H_{\text{loc}}^s(D) : a(u, \varphi) = 0 \text{ for all } \varphi \in C_0^\infty(D)\},$$

which consists of H_{loc}^s -functions being s -harmonic and vanishing outside Ω , where

$$H_{\text{loc}}^s(D) = \{u \in L^2(D) : u \in H^s(K) \text{ for all compact } K \subset D\}.$$

However, for functions $u \in X_{\text{loc}}^s(D)$ we can only prove a non-local Caccioppoli inequality, since we cannot guarantee that $u \in L^\infty(K)$ for each compact $K \subset D$.

7. \mathcal{H} -Approximation of the inverse of the stiffness matrix

Theorem 23. *Let $K \subset D$ be compact. Then there is a constant $c > 0$ such that*

$$|u|_{H^s(K)} \leq c \|u\|_{L^2(\Omega)} \quad \text{for all } u \in X_{\text{loc}}^s(D).$$

Proof. We follow the same approach as in the proof of Theorem 22. Only the terms I_2 and J are handled in a different way.

$$\begin{aligned} I_2 &= \int_{\Omega \setminus D} \int_D \frac{u(x) \varphi(y)}{|y-x|^{d+2s}} dy dx \leq \int_{K'} \int_{\Omega \setminus D} \frac{|u(x)| |u(y)|}{|y-x|^{d+2s}} dx dy \\ &\leq \text{dist}(K', \partial D)^{-d-2s} \|u\|_{L^1(\Omega)}^2 \leq C \|u\|_{L^2(\Omega)}^2. \end{aligned}$$

Then J is estimated:

$$\begin{aligned} |J| &\leq \int_{\Omega} \int_{\mathbb{R}^d \setminus D} \frac{|u(x)| |\varphi(x)|}{|y-x|^{d+2s}} dy dx \leq \int_{K'} |u(x)|^2 \int_{\mathbb{R}^d \setminus D} |y-x|^{-d-2s} dy dx \\ &\leq \int_{K'} |u(x)|^2 \int_{\mathbb{R}^d \setminus B_\sigma(x)} |y-x|^{-d-2s} dy dx = \kappa_{d,s}(\sigma) \|u\|_{L^2(D)}^2. \end{aligned}$$

From $I_1 \leq 2(|I_2| + |J|)$ we finally obtain

$$|u|_{H^s(K)} \leq c \|u\|_{L^2(\Omega)}.$$

□

The Caccioppoli inequality is important for the proof of the following lemma.

Lemma 28. *The space $X_{\text{loc}}^s(D)$ is a closed subspace of $L^2(\mathbb{R}^d)$.*

Proof. Let $\{u_k\}_{k \in \mathbb{N}} \subset X_{\text{loc}}^s(D)$ converge to u in $L^2(\mathbb{R}^d)$ and let $K \subset D$ be compact. According to Theorem 23, the sequence $\{u_k\}_{k \in \mathbb{N}}$ is bounded on K ,

$$|u_k|_{H^s(K)} \leq c \|u_k\|_{L^2(\mathbb{R}^d)} \leq C.$$

Due to the Banach-Alaoglu theorem (see [83]), a sub-sequence $\{u_{i_k}\}_{k \in \mathbb{N}}$ converges weakly in $H^s(K)$ to $\hat{u} \in H^s(K)$. Hence, for any $v \in L^2(K)$ we have

$$(u, v)_{L^2(K)} = \lim_{k \rightarrow \infty} (u_{i_k}, v)_{L^2(K)} = (\hat{u}, v)_{L^2(K)},$$

which proves that $u = \hat{u} \in H^s(K)$. Notice that this holds for all compact subsets of D . Since the functional $a(\cdot, \varphi) : \tilde{L}^2(\mathbb{R}^d) \cap H_{\text{loc}}^s(D) \rightarrow \mathbb{R}$ for $\varphi \in C_0^\infty(D)$ (see Lemma 5), we see by the same argument that $a(u, \varphi) = 0$. Hence, $u \in X_{\text{loc}}^s(D)$ is proved and $X_{\text{loc}}^s(D)$ is closed in $L^2(\mathbb{R}^d)$. □

Before we can start to construct an approximation space V , we need a Poincaré inequality for functions $u \in H^s(D)$.

Theorem 24. *For any $u \in H^s(D)$ we set $\bar{u} = |D|^{-1} \int_D u$. Then*

$$\|u - \bar{u}\|_{L^2(D)} \leq \sqrt{\frac{(\text{diam } D)^d}{|D|}} (\text{diam } D)^s |u|_{H^s(D)}.$$

7. \mathcal{H} -Approximation of the inverse of the stiffness matrix

Proof. Using the Cauchy-Schwarz inequality

$$\int_D |u(x) - \bar{u}|^2 dx = \frac{1}{|D|^2} \int_D \left| \int_D u(x) - u(y) dy \right|^2 dx \leq \frac{1}{|D|} \int_D \int_D |u(x) - u(y)|^2 dy dx,$$

we obtain

$$\int_D |u(x) - \bar{u}|^2 dx \leq \frac{(\text{diam } D)^{d+2s}}{|D|} \int_D \int_D \frac{|u(x) - u(y)|^2}{|x - y|^{d+2s}} dy dx.$$

□

With this we have all the building blocks together to construct V .

Lemma 29. *Let $B \subset D$. Then for any $k \in \mathbb{N}$ there is a subspace $V \subset X_{\text{loc}}^s(B)$ satisfying $\dim V \leq k$ so that*

$$\text{dist}_{L^2(D)}(u, V) \leq c_A \left(\frac{\text{diam } D}{\sqrt[d]{k}} \right)^s |u|_{H^s(D)}$$

for each $u \in X_{\text{loc}}^s(D)$, where c_A depends only on s and the shape of D .

Proof. We decompose D into k quasi-uniform and shape-regular sub-domains D_i , i.e. there is $c > 0$ such that

$$\text{diam } D_i \leq \frac{c}{\sqrt[d]{k}} \text{diam } D \quad \text{and} \quad |D_i| \geq c (\text{diam } D_i)^d, \quad i = 1, \dots, k.$$

Let

$$W = \{v \in L^2(\mathbb{R}^d) : v \text{ is constant on each } D_i, i = 1, \dots, k \text{ and } v|_{\mathbb{R}^d \setminus D} = 0\}.$$

Then $\dim W \leq k$ and according to Theorem 24 for $u \in H^s(D_i)$ it holds that

$$\int_{D_i} |u - \bar{u}_i|^2 dx \leq \frac{(\text{diam } D_i)^{d+2s}}{|D_i|} \int_{D_i} \int_{D_i} \frac{|u(x) - u(y)|^2}{|x - y|^{d+2s}} dy dx,$$

where $\bar{u}_i := |D_i|^{-1} \int_{D_i} u$ is the mean value of u in D_i . The properties of the decomposition of D into the D_i lead to

$$\int_{D_i} |u - \bar{u}_i|^2 dx \leq \frac{c^{2s-1}}{k^{2s/d}} (\text{diam } D)^{2s} \int_{D_i} \int_{D_i} \frac{|u(x) - u(y)|^2}{|x - y|^{d+2s}} dy dx.$$

Summation over all i yields

$$\|u - \bar{u}\|_{L^2(D)} \leq \frac{c^{s-1/2}}{k^{s/d}} (\text{diam } D)^s |u|_{H^s(D)}$$

with $\bar{u} \in W$ defined by $\bar{u}|_{D_i} = \bar{u}_i$ and $\bar{u}|_{\mathbb{R}^d \setminus D} = 0$.

In order to guarantee that the approximation is done from a subset of $X_{\text{loc}}^s(B)$, we project W onto $X_{\text{loc}}^s(B)$. Let $P : L^2(\mathbb{R}^d) \rightarrow X_{\text{loc}}^s(B)$ be the $L^2(\mathbb{R}^d)$ -orthogonal projection onto $X_{\text{loc}}^s(B)$ and let

7. \mathcal{H} -Approximation of the inverse of the stiffness matrix

$V = P(W)$. P exists, since $X_{\text{loc}}^s(B)$ is closed in $L^2(\mathbb{R}^d)$, see Lemma 28. Keeping in mind that P has norm one and $u \in X_{\text{loc}}^s(D) \subset X_{\text{loc}}^s(B)$, we obtain

$$\begin{aligned} \|u\|_{L^2(\mathbb{R}^d \setminus D)}^2 + \text{dist}_{L^2(D)}^2(u, V) &\leq \|P(u - 0)\|_{L^2(\mathbb{R}^d \setminus D)}^2 + \|P(u - \bar{u})\|_{L^2(D)}^2 = \|P(u - \bar{u})\|_{L^2(\mathbb{R}^d)}^2 \\ &\leq \|u\|_{L^2(\mathbb{R}^d \setminus D)}^2 + \|u - \bar{u}\|_{L^2(D)}^2, \end{aligned}$$

which proves the assertion. \square

Notice that if the orthogonal projection $\tilde{P} : L^2(\mathbb{R}^d) \rightarrow X_{\text{loc}}^s(D)$ is used to construct V instead of P , it cannot be guaranteed that the dimension of V depends on k . This is because V would consist of s -harmonic functions in D vanishing outside of D . Therefore, the detour via $X_{\text{loc}}^s(B)$ is necessary.

7.3.3. Approximation result

Lemma 30. *Assume that $B \subset D$ is a domain such that for some $\rho > 0$ it holds that*

$$0 < \text{diam } B \leq \rho \text{dist}(B, \partial D).$$

Then for any $k \in \mathbb{N}$ there is a subspace $V \subset X_{\text{loc}}^s(B)$ satisfying $\dim V \leq k$ so that

$$\text{dist}_{L^2(B)}(u, V) \leq c_A c_{\mathcal{L}} \left(\frac{\rho}{\sqrt[k]{k}} \right)^s \|u\|_{L^2(B)} \quad (68)$$

for each $u \in X^s(D)$. The constants c_A and $c_{\mathcal{L}}$ are from the Lemma 29 and Theorem 22, respectively.

Proof. Choose $V \subset X_{\text{loc}}^s(B)$ as in Lemma 29, then it holds

$$\text{dist}_{L^2(B)}(u, V) \leq c_A \left(\frac{\text{diam } D}{\sqrt[k]{k}} \right)^s |u|_{H^s(B)}.$$

Since $u \in X^s(D) \subset X_{\text{loc}}^s(D)$, we can apply Theorem 22:

$$\text{dist}_{L^2(B)}(u, V) \leq c_A c_{\mathcal{L}} \left(\frac{\rho}{\sqrt[k]{k}} \right)^s |u|_{H^s(D)}.$$

\square

Although Lemma 30 can be applied to approximate the Green's function, it does not satisfy our requirements, since the approximation error does not decay exponentially w.r.t. k . To obtain such an error estimate, Lemma 30 has to be applied to a sequence of domains K_i , $i = 0, \dots, l \in \mathbb{N}$, with

$$B = K_l \subset K_{l-1} \subset \dots \subset K_0 \subset D.$$

This is not possible here, since we can not guarantee that $v := \arg \text{dist}_{L^2(B)}(u, V) \in \tilde{H}^s(\Omega)$. Obviously, it holds that $v \in X_{\text{loc}}^s(B)$, however, this not enough to apply Theorem 22, the Caccioppoli inequality, to v . The main issue is that we cannot prove that a function $v \in X_{\text{loc}}^s(B)$ is s -harmonic in the interior of B . In contrast to harmonic functions u , where $u \in H_{\text{loc}}^1(B)$ is enough to show that u is continuous in the interior of B ; see [41], this is not true for s -harmonic functions. Here, the $H^s(\mathbb{R}^d)$ regularity is necessary, see [80]. Nevertheless, we can show that the inverse of the stiffness matrix can be approximated by \mathcal{H} -matrices.

For this Lemma 30 will now be applied with algebraic decay to $G(x, \cdot)$ on X_w with $x \in X_q$.

7. \mathcal{H} -Approximation of the inverse of the stiffness matrix

Lemma 31. *Let $b = q \times w$ be a block and assume that there is $\rho > 0$ such that*

$$0 < \text{diam } X_w \leq \rho \text{ dist}(X_q, X_w).$$

Then for any $\varepsilon > 0$ there is a separable approximation

$$G_k(x, y) = \sum_{m=1}^k u_m(x) v_m(y) \text{ with } k \leq k_\varepsilon := c_A c_{\mathcal{L}} \left(\frac{\rho}{\sqrt[d]{k}} \right)^s,$$

so that for all $x \in X_w$

$$\|G(x, \cdot) - G_k(x, \cdot)\|_{L^2(X_w)} \leq \varepsilon \|G(x, \cdot)\|_{L^2(\hat{X}_w)}, \quad (69)$$

where $\hat{X}_w := \{y \in \Omega : 2\rho \text{ dist}(y, X_w) < \text{diam } X_w\}$.

Proof. Note that due to $\text{dist}(X_q, \hat{X}_w) > 0$, we have $G(x, \cdot) \in X^s(\hat{X}_w)$ for all $x \in X_q$. Since in addition $\text{diam } X_w \leq 2\rho \text{ dist}(X_w, \partial\hat{X}_w)$, Lemma 30 can be applied with ρ replaced by 2ρ . Let $\{v_1, \dots, v_k\}$ be a basis of the subspace $W \subset X^s(B)$ with $B \subset X_w$ and

$$k = \dim W \leq c_A c_{\mathcal{L}} \left(\frac{\rho}{\sqrt[d]{k}} \right)^s.$$

According to (68), $G(x, \cdot)$ can be decomposed into $G(x, \cdot) = \hat{G}(x, \cdot) + r_x$ with $\hat{G}(x, \cdot) \in W$ and $\|r_x\|_{L^2(X_w)} \leq \varepsilon \|G(x, \cdot)\|_{L^2(\hat{X}_w)}$. Expressing $\hat{G}(x, \cdot)$ by means of the basis of W , we obtain

$$\hat{G}(x, \cdot) = \sum_{m=1}^k u_m(x) v_m(\cdot)$$

with coefficients $u_i(x)$ depending on the index $x \in X_q$. The function

$$G_k(x, y) := \sum_{m=1}^k u_m(x) v_m(y)$$

satisfies estimate (69). □

8. Uniform \mathcal{H} -matrices and \mathcal{H}^2 -matrices

As mentioned before, the assembling of the stiffness matrix of the fractional Laplacian is quite costly even if we use a standard \mathcal{H} -matrix approach. One possibility to reduce the computational effort even further is the use of uniform \mathcal{H} -matrices or even \mathcal{H}^2 -matrices. These are both special types of \mathcal{H} -matrices, which will be introduced later on in this section. First, we want to provide the necessary means to construct such matrices. To do so, we will provide a method to generalize the cross approximation presented in Section 6.2.2 to the kernel-independent construction of uniform \mathcal{H} -matrices and \mathcal{H}^2 -matrices for the stiffness matrix A . The method can also be applied to matrices $A \in \mathbb{R}^{M \times N}$ with entries of the form

$$a_{ij} = \int_{\Omega} \int_{\Omega} \kappa(x, y) \varphi_i(x) \psi_j(y) \, dy \, dx, \quad i = 1, \dots, M, \quad j = 1, \dots, N. \quad (70)$$

Here, φ_i and ψ_j denote locally supported ansatz and test functions. The kernel function κ is of the type

$$\kappa(x, y) = \xi(x) \zeta(y) f(x, y) \quad (71)$$

with a singular function $f(x, y) = |x - y|^{-\alpha}$, $\alpha > 0$, and functions ξ and ζ each depending on only one of the variables x and y . Such matrices result, for instance, from a Galerkin discretization of integral operators. In particular, this includes the single layer potential operator $\kappa(x, y) = |x - y|^{-1}$ and the double layer potential operator of the Laplacian in \mathbb{R}^3 for which $\kappa(x, y) = \frac{(x-y) \cdot n_y}{|x-y|^3} = \frac{x \cdot n_y}{|x-y|^3} - \frac{y \cdot n_y}{|x-y|^3}$. Note that collocation methods and Nyström methods can also be included by formally choosing $\varphi_i = \delta_{x_i}$ or $\psi_j = \delta_{x_j}$, where δ_x denotes the Dirac distribution centered at x . In contrast to \mathcal{H} -matrices for which the method is applied to blocks, in the case of uniform \mathcal{H} -matrices and \mathcal{H}^2 -matrices cluster bases have to be constructed. If this is to be done adaptively, special properties of the kernel have to be exploited, in order to be able to guarantee that the error is controlled also outside of the cluster. In particular, we will apply these techniques to the fractional Laplacian.

8.1. Interpolants and quadrature rules

For the construction of uniform \mathcal{H} -matrix approximations and \mathcal{H}^2 -matrix approximations (see Sections 8.3 and 8.4), quadrature rules for the computation of integrals

$$\int_X f(x, y) \, dx$$

will be required which depend only on the domain of integration $X \subset \mathbb{R}^d$ and which are valid in the whole far-field of X , i.e. for $y \in \mathcal{F}_\rho(X)$, where

$$\mathcal{F}_\rho(X) := \{y \in \mathbb{R}^d : \rho \operatorname{dist}(y, X) \geq \operatorname{diam} X\}$$

with given $\rho > 0$. Such quadrature formulas are usually based on polynomial interpolation together with a-priori error estimates. The aim of this section is to introduce new adaptive quadrature formulas which are controlled by a-posteriori error estimates.

8.1.1. Harmonic interpolants

In the special situation that $f(x, \cdot)$, $x \in X$, is harmonic in

$$X^c := \mathbb{R}^d \setminus \overline{X}$$

and vanishes at infinity it is possible to control the quadrature error for $y \in \mathcal{F}_\rho(X)$ also computationally. Notice that $f(x, y) = |x - y|^{-\alpha}$ is harmonic in \mathbb{R}^d , $d \geq 3$, only for $\alpha = d - 2$. Fractional exponents, including $\alpha = d + 2s$, will be treated later on in Section 8.1.2.

Harmonic functions $u : \Omega \rightarrow \mathbb{R}$ in an unbounded domain $\Omega \subset \mathbb{R}^d$ are known to satisfy the mean value property

$$u(x) = \frac{1}{|B_r|} \int_{B_r(x)} u(y) \, dy$$

for balls $B_r(x) \subset \Omega$ and the maximum principle

$$\max_{\Omega} |u| \leq \max_{\partial\Omega} |u|$$

provided u vanishes at infinity; see [46].

Let $\Sigma \subset \mathbb{R}^d$ be an unbounded domain such that (see Fig. 1)

$$\Sigma \supset \mathcal{F}_\rho(X) \quad \text{and} \quad \partial\Sigma \subset \mathcal{F}_{2\rho}(X). \quad (72)$$

A natural choice is $\Sigma = \mathcal{F}_\rho(X)$. Since our aim is to check the actual accuracy and we cannot afford

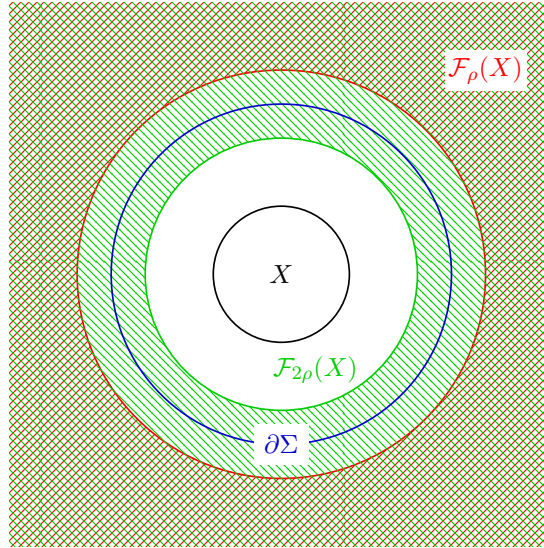


Figure 1: Σ and the far-fields $\mathcal{F}_{2\rho}(X)$ and $\mathcal{F}_\rho(X)$.

to inspect it on an infinite set, we introduce the finite set $M \subset \partial\Sigma$ to be close to $\partial\Sigma$, i.e., we assume that M satisfies

$$\text{dist}(y, M) \leq \delta, \quad y \in \partial\Sigma. \quad (73)$$

8. Uniform \mathcal{H} -matrices and \mathcal{H}^2 -matrices

Then we apply the cross approximation introduced in Section 6.2 to our problem. Let $r_0 = f$ and for $k = 0, 1, 2, \dots$ assume that r_k has already been defined. Let $x_{k+1} \in X$ be chosen such that

$$r_k(x_{k+1}, \cdot) \neq 0 \quad \text{in } M, \quad (74)$$

then set

$$r_{k+1}(x, y) := r_k(x, y) - \frac{r_k(x_{k+1}, y)}{r_k(x_{k+1}, y_{k+1})} r_k(x, y_{k+1}) \quad (75)$$

and $s_{k+1} := f - r_{k+1}$, where $y_{k+1} \in M$ denotes the maximum of $|r_k(x_{k+1}, \cdot)|$ in M . As we have seen already in (62), s_k interpolates f at the chosen nodes x_i , $i = 1, \dots, k$, for all $y \in \mathcal{F}_\rho(X)$, i.e.,

$$s_k(x_i, y) = f(x_i, y), \quad i = 1, \dots, k,$$

and belongs to $F_k := \text{span}\{f(\cdot, y_1), \dots, f(\cdot, y_k)\}$. In addition, the choice of $(x_k, y_k) \in X \times M$ guarantees unisolvency, which can be seen from

$$\det C_k = r_0(x_1, y_1) \cdot \dots \cdot r_{k-1}(x_k, y_k) \neq 0,$$

where $C_k \in \mathbb{R}^{k \times k}$ denotes the matrix with the entries $(C_k)_{ij} = f(x_i, y_j)$, $i, j = 1, \dots, k$. Hence, one can define the Lagrange functions for the system and the nodes x_i , i.e. $L_k^{(j)}(x_i) = \delta_{ij}$, $i, j = 1, \dots, k$, as

$$L_k^{(i)}(x) := \frac{\det C_k^{(i)}(x)}{\det C_k} \in F_k, \quad i = 1, \dots, k,$$

where $C_k^{(i)}(x) \in \mathbb{R}^{k \times k}$ results from C_k by replacing its i -th row with the vector

$$v_k(x) := \begin{bmatrix} f(x, y_1) \\ \vdots \\ f(x, y_k) \end{bmatrix}.$$

Another representation of the vector $L_k \in \mathbb{R}^k$ of Lagrange functions $L_k^{(i)}$ is

$$L_k(x) = C_k^{-T} v_k(x). \quad (76)$$

Due to the uniqueness of the interpolation, s_k has the representation

$$s_k(x, y) = \sum_{i=1}^k f(x_i, y) L_k^{(i)}(x) = v_k(x)^T C_k^{-1} z_k(y), \quad (77)$$

where $z_k(y) := [f(x_1, y), \dots, f(x_k, y)]^T$.

For an adaptive procedure it remains to control the interpolation error $f - s_k = r_k$ in $X \times \mathcal{F}_\rho(X)$. The following obvious property follows from (75) via induction.

Lemma 32. *If $f(x, \cdot)$ is harmonic in X^c and vanishes at infinity for all $x \in X$, then so do $s_k(x, \cdot)$ and $r_k(x, \cdot)$.*

8. Uniform \mathcal{H} -matrices and \mathcal{H}^2 -matrices

The following lemma shows that although $M \subset \partial\Sigma$ is a finite set, it can be used to find an upper bound on the maximum of $r_k(x, \cdot)$ in the unbounded domain $\mathcal{F}_\rho(X)$.

Lemma 33. *Let the assumptions of Lemma 32 be valid and let $2\rho\varrho\delta < \text{diam } X$, where $\varrho = (\sqrt[d]{2} - 1)^{-1} + 2$. Then there is $c_k > 0$ such that for $x \in X$ it holds*

$$\max_{y \in \mathcal{F}_\rho(X)} |f(x, y) - s_k(x, y)| \leq 2 \max_{y \in M} |f(x, y) - s_k(x, y)| + c_k \varrho \delta,$$

where $c_k := \|\nabla_y r_k(x, \cdot)\|_\infty$.

Proof. Let $x \in X$ and $y \in \partial\Sigma$. We define the set

$$N := \{z \in B_{\varrho\delta}(y) : r_k(x, z) = 0\}$$

of zeros in $B_{\varrho\delta}(y)$. If $N \neq \emptyset$ then with $z \in N$

$$|r_k(x, y)| = \left| \int_0^1 (y - z) \cdot \nabla_y r_k(x, z + t(y - z)) dt \right| \leq c_k \varrho \delta.$$

In the other case $N = \emptyset$, our aim is to find $y' \in M$ such that $|r_k(x, y)| \leq 2|r_k(x, y')|$. r_k does not change its sign and is harmonic in $B_{\varrho\delta}(y)$ due to $B_{\varrho\delta}(y) \subset X^c$, which follows from (72) as

$$2\rho \text{dist}(B_{\varrho\delta}(y), X) \geq 2\rho \text{dist}(y, X) - 2\rho\varrho\delta \geq \text{diam } X - 2\rho\varrho\delta > 0.$$

Due to the assumption (73) we can find $y' \in B_\delta(y) \cap M$. Then $B_{(\varrho-2)\delta}(y) \subset B_{(\varrho-1)\delta}(y') \subset B_{\varrho\delta}(y)$. Hence, the mean value property (applied to r_k if r_k is positive or to $-r_k$ if r_k is negative) shows

$$\begin{aligned} |r_k(x, y)| &= \frac{1}{|B_{(\varrho-2)\delta}|} \int_{B_{(\varrho-2)\delta}(y)} |r_k(x, z)| dz \leq \frac{1}{|B_{(\varrho-2)\delta}|} \int_{B_{(\varrho-1)\delta}(y')} |r_k(x, z)| dz \\ &= \frac{|B_{(\varrho-1)\delta}|}{|B_{(\varrho-2)\delta}|} |r_k(x, y')| = \left(\frac{\varrho-1}{\varrho-2} \right)^d |r_k(x, y')| = 2|r_k(x, y')|. \end{aligned}$$

Since r_k vanishes at infinity, (72) together with the maximum principle shows

$$\max_{y \in \mathcal{F}_\rho(X)} |r_k(x, y)| \leq \max_{y \in \Sigma} |r_k(x, y)| \leq \max_{y \in \partial\Sigma} |r_k(x, y)| \leq 2 \max_{y' \in M} |r_k(x, y')| + c_k \varrho \delta.$$

□

Notice that due to (77) we have

$$\nabla_y r_k(x, y) = \nabla_y f(x, y) - \nabla_y s_k(x, y) = \nabla_y f(x, y) - \sum_{i=1}^k L_k^{(i)}(x) \nabla_y f(x_i, y).$$

Hence,

$$c_k = \|\nabla_y r_k(x, \cdot)\|_\infty \leq (1 + \Lambda_k) \max_{x \in X} \|\nabla_y f(x, \cdot)\|_\infty$$

with the Lebesgue constant $\Lambda_k(x) := \sum_{i=1}^k |L_k^{(i)}(x)|$. Although it seems that $\Lambda_k(x) \sim k$ in practice, there is no proof for this observation up to now. A related topic in interpolation theory are *Leja points*; see [68].

To see that this special kind of interpolation is more efficient than polynomial interpolation, we present the following example.

8. Uniform \mathcal{H} -matrices and \mathcal{H}^2 -matrices

Example 1. Let $X \subset \mathbb{R}^3$ be 1000 points forming a uniform mesh of the unit cube $[0, 1]^3$. We choose $\Sigma = \{x \in \mathbb{R}^3 : |x| > 10\}$. M is a discretization of $\partial\Sigma$ with 768 points. We consider $f(x, y) = |x - y|^{-1}$ and compare the quality of s_k with the quality of the interpolating tensor Chebyshev polynomial of degree k . Table 6 shows the maximum point wise error measured at $X \times M$; see also Fig. 2.

k	8	27	64	125	216	343
Cross approximation	3.93e-4	1.74e-6	2.76e-9	1.13e-12	3.35e-14	6.60e-15
Chebyshev interpolation	3.24e-4	7.03e-6	2.15e-7	5.13e-9	1.23e-10	3.77e-12

Table 6: Approximation error of s_k and tensor Chebyshev interpolation polynomial of degree k .

Table 7 compares the cross approximation with a sparse grid interpolation obtained from the Sparse Grid Matlab Kit; see [9].

k	7	25	69	165	351
Cross approximation	9.25e-4	3.50e-6	1.82e-9	8.74e-14	3.10e-15
Sparse grid interpolation	1.10e-3	9.43e-5	7.29e-6	5.08e-07	3.25e-08

Table 7: Approximation error of s_k and sparse grid interpolation polynomial for k nodes.

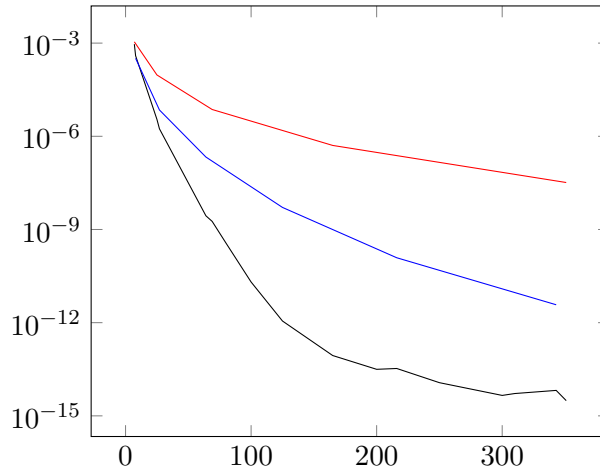


Figure 2: Error versus k of the cross approximation (black), Chebyshev interpolation (blue), and sparse grid interpolation (red).

8.1.2. s -harmonic interpolants

The next step is to adapt Lemma 32 and Lemma 33 to the fractional Laplacian, i.e. $f(x, y) = |x - y|^{-d-2s}$. For Lemma 32, this is quite obvious.

8. Uniform \mathcal{H} -matrices and \mathcal{H}^2 -matrices

Lemma 34. *If $f(x, \cdot)$ is s -harmonic in X^c and vanishes at infinity for all $x \in X$, then so do $s_k(x, \cdot)$ and $r_k(x, \cdot)$.*

Adapting Lemma 33 is more complicated. The lemma is based on two fundamental properties of harmonic functions, the mean value property and the maximum principle. For the fractional Laplacian, this becomes an issue, since according to [22] there is no comparable statement to the maximum principle and since the s -mean value property is a non-local property. However, as the next lemma shows, there is a Harnack inequality for s -harmonic functions.

Lemma 35. *Let u be a s -harmonic function on Ω with $u \geq 0$ in \mathbb{R}^d and let $\overline{B_{2R}(\xi)} \subset \Omega$. Then for $x, y \in B_R(\xi)$ it holds*

$$u(x) \leq M u(y), \quad M := \left(\frac{R^2 - |x - \xi|^2}{R^2 - |y - \xi|^2} \right)^s \left(\frac{R + |y - \xi|}{R - |x - \xi|} \right)^d. \quad (78)$$

Proof. For s -harmonic functions u in $B_R(\xi)$ we have the following representation using the Poisson kernel

$$u(x) = \mathcal{P}_{\xi, R} u(x) = a_s \int_{\mathbb{R}^d \setminus B_R(\xi)} \left(\frac{R^2 - |x - \xi|^2}{|z - \xi|^2 - R^2} \right)^s \frac{u(z)}{|z - x|^d} dz, \quad x \in B_R(\xi).$$

Hence, for $x, y \in B_R(\xi)$ we obtain

$$\begin{aligned} \frac{u(x)}{u(y)} &= \left(\frac{R^2 - |x - \xi|^2}{R^2 - |y - \xi|^2} \right)^s \frac{\int_{\mathbb{R}^d \setminus B_R(\xi)} u(z) (|z - \xi|^2 - R^2)^{-s} |z - x|^{-d} dz}{\int_{\mathbb{R}^d \setminus B_R(\xi)} u(z) (|z - \xi|^2 - R^2)^{-s} |z - y|^{-d} dz} \\ &\leq \left(\frac{R^2 - |x - \xi|^2}{R^2 - |y - \xi|^2} \right)^s \left(\frac{R - |x - \xi|}{R + |y - \xi|} \right)^{-d} \end{aligned}$$

due to $|z - x| \geq ||z - \xi| - |x - \xi|| \geq |R - |x - \xi||$ and $|z - y| \leq |z - \xi| + |y - \xi| \leq R + |y - \xi|$. The associated integrals

$$\int_{\mathbb{R}^d \setminus B_R(\xi)} \frac{u(z)}{(|z - \xi|^2 - R^2)^s} dz = \int_{\mathbb{R}^d \setminus B_{2R}(\xi)} \frac{u(z)}{(|z - \xi|^2 - R^2)^s} dz + \int_{B_{2R}(\xi) \setminus B_R(\xi)} \frac{u(z)}{(|z - \xi|^2 - R^2)^s} dz$$

are finite, since a s -harmonic function is Lebesgue measurable in \mathbb{R}^d and continuous in Ω . Therefore the first summand is limited by $(3R^2)^{-s} \|u\|_{L^1(\mathbb{R}^d)}$ and for the second one we use spherical coordinates

$$\int_{B_{2R}(\xi) \setminus B_R(\xi)} \frac{u(z)}{(|z - \xi|^2 - R^2)^s} dz \leq C \|u\|_{L^\infty(B_{2R}(\xi) \setminus B_R(\xi))} \int_R^{2R} \frac{2r}{(r^2 - R^2)^s} r^{d-2} dr < \infty.$$

□

The non-locality causes the sign of u to be prescribed on the whole space \mathbb{R}^d . By adapting the work of [61], we can formulate a Harnack inequality with no requirements for the sign of u .

8. Uniform \mathcal{H} -matrices and \mathcal{H}^2 -matrices

Lemma 36. *Let u be a s -harmonic function in Ω and let $\overline{B_{2R}(\xi)} \subset \Omega$. Then for $x, y \in B_R(\xi)$, it holds*

$$u(x) \leq M u(y) + M \mathcal{P}_{\xi, 2R} u^-(y),$$

where M is defined in (78) and u^- is the negative part of u .

Proof. By using $u = u^+ - u^-$, we obtain

$$u(x) = \mathcal{P}_{\xi, 2R} u(x) = \mathcal{P}_{\xi, 2R} [u^+ - u^-](x) \leq \mathcal{P}_{\xi, 2R} u^+(x).$$

Since $\mathcal{P}_{\xi, 2R} u^+$ fulfills the requirements of Lemma 35, the lemma can be applied

$$u(x) \leq \mathcal{P}_{\xi, 2R} u^+(x) \leq M \mathcal{P}_{\xi, 2R} u^+(y) = M \mathcal{P}_{\xi, 2R} [u + u^-](y) = M[u(y) + \mathcal{P}_{\xi, 2R} u^-(y)].$$

□

However, $\mathcal{P}_{\xi, 2R} u^-$ has to be calculated. Therefore, this lemma is not an adequate replacement for the mean value property.

Instead of the s -harmonicity, we rely on other properties of f , the smoothness and the decay at infinity. We can reduce the maximization to a bounded domain

$$\Sigma_R := \{y \in \Sigma : \text{dist}(y, X) < R\},$$

where $R > 0$ is chosen such that for $x \in X$

$$\max_{y \in \Sigma \setminus \Sigma_R} |r_k(x, y)| \leq \max_{y \in \Sigma_R} |r_k(x, y)|. \quad (79)$$

Such an R exists due the decay of r_k

$$|r_k(x, y)| \leq c_k R^{-\frac{d}{k}}, \quad x \in X, \text{dist}(y, X) = R.$$

Analogous to the harmonic case, we introduce the finite set $M_R \subset \Sigma_R$ to be close to Σ_R , i.e., we assume that M_R satisfies

$$\text{dist}(y, M_R) \leq \delta, \quad y \in \Sigma_R. \quad (80)$$

Additionally, due to the smoothness of $f(x, y) = |x - y|^{-d-2s} r_k(x, \cdot)$ satisfies a Lipschitz condition, i.e. there exists a constant $c_L > 0$ such that

$$|r_k(x, y) - r_k(x, y')| \leq c_L |y - y'| \quad \text{for } y, y' \in \Sigma_R. \quad (81)$$

Lemma 37. *Let r_k vanish at infinity for all $x \in X$ and satisfy (81). Let $2\varrho\rho\delta < \text{diam } X$, where $\varrho := 1/(1 - 2^{-1/d})$. Then there is $c_k > 0$ such that for $x \in X$*

$$\max_{y \in F_\rho(X)} |f(x, y) - s_k(x, y)| \leq \max_{y \in M_R} |f(x, y) - s_k(x, y)| + (c_k + c_L)\varrho\delta,$$

where $c_k := \|\nabla r_k(x, \cdot)\|_\infty$ and c_L is defined in (81).

8. Uniform \mathcal{H} -matrices and \mathcal{H}^2 -matrices

Proof. Let $x \in X$ and $y \in \Sigma_R$. We define the set

$$N := \{z \in B_{\varrho\delta}(y) : r_k(x, z) = 0\}$$

of zeros in $B_{\varrho\delta}(y)$. If $N \neq \emptyset$ then with $z \in N$

$$|r_k(x, y)| = \left| \int_0^1 (y - z) \cdot \nabla r_k(x, z + t(y - z)) dt \right| \leq c_k \varrho\delta.$$

Next, we consider the case $N = \emptyset$. r_k does not change its sign in $B_{\varrho\delta}(y)$ and $B_{\varrho\delta}(y) \subset X^c$, which follows from (72) as

$$2\rho \operatorname{dist}(B_{\varrho\delta}(y), X) \geq 2\rho \operatorname{dist}(y, X) - 2\rho\varrho\delta \geq \operatorname{diam} X - 2\rho\varrho\delta > 0.$$

Due to the assumption (80) we can find $y' \in M_R$ with $y' \in B_\delta(y) \cap M_R$. Using (81), this leads to

$$r_k(x, y) \leq r_k(x, y') + c_L |y - y'| \leq r_k(x, y') + c_L \varrho\delta,$$

if $r_k(x, y) > r_k(x, y') > 0$ and to

$$-r_k(x, y) \leq -r_k(x, y') + c_L |y - y'| \leq -r_k(x, y') + c_L \varrho\delta,$$

if $r_k(x, y) < r_k(x, y') < 0$. The two remaining cases are obvious. Due to (79) we obtain that

$$\max_{y \in F_\rho(X)} |r_k(x, y)| \leq \max_{y \in \Sigma_R} |r_k(x, y)| \leq \max_{y' \in M_R} |r_k(x, y')| + (c_k + c_L) \varrho\delta.$$

□

As it can be seen, Lemma 37 holds for all $\alpha > 0$, since we no longer exploit the fact that r_k is either harmonic or s -harmonic. Instead, we only use the decay and smoothness of r_k .

8.2. Exponential error estimates for multivariate interpolation

For analyzing the error of the cross approximation, the remainder r_k has to be estimated. Theorem 18 establishes a connection of r_k with the best approximation in an arbitrary system $\Xi = \{\xi_1, \dots, \xi_k\}$ of functions and Theorem 17 presents a qualitative estimate for a polynomial system Ξ . For the uniqueness of polynomial interpolation it has to be assumed that the Vandermonde matrix $[\xi_j(x_i)]_{ij} \in \mathbb{R}^{k \times k}$ is non-singular. The goal of the following section is to provide new error estimates for the convergence of the cross approximation which avoids the unisolvency assumption by employing radial basis functions (RBFs) for the system Ξ instead of polynomials as the former type of functions are positive definite; see e.g. [24]. Since the interpolation error of RBFs is governed by the fill distance (see (83)), we will be able to state a rule for choosing the next pivotal point x_k (in addition to (74)) leading to fast convergence.

Although RBFs lead to a positive definite Vandermonde matrix A , its numerical stability might be an issue. The eigenvalues of A depend significantly on the distribution of the points and in particular on their distances. A typical measure for this is the *separation distance*

$$q_{X_k} := \frac{1}{2} \min_{x, y \in X_k, x \neq y} \|x - y\|_2.$$

8. Uniform \mathcal{H} -matrices and \mathcal{H}^2 -matrices

In our case, i.e. for the Gaussian kernel, $\Phi(x, y) = \exp(-\beta|x-y|^2)$ with $\beta > 0$, the smallest eigenvalue of A can be estimated by

$$\lambda_{\min}(A) \geq C(2\beta)^{-d/2} \exp\left(-\frac{40.71d^2}{q_{X_k}^2\beta}\right) q_{X_k}^{-d},$$

where $C = C(d) > 0$ is a d -dependent constant; see [84]. One of the main aims of the techniques presented here is a uniform coverage of the considered domain with interpolation points and no generation of local clusters of points, so also from the numerical point of view the Vandermonde matrix A is expected to behave in a stable way.

We consider functions f of the form

$$f(x, y) = \frac{1}{|x-y|^\alpha}, \quad \alpha > 0,$$

on two domains X, Y satisfying

$$\text{diam } X \leq \rho \text{dist}(X, Y) \quad \text{and} \quad \text{diam } Y \leq c_0 \text{diam } X,$$

where c_0 is a positive constant. The validity of the latter condition usually results from a partitioning of the computational domain $\Omega \times \Omega$ induced by a hierarchical partitioning of the matrix (70). Here, the choices $Y = M$ and $Y = M_R$ are of particular importance, where the sets $M \subset \partial\Sigma \subset \mathcal{F}_{2\rho}(X)$ and $M_R \subset \partial\Sigma_R \subset \mathcal{F}_{2\rho}(X)$ are introduced in Sections 8.1.1 and 8.1.2, respectively. Notice that $\text{diam } M \leq \text{diam } M_R \leq \text{diam } \partial\mathcal{F}_\rho(X) \leq \text{diam } X + 2 \text{dist}(X, \partial\mathcal{F}_\rho(X)) = (1 + 2/\rho) \text{diam } X$.

In order to employ RBFs for the system Ξ , we have to apply two additional steps. The first step is to extend the function f outside of $X \times Y$ by

$$\tilde{f}(x, y) := \tilde{f}(x-y) := \begin{cases} \sigma^\alpha, & \text{if } |x-y| \leq \sigma, \\ |x-y|^{-\alpha}, & \text{if } \sigma < |x-y| \leq \sigma + 2\vartheta, \\ -\frac{\sigma + 2\vartheta - |x-y|}{\vartheta(\sigma + \vartheta)^\alpha}, & \text{if } \sigma + \vartheta < |x-y| \leq \sigma + 2\vartheta, \\ 0, & \text{if } |x-y| > \sigma + 2\vartheta, \end{cases}$$

where $\sigma := \text{dist}(X, Y)$ and $\vartheta := \text{diam } X + \text{diam } Y$. Obviously, it holds that $\tilde{f} = f$ on $X \times Y$. The second step is to smooth \tilde{f} by using the smoothness kernel $g_m(x) := (m/\pi)^{\frac{d}{2}} e^{-m\|x\|_2^2}$ for $m \in \mathbb{N}$ and $x \in \mathbb{R}^d$, i.e. $\tilde{f}_m = \tilde{f} * g_m$. Since \tilde{f} is continuous, it holds according to [84, Thm. 5.20] that \tilde{f}_m converges to \tilde{f} for $m \rightarrow \infty$. Let $\Phi_m(x, y) := (m/2\pi)^{\frac{d}{2}} e^{-\frac{m}{2}\|x-y\|_2^2}$. For fixed $m \in \mathbb{N}$ and for $y \in Y$ we interpolate f with the radial basis function

$$p_y(x) := \sum_{i=1}^k f(x_i, y) L_i^{\Phi_m}(x) \tag{82}$$

on the data set $X_k = \{x_1, \dots, x_k\}$. Here, L_j^k , $j = 1, \dots, k$, are the Lagrange functions for Φ_m and X_k .

Lemma 38. *Let $m \in \mathbb{N}$. Then for $x \in X$, $y \in Y$*

$$|f(x, y) - p_y(x)| \leq (1 + \Lambda_k^\Phi) \|f - f_m\|_{L^\infty(X \times Y)} + c \lambda^{1/h_{X_k, X}} \|f\|_{L^2(X \times Y)},$$

8. Uniform \mathcal{H} -matrices and \mathcal{H}^2 -matrices

where $0 < \lambda < 1$ depends on Φ_m and X_k , $c > 0$ is a constant, $\Lambda_k^\kappa := \sup_{x \in X} \sum_{i=1}^k |L_i^{\Phi_m}(x)|$ denotes the Lebesgue constant and the fill distance

$$h_{X_k, X} := \sup_{x \in X} \text{dist}(x, X_k). \quad (83)$$

The proof of the lemma can be found in [10, 11].

The convergence can be controlled by choosing the node x_{k+1} such that the fill distance $h_{X_{k+1}, X}$ is minimized from step k to step $k+1$. This minimization problem can be solved efficiently, i.e. with logarithmic-linear complexity, with the approximate nearest neighbor search described in [6, 7, 8].

Remark. In practice, we replace possibly uncountable sets X with a sufficiently fine mesh. In our applications, X is a discrete cloud of points.

If we choose the pivots x_1, \dots, x_k such that the fill distance behaves like $h_{X_k, X} \sim k^{-1/d}$, Lemma 38 shows exponential convergence of p_y w.r.t. k provided the Lebesgue constant grows sub-exponentially.

Applying the results of the previous lemma to the remainder r_k , we obtain the following result for interpolating f on $X \times Y$. Notice that this result shows that the convergence is governed only by the fill distance. Hence, the unisolvency assumption on the nodes x_1, \dots, x_k in the older convergence proof of ACA (which was based on polynomials; see [13]) can be dropped.

Theorem 25. For $y \in Y$ let p_y denote the radial basis function interpolant (82) for $f_y := f(\cdot, y) = |\cdot - y|^{-\alpha}$. Choosing $y_1, \dots, y_k \in Y$ such that

$$|\det C_k^{(i)}(y)| \leq c_M |\det C_k|, \quad 1 \leq i \leq k, y \in Y,$$

where $c_M > 1$ is a constant, it holds that

$$|r_k(x, y)| \leq c(c_M k + 1) \lambda^{1/h_{X_k, X}},$$

where $X_k := \{x_1, \dots, x_k\}$.

Proof. Let the vector of the Lagrange functions L_i^κ , $i = 1, \dots, k$, corresponding to the radial basis function κ and the nodes x_1, \dots, x_k be given by

$$L^\kappa(x) = \begin{bmatrix} L_1^\kappa(x) \\ \vdots \\ L_k^\kappa(x) \end{bmatrix}.$$

Using (77), we obtain

$$\begin{aligned} r_k(x, y) &= f(x, y) - v_k(x)^T C_k^{-1} w_k(y) \\ &= f(x, y) - w_k(y)^T L^\kappa(x) - [v_k(x) - C_k L^\kappa(x)]^T C_k^{-1} w_k(y) \\ &= f_y(x) - p_y(x) - \sum_{i=1}^k [C_k^{-1} w_k(y)]_i [f_{y_i}(x) - p_{y_i}(x)] \\ &= f_y(x) - p_y(x) - \sum_{i=1}^k \frac{\det C_k^{(i)}(y)}{\det C_k} [f_{y_i}(x) - p_{y_i}(x)], \end{aligned}$$

where the last line follows from Cramer's rule. The assertion follows from the triangle inequality and Lemma 38. \square

8. Uniform \mathcal{H} -matrices and \mathcal{H}^2 -matrices

Remark. In practice, Y will be replaced by a discrete set of points. For the choices $Y = M$ or $Y = M_R$, it is sufficient to choose the nodes $y_1, \dots, y_k \in Y$ according to the condition

$$|r_{k-1}(x_k, y_k)| \geq |r_{k-1}(x_k, y)| \quad \text{for all } y \in Y,$$

which is much easier to check in practice and which leads to the estimate

$$|\det C_k^{(i)}(y)| \leq 2^{k-i} |\det C_k|, \quad 1 \leq i \leq k, y \in Y;$$

for details see [13].

8.3. Uniform \mathcal{H} -matrix

Hierarchical matrices are well-suited for treating non-local operators with logarithmic-linear complexity; see [13, 18, 51].

In order to approximate the matrix (70) more efficiently, we employ uniform \mathcal{H} -matrices; see [50].

Definition 8. A cluster basis Φ for the rank distribution $(k_q)_{q \in T_I}$ is a family $\Phi = (\Phi(q))_{q \in T_I}$ of matrices $\Phi(q) \in \mathbb{R}^{|q| \times k_q}$.

Definition 9. Let Φ and Ψ be cluster bases for T_I and T_J . A matrix $A \in \mathbb{R}^{|I| \times |J|}$ satisfying

$$A|_{qw} = \Phi(q) F(q, w) \Psi(w)^H \quad \text{for all } q \times w \in P_{\text{adm}}$$

with some $F(q, w) \in \mathbb{R}^{k_q^\Phi \times k_w^\Psi}$ is called uniform hierarchical matrix for Φ and Ψ .

The storage required for the coupling matrices $F(q, w)$ is of the order $k \min\{|I|, |J|\}$ if for the sake of simplicity it is assumed that $k_q \leq k$ for all $q \in T_I$. Additionally, it is not useful to choose $k_q > |q|$. The cluster bases Φ and Ψ require $k[|I|L(T_I) + |J|L(T_J)]$ units of storage; see [55].

In the following we employ the method from Sect. 8.1 to construct a uniform \mathcal{H} -matrix approximation to an arbitrary block $q \times w \in P_{\text{adm}}$ of matrix (70). Let $\varepsilon > 0$ be given and $[x]_q = \{x_\alpha^q, \alpha \in \vartheta_q\} \subset X_q$ and $[v]_q = \{v_\alpha^q, \alpha \in \sigma_q\} \subset \mathcal{F}_\rho(X_q)$ be the pivots chosen in (75) such that

$$|f(x, y) - \sum_{\alpha \in \vartheta_q} L_\alpha^q(x) f(x_\alpha^q, y)| < \varepsilon, \quad x \in X_q, y \in \mathcal{F}_\rho(X_q), \quad (84)$$

for each cluster q . Here, $L^q(x) := f(x, [v]_q) f^{-1}([x]_q, [v]_q)$ denotes the vector of Lagrange functions defined in (76). ϑ_q and σ_q denote index sets with cardinality k . From Theorem 25 we know that $k \sim |\log \varepsilon|^d$. Similarly, for $w \in T_J$ let $[y]_w = \{y_\beta^w, \beta \in \sigma_w\} \subset Y_w$ and $[z]_w = \{z_\beta^w, \beta \in \vartheta_w\} \subset \mathcal{F}_\rho(Y_w)$ be chosen such that

$$|f(x, y) - \sum_{\beta \in \sigma_w} f(x, y_\beta^w) L_\beta^w(y)| < \varepsilon, \quad x \in \mathcal{F}_\rho(Y_w), y \in Y_w, \quad (85)$$

where $L^w(y) := f^{-1}([z]_w, [y]_w) f([z]_w, y)$. For $x \in X_q$ and $y \in Y_w$ this yields the dual interpolation

$$f(x, y) \approx \sum_{\alpha \in \vartheta_q} L_\alpha^q(x) f(x_\alpha^q, y) \approx \sum_{\alpha \in \vartheta_q, \beta \in \sigma_w} L_\alpha^q(x) f(x_\alpha^q, y_\beta^w) L_\beta^w(y)$$

8. Uniform \mathcal{H} -matrices and \mathcal{H}^2 -matrices

with corresponding interpolation error

$$\begin{aligned}
|f(x, y) - \sum_{\alpha \in \vartheta_q, \beta \in \sigma_w} L_\alpha^q(x) f(x_\alpha^q, y_\beta^w) L_\beta^w(y)| &\leq |f(x, y) - \sum_{\alpha \in \vartheta_q} L_\alpha^q(x) f(x_\alpha^q, y)| + \\
&\quad + \sum_{\alpha \in \vartheta_q} |L_\alpha^q(x)| (|f(x_\alpha^q, y) - \sum_{\beta \in \sigma_w} f(x_\alpha^q, y_\beta^w) L_\beta^w(y)|) \\
&\leq \varepsilon + \varepsilon \sum_{\alpha \in \vartheta_q} |L_\alpha^q(x)| = (1 + \Lambda_k^q) \varepsilon
\end{aligned} \tag{86}$$

and the Lebesgue constant $\Lambda_k^q \geq 1$. We define the matrix B of rank at most k

$$\begin{aligned}
b_{ij} &= \sum_{\alpha \in \vartheta_q, \beta \in \sigma_w} f(x_\alpha^q, y_\beta^w) \int_{X_q} L_\alpha^q(x) \varphi_i(x) \xi(x) dx \int_{Y_w} L_\beta^w(y) \psi_j(y) \zeta(y) dy \\
&= [\Phi(q) F(q, w) \Psi(w)^T]_{ij},
\end{aligned} \tag{87}$$

where ξ and ζ are the functions defined in (71). Notice that both matrices

$$[\Phi(q)]_{i\alpha} := \int_{X_q} L_\alpha^q(x) \varphi_i(x) \xi(x) dx \quad \text{and} \quad [\Psi(w)]_{j\beta} := \int_{Y_w} L_\beta^w(y) \psi_j(y) \zeta(y) dy$$

are associated only with q and w , respectively, and can be precomputed independently of each other. Only the matrix $F(q, w) \in \mathbb{R}^{k \times k}$ with $[F(q, w)]_{\alpha\beta} := f(x_\alpha^q, y_\beta^w)$ depends on both clusters q and w .

Remark. Since the vector of Lagrange functions $L^q(x)$ has the representation $L^q(x) = C_k^{-1} v_k(x)$, the matrices $\Phi(q) \in \mathbb{R}^{|\vartheta_q| \times |\vartheta_q|}$ can be found from solving the linear system

$$C_k \Phi(q) = \left[\int_{X_q} v_k(x) \varphi_i(x) \xi(x) dx \right]_i.$$

With $\|\varphi_i\|_{L^1} = 1 = \|\psi_j\|_{L^1}$ the Cauchy-Schwarz inequality implies

$$\begin{aligned}
|a_{ij} - b_{ij}| &\leq \int_{Y_w} \int_{X_q} |f(x, y) - \sum_{\alpha \in \vartheta_q, \beta \in \sigma_w} L_\alpha^q(x) f(x_\alpha^q, y_\beta^w) L_\beta^w(y)| |\xi(x)| |\varphi_i(x)| |\zeta(y)| |\varphi_j(y)| dx dy \\
&\stackrel{(86)}{\leq} 2\Lambda_k^q \|\xi\|_\infty \|\zeta\|_\infty \varepsilon.
\end{aligned}$$

and thus

$$\begin{aligned}
\|A|_{qw} - B\|_2^2 &\leq \|A|_{qw} - B\|_F^2 = \|A|_{qw} - \Phi(q) F(q, w) \Psi(w)^T\|_F^2 = \sum_{i \in q, j \in w} |a_{ij} - b_{ij}|^2 \\
&\leq (2\Lambda_k^q \|\xi\|_\infty \|\zeta\|_\infty)^2 |q| |w| \varepsilon^2.
\end{aligned} \tag{88}$$

Notice that the computation of the double integral for a single entry of the Galerkin matrix (70) is replaced with two single integrals in (87).

By exploiting the structure of f , we can use a reference geometry for the computation of the interpolation points. Since f only dependence on the distance between x and y , the reference element

Algorithm 2 Efficient computation of Φ

Apply the ACA on the reference geometry, i.e. on X_{ref} and $\partial\Sigma_{ref}$
 Perform an QR-decomposition on C^{ref} with $C_{ij}^{ref} = f(x_i^{ref}, y_j^{ref})$
for each Cluster X_q belonging to an admissible block **do**
 for $i = 1, \dots, k$ **do**
 $x_i := \text{diam } X_q x_i^{ref} + \xi_q$
 $y_i := \text{diam } X_q y_i^{ref} + \xi_q$
 end for
 for $i = 1, \dots, k$ **do**
 Solve $C^{ref} \Phi_i = (\text{diam } X_q)^\alpha [\int_{X_q} v_k(x) \varphi_i(x) \xi(x) dx]_i$
 end for
end for

can be placed in the origin. Additionally, by using a scaling argument the uniform approximation can be performed on a unit sphere. The set $\partial\Sigma_{ref}$ is defined by the parameter ρ of the original geometry and by X_{ref} is discretization of the unit sphere denoted. Let be $b = q \times w$ be an admissible block and denote by ξ_q and ξ_w the center of the clusters X_q and X_w , respectively. Then we formulate Algorithm 2 to compute efficiently the matrices Φ and Ψ . Since the stiffness matrix A is a symmetric matrix, it is sufficient to only compute the matrices Φ .

The huge advantage is that instead of applying the ACA to each cluster, the ACA has only to be applied to the reference geometry. Additionally, the costs to solve the linear equation systems can also be significantly reduced, since for each equation system the same matrix C^{ref} is used. Note the Algorithm 2 can only be applied in this way, when for the admissible condition also spheres $B_{\text{diam } X_q}(\xi_q)$ and $B_{\text{diam } X_w}(\xi_w)$ are used.

8.4. \mathcal{H}^2 -matrix

In order to reduce the amount of storage for storing the bases Φ and Ψ one can establish a recursive relation among the basis vectors. The corresponding structures are \mathcal{H}^2 -matrices; see [18, 55]. This sub-structure of \mathcal{H} -matrices is even mandatory if a logarithmic-linear complexity is to be achieved for high-frequency Helmholtz problems. To this end, *directional \mathcal{H}^2 -matrices* have been introduced in [15].

Definition 10. A cluster basis $U = (U(q))_{q \in T_I}$ is called nested if for each $q \in T_I \setminus \mathcal{L}(T_I)$ there are transfer matrices $T_{q'q} \in \mathbb{R}^{k_{q'} \times k_q}$ such that for the restriction of the matrix $U(q)$ to the rows q' it holds that

$$U(q)|_{q'} = U(q') T_{q'q} \quad \text{for all } q' \in S_I(q).$$

For estimating the complexity of storing a nested cluster basis U notice that the set of leaf clusters $\mathcal{L}(T_I)$ constitutes a partition of I and for each leaf cluster $q \in \mathcal{L}(T_I)$ at most $k|q|$ entries have to be stored. Hence, $\sum_{q \in \mathcal{L}(T_I)} k|q| = k|I|$ units of storage are required for the leaf matrices $U(q)$, $q \in \mathcal{L}(T_I)$. The storage required for the transfer matrices is of the order $k|I|$, too; see [55].

8. Uniform \mathcal{H} -matrices and \mathcal{H}^2 -matrices

Definition 11. A matrix $A \in \mathbb{R}^{|I| \times |J|}$ is called \mathcal{H}^2 -matrix if there are nested cluster bases U and V such that for $q \times w \in P_{\text{adm}}$

$$A|_{qw} = U(q) F(q, w) V^H(w)$$

with coupling matrices $F(q, w) \in \mathbb{R}^{k_q^U \times k_w^V}$.

Hence, the total storage required for an \mathcal{H}^2 -matrix is of the order $k(|I| + |J|)$.

Remark. It may be advantageous to consider only nested bases for clusters t having a minimal cardinality $n_{\min}^{\mathcal{H}^2} \geq n_{\min}^{\mathcal{H}}$. Blocks consisting of smaller clusters are treated with \mathcal{H} -matrices.

We define the matrices $U(q) \in \mathbb{R}^{|q| \times k_q}$, $q \in T_I$, by the following recursion. If $q \in T \setminus \mathcal{L}(T_I)$ then the set of sons $S_I(q)$ is non-empty and we define

$$U(q)|_{q'} = U(q') T_{q'q}^U, \quad q' \in S_I(q),$$

with the transfer matrix

$$T_{q'q}^U := f([x]_{q'}, [v]_q) f^{-1}([x]_q, [v]_q) \in \mathbb{R}^{k_{q'} \times k_q}.$$

For leaf clusters $q \in \mathcal{L}(T_I)$ we set $U(q) = \Phi(q)$. Similarly, we define matrices $V(w) \in \mathbb{R}^{|w| \times k_w}$, $w \in T_J$, using transfer matrices

$$T_{w'w}^V := f^T([z]_w, [y]_{w'}) f^{-T}([z]_{w'}, [y]_w) \in \mathbb{R}^{k_{w'} \times k_w}.$$

Then $U := (U(q))_{q \in T_I}$ and $V := (V(w))_{w \in T_J}$ are nested bases.

Lemma 39. Assuming that $\max_{q \in T_I, w \in T_J} \{\|U(q)\|_F, \|V(w)\|_F, \|T_{q'q}^U\|_F\} \leq \gamma$ and $k_q \leq k$ it holds that there exists a constant $c > 0$ such that

$$\|A|_{qw} - U(q) F(q, w) V(w)^T\|_F \leq c(L - \ell) \sqrt{|q||w|} \|\xi\|_\infty \|\zeta\|_\infty \varepsilon, \quad q \times w \in P_{\text{adm}},$$

where ℓ denotes the level of $q \times w$.

Proof. Let $q \in T_I \setminus \mathcal{L}(T_I)$ and $w \in T_J \setminus \mathcal{L}(T_J)$. For $q' \in S_I(q)$ and $w' \in S_J(w)$ we have

$$\begin{aligned} U(q)|_{q'} F(q, w) V(w)|_{w'}^T &= U(q') T_{q'q}^U F(q, w) (T_{w'w}^V)^T V(w')^T \\ &= U(q') F(q', w') V(w')^T - U(q') D(q', w') V(w')^T, \end{aligned} \tag{89}$$

where $D(q', w') := F(q', w') - T_{q'q}^U F(q, w) (T_{w'w}^V)^T$. Using

$$\|D(q', w')\|_F^2 \leq 2\|F(q', w') - T_{q'q}^U F(q, w)\|_F^2 + 2\|T_{q'q}^U\|_F^2 \|F(q, w) - F(q, w) (T_{w'w}^V)^T\|_F^2,$$

one observes that the previous expression consists of matrices with entries

$$f(x_i, y_j) - f(x_i, [v]_q) f^{-1}([x]_q, [v]_q) f([x]_q, y_j), \quad i \in q', j \in w',$$

and

$$f(x_i, y_j) - f(x_i, [y]_w) f^{-1}([w]_w, [y]_w) f([w]_w, y_j), \quad i \in q, j \in w',$$

8. Uniform \mathcal{H} -matrices and \mathcal{H}^2 -matrices

which can be estimated using (84) and (85) due to $x_i \in X_q \subset \mathcal{F}_\rho(Y_w)$ and $y_j \in Y_w \subset \mathcal{F}_\rho(X_q)$. Thus,

$$\|D(q', w')\|_F \leq \sqrt{2(1+\gamma^2)}\sqrt{|q'w'|}\varepsilon.$$

By induction we prove that $\|A|_{qw} - U(q)F(q, r)V(w)^T\|_F \leq \gamma^2\sqrt{2(1+\gamma^2)}(L-\ell)\sqrt{|q|w|}\|\xi\|_\infty\|\zeta\|_\infty\varepsilon$, where ℓ denotes the maximum of the levels of q and w . If both q and w are leaves, then $\|A|_{qw} - \Phi(q)F(q, w)\Psi(w)^T\| \leq 2\Lambda_k^q\sqrt{|q|w|}\|\xi\|_\infty\|\zeta\|_\infty\varepsilon$ due to (88). From (89) we see

$$\begin{aligned} \|A|_{q'w'} - U(q)|_{q'}F(q, w)V(w)|_{w'}^T\|_F &\leq \|A|_{q'w'} - U(q')F(q', w')V(w')^T\|_F + \|U(q')D(q', w')V(w')^T\|_F \\ &\leq \gamma^2\sqrt{2(1+\gamma^2)}(L-\ell-1)\sqrt{|q'|w'|}\|\xi\|_\infty\|\zeta\|_\infty\varepsilon + \gamma^2\sqrt{2(1+\gamma^2)}\sqrt{|q'|w'|}\varepsilon \\ &\leq \gamma^2\sqrt{2(1+\gamma^2)}(L-\ell)\sqrt{|q'|w'|}\|\xi\|_\infty\|\zeta\|_\infty\varepsilon. \end{aligned}$$

This shows

$$\begin{aligned} \|A|_{qw} - U(q)F(q, w)V(w)^T\|_F^2 &= \sum_{q' \in S_I(q), w' \in S_J(w)} \|A|_{q'w'} - U(q)|_{q'}F(q, w)V(w)|_{w'}^T\|_F^2 \\ &\leq 2\gamma^4(1+\gamma^2)(L-\ell)^2(\|\xi\|_\infty\|\zeta\|_\infty\varepsilon)^2 \sum_{q' \in S_I(q), w' \in S_J(w)} |q'|w'| \\ &= 2\gamma^4(1+\gamma^2)(L-\ell)^2(\|\xi\|_\infty\|\zeta\|_\infty\varepsilon)^2|q|w|. \end{aligned}$$

The same kind of estimate holds if q or w is a leaf, because then $U(q) = \Phi(q)$ or $V(w) = \Psi(w)$. \square

Remark. Lemma 39 can also be applied to uniform \mathcal{H} -matrix blocks.

9. Numerical results

The focus of the following numerical tests lies on three problems. First, we focus on the error of numerical integration for singular integrals of the type (22) and (23). For this purpose, we verify for two selected singularity cases whether the error estimates from the Theorems 12 and 13 hold true. Additionally, we compare the two approaches, the nonlinear transformation to unit cubes and the nonlinear transformation to suitable reference elements, presented in Chapters 3 and 5. The second and the third problem are fractional diffusion processes with different geometries. To be more precise, the second problem is (10), where an analytical solution is known. There, the rules presented in Lemma 19 are validated and we show that a coarse \mathcal{H} -matrix approximation of the inverse of the stiffness matrix is well suited as a preconditioner. In the last example, the standard \mathcal{H} -matrix approach is compared with the uniform \mathcal{H} -matrix approach and the \mathcal{H}^2 -matrix approach, as presented in Chapter 8. All computations were performed on a single computation node consisting of two Intel E5-2630 v4 processors with 64 GB RAM. The implementation is based on the C++ software library AHMED [13]: Another software library on Hierarchical Matrices for Elliptic Differential equations. In the process, the library was supplemented with the methods presented in this dissertation and their necessary frameworks. This includes the singularity removal techniques from Chapters 3 and 5, the uniform \mathcal{H} -matrix and the \mathcal{H}^2 -matrix approximations from Chapter 8.

9.1. Singular integrals

We consider the integrals (22) and (23). To exemplify the numerical errors presented in Chapter 4, we choose for the first two tetrahedra t_1 and t_2 such that both share a common face, and linear basis functions such that $t_1 \not\subset \text{supp } \varphi_i$ and $t_2 \not\subset \text{supp } \varphi_j$. For the second integral we choose a tetrahedron t and panel τ sharing a common edge, and a linear basis function with $\varphi_i = \varphi_j$. Then the integrals simplify to:

$$I_1 := - \int_{t_1} \int_{t_2} \frac{\varphi_i(y) \varphi_j(x)}{|x-y|^{3+2s}} dy dx \quad \text{and} \quad I_2 := \int_t \varphi_i^2(x) \int_\tau \frac{(y-x)^T n_\tau(y)}{|x-y|^{3+2s}} ds_y dx.$$

After applying the respective Duffy transformation, a three-dimensional integral must be computed numerically in both cases. In the following, we focus only on the stronger singularities, i.e. we set $s = 0.8$.

First, we consider the Duffy transformation presented in Chapter 3. Since the integrals cannot be integrated analytically, we replace the exact values $I_1 = I[\tilde{k}_{1,F}]$ and $I_2 = I[\tilde{k}_{2,E}]$ by $Q^{20}[\tilde{k}_{1,F}]$ and $Q^{20}[\tilde{k}_{2,E}]$, respectively, where Q^{20} denotes the approximation of the integral with 20 Gauss points per dimension.

In Figure 3, the error of the numerical integration E^n , $n = 2, \dots, 7$, is shown for four different diameters h . Notice that the error is plotted logarithmically. Based on the Theorems 12 and 13, one expects $\log(E^n)$ to be linear w.r.t. the number of Gauss points. This can also be observed in the Figures 3a and 3b. Obviously, h has no influence on the slope of the curves.

Next, we repeat the example, however, using the cubature formulas described in Chapter 5. Remember, the difference between the two approaches is only the nonlinear transformation. Instead of mapping the integration domain to a six-dimensional unit cube, respectively a five-dimensional unit cube, the integration domain is mapped to suitable reference elements. The regularized integrands

9. Numerical results

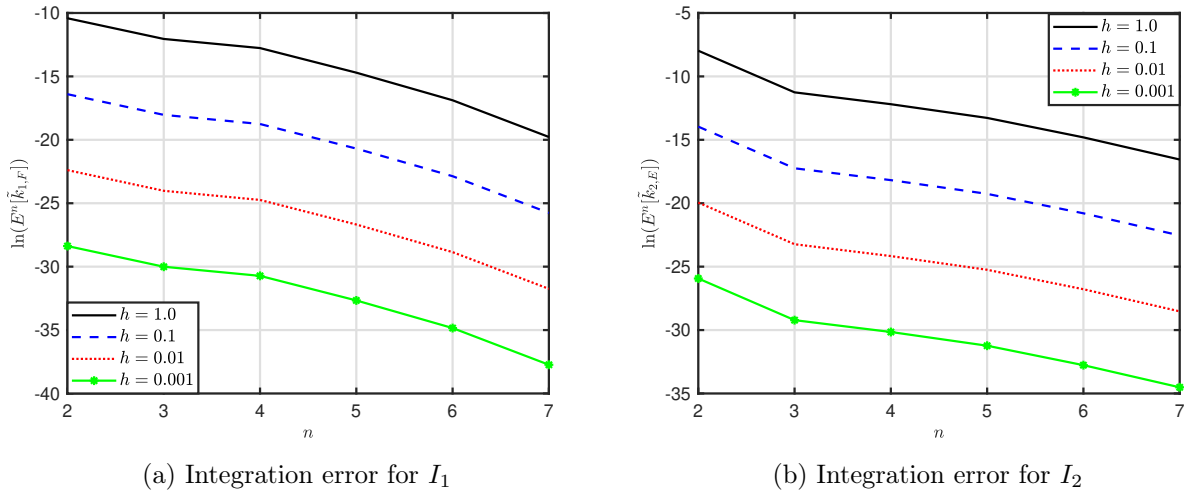


Figure 3: Integration error for different values of h using tensor Gauss quadrature formulas

are denoted by $\hat{k}_{1,F}$ and $\hat{k}_{2,E}$. As reference value for the exact integral, we still use $Q^{20}[\tilde{k}_{1,F}]$ and $Q^{20}[\tilde{k}_{2,E}]$, respectively.

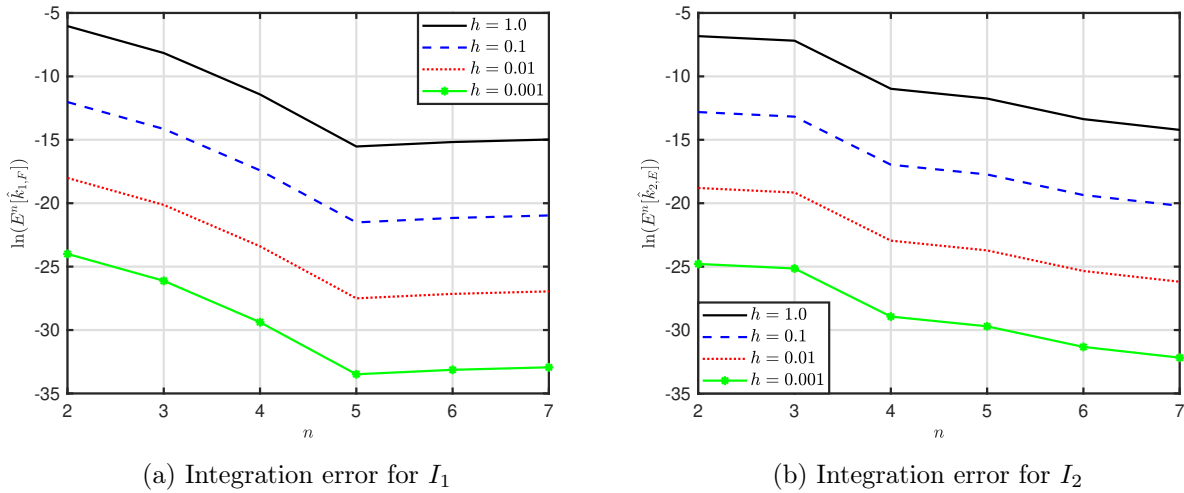


Figure 4: Integration error for different values of h using symmetric cubature formulas

Figure 4 illustrates the error of numerical integration E^n , $n = 2, \dots, 7$, for four different diameters h . Based on n , the symmetric cubature formulas for the tetrahedron and the panel are chosen as described in Section 5, i.e. for the numerical integration of the tetrahedron a rule with at least $n^3/6$ evaluation points is used and for the numerical integration of the panel a rule with at least $n^2/2$ evaluation points is used. For I_2 the numerical integration behaves as expected, the slope of the graphs is almost linear. However, the graphs in Figure 4a behave differently. For $n = 2, \dots, 5$ the graphs decrease linearly as Theorem 12 indicates. But for $n = 6, 7$ the error plots are slightly

9. Numerical results

increasing. We suppose that the issue here is that for the numerical integration three different types of quadrature rules are used: a Gaussian quadrature rule, a symmetric cubature rule for panels and a symmetric cubature rule for tetrahedra. To obtain a more stable approach we suggest to split up the last two sub-domain such that each new sub-domain can be described by one inequality w.r.t. ω , since then all appearing integrals can be computed via the symmetric cubature rule for tetrahedra.

However, for our main purpose, the approximation of the entries of the stiffness matrix, we do not need such a fine approximation of the integrals. If we take a look at Figure 5, we see the relative errors of the numerical integration displayed for both approximation schemes, the one introduced in Chapter 3 and the one introduced in Chapter 5, for $h = 0.0001$, respectively. In both cases, the relative error decreases exponentially and it is less than 1% for $n = 4$. Even for $n = 3$ the error is about by 5%. For the approximation of the entries of the stiffness this is sufficient.

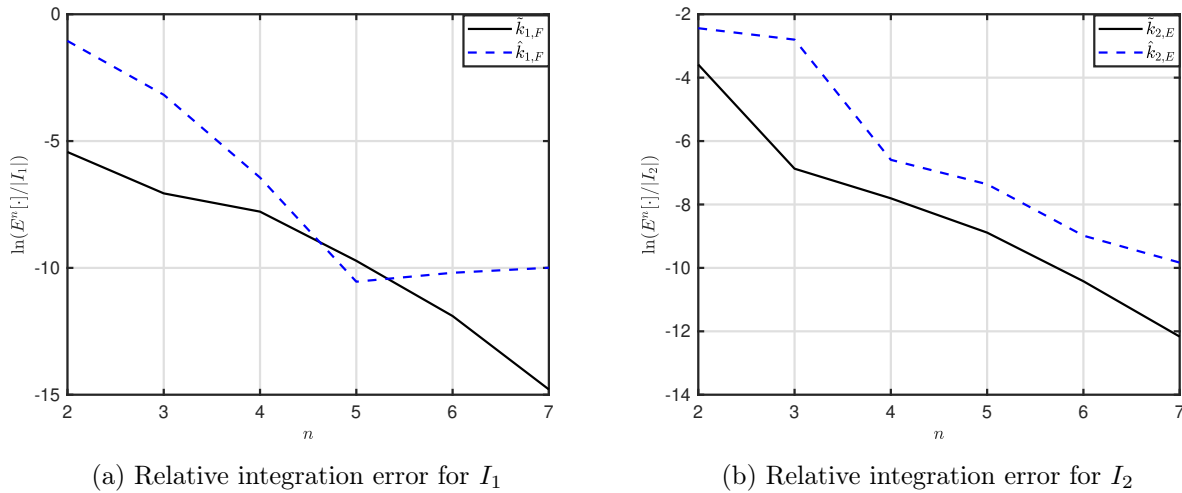


Figure 5: Comparison of the relative errors for $h = 0.0001$

As the Figures 3 to 5 have shown, both approaches presented are suitable to approximate the integrals I_1 and I_2 . The Duffy transformation to the six-dimensional unit cube, five-dimensional unit cube, respectively, produces more accurate approximations. On the other hand, the procedure presented in Chapter 5 is much faster, as shown in Table 8.

In Table 8, the number of evaluations of the kernel for the numerical integration for each case is calculated for $n = 2, \dots, 7$ and the corresponding methods are compared by the ratio of the evaluations of the kernel. As Table 8 displays computing the integrals I_1 and I_2 is an expensive task. Note, the computation of entry of the stiffness matrix consists of multiple integrals of the type of I_1 and I_2 , if the support of the linear basis functions corresponding to this entry overlap. Therefore, it is mandatory to compute this integral in an efficient way and the method presented in Chapter 5 provides that, e.g. the cubature approach requires 16% less evaluations of the kernel compared to the tensor Gauss quadrature. This is due to the fact that the symmetric cubature rule for tetrahedra dominates the costs here and the rule was chosen such that number of evaluation points is roughly at $n^3/6$. For I_2 we also obtain a good speed up. Actually, it is more than we expect for the bigger values of n . This can be explained by the choice of the number of evaluation points of the symmetric

9. Numerical results

n	2	3	4	5	6	7
$\tilde{k}_{1,F}$	136	459	1 088	2 125	3 672	5 831
$\hat{k}_{1,F}$	23	74	174	334	588	917
ratio	17%	16%	16%	16%	16%	16%
$\tilde{k}_{2,E}$	32	108	256	500	864	1 372
$\hat{k}_{2,E}$	13	25	46	71	108	150
ratio	40%	23%	18%	14%	13%	11%

Table 8: Number of evaluations of the kernel

cubature rule for the panel. Since we do not use exactly at least $n^2/2$ points, but mostly rounded off, the speed up is better than expected.

9.2. Fractional diffusion process on a unit ball

For the second part of the numerical results, we consider (1), the fractional Poisson problem, where we set $f = 1$ and $\Omega = B_1(0) \subset \mathbb{R}^3$:

$$\begin{aligned} (-\Delta)^s u &= 1 && \text{in } B_1(0), \\ u &= 0 && \text{on } \mathbb{R}^3 \setminus B_1(0). \end{aligned}$$

As mentioned in Section 2.3 the analytic solution of the problem,

$$u(x) = \frac{2^{-2s}}{\Gamma(1+s)^2} (1 - |x|^2)^s,$$

is well-known (see [2]) and displayed in Figure 6a and 6b for $x_3 = 0$ and for two different values of s . Following the approach described in Section 2.4, we discretize the problem. Notice that according to Lemma 7 the interior angles of the panels should not be chosen too small, otherwise the Duffy transformation becomes unstable. Here, we use the transformation displayed in Chapter 5. For the computation of the stiffness matrix we use the lower bound on the number of Gauss points per dimension presented in Lemma 19 and adapt it to the symmetric cubature rules for panels and the tetrahedra, respectively. The stiffness matrix A is computed in two different ways, first as a dense matrix and second it is approximated by an \mathcal{H} -matrix, where the admissible blocks are computed via the ACA. The accuracy of the ACA is adapted to the fineness of the discretization of the unit sphere. The resulting finite element solutions are denoted by u_{FEM} and u_{ACA} , respectively.

Figure 7 shows the error between the exact solution u and the finite element solution u_{FEM} together with the theoretical error estimate of Theorem 8 in a log-log scale. Notice that for $s = 0.8$ we are not able to compute u_{FEM} for the finest discretization, since the computation of the dense matrix exceeds the available memory of 64 GB RAM.

9. Numerical results

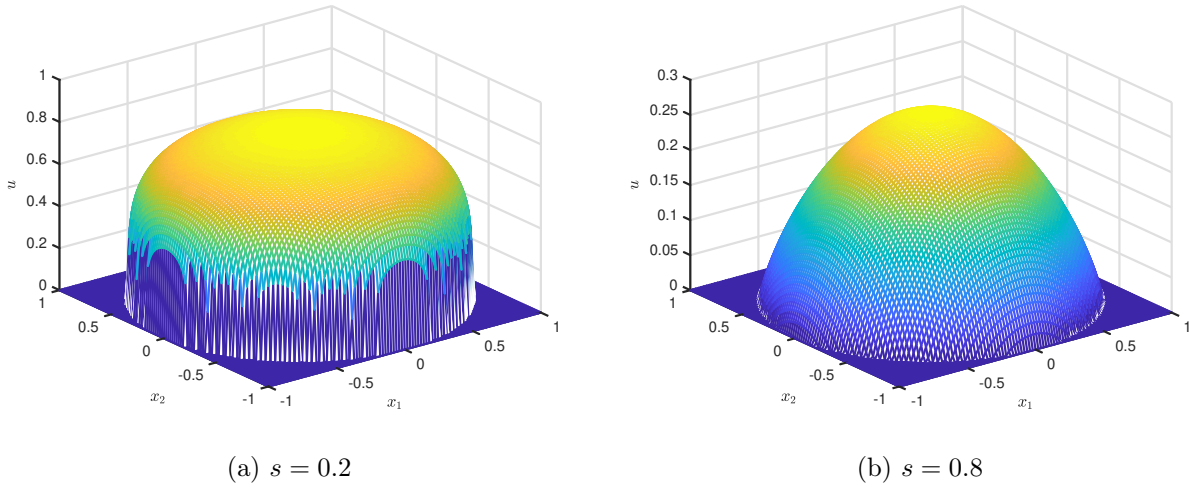


Figure 6: Exact solution u

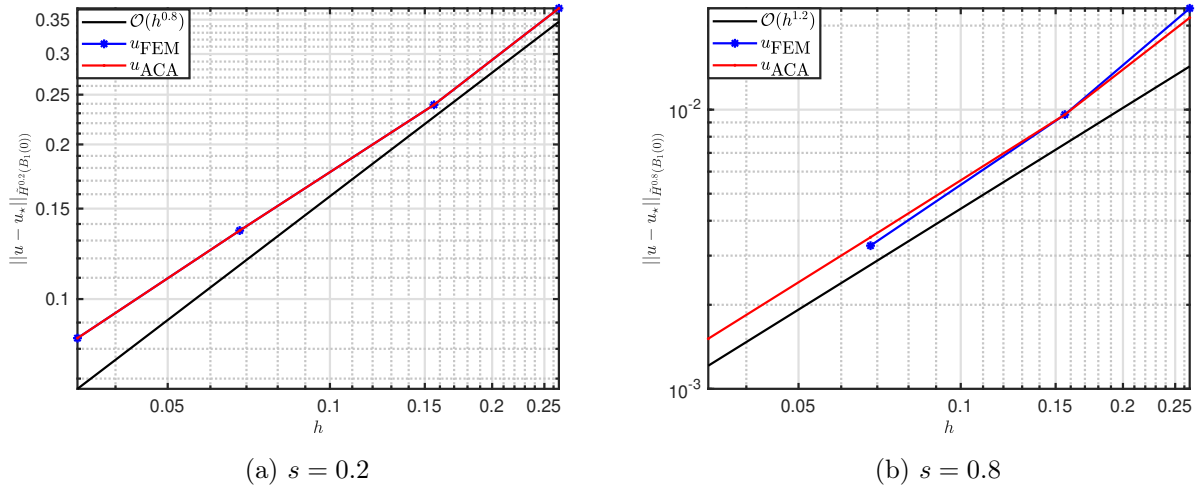


Figure 7: Absolute error between the analytic and numerical solution

According to [2], it holds that $u \in H^{s+1/2-\varepsilon}(B_1(0))$. Hence, we would expect a convergence rate less than $1/2$ w.r.t. h . As it can be seen in Figure 7, the convergence rates are better than expected. For both cases we obtain an optimal rate of $1 - s$ and $2 - s$, respectively; cf. Theorem 8. This may be due to the fact that the analytical solution is a smooth function in the interior of $B_1(0)$ as the singularity of u is located on the boundary $\partial B_1(0)$. Moreover, for the numerical computations a (inner) polyhedral approximation of $B_1(0)$ is used.

Since we have numerically verified that the \mathcal{H} -matrix approximation of A is working, we can study the benefits of this approach.

In Table 9 the results for the storage requirements are illustrated for $s = 0.2$ and for $s = 0.8$. The

9. Numerical results

	$s = 0.2$				$s = 0.8$			
	219	1 130	17 563	144 716	219	1 130	17 563	144 716
N	219	1 130	17 563	144 716	219	1 130	17 563	144 716
A	0.2	4.9	1 177.4	79 899.3	0.2	4.9	1 177.4	79 899.3
$A_{\mathcal{H}}$	0.2	4.8	362.9	6 072.9	0.2	4.8	374.8	6 458.9
compr. rate	100%	98%	32%	8%	100%	98%	31%	8%

Table 9: Storage requirements for the stiffness matrix in MB for two different values of s

compression rate is defined as the ratio between the storage requirements between A and $A_{\mathcal{H}}$. For the coarse grids we cannot save anything, because most of the blocks are too small to apply the ACA efficiently. But we can see a significant saving with the finer grids. Only 8% of the original memory is needed for $A_{\mathcal{H}}$ for the finest discretization. This is a saving of over 70 GB for both cases. The results for $s = 0.2$ are slightly better than for $s = 0.8$, because for $s = 0.2$ the rank of the blocks is smaller.

Similar observations can be made about the computation time for the setting up the stiffness matrix.

	$s = 0.2$				$s = 0.8$			
	219	1 130	17 563	144 716	219 s	1 130	17 563	144 716
N	219	1 130	17 563	144 716	219 s	1 130	17 563	144 716
A	0.6 s	6.1 s	706.0 s	45 338.2 s	0.6 s	60.5 s	1 183.2 s	63 424.1 s
$A_{\mathcal{H}}$	0.6 s	6.3 s	297.9 s	7 041.4 s	0.6 s	60.1 s	783.3 s	25 487.6 s
time ratio	100%	103%	42%	16%	100%	99%	66%	40%

Table 10: Computation time for the setting of the stiffness matrix for two different values of s

The time for setting up the stiffness matrix and the speed up between the methods is displayed in Table 10. Again, for the small examples almost no block is approximated and therefore we gain no advantage. For the finer grids, however, a large speed up can be seen. The computation is more than five times faster for the \mathcal{H} -matrix approach compared to the dense matrix for $s = 0.2$ and more than two times faster for $s = 0.8$. Thus, also note that a big difference between the values of s can be observed. This is mainly due to quadrature rules being used. As we have seen in Figure 7 the solutions for $s = 0.2$ have smaller errors compared to the solutions for $s = 0.8$ and this accuracy has to be paid by the quadrature rules.

As the final point, we focus on solving the linear system of equations and the utility of $A_{\mathcal{H}}^{-1}$, the rough approximation of the inverse of the stiffness matrix, as a preconditioner. $\varepsilon_{A_{\mathcal{H}}^{-1}}$, the accuracy of the approximation of the preconditioner, is set to 0.1 for all geometries and for both values of s .

Table 11 presents an overview over the time being needed to solve the linear system of equation for $s = 0.2$ and $s = 0.8$, respectively. There are three different cases listed: the dense stiffness matrix A , the \mathcal{H} -matrix $A_{\mathcal{H}}$ and the \mathcal{H} -matrix $A_{\mathcal{H}}^{\text{precond}}$, where we used $A_{\mathcal{H}}^{-1}$ as a preconditioner. Note

9. Numerical results

N	$s = 0.2$				$s = 0.8$			
	219	1 130	17 563	144 716	219	1 130	17 563	144 716
A	0.01 s	0.07 s	13.76 s	123 326 s	0.02 s	0.16 s	25.19 s	–
$A_{\mathcal{H}}$	0.01 s	0.10 s	4.83 s	88.05 s	0.04 s	0.13 s	7.42 s	224.59 s
$A_{\mathcal{H}}^{\text{precond}}$	0.02 s	0.14 s	7.68 s	158.98 s	0.02 s	0.12 s	5.61 s	134.95 s

Table 11: Computation time for the setting of the stiffness matrix for two different values of s

that for the finest geometry the linear system of equations w.r.t. A could not be solved, since the computation of A itself exceeded the available memory. Additionally, Table 11 illustrates that for the finer geometries the \mathcal{H} -matrix approach is far more efficient in comparison to the dense matrix. Both approaches behave similar for the coarse grids. The reason for this is again that here almost no block is admissible and therefore there is no significant difference between A and $A_{\mathcal{H}}$.

Interesting are the results for the preconditioner. By having a closer look at Table 11, we can see that for $s = 0.2$ applying the preconditioner costs more than not using it, while for $s = 0.8$ the preconditioner provides a good speed up by a factor of two.

N	$s = 0.2$				$s = 0.8$			
	219	1 130	17 563	144 716	219	1 130	17 563	144 716
CG	25	35	37	53	21	37	71	136
PCG	4	6	6	6	5	6	10	17

Table 12: Number of steps for solving the system for two different values of s

Table 12 gives insight to this. There, the number of steps for solving the linear systems by the CG-method, respectively the PCG-method, are listed. First of all, it is obvious that $A_{\mathcal{H}}^{-1}$ is a good choice for preconditioning, since the number steps needed to solve the system are reduced drastically. For $s = 0.2$ the preconditioning is almost optimal, since the number of steps is constant w.r.t. N , i.e. $\varepsilon_{A_{\mathcal{H}}^{-1}}$ can be chosen smaller to achieve sufficient results. As mentioned in Chapter 7, the reason for this is that the condition of the stiffness matrix scales as $\mathcal{O}(h^{-2s})$. Actually, for $s = 0.2$ the linear system of equations may be well-conditioned enough in order to do without preconditioning, while for $s = 0.8$ the preconditioning proves to be quite useful.

9.3. Fractional diffusion process on an ellipse

For the last example, we consider again (1), the fractional Poisson problem, where we set $f = 1$ and $\Omega := \{x \in \mathbb{R}^3 : x_1^2 + x_2^2 + x_3^2/9 = 1\} \subset \mathbb{R}^3$:

$$\begin{aligned} (-\Delta)^s u &= 1 && \text{in } \Omega, \\ u &= 0 && \text{on } \mathbb{R}^3 \setminus \Omega. \end{aligned}$$

The general setup and our approach are the same as in Section 9.2, i.e. for the singularity removal the Duffy transformation introduced in Chapter 5 is used and the quadrature rules are chosen via Lemma 19. We compare three types of \mathcal{H} -matrix approximations of A using the same block cluster tree generated with $\rho = 0.8$. The first one is generated via standard ACA, the second one is a uniform \mathcal{H} -matrix approximation and the third one is an \mathcal{H}^2 -matrix approximation. Due to the Galerkin approach, we choose various volume discretizations of the ellipse Ω as the computational domain, the Dirichlet data $g \equiv 1$, the order of the fractional Laplacian is $s = 0.8$ and the accuracy $\varepsilon_{\text{ACA}}^{\mathcal{H}}$ of the ACA for \mathcal{H} -blocks depends on the discretization of Ω .

Since no analytical solution is known for this geometry, we cannot directly verify the accuracy of the numerical solution u_h . Since we already exemplified in Section 9.2 that the standard \mathcal{H} -matrix approximation performs well, it is used here as a reference value for the numerical verification of the other two methods. To be more precise for each grid we calculate e_h the mean relative error between the solutions of the discretized problem, i.e.

$$e_h(u_{\star}^N) := \frac{1}{N} \sum_{i=1}^N \frac{|(u_{\mathcal{H}}^N)_i - (u_{\star}^N)_i|}{|(u_{\mathcal{H}}^N)_i|}, \quad u_{\mathcal{H}}^N, u_{\star}^N \in \mathbb{R}^N, \star \in \{\mathcal{H}_u, \mathcal{H}^2\}.$$

Notice, $u_{\mathcal{H}}^N, u_{\mathcal{H}_u}^N$ and $u_{\mathcal{H}^2}^N$ are the solutions of corresponding discretized problems.

Table 13 shows the minimum sizes of the respective clusters $n_{\min}^{\mathcal{H}}$, $n_{\min}^{\mathcal{H}_u}$, and $n_{\min}^{\mathcal{H}^2}$, the accuracy of the respective used ACAs $\varepsilon_{\text{ACA}}^{\mathcal{H}}$, $\varepsilon_{\text{ACA}}^{\mathcal{H}_u}$, and $\varepsilon_{\text{ACA}}^{\mathcal{H}^2}$ and the error e_h . The accuracies $\varepsilon_{\text{ACA}}^{\mathcal{H}_u}$ and $\varepsilon_{\text{ACA}}^{\mathcal{H}^2}$

N	\mathcal{H} -matrix		uniform \mathcal{H} -matrix			\mathcal{H}^2 -matrix		
	$n_{\min}^{\mathcal{H}}$	$\varepsilon_{\text{ACA}}^{\mathcal{H}}$	$n_{\min}^{\mathcal{H}_u}$	$\varepsilon_{\text{ACA}}^{\mathcal{H}_u}$	e_h	$n_{\min}^{\mathcal{H}^2}$	$\varepsilon_{\text{ACA}}^{\mathcal{H}^2}$	e_h
7 100	30	$1.0e - 2$	100	$1.0e - 2$	$4.0e - 2$	100	$1.0e - 2$	$3.8e - 2$
62 964	60	$1.0e - 3$	200	$1.0e - 3$	$1.1e - 2$	200	$1.0e - 3$	$1.0e - 2$
528 747	60	$1.0e - 4$	400	$1.0e - 4$	$4.2e - 2$	400	$1.0e - 4$	$3.8e - 2$

Table 13: Comparison between the three different \mathcal{H} -matrix approximations

for the uniform \mathcal{H} -matrix blocks, respectively for the \mathcal{H}^2 -blocks, were adjusted so that all methods produce almost the same error e_h . Note that $n_{\min}^{\mathcal{H}_u}$ and $n_{\min}^{\mathcal{H}^2}$ denote the minimal size of blocks being approximated via the uniform approach, respectively the \mathcal{H}^2 -matrix approach.

Since all three methods generate similar errors, we can compare the different \mathcal{H} -matrix approximations amongst each other. First we start with setting up the stiffness matrix. In Table 13 the

9. Numerical results

N	\mathcal{H} -matrix	\mathcal{H}_u -matrix		\mathcal{H}^2 -matrix	
	$A_{\mathcal{H}}$	precalculations	$A_{\mathcal{H}_u}$	precalculations	$A_{\mathcal{H}^2}$
7 100	60.0 s	0.1 s	54.2 s	0.1 s	54.6 s
62 964	3 047.7 s	1.4 s	2 914.7 s	1.1 s	2 929.2 s
526 747	95 615.0 s	27.6 s	87 709.6 s	19.2 s	87 902.1 s

Table 14: Time comparison for setting up the stiffness matrix

time being needed to set up the stiffness matrix is listed. We can observe that both methods that are based on a uniform approximation need almost the same time, while they are both faster than the standard \mathcal{H} -matrix method. For the finest geometry the CPU time for approximating A is reduced by almost 10%, i.e. more than two hours. The speed up is due to the uniform approximation, since the costly numerical integral is done beforehand. The more blocks are approximated with a uniform method, the faster is the setting up of the matrix.

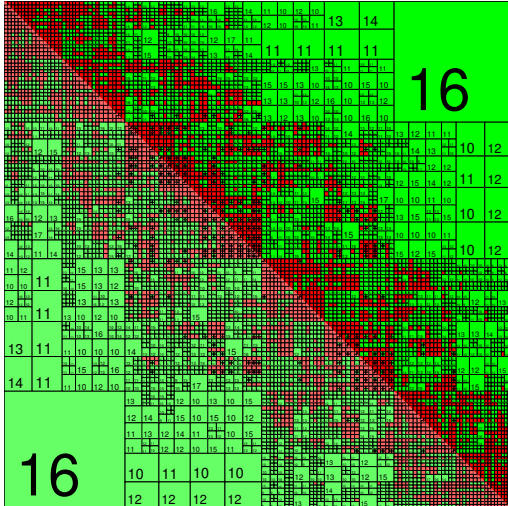


Figure 8: $A_{\mathcal{H}}$ for $N = 7100$

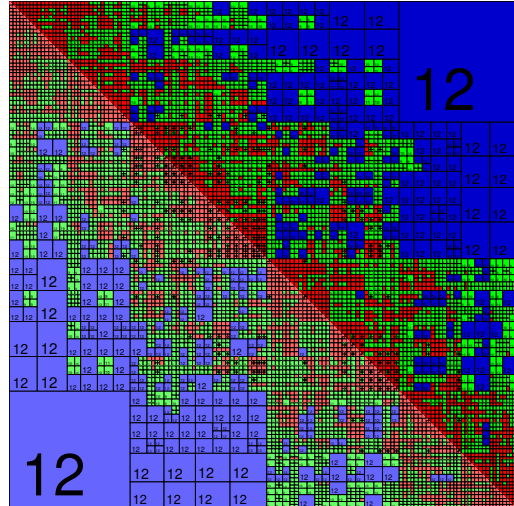


Figure 9: $A_{\mathcal{H}^2}$ for $N = 7100$

This can be seen from Figs. 8 and 9. These figures show the matrix A for the coarsest discretization, which was approximated as an \mathcal{H} -matrix and \mathcal{H}^2 -matrix, respectively. The red blocks were calculated entry by entry, the green and blue blocks are low-rank approximations calculated via ACA and uniform approach, respectively, and the numbers in the low-rank blocks are the ranks $k_{\mathcal{H}}$ and $k_{\mathcal{H}^2}$, respectively. As it can be seen, the ranks $k_{\mathcal{H}}$ and $k_{\mathcal{H}^2}$ of corresponding blocks hardly differ. This is due to the difference in accuracy between $\varepsilon_{ACA}^{\mathcal{H}}$ and $\varepsilon_{ACA}^{\mathcal{H}^2}$. Obviously, the difference in rank grows larger if the accuracies are equal. Theoretically, $k_{\mathcal{H}}$ is smaller than $k_{\mathcal{H}^2}$, since $k_{\mathcal{H}}$ is tailored to the block, while $k_{\mathcal{H}^2}$ is the result of a uniform approximation. For this example we omit the uniform \mathcal{H} -matrix, since in this case the matrix is identical to the \mathcal{H}^2 -matrix, because the critical

9. Numerical results

parameters are for both cases identical, i.e. $\varepsilon_{\text{ACA}}^{\mathcal{H}_u} = \varepsilon_{\text{ACA}}^{\mathcal{H}^2}$ and $\rho_{\mathcal{H}^2} = \rho_{\mathcal{H}_u}$.

Of course not only the CPU time benefits from the small difference between $k_{\mathcal{H}}$ and $k_{\mathcal{H}^2}$, but also the storage requirements as can be seen from Table 15. For each selected discretization, less storage is

N	\mathcal{H} -matrix		uniform \mathcal{H} -matrix		\mathcal{H}^2 -matrix	
	memory	compr. rate	memory	compr. rate	memory	compr. rate
7 100	61 MB	31.7%	56 MB	28.9%	56 MB	29.1%
62 964	1 502 MB	9.9%	1 353 MB	8.9%	1 356 MB	8.9%
528 747	27 195 MB	2.5%	21 350 MB	2.0%	20 938 MB	2.0%

Table 15: Memory comparison between \mathcal{H} -, uniform \mathcal{H} - and \mathcal{H}^2 -matrices

required when using the method presented in Chapter 8. For example, the finest discretization requires almost 25% less storage (i.e. more than 6 GB). In addition, the uniform \mathcal{H} -matrix approximation and the \mathcal{H}^2 -approximation become more efficient the larger the number of degrees of freedom N becomes, since the precomputations can be exploited for an increasingly larger part of the matrix. Notice, the memory requirements for the precomputations are already included in Table 15.

As a last point we consider the runtime of the CG-method for all \mathcal{H} -matrix approximations. Table 16 displays the time needed to solve the resulting linear system via the CG-method and how

N	\mathcal{H} -matrix		uniform \mathcal{H} -matrix		\mathcal{H}^2 -matrix	
	t_{CG}	CG steps	t_{CG}	CG steps	t_{CG}	CG steps
7 100	1.1 s	52	1.0 s	52	1.3 s	64
62 964	54.4 s	91	57.0 s	99	57.8 s	99
528 747	1 485.6 s	175	2 397.1 s	196	3 200.1 s	197

Table 16: Time comparison for solving the linear system

many steps were needed for the algorithm. Notice that the solving of the linear system is not parallelized. The interesting issue is that here for the first time the standard \mathcal{H} -matrix approximation is fastest. The uniform \mathcal{H} -matrix approximation is a little bit slower and becomes slower the larger N becomes. The same applies for the \mathcal{H}^2 -matrix. However, here the problems are larger, since the matrix is worse conditioned which can be seen by number of CG steps needed. The issue gets better, though, when the time per CG step is considered. In this context the \mathcal{H} -matrix is two times faster than \mathcal{H}^2 -matrix and 1.4 times faster than the uniform \mathcal{H} -matrix for the finest geometry. Actually, this is not so surprising since the costs for the matrix-vector-multiplication for the uniform \mathcal{H} -matrix block is more expensive than the standard \mathcal{H} -matrix block, since we have to consider an additional matrix (see Section 8.3). Additionally, in most cases $k_{\mathcal{H}_u}$ is larger than $k_{\mathcal{H}}$. This is obvious, since for each block $k_{\mathcal{H}}$ is specially adapted to it, while $k_{\mathcal{H}_u}$ is only tailored to the worst case (see Algorithm 2).

9. Numerical results

Theoretically, the \mathcal{H}^2 -matrix should be more efficient than the standard \mathcal{H} -matrix (see [51]). The issue is that this holds true if the rank of the son clusters is always smaller than the rank of the father cluster. This assumption is violated by our implementation, since for each cluster belonging to an \mathcal{H}^2 -admissible block a uniform approximation is performed via a reference element similar to Algorithm 2. This can also be observed in Figure 9. Therefore, each \mathcal{H}^2 -admissible block has the same rank $k_{\mathcal{H}^2}$ and each transfer matrix between clusters belonging to such an admissible has the dimension of $k_{\mathcal{H}^2} \times k_{\mathcal{H}^2}$. Therefore, matrix-vector multiplication for \mathcal{H}^2 -matrices is slower than the matrix-vector multiplication for the standard \mathcal{H} -matrix. A simple way to improve this issue would be to parallelize the matrix-vector multiplication. While this would not improve the basic problem, it would drastically reduce the total time required to solve the linear system of equations.

10. Conclusion

10.1. Summary

As we have seen, the aim of the dissertation is to handle the fractional Laplacian efficiently numerically, with the special focus on three dimensions. To this end, Chapter 1 laid the theoretical foundation. It is especially interesting to see how closely related the operator is to the Laplace operator. Nevertheless, there are serious differences between the two due to the nonlinearity of the fractional Laplacian, cf. for example the mean value properties. Moreover, the weak formulation of the fractional Laplacian looks more like the BEM formulation of the Laplace operator than the weak formulation of the Laplace operator. Therefore, the computation of the entries of the stiffness matrix is also very complex and time-consuming. In total, we spent three chapters on it. The time-consuming part here is the singularity removal. In Chapter 3 we introduced new tensor Gauss quadrature formulas for integrals of the type (22) and (23). The tensor Gauss quadrature approach is necessary for the error estimates being applied in the following chapter, Chapter 4. There, based on the error estimates for the finite element solution we derived rules on the minimal number of Gauss points per dimension w.r.t. the discretization size. However, from a computational point of view the tensor approach is not ideal, because the integration domain consisting of tetrahedra and panels has to be blown up to multidimensional unit cubes. Therefore, in Chapter 5 we went back to the singularity removal. In contrast to the standard Duffy transformation, we applied here another kind of nonlinear transformation. Instead of blowing up the whole geometry to a six-dimensional unit cube, we have shown that it is enough to map only the geometry regarding ξ to a unit cube and for the remaining variables η the forking inequality chains can be exploited to map the geometry to suitable reference elements, e.g. to a combination of unit panels and unit tetrahedra. In Section 9.1 it is illustrated that the cubature approach is significantly faster than the standard tensor Gauss quadrature approach.

After we provided efficient means to compute the entries of the stiffness matrix, we focused on an approximation of the matrix itself. In Chapter 6 we laid out the foundation for it and have shown that the stiffness matrix can be approximated by an \mathcal{H} -matrix. Unfortunately, we were not able to fully adapt the approach of [13] concerning the approximation of the inverse of the stiffness matrix. The issue is that we cannot prove that for $u \in X_{\text{loc}}(D)$ it holds that $u \in L^\infty(K)$ for each compact subset $K \subset D$. If this statement is true then it could be easily proven that the error of the \mathcal{H} -matrix approximation of the inverse stiffness matrix is decaying exponentially w.r.t. the rank. Nevertheless, we were able to provide a local Caccioppoli inequality for the fractional Laplacian. Chapter 8 provides two additional \mathcal{H} -matrix approximations, the uniform \mathcal{H} -matrix and the \mathcal{H}^2 -matrix. Both approaches are introduced in the Sections 8.3 and 8.4, respectively. Both methods can be computed via a new version of the ACA that we derive in Section 8.1. Additionally, we have shown that this new kind of approximation can be applied to functions f , where $f(x, y) = |x - y|^\alpha$ with $\alpha < 0$. This means that the method can also be used for the numerical treatment of the Laplace operator. As a next step we compared these three different methods with each other and observed that w.r.t. the time needed to set up the matrix and the memory requirements, the two methods from Chapter 8 are superior, as predicted by the theory. Only for solving the linear equation system the standard \mathcal{H} -matrix approach is faster.

10.2. Outlook

Future research might improve some of the presented methods. For example, in Section 9.3 we discussed that the issue for \mathcal{H}^2 -matrix approach is that there is no decrease of the rank along the cluster tree. Therefore, we can observe that there are way less performance improvements as we would expect. The main problem is that for each cluster the same admissible parameter ρ is used. Therefore, each cluster has the same rank $k_{\mathcal{H}^2}$. To solve this issue, we could introduce a new parameter $\hat{n}_{\min}^{\mathcal{H}^2}$ with $n_{\min}^{\mathcal{H}} \leq \hat{n}_{\min}^{\mathcal{H}^2} < n_{\min}^{\mathcal{H}^2}$ to artificially deepen the cluster tree being used for the \mathcal{H}^2 -matrix approximation. However, for these new generated clusters we have to ensure that the uniform cross approximation is executed with a new admissible parameter $\hat{\rho}$ being smaller than ρ such that $\hat{k}_{\mathcal{H}^2}$, the rank of uniform cross approximation for these new clusters, is smaller than $k_{\mathcal{H}^2}$. In order to ensure that $\hat{\rho} \leq \rho$ the far-fields of the corresponding leaf cluster of the cluster tree w.r.t. $n_{\min}^{\mathcal{H}^2}$ are used instead of the far-fields of the individual clusters for the uniform cross approximation. Unfortunately, this is not enough guarantee that $\hat{\rho} < \rho$. The issue is the curse of dimensions. Due to the construction of the cluster tree via the PCA neither the diameter of the new clusters decreases significantly nor does the distance between the new clusters and the specially selected far-fields increases significantly on the first new added levels of the cluster tree. If the cluster tree w.r.t. $\hat{n}_{\min}^{\mathcal{H}^2}$ is deep enough, then $\hat{\rho} < \rho$ can be guaranteed for most of the leaf clusters. However, a new issue can occur, namely that for these leafs the accuracy of the approximation has to be adjusted, which may more or less negates the effect of $\hat{\rho}$ or even worsen the situation. This adjustment of the accuracy may be necessary due to Theorem 39. All in all, this idea is a balancing problem between $\hat{n}_{\min}^{\mathcal{H}^2}$ and the accuracy of the approximation.

Until now we applied the uniform cross approximation presented in Section 8.1 only on admissible matrix blocks. It would be particularly interesting to see whether these methods can also be applied efficiently on a smaller scale. Using the geometric insights from Section 5, one could create new uniform quadrature rules for nearly singular integrals and for the integrals arising in the Duffy transformation. The basic idea is to split up the integrals and perform the costly numerical integration as precomputations. Hereby, the costs are significantly reduced since in the case of the nearly singular integrals only two independent three-dimensional integrals have to be computed instead of one six-dimensional integral. However, there are still some open questions here. Is the number of interpolations points less than the total number of Gauss points needed for the numerical interpolation? Is it efficient to perform a uniform approximation for each tetrahedron? How to select the discrete set M_R efficiently? Since the discretization is only quasi-uniform the distance between two tetrahedra can be less than the mean diameter h . Therefore, for each tetrahedron M_R must be selected appropriately. Another possibility would be to set ρ to a smaller value, in order to use a reference element in the same sense as in Algorithm 2 in Section 8.3. However, if we follow this approach the question is if the method is still efficient and faster than the standard multi-dimensional numerical integration.

A similar question can be asked regarding the entries of the non-admissible blocks. Let us consider a matrix entry a_{ij} belonging to a non-admissible block b_{qw} . Although the clusters X_t and X_s do not satisfy the geometric admissibility condition, the supports of the linear basis function φ_i and φ_j can still satisfy it. It is obvious that for the precomputations a reference element can be used to reduce computational costs. However, in order to obtain a numerical stable method the quasi uniformity of the tetrahedra has to be considered. Therefore, the main issue is how to keep the process stable and also efficient at the same time.

A. Appendix: Duffy Transformation

In this chapter we present the treatment of the singular integrals from Chapter 3 in detail. This includes resolving the min and max constraints and generating suitable forking inequality chains. Note that the numbering of the sub-domains D_i does not have to match the numbering of the Duffy transformations \mathcal{D}_i in the individual singularity cases. As we have seen in Chapter 3 some sub-domains require a different transformation and were therefore moved backwards in the numbering.

A.1. Interaction between two tetrahedra

We first start with the interaction between two tetrahedra. Note that the first two singularity cases have already been treated in detail in the Sections 3.2.1 and 3.2.2.

A.1.1. Singularity on a face

In this section we study the singularity case that the two tetrahedra share a common face. The result for the Duffy transformation is already presented in Section 3.2.3. Here, the remaining intermediate steps that were previously omitted are presented.

A.1.1.1. Derivation of the integration domains

As we have seen in Section 3.2.3, the changing of the integration order leads to the following set:

$$D := \left\{ \begin{array}{l} -1 \leq \tilde{z}_1 \leq 1 \\ \max\{-1, -1 + \tilde{z}_1\} \leq \tilde{z}_2 \leq \min\{1, 1 + \tilde{z}_1\} \\ 0 \leq \tilde{z}_3 \leq \min\{1, 1 + \tilde{z}_1\} + \min\{0, -\tilde{z}_2\} \\ \max\{0, -\tilde{z}_2, -\tilde{z}_1 + \tilde{z}_3, \tilde{z}_2 - \tilde{z}_1 + \tilde{z}_3\} \leq \tilde{x}_1 \leq \min\{1, 1 - \tilde{z}_1\} \\ \max\{0, -\tilde{z}_2\} \leq \tilde{x}_2 \leq \tilde{x}_1 + \min\{0, \tilde{z}_1 - \tilde{z}_2 - \tilde{z}_3\} \\ 0 \leq \tilde{z}_4 \leq \tilde{x}_1 - \tilde{x}_2 \end{array} \right\},$$

where we have already considered the first sub-domain D_1 :

$$D_1 := \left\{ \begin{array}{l} -1 \leq \tilde{z}_1 \leq 0 \\ -1 \leq \tilde{z}_2 \leq \tilde{z}_1 \\ 0 \leq \tilde{z}_3 \leq \tilde{z}_1 - \tilde{z}_2 \\ -\tilde{z}_2 \leq \tilde{x}_1 \leq 1 \\ -\tilde{z}_2 \leq \tilde{x}_2 \leq \tilde{x}_1 \\ 0 \leq \tilde{z}_4 \leq \tilde{x}_1 - \tilde{x}_2 \end{array} \right\}.$$

In order to get the remaining subsets, we must understand that the dependencies of the variables among themselves arose from splitting the inequalities. This idea is slightly different to (28), since we do not interleave two inequality chains, but we construct an artificial dependency between them:

$$\left\{ \begin{array}{l} -1 \leq \tilde{z}_1 \leq 0 \\ -1 \leq \tilde{z}_2 \leq 0 \end{array} \right\} = \left\{ \begin{array}{l} -1 \leq \tilde{z}_1 \leq 0 \\ -1 \leq \tilde{z}_2 \leq \tilde{z}_1 \end{array} \right\} \cup \left\{ \begin{array}{l} -1 \leq \tilde{z}_1 \leq 0 \\ \tilde{z}_1 \leq \tilde{z}_2 \leq 0 \end{array} \right\}.$$

A. Appendix: Duffy Transformation

The same applies, of course, to the procedure for \tilde{z}_3 :

$$\left\{ \begin{array}{l} -1 \leq \tilde{z}_1 \leq 0 \\ \tilde{z}_1 \leq \tilde{z}_2 \leq 0 \\ 0 \leq \tilde{z}_3 \leq 1 + \tilde{z}_1 \end{array} \right\} = \left\{ \begin{array}{l} -1 \leq \tilde{z}_1 \leq 0 \\ \tilde{z}_1 \leq \tilde{z}_2 \leq 0 \\ 0 \leq \tilde{z}_3 \leq \tilde{z}_1 - \tilde{z}_2 \end{array} \right\} \cup \left\{ \begin{array}{l} -1 \leq \tilde{z}_1 \leq 0 \\ \tilde{z}_1 \leq \tilde{z}_2 \leq 0 \\ \tilde{z}_1 - \tilde{z}_2 \leq \tilde{z}_3 \leq 1 + \tilde{z}_1 \end{array} \right\}.$$

This leads to two extra sub-domains:

$$D_2 := \left\{ \begin{array}{l} -1 \leq \tilde{z}_1 \leq 0 \\ -1 \leq \tilde{z}_2 \leq \tilde{z}_1 \\ \tilde{z}_1 - \tilde{z}_2 \leq \tilde{z}_3 \leq 1 + \tilde{z}_1 \\ -\tilde{z}_1 + \tilde{z}_3 \leq \tilde{x}_1 \leq 1 \\ -\tilde{z}_2 \leq \tilde{x}_2 \leq \tilde{x}_1 + \tilde{z}_1 - \tilde{z}_2 - \tilde{z}_3 \\ 0 \leq \tilde{z}_4 \leq \tilde{x}_1 - \tilde{x}_2 \end{array} \right\}, \quad D_3 := \left\{ \begin{array}{l} -1 \leq \tilde{z}_1 \leq 0 \\ \tilde{z}_1 \leq \tilde{z}_2 \leq 0 \\ 0 \leq \tilde{z}_3 \leq 1 + \tilde{z}_1 \\ -\tilde{z}_1 + \tilde{z}_3 \leq \tilde{x}_1 \leq 1 \\ -\tilde{z}_2 \leq \tilde{x}_2 \leq \tilde{x}_1 + \tilde{z}_1 - \tilde{z}_2 - \tilde{z}_3 \\ 0 \leq \tilde{z}_4 \leq \tilde{x}_1 - \tilde{x}_2 \end{array} \right\}.$$

However, such dependencies are not always necessary, as we see here:

$$D_4 := \left\{ \begin{array}{l} -1 \leq \tilde{z}_1 \leq 0 \\ 0 \leq \tilde{z}_2 \leq 1 + \tilde{z}_1 \\ 0 \leq \tilde{z}_3 \leq 1 + \tilde{z}_1 - \tilde{z}_2 \\ \tilde{z}_2 - \tilde{z}_1 + \tilde{z}_3 \leq \tilde{x}_1 \leq 1 \\ 0 \leq \tilde{x}_2 \leq \tilde{x}_1 + \tilde{z}_1 - \tilde{z}_2 - \tilde{z}_3 \\ 0 \leq \tilde{z}_4 \leq \tilde{x}_1 - \tilde{x}_2 \end{array} \right\}$$

For the case $0 \leq \tilde{z}_1 \leq 1$ the procedure and the ideas are the same. Here, five sub-domains are needed to resolve the min and max conditions:

$$D_5 := \left\{ \begin{array}{l} 0 \leq \tilde{z}_1 \leq 1 \\ -1 + \tilde{z}_1 \leq \tilde{z}_2 \leq 0 \\ 0 \leq \tilde{z}_3 \leq \tilde{z}_1 - \tilde{z}_2 \\ -\tilde{z}_2 \leq \tilde{x}_1 \leq 1 - \tilde{z}_1 \\ -\tilde{z}_2 \leq \tilde{x}_2 \leq \tilde{x}_1 \\ 0 \leq \tilde{z}_4 \leq \tilde{x}_1 - \tilde{x}_2 \end{array} \right\}, \quad D_6 := \left\{ \begin{array}{l} 0 \leq \tilde{z}_1 \leq 1 \\ -1 + \tilde{z}_1 \leq \tilde{z}_2 \leq 0 \\ \tilde{z}_1 - \tilde{z}_2 \leq \tilde{z}_3 \leq 1 \\ -\tilde{z}_1 + \tilde{z}_3 \leq \tilde{x}_1 \leq 1 - \tilde{z}_1 \\ -\tilde{z}_2 \leq \tilde{x}_2 \leq \tilde{x}_1 + \tilde{z}_1 - \tilde{z}_2 - \tilde{z}_3 \\ 0 \leq \tilde{z}_4 \leq \tilde{x}_1 - \tilde{x}_2 \end{array} \right\}$$

$$D_7 := \left\{ \begin{array}{l} 0 \leq \tilde{z}_1 \leq 1 \\ 0 \leq \tilde{z}_2 \leq \tilde{z}_1 \\ 0 \leq \tilde{z}_3 \leq \tilde{z}_1 - \tilde{z}_2 \\ 0 \leq \tilde{x}_1 \leq 1 - \tilde{z}_1 \\ 0 \leq \tilde{x}_2 \leq \tilde{x}_1 \\ 0 \leq \tilde{z}_4 \leq \tilde{x}_1 - \tilde{x}_2 \end{array} \right\}, \quad D_8 := \left\{ \begin{array}{l} 0 \leq \tilde{z}_1 \leq 1 \\ 0 \leq \tilde{z}_2 \leq \tilde{z}_1 \\ \tilde{z}_1 - \tilde{z}_2 \leq \tilde{z}_3 \leq 1 - \tilde{z}_2 \\ \tilde{z}_2 - \tilde{z}_1 + \tilde{z}_3 \leq \tilde{x}_1 \leq 1 - \tilde{z}_1 \\ 0 \leq \tilde{x}_2 \leq \tilde{x}_1 + \tilde{z}_1 - \tilde{z}_2 - \tilde{z}_3 \\ 0 \leq \tilde{z}_4 \leq \tilde{x}_1 - \tilde{x}_2 \end{array} \right\}$$

$$\text{and } D_9 := \left\{ \begin{array}{l} 0 \leq \tilde{z}_1 \leq 1 \\ \tilde{z}_1 \leq \tilde{z}_2 \leq 1 \\ 0 \leq \tilde{z}_3 \leq 1 - \tilde{z}_2 \\ \tilde{z}_2 - \tilde{z}_1 + \tilde{z}_3 \leq \tilde{x}_1 \leq 1 - \tilde{z}_1 \\ 0 \leq \tilde{x}_2 \leq \tilde{x}_1 + \tilde{z}_1 - \tilde{z}_2 - \tilde{z}_3 \\ 0 \leq \tilde{z}_4 \leq \tilde{x}_1 - \tilde{x}_2 \end{array} \right\}.$$

A. Appendix: Duffy Transformation

All in all, we obtain that

$$D = \bigcup_{i=1}^9 D_i.$$

A.1.1.2. Preparations for the nonlinear transformation

The next step is to establish for each sub-domain a forking inequality chain and to introduce a set of new variables $\omega \in \mathbb{R}^6$ representing the forking inequality chain.

Sub-domain D_1 Since we get here an inequality chain,

$$0 \leq -\tilde{z}_1 \leq -\tilde{z}_1 + \tilde{z}_3 \leq -\tilde{z}_2 \leq -\tilde{z}_2 + \tilde{z}_4 \leq \tilde{x}_1 - \tilde{x}_2 - \tilde{z}_2 \leq \tilde{x}_1 \leq 1,$$

that fulfills our requirements, namely the variables which do not describe the singularity are in the first two chain links, a split up of D_1 is not necessary. Therefore, it is possible to proceed with the introduction of the new set of variables $\omega \in \mathbb{R}^6$ that reflect this ordering:

$$\omega_1 := \tilde{x}_1, \omega_2 := \tilde{x}_1 - \tilde{x}_2 - \tilde{z}_2, \omega_3 := -\tilde{z}_2 + \tilde{z}_4, \omega_4 := -\tilde{z}_2, \omega_5 := -\tilde{z}_1 - \tilde{z}_3, \omega_6 := -\tilde{z}_1.$$

$$\int_0^1 \int_0^{\omega_1} \int_0^{\omega_2} \int_0^{\omega_3} \int_0^{\omega_4} \int_0^{\omega_5} \tilde{k}_1 \left(\begin{bmatrix} 1 - \omega_1 \\ \omega_1 - \omega_2 + \omega_4 \\ \omega_3 - \omega_4 \end{bmatrix}, \begin{bmatrix} 1 - \omega_1 + \omega_6 \\ \omega_1 - \omega_2 \\ \omega_5 - \omega_6 \end{bmatrix} \right) d\omega.$$

Sub-domain D_2 For D_2 a split has to be done, since the forking inequality chain,

$$\begin{aligned} 0 &\leq -\tilde{z}_1 \leq -\tilde{z}_2 \leq -\tilde{z}_1 + \tilde{z}_3 \leq \tilde{x}_1 - \tilde{x}_2 - \tilde{z}_2 \leq \tilde{x}_1 \leq 1, \\ 0 &\leq -\tilde{z}_1 \leq -\tilde{z}_2 \leq -\tilde{z}_2 + \tilde{z}_4 \leq \tilde{x}_1 - \tilde{x}_2 - \tilde{z}_2 \leq \tilde{x}_1 \leq 1. \end{aligned}$$

splits up after the second chain link, which is one link too early:

$$D_2 = \left\{ \begin{array}{l} -1 \leq \tilde{z}_1 \leq 0 \\ -1 \leq \tilde{z}_2 \leq \tilde{z}_1 \\ \tilde{z}_1 - \tilde{z}_2 \leq \tilde{z}_3 \leq 1 + \tilde{z}_1 \\ -\tilde{z}_1 + \tilde{z}_3 \leq \tilde{x}_1 \leq 1 \\ -\tilde{z}_2 \leq \tilde{x}_2 \leq \tilde{x}_1 + \tilde{z}_1 - \tilde{z}_2 - \tilde{z}_3 \\ 0 \leq \tilde{z}_4 \leq -\tilde{z}_1 + \tilde{z}_2 + \tilde{z}_3 \end{array} \right\} \cup \left\{ \begin{array}{l} -1 \leq \tilde{z}_1 \leq 0 \\ -1 \leq \tilde{z}_2 \leq \tilde{z}_1 \\ \tilde{z}_1 - \tilde{z}_2 \leq \tilde{z}_3 \leq -\tilde{z}_2 + \tilde{z}_4 + \tilde{z}_1 \\ -\tilde{z}_1 + \tilde{z}_3 \leq \tilde{x}_1 \leq 1 \\ -\tilde{z}_2 \leq \tilde{x}_2 \leq \tilde{x}_1 + \tilde{z}_1 - \tilde{z}_2 - \tilde{z}_3 \\ 0 \leq \tilde{z}_4 \leq \tilde{x}_1 - \tilde{x}_2 \end{array} \right\}.$$

This implies for the first sub-domain,

$$0 \leq -\tilde{z}_1 \leq -\tilde{z}_2 \leq -\tilde{z}_2 + \tilde{z}_4 \leq -\tilde{z}_1 + \tilde{z}_3 \leq \tilde{x}_1 - \tilde{x}_2 - \tilde{z}_2 \leq \tilde{x}_1 \leq 1,$$

and for the second one,

$$0 \leq -\tilde{z}_1 \leq -\tilde{z}_2 \leq -\tilde{z}_1 + \tilde{z}_3 \leq -\tilde{z}_2 + \tilde{z}_4 \leq \tilde{x}_1 - \tilde{x}_2 - \tilde{z}_2 \leq \tilde{x}_1 \leq 1,$$

Therefore, we now have for each sub-domain a suitable inequality chain and we can present for each domain a matching set of variables $\omega \in \mathbb{R}^6$:

$$\omega_1 := \tilde{x}_1, \omega_2 := \tilde{x}_1 - \tilde{x}_2 - \tilde{z}_2, \omega_3 := -\tilde{z}_1 + \tilde{z}_3, \omega_4 := -\tilde{z}_2 + \tilde{z}_4, \omega_5 := -\tilde{z}_2, \omega_6 := -\tilde{z}_1,$$

A. Appendix: Duffy Transformation

$$\int_0^1 \int_0^{\omega_1} \int_0^{\omega_2} \int_0^{\omega_3} \int_0^{\omega_4} \int_0^{\omega_5} \tilde{k}_1 \left(\begin{bmatrix} 1 - \omega_1 \\ \omega_1 - \omega_2 + \omega_5 \\ \omega_4 - \omega_5 \end{bmatrix}, \begin{bmatrix} 1 - \omega_1 + \omega_6 \\ \omega_1 - \omega_2 \\ \omega_3 - \omega_6 \end{bmatrix} \right) d\omega$$

and

$$\omega_1 := \tilde{x}_1, \omega_2 := \tilde{x}_1 - \tilde{x}_2 - \tilde{z}_2, \omega_3 := -\tilde{z}_2 + \tilde{z}_4, \omega_4 := -\tilde{z}_1 + \tilde{z}_3, \omega_5 := -\tilde{z}_2, \omega_6 := -\tilde{z}_1,$$

$$\int_0^1 \int_0^{\omega_1} \int_0^{\omega_2} \int_0^{\omega_3} \int_0^{\omega_4} \int_0^{\omega_5} \tilde{k}_1 \left(\begin{bmatrix} 1 - \omega_1 \\ \omega_1 - \omega_2 + \omega_5 \\ \omega_3 - \omega_5 \end{bmatrix}, \begin{bmatrix} 1 - \omega_1 + \omega_6 \\ \omega_1 - \omega_2 \\ \omega_4 - \omega_6 \end{bmatrix} \right) d\omega.$$

Sub-domain D_3 First we take a look at the inequality chain corresponding to D_3 :

$$\begin{aligned} 0 &\leq -\tilde{z}_2 \leq -\tilde{z}_1 \leq -\tilde{z}_1 + \tilde{z}_3 \leq \tilde{x}_1 - \tilde{x}_2 - \tilde{z}_2 \leq \tilde{x}_1 \leq 1, \\ 0 &\leq -\tilde{z}_2 \leq -\tilde{z}_2 + \tilde{z}_4 \leq \tilde{x}_1 - \tilde{x}_2 - \tilde{z}_2 \leq \tilde{x}_1 \leq 1. \end{aligned}$$

Since the chain splits one link too early, again, we have to subdivide D_3 :

$$D_3 = \left\{ \begin{array}{l} -1 \leq \tilde{z}_1 \leq 0 \\ \tilde{z}_1 \leq \tilde{z}_2 \leq 0 \\ 0 \leq \tilde{z}_3 \leq 1 + \tilde{z}_1 \\ -\tilde{z}_1 + \tilde{z}_3 \leq \tilde{x}_1 \leq 1 \\ -\tilde{z}_2 \leq \tilde{x}_2 \leq \tilde{x}_1 + \tilde{z}_1 - \tilde{z}_2 - \tilde{z}_3 \\ 0 \leq \tilde{z}_4 \leq -\tilde{z}_1 + \tilde{z}_2 + \tilde{z}_3 \end{array} \right\} \cup \left\{ \begin{array}{l} -1 \leq \tilde{z}_1 \leq 0 \\ \tilde{z}_1 \leq \tilde{z}_2 \leq 0 \\ 0 \leq \tilde{z}_3 \leq \tilde{z}_1 - \tilde{z}_2 + \tilde{z}_4 \\ -\tilde{z}_1 + \tilde{z}_3 \leq \tilde{x}_1 \leq 1 \\ -\tilde{z}_2 \leq \tilde{x}_2 \leq \tilde{x}_1 + \tilde{z}_1 - \tilde{z}_2 - \tilde{z}_3 \\ 0 \leq \tilde{z}_4 \leq \tilde{x}_1 - \tilde{x}_2 \end{array} \right\}$$

The interesting point here is that the first sub-domain satisfies a forking inequality chain, which is not suitable for our approach:

$$\begin{aligned} 0 &\leq -\tilde{z}_2 \leq -\tilde{z}_1 \leq -\tilde{z}_1 + \tilde{z}_3 \leq \tilde{x}_1 - \tilde{x}_2 - \tilde{z}_2 \leq \tilde{x}_1 \leq 1, \\ 0 &\leq -\tilde{z}_2 \leq -\tilde{z}_2 + \tilde{z}_4 \leq -\tilde{z}_1 + \tilde{z}_3 \leq \tilde{x}_1 - \tilde{x}_2 - \tilde{z}_2 \leq \tilde{x}_1 \leq 1. \end{aligned}$$

Although the inequality chain now splits at the appropriate link, the resulting chains are not independent of each other, because both end on \tilde{z}_2 . In order to resolve this an additional split up is necessary:

$$\left\{ \begin{array}{l} -1 \leq \tilde{z}_1 \leq 0 \\ \tilde{z}_1 \leq \tilde{z}_2 \leq 0 \\ 0 \leq \tilde{z}_3 \leq 1 + \tilde{z}_1 \\ -\tilde{z}_1 + \tilde{z}_3 \leq \tilde{x}_1 \leq 1 \\ -\tilde{z}_2 \leq \tilde{x}_2 \leq \tilde{x}_1 + \tilde{z}_1 - \tilde{z}_2 - \tilde{z}_3 \\ 0 \leq \tilde{z}_4 \leq -\tilde{z}_1 + \tilde{z}_2 \end{array} \right\} \cup \left\{ \begin{array}{l} \tilde{z}_2 - \tilde{z}_4 \leq \tilde{z}_1 \leq 0 \\ \tilde{z}_1 \leq \tilde{z}_2 \leq 0 \\ 0 \leq \tilde{z}_3 \leq \tilde{z}_1 - \tilde{z}_2 + \tilde{z}_4 \\ -\tilde{z}_1 + \tilde{z}_3 \leq \tilde{x}_1 \leq 1 \\ -\tilde{z}_2 \leq \tilde{x}_2 \leq \tilde{x}_1 + \tilde{z}_1 - \tilde{z}_2 - \tilde{z}_3 \\ 0 \leq \tilde{z}_4 \leq \tilde{x}_1 - \tilde{x}_2 \end{array} \right\}$$

Then we can introduce for each sub-domain a new set of variables $\omega \in \mathbb{R}^6$:

$$\omega_1 := \tilde{x}_1, \omega_2 := \tilde{x}_1 - \tilde{x}_2 - \tilde{z}_2, \omega_3 := -\tilde{z}_1 + \tilde{z}_3, \omega_4 := -\tilde{z}_1, \omega_5 := -\tilde{z}_2 + \tilde{z}_4, \omega_6 := -\tilde{z}_2,$$

A. Appendix: Duffy Transformation

$$\int_0^1 \int_0^{\omega_1} \int_0^{\omega_2} \int_0^{\omega_3} \int_0^{\omega_4} \int_0^{\omega_5} \tilde{k}_1 \left(\begin{bmatrix} 1 - \omega_1 \\ \omega_1 - \omega_2 + \omega_6 \\ \omega_5 - \omega_6 \end{bmatrix}, \begin{bmatrix} 1 - \omega_1 + \omega_4 \\ \omega_1 - \omega_2 \\ \omega_3 - \omega_4 \end{bmatrix} \right) d\omega$$

$$\omega_1 := \tilde{x}_1, \omega_2 := \tilde{x}_1 - \tilde{x}_2 - \tilde{z}_2, \omega_3 := -\tilde{z}_1 + \tilde{z}_3, \omega_4 := -\tilde{z}_1, \omega_5 := -\tilde{z}_2 + \tilde{z}_4, \omega_6 := -\tilde{z}_2,$$

$$\int_0^1 \int_0^{\omega_1} \int_0^{\omega_2} \int_0^{\omega_3} \int_0^{\omega_4} \int_0^{\omega_5} \tilde{k}_1 \left(\begin{bmatrix} 1 - \omega_1 \\ \omega_1 - \omega_2 + \omega_6 \\ \omega_4 - \omega_6 \end{bmatrix}, \begin{bmatrix} 1 - \omega_1 + \omega_5 \\ \omega_1 - \omega_2 \\ \omega_3 - \omega_5 \end{bmatrix} \right) d\omega$$

$$\omega_1 := \tilde{x}_1, \omega_2 := \tilde{x}_1 - \tilde{x}_2 - \tilde{z}_2, \omega_3 := \tilde{z}_4 - \tilde{z}_2, \omega_4 := \tilde{z}_3 - \tilde{z}_1, \omega_5 := -\tilde{z}_1, \omega_6 := -\tilde{z}_2,$$

$$\int_0^1 \int_0^{\omega_1} \int_0^{\omega_2} \int_0^{\omega_3} \int_0^{\omega_4} \int_0^{\omega_5} \tilde{k}_1 \left(\begin{bmatrix} 1 - \omega_1 \\ \omega_1 - \omega_2 + \omega_6 \\ \omega_3 - \omega_6 \end{bmatrix}, \begin{bmatrix} 1 - \omega_1 + \omega_5 \\ \omega_1 - \omega_2 \\ \omega_4 - \omega_5 \end{bmatrix} \right) d\omega$$

Sub-domain D_4 For the fourth domain we get a forking inequality chain,

$$\begin{aligned} 0 &\leq -\tilde{z}_1 \leq -\tilde{z}_1 + \tilde{z}_2 \leq -\tilde{z}_1 + \tilde{z}_2 + \tilde{z}_3 \leq \tilde{x}_1 - \tilde{x}_2 \leq \tilde{x}_1 \leq 1, \\ 0 &\leq \tilde{z}_4 \leq \tilde{x}_1 - \tilde{x}_2 \leq \tilde{x}_1 \leq 1, \end{aligned}$$

which splits up one link too early. Therefore, D_4 is subdivided:

$$D_4 = \left\{ \begin{array}{l} -1 \leq \tilde{z}_1 \leq 0 \\ 0 \leq \tilde{z}_2 \leq 1 + \tilde{z}_1 \\ 0 \leq \tilde{z}_3 \leq 1 + \tilde{z}_1 - \tilde{z}_2 \\ \tilde{z}_2 - \tilde{z}_1 + \tilde{z}_3 \leq \tilde{x}_1 \leq 1 \\ 0 \leq \tilde{x}_2 \leq \tilde{x}_1 + \tilde{z}_1 - \tilde{z}_2 - \tilde{z}_3 \\ 0 \leq \tilde{z}_4 \leq -\tilde{z}_1 + \tilde{z}_2 + \tilde{z}_3 \end{array} \right\} \cup \left\{ \begin{array}{l} -1 \leq \tilde{z}_1 \leq 0 \\ 0 \leq \tilde{z}_2 \leq 1 + \tilde{z}_1 \\ 0 \leq \tilde{z}_3 \leq \tilde{z}_1 - \tilde{z}_2 + \tilde{z}_4 \\ \tilde{z}_2 - \tilde{z}_1 + \tilde{z}_3 \leq \tilde{x}_1 \leq 1 \\ 0 \leq \tilde{x}_2 \leq \tilde{x}_1 + \tilde{z}_1 - \tilde{z}_2 - \tilde{z}_3 \\ 0 \leq \tilde{z}_4 \leq \tilde{x}_1 - \tilde{x}_2 \end{array} \right\}.$$

Then a new set of variables $\omega \in \mathbb{R}^6$ is established to represent this structure:

$$\omega_1 := \tilde{x}_1, \omega_2 := \tilde{x}_1 - \tilde{x}_2, \omega_3 := -\tilde{z}_1 + \tilde{z}_2 + \tilde{z}_3, \omega_4 := -\tilde{z}_1 + \tilde{z}_2, \omega_5 := \tilde{z}_2, \omega_6 := \tilde{z}_4,$$

$$\int_0^1 \int_0^{\omega_1} \int_0^{\omega_2} \int_0^{\omega_3} \int_0^{\omega_4} \int_0^{\omega_5} \tilde{k}_1 \left(\begin{bmatrix} 1 - \omega_1 \\ \omega_1 - \omega_2 \\ \omega_6 \end{bmatrix}, \begin{bmatrix} 1 - \omega_1 + \omega_5 \\ \omega_1 - \omega_2 + \omega_4 - \omega_5 \\ \omega_3 - \omega_4 \end{bmatrix} \right) d\omega$$

$$\omega_1 := \tilde{x}_1, \omega_2 := \tilde{x}_1 - \tilde{x}_2, \omega_3 := \tilde{z}_4, \omega_4 := -\tilde{z}_1 + \tilde{z}_2 + \tilde{z}_3, \omega_5 := -\tilde{z}_1 + \tilde{z}_2, \omega_6 := -\tilde{z}_1,$$

$$\int_0^1 \int_0^{\omega_1} \int_0^{\omega_2} \int_0^{\omega_3} \int_0^{\omega_4} \int_0^{\omega_5} \tilde{k}_1 \left(\begin{bmatrix} 1 - \omega_1 \\ \omega_1 - \omega_2 \\ \omega_3 \end{bmatrix}, \begin{bmatrix} 1 - \omega_1 + \omega_6 \\ \omega_1 - \omega_2 + \omega_5 - \omega_6 \\ \omega_4 - \omega_5 \end{bmatrix} \right) d\omega$$

A. Appendix: Duffy Transformation

Sub-domain D_5 At first glance D_5 is a little special, because the forking inequality chain behaves differently,

$$\begin{aligned} 0 &\leq \tilde{z}_1 \leq \tilde{z}_1 - \tilde{z}_2 \leq \tilde{x}_1 - \tilde{x}_2 + \tilde{z}_4 \leq \tilde{x}_1 - \tilde{x}_2 + \tilde{z}_1 - \tilde{z}_2 \leq \tilde{x}_1 + \tilde{z}_1 \leq 1, \\ 0 &\leq \tilde{z}_3 \leq \tilde{z}_1 - \tilde{z}_2 \leq \tilde{x}_1 - \tilde{x}_2 + \tilde{z}_4 \leq \tilde{x}_1 - \tilde{x}_2 + \tilde{z}_1 - \tilde{z}_2 \leq \tilde{x}_1 + \tilde{z}_1 \leq 1. \end{aligned}$$

The forking happens one link further as necessary. As we have seen in Lemma 8, this is not a problem. Therefore, D_5 does not need to be further refined and the procedure can be continued:

$$\omega_1 := \tilde{x}_1 + \tilde{z}_1, \omega_2 := \tilde{x}_1 - \tilde{x}_2 + \tilde{z}_1 - \tilde{z}_2, \omega_3 := \tilde{x}_1 - \tilde{x}_2 + \tilde{z}_4, \omega_4 := \tilde{z}_1 - \tilde{z}_2, \omega_5 := \tilde{z}_1, \omega_6 := \tilde{z}_3,$$

$$\int_0^1 \int_0^{\omega_1} \int_0^{\omega_2} \int_0^{\omega_3} \int_0^{\omega_4} \int_0^{\omega_5} \tilde{k}_1 \left(\begin{bmatrix} 1 - \omega_1 + \omega_5 \\ \omega_1 - \omega_2 + \omega_4 - \omega_5 \\ \omega_3 - \omega_4 \end{bmatrix}, \begin{bmatrix} 1 - \omega_1 \\ \omega_1 - \omega_2 \\ \omega_6 \end{bmatrix} \right) d\omega$$

Sub-domain D_6 As we can see,

$$\begin{aligned} 0 &\leq \tilde{z}_1 \leq \tilde{z}_1 - \tilde{z}_2 \leq \tilde{z}_3 \leq \tilde{x}_1 - \tilde{x}_2 + \tilde{z}_1 - \tilde{z}_2 \leq \tilde{x}_1 + \tilde{z}_1 \leq 1, \\ 0 &\leq \tilde{z}_1 \leq \tilde{z}_1 - \tilde{z}_2 \leq \tilde{z}_1 - \tilde{z}_2 + \tilde{z}_4 \leq \tilde{x}_1 - \tilde{x}_2 + \tilde{z}_1 - \tilde{z}_2 \leq \tilde{x}_1 + \tilde{z}_1 \leq 1, \end{aligned}$$

D_6 has to be divided up in order to satisfy a matching forking inequality chain:

$$D_6 := \left\{ \begin{array}{l} 0 \leq \tilde{z}_1 \leq 1 \\ -1 + \tilde{z}_1 \leq \tilde{z}_2 \leq 0 \\ \tilde{z}_1 - \tilde{z}_2 \leq \tilde{z}_3 \leq 1 \\ -\tilde{z}_1 + \tilde{z}_3 \leq \tilde{x}_1 \leq 1 - \tilde{z}_1 \\ -\tilde{z}_2 \leq \tilde{x}_2 \leq \tilde{x}_1 + \tilde{z}_1 - \tilde{z}_2 - \tilde{z}_3 \\ 0 \leq \tilde{z}_4 \leq -\tilde{z}_1 + \tilde{z}_2 + \tilde{z}_3 \end{array} \right\} \cup \left\{ \begin{array}{l} 0 \leq \tilde{z}_1 \leq 1 \\ -1 + \tilde{z}_1 \leq \tilde{z}_2 \leq 0 \\ \tilde{z}_1 - \tilde{z}_2 \leq \tilde{z}_3 \leq \tilde{z}_1 - \tilde{z}_2 + \tilde{z}_4 \\ -\tilde{z}_1 + \tilde{z}_3 \leq \tilde{x}_1 \leq 1 - \tilde{z}_1 \\ -\tilde{z}_2 \leq \tilde{x}_2 \leq \tilde{x}_1 + \tilde{z}_1 - \tilde{z}_2 - \tilde{z}_3 \\ 0 \leq \tilde{z}_4 \leq \tilde{x}_1 - \tilde{x}_2 \end{array} \right\}.$$

According to the inequality chains, a new set of variables $\omega \in \mathbb{R}^6$ is introduced for each sub-domain:

$$\omega_1 := \tilde{x}_1 + \tilde{z}_1, \omega_2 := \tilde{x}_1 - \tilde{x}_2 + \tilde{z}_1 - \tilde{z}_2, \omega_3 := \tilde{z}_3, \omega_4 := \tilde{z}_1 - \tilde{z}_2 + \tilde{z}_4, \omega_5 := \tilde{z}_1 - \tilde{z}_2, \omega_6 := \tilde{z}_1,$$

$$\int_0^1 \int_0^{\omega_1} \int_0^{\omega_2} \int_0^{\omega_3} \int_0^{\omega_4} \int_0^{\omega_5} \tilde{k}_1 \left(\begin{bmatrix} 1 - \omega_1 + \omega_6 \\ \omega_1 - \omega_2 + \omega_5 - \omega_6 \\ \omega_4 - \omega_5 \end{bmatrix}, \begin{bmatrix} 1 - \omega_1 \\ \omega_1 - \omega_2 \\ \omega_3 \end{bmatrix} \right) d\omega,$$

$$\omega_1 := \tilde{x}_1 + \tilde{z}_1, \omega_2 := \tilde{x}_1 - \tilde{x}_2 + \tilde{z}_1 - \tilde{z}_2, \omega_3 := \tilde{z}_1 - \tilde{z}_2 + \tilde{z}_4, \omega_4 := \tilde{z}_3, \omega_5 := \tilde{z}_1 - \tilde{z}_2, \omega_6 := \tilde{z}_1,$$

$$\int_0^1 \int_0^{\omega_1} \int_0^{\omega_2} \int_0^{\omega_3} \int_0^{\omega_4} \int_0^{\omega_5} \tilde{k}_1 \left(\begin{bmatrix} 1 - \omega_1 + \omega_6 \\ \omega_1 - \omega_2 + \omega_5 - \omega_6 \\ \omega_3 - \omega_5 \end{bmatrix}, \begin{bmatrix} 1 - \omega_1 \\ \omega_1 - \omega_2 \\ \omega_4 \end{bmatrix} \right) d\omega.$$

A. Appendix: Duffy Transformation

Sub-domain D_7 For D_7 we do not have to do anything, because a matching inequality chain already exists,

$$0 \leq \tilde{z}_2 \leq \tilde{z}_2 + \tilde{z}_3 \leq \tilde{z}_1 \leq \tilde{z}_4 + \tilde{z}_1 \leq \tilde{x}_1 - \tilde{x}_2 + \tilde{z}_1 \leq \tilde{x}_1 + \tilde{z}_1 \leq 1.$$

Thus a matching set of variables $\omega \in \mathbb{R}^6$ can already be presented:

$$\omega_1 := \tilde{x}_1 + \tilde{z}_1, \omega_2 := \tilde{x}_1 - \tilde{x}_2 + \tilde{z}_1, \omega_3 := \tilde{z}_1 + \tilde{z}_4, \omega_4 := \tilde{z}_1, \omega_5 := \tilde{z}_2 + \tilde{z}_3, \omega_6 := \tilde{z}_2,$$

$$\int_0^1 \int_0^{\omega_1} \int_0^{\omega_2} \int_0^{\omega_3} \int_0^{\omega_4} \int_0^{\omega_5} \tilde{k}_1 \left(\begin{bmatrix} 1 - \omega_1 + \omega_4 \\ \omega_1 - \omega_2 \\ \omega_3 - \omega_4 \end{bmatrix}, \begin{bmatrix} 1 - \omega_1 \\ \omega_1 - \omega_2 + \omega_6 \\ \omega_5 - \omega_6 \end{bmatrix} \right) d\omega.$$

Sub-domain D_8 Next we consider D_8 ,

$$0 \leq \tilde{z}_2 \leq \tilde{z}_1 \leq \tilde{z}_2 + \tilde{z}_3 \leq \tilde{x}_1 - \tilde{x}_2 + \tilde{z}_1 \leq \tilde{x}_1 + \tilde{z}_1 \leq 1,$$

$$0 \leq \tilde{z}_2 \leq \tilde{z}_1 \leq \tilde{z}_1 + \tilde{z}_4 \leq \tilde{x}_1 - \tilde{x}_2 + \tilde{z}_1 \leq \tilde{x}_1 + \tilde{z}_1 \leq 1,$$

where again a split up is needed:

$$D_8 = \left\{ \begin{array}{l} 0 \leq \tilde{z}_1 \leq 1 \\ 0 \leq \tilde{z}_2 \leq \tilde{z}_1 \\ \tilde{z}_1 - \tilde{z}_2 \leq \tilde{z}_3 \leq 1 - \tilde{z}_2 \\ -\tilde{z}_1 + \tilde{z}_2 + \tilde{z}_3 \leq \tilde{x}_1 \leq 1 - \tilde{z}_1 \\ 0 \leq \tilde{x}_2 \leq \tilde{x}_1 + \tilde{z}_1 - \tilde{z}_2 - \tilde{z}_3 \\ 0 \leq \tilde{z}_4 \leq -\tilde{z}_1 + \tilde{z}_2 + \tilde{z}_3 \end{array} \right\} \cup \left\{ \begin{array}{l} 0 \leq \tilde{z}_1 \leq 1 \\ 0 \leq \tilde{z}_2 \leq \tilde{z}_1 \\ \tilde{z}_1 - \tilde{z}_2 \leq \tilde{z}_3 \leq \tilde{z}_1 - \tilde{z}_2 + \tilde{z}_4 \\ -\tilde{z}_1 + \tilde{z}_2 + \tilde{z}_3 \leq \tilde{x}_1 \leq 1 - \tilde{z}_1 \\ 0 \leq \tilde{x}_2 \leq \tilde{x}_1 + \tilde{z}_1 - \tilde{z}_2 - \tilde{z}_3 \\ 0 \leq \tilde{z}_4 \leq \tilde{x}_1 - \tilde{x}_2 \end{array} \right\}.$$

Then we introduce the new set of variables matching the forking inequality chains:

$$\omega_1 := \tilde{x}_1 + \tilde{z}_1, \omega_2 := \tilde{x}_1 - \tilde{x}_2 + \tilde{z}_1, \omega_3 := \tilde{z}_2 + \tilde{z}_3, \omega_4 := \tilde{z}_1 + \tilde{z}_4, \omega_5 := \tilde{z}_1, \omega_6 := \tilde{z}_2,$$

$$\int_0^1 \int_0^{\omega_1} \int_0^{\omega_2} \int_0^{\omega_3} \int_0^{\omega_4} \int_0^{\omega_5} \tilde{k}_1 \left(\begin{bmatrix} 1 - \omega_1 + \omega_5 \\ \omega_1 - \omega_2 \\ \omega_4 - \omega_5 \end{bmatrix}, \begin{bmatrix} 1 - \omega_1 \\ \omega_1 - \omega_2 + \omega_6 \\ \omega_3 - \omega_6 \end{bmatrix} \right) d\omega$$

$$\omega_1 := \tilde{x}_1 + \tilde{z}_1, \omega_2 := \tilde{x}_1 - \tilde{x}_2 + \tilde{z}_1, \omega_3 := \tilde{z}_1 + \tilde{z}_4, \omega_4 := \tilde{z}_2 + \tilde{z}_3, \omega_5 := \tilde{z}_1, \omega_6 := \tilde{z}_2,$$

$$\int_0^1 \int_0^{\omega_1} \int_0^{\omega_2} \int_0^{\omega_3} \int_0^{\omega_4} \int_0^{\omega_5} \tilde{k}_1 \left(\begin{bmatrix} 1 - \omega_1 + \omega_5 \\ \omega_1 - \omega_2 \\ \omega_3 - \omega_5 \end{bmatrix}, \begin{bmatrix} 1 - \omega_1 \\ \omega_1 - \omega_2 + \omega_6 \\ \omega_4 - \omega_6 \end{bmatrix} \right) d\omega$$

Sub-domain D_9 The treatment of the last sub-domain is analogous to the treatment of D_3 . As we can see,

$$0 \leq \tilde{z}_1 \leq \tilde{z}_2 \leq \tilde{z}_2 + \tilde{z}_3 \leq \tilde{x}_1 - \tilde{x}_2 + \tilde{z}_1 \leq \tilde{x}_1 + \tilde{z}_1 \leq 1,$$

$$0 \leq \tilde{z}_1 \leq \tilde{z}_4 + \tilde{z}_1 \leq \tilde{x}_1 - \tilde{x}_2 + \tilde{z}_1 \leq \tilde{x}_1 + \tilde{z}_1 \leq 1,$$

A. Appendix: Duffy Transformation

there are two problems concerning the forking inequality chain. First, the chain splits up one link to early and second, both chains are not independent of each other after the split up. To solve this issue, D_9 is divided up in two steps:

$$\left\{ \begin{array}{l} 0 \leq \tilde{z}_1 \leq 1 \\ \tilde{z}_1 \leq \tilde{z}_2 \leq 1 \\ 0 \leq \tilde{z}_3 \leq 1 - \tilde{z}_2 \\ \tilde{z}_2 - \tilde{z}_1 + \tilde{z}_3 \leq \tilde{x}_1 \leq 1 - \tilde{z}_1 \\ 0 \leq \tilde{x}_2 \leq \tilde{x}_1 + \tilde{z}_1 - \tilde{z}_2 - \tilde{z}_3 \\ 0 \leq \tilde{z}_4 \leq -\tilde{z}_1 + \tilde{z}_2 + \tilde{z}_3 \end{array} \right\} \cup \left\{ \begin{array}{l} 0 \leq \tilde{z}_1 \leq 1 \\ \tilde{z}_1 \leq \tilde{z}_2 \leq 1 \\ 0 \leq \tilde{z}_3 \leq \tilde{z}_1 + \tilde{z}_4 - \tilde{z}_2 \\ \tilde{z}_2 - \tilde{z}_1 + \tilde{z}_3 \leq \tilde{x}_1 \leq 1 - \tilde{z}_1 \\ 0 \leq \tilde{x}_2 \leq \tilde{x}_1 + \tilde{z}_1 - \tilde{z}_2 - \tilde{z}_3 \\ 0 \leq \tilde{z}_4 \leq \tilde{x}_1 - \tilde{x}_2 \end{array} \right\}.$$

And then the first resulting sub-domain is split up again:

$$\left\{ \begin{array}{l} 0 \leq \tilde{z}_1 \leq 1 \\ \tilde{z}_1 \leq \tilde{z}_2 \leq 1 \\ 0 \leq \tilde{z}_3 \leq 1 - \tilde{z}_2 \\ \tilde{z}_2 - \tilde{z}_1 + \tilde{z}_3 \leq \tilde{x}_1 \leq 1 - \tilde{z}_1 \\ 0 \leq \tilde{x}_2 \leq \tilde{x}_1 + \tilde{z}_1 - \tilde{z}_2 - \tilde{z}_3 \\ 0 \leq \tilde{z}_4 \leq -\tilde{z}_1 + \tilde{z}_2 \end{array} \right\} \cup \left\{ \begin{array}{l} 0 \leq \tilde{z}_1 \leq 1 \\ \tilde{z}_1 \leq \tilde{z}_2 \leq \tilde{z}_1 + \tilde{z}_4 \\ 0 \leq \tilde{z}_3 \leq 1 - \tilde{z}_2 \\ \tilde{z}_2 - \tilde{z}_1 + \tilde{z}_3 \leq \tilde{x}_1 \leq 1 - \tilde{z}_1 \\ 0 \leq \tilde{x}_2 \leq \tilde{x}_1 + \tilde{z}_1 - \tilde{z}_2 - \tilde{z}_3 \\ 0 \leq \tilde{z}_4 \leq -\tilde{z}_1 + \tilde{z}_2 + \tilde{z}_3 \end{array} \right\}.$$

For each of these three domains we establish a new set of variables $\omega \in \mathbb{R}^6$ according to the forking inequality chains:

$$\omega_1 := \tilde{x}_1 + \tilde{z}_1, \omega_2 := \tilde{x}_1 - \tilde{x}_2 + \tilde{z}_1, \omega_3 := \tilde{z}_2 + \tilde{z}_3, \omega_4 := \tilde{z}_2, \omega_5 := \tilde{z}_1 + \tilde{z}_4, \omega_6 := \tilde{z}_1,$$

$$\int_0^1 \int_0^{\omega_1} \int_0^{\omega_2} \int_0^{\omega_3} \int_0^{\omega_4} \int_0^{\omega_5} \tilde{k}_1 \left(\begin{bmatrix} 1 - \omega_1 + \omega_6 \\ \omega_1 - \omega_2 \\ \omega_5 - \omega_6 \end{bmatrix}, \begin{bmatrix} 1 - \omega_1 \\ \omega_1 - \omega_2 + \omega_4 \\ \omega_3 - \omega_4 \end{bmatrix} \right) d\omega,$$

$$\omega_1 := \tilde{x}_1 + \tilde{z}_1, \omega_2 := \tilde{x}_1 - \tilde{x}_2 + \tilde{z}_1, \omega_3 := \tilde{z}_2 + \tilde{z}_3, \omega_4 := \tilde{z}_1 + \tilde{z}_4, \omega_5 := \tilde{z}_2, \omega_6 := \tilde{z}_1,$$

$$\int_0^1 \int_0^{\omega_1} \int_0^{\omega_2} \int_0^{\omega_3} \int_0^{\omega_4} \int_0^{\omega_5} \tilde{k}_1 \left(\begin{bmatrix} 1 - \omega_1 + \omega_6 \\ \omega_1 - \omega_2 \\ \omega_4 - \omega_6 \end{bmatrix}, \begin{bmatrix} 1 - \omega_1 \\ \omega_1 - \omega_2 + \omega_5 \\ \omega_3 - \omega_5 \end{bmatrix} \right) d\omega,$$

$$\omega_1 := \tilde{x}_1 + \tilde{z}_1, \omega_2 := \tilde{x}_1 - \tilde{x}_2 + \tilde{z}_1, \omega_3 := \tilde{z}_1 + \tilde{z}_4, \omega_4 := \tilde{z}_2 + \tilde{z}_3, \omega_5 := \tilde{z}_1, \omega_6 := \tilde{z}_2,$$

$$\int_0^1 \int_0^{\omega_1} \int_0^{\omega_2} \int_0^{\omega_3} \int_0^{\omega_4} \int_0^{\omega_5} \tilde{k}_1 \left(\begin{bmatrix} 1 - \omega_1 + \omega_6 \\ \omega_1 - \omega_2 \\ \omega_3 - \omega_6 \end{bmatrix}, \begin{bmatrix} 1 - \omega_1 \\ \omega_1 - \omega_2 + \omega_5 \\ \omega_4 - \omega_5 \end{bmatrix} \right) d\omega,$$

A.1.2. Two identical tetrahedra

Next, we consider the singularity case that the two tetrahedra are identical.

A.1.2.1. Derivation of the integration domains

As in the case of a singularity along one side, also in the case that the two tetrahedra are identical, a set described by min and max conditions arises by swapping the integration order, see Section 3.2.4:

$$D := \left\{ \begin{array}{l} -1 \leq \tilde{z}_1 \leq 1 \\ -1 + \max\{0, \tilde{z}_1\} \leq \tilde{z}_2 \leq 1 + \min\{0, \tilde{z}_1\} \\ -1 + \max\{0, \tilde{z}_1\} + \max\{0, -\tilde{z}_2\} \leq \tilde{z}_3 \leq 1 + \min\{0, \tilde{z}_1\} + \min\{0, -\tilde{z}_2\} \\ \max\{0, -\tilde{z}_1, -\tilde{z}_2, -\tilde{z}_3, \\ -\tilde{z}_2 - \tilde{z}_3, \tilde{z}_2 - \tilde{z}_1, -\tilde{z}_1 + \tilde{z}_3, \tilde{z}_2 - \tilde{z}_1 + \tilde{z}_3\} \leq \tilde{x}_1 \leq 1 + \min\{0, -\tilde{z}_1\} \\ \max\{0, -\tilde{z}_2\} \leq \tilde{x}_2 \leq \tilde{x}_1 + \min\{0, \tilde{z}_1 - \tilde{z}_2, \tilde{z}_1 - \tilde{z}_2 - \tilde{z}_3\} \\ \max\{0, -\tilde{z}_3\} \leq \tilde{x}_3 \leq \tilde{x}_1 - \tilde{x}_2 + \min\{0, \tilde{z}_1 - \tilde{z}_2 - \tilde{z}_3\} \end{array} \right\}.$$

The first step here is to resolve the min and max conditions. The ideas are the same is in Appendix A.1.1. Starting with

$$-1 \leq \tilde{z}_1 \leq 0 \quad \text{and} \quad -1 \leq \tilde{z}_2 \leq \tilde{z}_1,$$

the condition on \tilde{z}_3 has to be divided into three parts to server the min and max conditions:

$$D_1 := \left\{ \begin{array}{l} -1 \leq \tilde{z}_1 \leq 0 \\ -1 \leq \tilde{z}_2 \leq \tilde{z}_1 \\ -1 - \tilde{z}_2 \leq \tilde{z}_3 \leq 0 \\ -\tilde{z}_2 - \tilde{z}_3 \leq \tilde{x}_1 \leq 1 \\ -\tilde{z}_2 \leq \tilde{x}_2 \leq \tilde{x}_1 \\ -\tilde{z}_3 \leq \tilde{x}_3 \leq \tilde{x}_1 - \tilde{x}_2 \end{array} \right\}, \quad D_2 := \left\{ \begin{array}{l} -1 \leq \tilde{z}_1 \leq 0 \\ -1 \leq \tilde{z}_2 \leq \tilde{z}_1 \\ 0 \leq \tilde{z}_3 \leq \tilde{z}_1 - \tilde{z}_2 \\ -\tilde{z}_2 \leq \tilde{x}_1 \leq 1 \\ -\tilde{z}_2 \leq \tilde{x}_2 \leq \tilde{x}_1 \\ 0 \leq \tilde{x}_3 \leq \tilde{x}_1 - \tilde{x}_2 \end{array} \right\},$$

$$\text{and} \quad D_3 := \left\{ \begin{array}{l} -1 \leq \tilde{z}_1 \leq 0 \\ -1 \leq \tilde{z}_2 \leq \tilde{z}_1 \\ \tilde{z}_1 - \tilde{z}_2 \leq \tilde{z}_3 \leq 1 + \tilde{z}_1 \\ -\tilde{z}_1 + \tilde{z}_3 \leq \tilde{x}_1 \leq 1 \\ -\tilde{z}_2 \leq \tilde{x}_2 \leq \tilde{x}_1 + \tilde{z}_1 - \tilde{z}_2 - \tilde{z}_3 \\ 0 \leq \tilde{x}_3 \leq \tilde{x}_1 - \tilde{x}_2 + \tilde{z}_1 - \tilde{z}_2 - \tilde{z}_3 \end{array} \right\}.$$

The next case being studied is $\tilde{z}_1 \leq \tilde{z}_2 \leq 0$. Here, three split ups are needed to get sub-domains with a feasible representation:

$$D_4 := \left\{ \begin{array}{l} -1 \leq \tilde{z}_1 \leq 0 \\ \tilde{z}_1 \leq \tilde{z}_2 \leq 0 \\ -1 - \tilde{z}_2 \leq \tilde{z}_3 \leq \tilde{z}_1 - \tilde{z}_2 \\ -\tilde{z}_2 - \tilde{z}_3 \leq \tilde{x}_1 \leq 1 \\ -\tilde{z}_2 \leq \tilde{x}_2 \leq \tilde{x}_1 + \tilde{z}_1 - \tilde{z}_2 \\ -\tilde{z}_3 \leq \tilde{x}_3 \leq \tilde{x}_1 - \tilde{x}_2 \end{array} \right\}, \quad D_5 := \left\{ \begin{array}{l} -1 \leq \tilde{z}_1 \leq 0 \\ \tilde{z}_1 \leq \tilde{z}_2 \leq 0 \\ \tilde{z}_1 - \tilde{z}_2 \leq \tilde{z}_3 \leq 0 \\ -\tilde{z}_1 \leq \tilde{x}_1 \leq 1 \\ -\tilde{z}_2 \leq \tilde{x}_2 \leq \tilde{x}_1 + \tilde{z}_1 - \tilde{z}_2 \\ -\tilde{z}_3 \leq \tilde{x}_3 \leq \tilde{x}_1 - \tilde{x}_2 + \tilde{z}_1 - \tilde{z}_2 - \tilde{z}_3 \end{array} \right\}$$

$$\text{and} \quad D_6 := \left\{ \begin{array}{l} -1 \leq \tilde{z}_1 \leq 0 \\ \tilde{z}_1 \leq \tilde{z}_2 \leq 0 \\ 0 \leq \tilde{z}_3 \leq 1 + \tilde{z}_1 \\ -\tilde{z}_1 + \tilde{z}_3 \leq \tilde{x}_1 \leq 1 \\ -\tilde{z}_2 \leq \tilde{x}_2 \leq \tilde{x}_1 + \tilde{z}_1 - \tilde{z}_2 - \tilde{z}_3 \\ 0 \leq \tilde{x}_3 \leq \tilde{x}_1 - \tilde{x}_2 + \tilde{z}_1 - \tilde{z}_2 - \tilde{z}_3 \end{array} \right\}.$$

A. Appendix: Duffy Transformation

Then we consider $0 \leq \tilde{z}_2 \leq 1 + \tilde{z}_1$ and obtain:

$$D_7 := \left\{ \begin{array}{l} -1 \leq \tilde{z}_1 \leq 0 \\ 0 \leq \tilde{z}_2 \leq 1 + \tilde{z}_1 \\ -1 \leq \tilde{z}_3 \leq \tilde{z}_1 - \tilde{z}_2 \\ -\tilde{z}_3 \leq \tilde{x}_1 \leq 1 \\ 0 \leq \tilde{x}_2 \leq \tilde{x}_1 + \tilde{z}_1 - \tilde{z}_2 \\ -\tilde{z}_3 \leq \tilde{x}_3 \leq \tilde{x}_1 - \tilde{x}_2 \end{array} \right\}, \quad D_8 := \left\{ \begin{array}{l} -1 \leq \tilde{z}_1 \leq 0 \\ 0 \leq \tilde{z}_2 \leq 1 + \tilde{z}_1 \\ \tilde{z}_1 - \tilde{z}_2 \leq \tilde{z}_3 \leq 0 \\ \tilde{z}_2 - \tilde{z}_1 \leq \tilde{x}_1 \leq 1 \\ 0 \leq \tilde{x}_2 \leq \tilde{x}_1 + \tilde{z}_1 - \tilde{z}_2 \\ -\tilde{z}_3 \leq \tilde{x}_3 \leq \tilde{x}_1 - \tilde{x}_2 + \tilde{z}_1 - \tilde{z}_2 - \tilde{z}_3 \end{array} \right\}$$

$$\text{and } D_9 := \left\{ \begin{array}{l} -1 \leq \tilde{z}_1 \leq 0 \\ 0 \leq \tilde{z}_2 \leq 1 + \tilde{z}_1 \\ 0 \leq \tilde{z}_3 \leq 1 + \tilde{z}_1 - \tilde{z}_2 \\ -\tilde{z}_1 + \tilde{z}_2 + \tilde{z}_3 \leq \tilde{x}_1 \leq 1 \\ 0 \leq \tilde{x}_2 \leq \tilde{x}_1 + \tilde{z}_1 - \tilde{z}_2 - \tilde{z}_3 \\ 0 \leq \tilde{x}_3 \leq \tilde{x}_1 - \tilde{x}_2 + \tilde{z}_1 - \tilde{z}_2 - \tilde{z}_3 \end{array} \right\}.$$

The procedure for the case $0 \leq \tilde{z}_1 \leq 1$ is analog. In total we get the same amount of domains:

$$D_{10} := \left\{ \begin{array}{l} 0 \leq \tilde{z}_1 \leq 1 \\ -1 + \tilde{z}_1 \leq \tilde{z}_2 \leq 0 \\ -1 + \tilde{z}_1 - \tilde{z}_2 \leq \tilde{z}_3 \leq 0 \\ -\tilde{z}_2 - \tilde{z}_3 \leq \tilde{x}_1 \leq 1 - \tilde{z}_1 \\ -\tilde{z}_2 \leq \tilde{x}_2 \leq \tilde{x}_1 \\ -\tilde{z}_3 \leq \tilde{x}_3 \leq \tilde{x}_1 - \tilde{x}_2 \end{array} \right\}, \quad D_{11} := \left\{ \begin{array}{l} 0 \leq \tilde{z}_1 \leq 1 \\ -1 + \tilde{z}_1 \leq \tilde{z}_2 \leq 0 \\ 0 \leq \tilde{z}_3 \leq \tilde{z}_1 - \tilde{z}_2 \\ -\tilde{z}_2 \leq \tilde{x}_1 \leq 1 - \tilde{z}_1 \\ -\tilde{z}_2 \leq \tilde{x}_2 \leq \tilde{x}_1 \\ 0 \leq \tilde{x}_3 \leq \tilde{x}_1 - \tilde{x}_2 \end{array} \right\},$$

$$D_{12} := \left\{ \begin{array}{l} 0 \leq \tilde{z}_1 \leq 1 \\ -1 + \tilde{z}_1 \leq \tilde{z}_2 \leq 0 \\ \tilde{z}_1 - \tilde{z}_2 \leq \tilde{z}_3 \leq 1 \\ -\tilde{z}_1 + \tilde{z}_3 \leq \tilde{x}_1 \leq 1 - \tilde{z}_1 \\ -\tilde{z}_2 \leq \tilde{x}_2 \leq \tilde{x}_1 + \tilde{z}_1 - \tilde{z}_2 - \tilde{z}_3 \\ 0 \leq \tilde{x}_3 \leq \tilde{x}_1 - \tilde{x}_2 + \tilde{z}_1 - \tilde{z}_2 - \tilde{z}_3 \end{array} \right\}, \quad D_{13} := \left\{ \begin{array}{l} 0 \leq \tilde{z}_1 \leq 1 \\ 0 \leq \tilde{z}_2 \leq \tilde{z}_1 \\ -1 + \tilde{z}_1 \leq \tilde{z}_3 \leq 0 \\ -\tilde{z}_3 \leq \tilde{x}_1 \leq 1 - \tilde{z}_1 \\ 0 \leq \tilde{x}_2 \leq \tilde{x}_1 \\ -\tilde{z}_3 \leq \tilde{x}_3 \leq \tilde{x}_1 - \tilde{x}_2 \end{array} \right\},$$

$$D_{14} := \left\{ \begin{array}{l} 0 \leq \tilde{z}_1 \leq 1 \\ 0 \leq \tilde{z}_2 \leq \tilde{z}_1 \\ 0 \leq \tilde{z}_3 \leq \tilde{z}_1 - \tilde{z}_2 \\ 0 \leq \tilde{x}_1 \leq 1 - \tilde{z}_1 \\ 0 \leq \tilde{x}_2 \leq \tilde{x}_1 \\ 0 \leq \tilde{x}_3 \leq \tilde{x}_1 - \tilde{x}_2 \end{array} \right\}, \quad D_{15} := \left\{ \begin{array}{l} 0 \leq \tilde{z}_1 \leq 1 \\ 0 \leq \tilde{z}_2 \leq \tilde{z}_1 \\ \tilde{z}_1 - \tilde{z}_2 \leq \tilde{z}_3 \leq 1 - \tilde{z}_2 \\ \tilde{z}_2 - \tilde{z}_1 + \tilde{z}_3 \leq \tilde{x}_1 \leq 1 - \tilde{z}_1 \\ 0 \leq \tilde{x}_2 \leq \tilde{x}_1 + \tilde{z}_1 - \tilde{z}_2 - \tilde{z}_3 \\ 0 \leq \tilde{x}_3 \leq \tilde{x}_1 - \tilde{x}_2 + \tilde{z}_1 - \tilde{z}_2 - \tilde{z}_3 \end{array} \right\},$$

$$D_{16} := \left\{ \begin{array}{l} 0 \leq \tilde{z}_1 \leq 1 \\ \tilde{z}_1 \leq \tilde{z}_2 \leq 1 \\ -1 + \tilde{z}_1 \leq \tilde{z}_3 \leq \tilde{z}_1 - \tilde{z}_2 \\ -\tilde{z}_3 \leq \tilde{x}_1 \leq 1 - \tilde{z}_1 \\ 0 \leq \tilde{x}_2 \leq \tilde{x}_1 + \tilde{z}_1 - \tilde{z}_2 \\ -\tilde{z}_3 \leq \tilde{x}_3 \leq \tilde{x}_1 - \tilde{x}_2 \end{array} \right\}, \quad D_{17} := \left\{ \begin{array}{l} 0 \leq \tilde{z}_1 \leq 1 \\ \tilde{z}_1 \leq \tilde{z}_2 \leq 1 \\ \tilde{z}_1 - \tilde{z}_2 \leq \tilde{z}_3 \leq 0 \\ \tilde{z}_2 - \tilde{z}_1 \leq \tilde{x}_1 \leq 1 - \tilde{z}_1 \\ 0 \leq \tilde{x}_2 \leq \tilde{x}_1 + \tilde{z}_1 - \tilde{z}_2 \\ -\tilde{z}_3 \leq \tilde{x}_3 \leq \tilde{x}_1 - \tilde{x}_2 + \tilde{z}_1 - \tilde{z}_2 - \tilde{z}_3 \end{array} \right\}$$

A. Appendix: Duffy Transformation

$$\text{and } D_{18} := \left\{ \begin{array}{l} 0 \leq \tilde{z}_1 \leq 1 \\ \tilde{z}_1 \leq \tilde{z}_2 \leq 1 \\ 0 \leq \tilde{z}_3 \leq 1 - \tilde{z}_2 \\ \tilde{z}_2 - \tilde{z}_1 + \tilde{z}_3 \leq \tilde{x}_1 \leq 1 - \tilde{z}_1 \\ 0 \leq \tilde{x}_2 \leq \tilde{x}_1 + \tilde{z}_1 - \tilde{z}_2 - \tilde{z}_3 \\ 0 \leq \tilde{x}_3 \leq \tilde{x}_1 - \tilde{x}_2 + \tilde{z}_1 - \tilde{z}_2 - \tilde{z}_3 \end{array} \right\}.$$

All in all, the domain D can now be described by 18 sub-domains, i.e.

$$D = \bigcup_{i=1}^{18} D_i.$$

A.1.2.2. Preparations for the non-linear transformation One advantage of this strongly structured domain D is that every sub-domain D_i satisfies already a forking inequality chain, which is suitable for our approach. Since the procedure is always analogous for each sub-domain, we will abbreviate the procedure and only state the results, i.e. the forking inequality chain and the new set of variables $\omega \in \mathbb{R}^6$ which reflect this ordering.

Sub-domain D_1 Forking inequality chain:

$$0 \leq -\tilde{z}_1 \leq -\tilde{z}_2 \leq -\tilde{z}_2 - \tilde{z}_3 \leq -\tilde{z}_2 + \tilde{x}_3 \leq \tilde{x}_1 - \tilde{x}_2 - \tilde{z}_2 \leq \tilde{x}_1 \leq 1.$$

Introduction of a new set of variables $\omega \in \mathbb{R}^6$ matching the inequality chain:

$$\omega_1 := \tilde{x}_1, \quad \omega_2 := \tilde{x}_1 - \tilde{x}_2 - \tilde{z}_2, \quad \omega_3 := -\tilde{z}_2 + \tilde{x}_3, \quad \omega_4 := -\tilde{z}_2 - \tilde{z}_3, \quad \omega_5 := -\tilde{z}_2, \quad \omega_6 := -\tilde{z}_1,$$

$$\int_0^1 \int_0^{\omega_1} \int_0^{\omega_2} \int_0^{\omega_3} \int_0^{\omega_4} \int_0^{\omega_5} \tilde{k}_1 \left(\left[\begin{array}{c} 1 - \omega_1 \\ \omega_1 - \omega_2 + \omega_5 \\ \omega_3 - \omega_5 \end{array} \right], \left[\begin{array}{c} 1 - \omega_1 + \omega_6 \\ \omega_1 - \omega_2 \\ \omega_3 - \omega_4 \end{array} \right] \right) d\omega.$$

Sub-domain D_2 Forking inequality chain:

$$0 \leq -\tilde{z}_1 \leq -\tilde{z}_1 + \tilde{z}_3 \leq -\tilde{z}_2 \leq \tilde{x}_3 - \tilde{z}_2 \leq \tilde{x}_1 - \tilde{x}_2 - \tilde{z}_2 \leq \tilde{x}_1 \leq 1.$$

Introduction of a new set of variables $\omega \in \mathbb{R}^6$ matching the inequality chain:

$$\begin{array}{lll} \omega_1 & := & \tilde{x}_1, & \omega_2 & := & \tilde{x}_1 - \tilde{x}_2 - \tilde{z}_2, & \omega_3 & := & \tilde{x}_3 - \tilde{z}_2, \\ \omega_4 & := & -\tilde{z}_2, & \omega_5 & := & -\tilde{z}_1 + \tilde{z}_3, & \omega_6 & := & -\tilde{z}_1, \end{array}$$

$$\int_0^1 \int_0^{\omega_1} \int_0^{\omega_2} \int_0^{\omega_3} \int_0^{\omega_4} \int_0^{\omega_5} \tilde{k}_1 \left(\left[\begin{array}{c} 1 - \omega_1 \\ \omega_1 - \omega_2 + \omega_4 \\ \omega_3 - \omega_4 \end{array} \right], \left[\begin{array}{c} 1 - \omega_1 + \omega_6 \\ \omega_1 - \omega_2 \\ \omega_3 - \omega_4 + \omega_5 - \omega_6 \end{array} \right] \right) d\omega.$$

A. Appendix: Duffy Transformation

Sub-domain D_3 Forking inequality chain:

$$0 \leq -\tilde{z}_1 \leq -\tilde{z}_2 \leq -\tilde{z}_1 + \tilde{z}_3 \leq \tilde{x}_3 - \tilde{z}_1 + \tilde{z}_3 \leq \tilde{x}_1 - \tilde{x}_2 - \tilde{z}_2 \leq \tilde{x}_1 \leq 1.$$

Introduction of a new set of variables $\omega \in \mathbb{R}^6$ matching the inequality chain:

$$\omega_1 := \tilde{x}_1, \omega_2 := \tilde{x}_1 - \tilde{x}_2 - \tilde{z}_2, \omega_3 := \tilde{x}_3 - \tilde{z}_1 + \tilde{z}_3, \omega_4 := -\tilde{z}_1 + \tilde{z}_3, \omega_5 := -\tilde{z}_2, \omega_6 := -\tilde{z}_1,$$

$$\int_0^1 \int_0^{\omega_1} \int_0^{\omega_2} \int_0^{\omega_3} \int_0^{\omega_4} \int_0^{\omega_5} \tilde{k}_1 \left(\begin{bmatrix} 1 - \omega_1 \\ \omega_1 - \omega_2 + \omega_5 \\ \omega_3 - \omega_4 \end{bmatrix}, \begin{bmatrix} 1 - \omega_1 + \omega_6 \\ \omega_1 - \omega_2 \\ \omega_3 - \omega_6 \end{bmatrix} \right) d\omega.$$

Sub-domain D_4 Forking inequality chain:

$$0 \leq -\tilde{z}_2 \leq -\tilde{z}_1 \leq -\tilde{z}_2 - \tilde{z}_3 \leq \tilde{x}_3 - \tilde{z}_2 \leq \tilde{x}_1 - \tilde{x}_2 - \tilde{z}_2 \leq \tilde{x}_1 \leq 1.$$

Introduction of a new set of variables $\omega \in \mathbb{R}^6$ matching the inequality chain:

$$\omega_1 := \tilde{x}_1, \omega_2 := \tilde{x}_1 - \tilde{x}_2 - \tilde{z}_2, \omega_3 := \tilde{x}_3 - \tilde{z}_2, \omega_4 := -\tilde{z}_2 + \tilde{z}_3, \omega_5 := -\tilde{z}_2, \omega_6 := -\tilde{z}_1,$$

$$\int_0^1 \int_0^{\omega_1} \int_0^{\omega_2} \int_0^{\omega_3} \int_0^{\omega_4} \int_0^{\omega_5} \tilde{k}_1 \left(\begin{bmatrix} 1 - \omega_1 \\ \omega_1 - \omega_2 + \omega_6 \\ \omega_3 - \omega_6 \end{bmatrix}, \begin{bmatrix} 1 - \omega_1 + \omega_5 \\ \omega_1 - \omega_2 \\ \omega_3 - \omega_4 \end{bmatrix} \right) d\omega.$$

Sub-domain D_5 Forking inequality chain:

$$0 \leq -\tilde{z}_2 \leq -\tilde{z}_2 - \tilde{z}_3 \leq -\tilde{z}_1 \leq \tilde{x}_3 - \tilde{z}_1 + \tilde{z}_3 \leq \tilde{x}_1 - \tilde{x}_2 - \tilde{z}_2 \leq \tilde{x}_1 \leq 1.$$

Introduction of a new set of variables $\omega \in \mathbb{R}^6$ matching the inequality chain:

$$\omega_1 := \tilde{x}_1, \omega_2 := \tilde{x}_1 - \tilde{x}_2 - \tilde{z}_2, \omega_3 := \tilde{x}_3 - \tilde{z}_1 + \tilde{z}_3, \omega_4 := -\tilde{z}_1, \omega_5 := -\tilde{z}_2 - \tilde{z}_3, \omega_6 := -\tilde{z}_2,$$

$$\int_0^1 \int_0^{\omega_1} \int_0^{\omega_2} \int_0^{\omega_3} \int_0^{\omega_4} \int_0^{\omega_5} \tilde{k}_1 \left(\begin{bmatrix} 1 - \omega_1 \\ \omega_1 - \omega_2 + \omega_6 \\ \omega_3 - \omega_4 + \omega_5 - \omega_6 \end{bmatrix}, \begin{bmatrix} 1 - \omega_1 + \omega_4 \\ \omega_1 - \omega_2 \\ \omega_3 - \omega_4 \end{bmatrix} \right) d\omega.$$

Sub-domain D_6 Forking inequality chain:

$$0 \leq -\tilde{z}_2 \leq -\tilde{z}_1 \leq -\tilde{z}_1 + \tilde{z}_3 \leq \tilde{x}_3 - \tilde{z}_1 + \tilde{z}_3 \leq \tilde{x}_1 - \tilde{x}_2 - \tilde{z}_2 \leq \tilde{x}_1 \leq 1.$$

Introduction of a new set of variables $\omega \in \mathbb{R}^6$ matching the inequality chain:

$$\omega_1 := \tilde{x}_1, \omega_2 := \tilde{x}_1 - \tilde{x}_2 - \tilde{z}_2, \omega_3 := \tilde{x}_3 - \tilde{z}_1 + \tilde{z}_3, \omega_4 := -\tilde{z}_1 + \tilde{z}_3, \omega_5 := -\tilde{z}_1, \omega_6 := -\tilde{z}_2,$$

$$\int_0^1 \int_0^{\omega_1} \int_0^{\omega_2} \int_0^{\omega_3} \int_0^{\omega_4} \int_0^{\omega_5} \tilde{k}_1 \left(\begin{bmatrix} 1 - \omega_1 \\ \omega_1 - \omega_2 + \omega_6 \\ \omega_3 - \omega_4 \end{bmatrix}, \begin{bmatrix} 1 - \omega_1 + \omega_5 \\ \omega_1 - \omega_2 \\ \omega_3 - \omega_5 \end{bmatrix} \right) d\omega.$$

A. Appendix: Duffy Transformation

Sub-domain D₇ Forking inequality chain:

$$0 \leq -\tilde{z}_1 \leq -\tilde{z}_1 + \tilde{z}_2 \leq -\tilde{z}_3 \leq \tilde{x}_3 \leq \tilde{x}_1 - \tilde{x}_2 \leq \tilde{x}_1 \leq 1.$$

Introduction of a new set of variables $\omega \in \mathbb{R}^6$ matching the inequality chain:

$$\omega_1 := \tilde{x}_1, \omega_2 := \tilde{x}_1 - \tilde{x}_2, \omega_3 := \tilde{x}_3, \omega_4 := -\tilde{z}_3, \omega_5 := -\tilde{z}_1 + \tilde{z}_2, \omega_6 := -\tilde{z}_1,$$

$$\int_0^1 \int_0^{\omega_1} \int_0^{\omega_2} \int_0^{\omega_3} \int_0^{\omega_4} \int_0^{\omega_5} \tilde{k}_1 \left(\begin{bmatrix} 1 - \omega_1 \\ \omega_1 - \omega_2 \\ \omega_3 \end{bmatrix}, \begin{bmatrix} 1 - \omega_1 + \omega_6 \\ \omega_1 - \omega_2 + \omega_5 - \omega_6 \\ \omega_3 - \omega_4 \end{bmatrix} \right) d\omega.$$

Sub-domain D₈ Forking inequality chain:

$$0 \leq -\tilde{z}_1 \leq -\tilde{z}_1 + \tilde{z}_2 \leq \tilde{x}_3 - \tilde{z}_1 + \tilde{z}_2 + \tilde{z}_3 \leq \tilde{x}_1 - \tilde{x}_2 \leq \tilde{x}_1 \leq 1,$$

$$0 \leq -\tilde{z}_3 \leq -\tilde{z}_1 + \tilde{z}_2 \leq \tilde{x}_3 - \tilde{z}_1 + \tilde{z}_2 + \tilde{z}_3 \leq \tilde{x}_1 - \tilde{x}_2 \leq \tilde{x}_1 \leq 1.$$

Introduction of a new set of variables $\omega \in \mathbb{R}^6$ matching the inequality chain:

$$\omega_1 := \tilde{x}_1, \omega_2 := \tilde{x}_1 - \tilde{x}_2, \omega_3 := \tilde{x}_3 - \tilde{z}_1 + \tilde{z}_2 + \tilde{z}_3, \omega_4 := -\tilde{z}_1 + \tilde{z}_2, \omega_5 := -\tilde{z}_3, \omega_6 := -\tilde{z}_1,$$

$$\int_0^1 \int_0^{\omega_1} \int_0^{\omega_2} \int_0^{\omega_3} \int_0^{\omega_4} \int_0^{\omega_5} \tilde{k}_1 \left(\begin{bmatrix} 1 - \omega_1 \\ \omega_1 - \omega_2 \\ \omega_3 - \omega_4 + \omega_5 \end{bmatrix}, \begin{bmatrix} 1 - \omega_1 + \omega_6 \\ \omega_1 - \omega_2 + \omega_4 - \omega_6 \\ \omega_3 - \omega_4 \end{bmatrix} \right) d\omega.$$

Sub-domain D₉ Forking inequality chain:

$$0 \leq -\tilde{z}_1 \leq -\tilde{z}_1 + \tilde{z}_2 \leq -\tilde{z}_1 + \tilde{z}_2 + \tilde{z}_3 \leq \tilde{x}_3 - \tilde{z}_1 + \tilde{z}_2 + \tilde{z}_3 \leq \tilde{x}_1 - \tilde{x}_2 \leq \tilde{x}_1 \leq 1.$$

Introduction of a new set of variables $\omega \in \mathbb{R}^6$ matching the inequality chain:

$$\omega_1 := \tilde{x}_1, \omega_2 := \tilde{x}_1 - \tilde{x}_2, \omega_3 := \tilde{x}_3 - \tilde{z}_1 + \tilde{z}_2 + \tilde{z}_3, \omega_4 := -\tilde{z}_1 + \tilde{z}_2 + \tilde{z}_3, \omega_5 := -\tilde{z}_1 + \tilde{z}_2, \omega_6 := -\tilde{z}_1,$$

$$\int_0^1 \int_0^{\omega_1} \int_0^{\omega_2} \int_0^{\omega_3} \int_0^{\omega_4} \int_0^{\omega_5} \tilde{k}_1 \left(\begin{bmatrix} 1 - \omega_1 \\ \omega_1 - \omega_2 \\ \omega_3 - \omega_4 \end{bmatrix}, \begin{bmatrix} 1 - \omega_1 + \omega_6 \\ \omega_1 - \omega_2 + \omega_5 - \omega_6 \\ \omega_3 - \omega_5 \end{bmatrix} \right) d\omega.$$

Sub-domain D₁₀ Forking inequality chain:

$$0 \leq \tilde{z}_1 \leq \tilde{z}_1 - \tilde{z}_2 \leq \tilde{z}_1 - \tilde{z}_2 - \tilde{z}_3 \leq \tilde{x}_3 + \tilde{z}_1 - \tilde{z}_2 - \tilde{z}_3 \leq \tilde{x}_1 - \tilde{x}_2 + \tilde{z}_1 - \tilde{z}_2 \leq \tilde{x}_1 + \tilde{z}_1 \leq 1.$$

Introduction of a new set of variables $\omega \in \mathbb{R}^6$ matching the inequality chain:

$$\omega_1 := \tilde{x}_1 + \tilde{z}_1, \omega_2 := \tilde{x}_1 - \tilde{x}_2 + \tilde{z}_1 - \tilde{z}_2, \omega_3 := \tilde{x}_3 + \tilde{z}_1 - \tilde{z}_2 - \tilde{z}_3, \omega_4 := \tilde{z}_1 - \tilde{z}_2 - \tilde{z}_3, \omega_5 := \tilde{z}_1 - \tilde{z}_2, \omega_6 := \tilde{z}_1,$$

$$\int_0^1 \int_0^{\omega_1} \int_0^{\omega_2} \int_0^{\omega_3} \int_0^{\omega_4} \int_0^{\omega_5} \tilde{k}_1 \left(\begin{bmatrix} 1 - \omega_1 + \omega_6 \\ \omega_1 - \omega_2 + \omega_5 - \omega_6 \\ \omega_3 - \omega_5 \end{bmatrix}, \begin{bmatrix} 1 - \omega_1 \\ \omega_1 - \omega_2 \\ \omega_3 - \omega_4 \end{bmatrix} \right) d\omega.$$

A. Appendix: Duffy Transformation

Sub-domain D_{11} Forking inequality chain:

$$\begin{aligned} 0 \leq \tilde{z}_1 \leq \tilde{z}_1 - \tilde{z}_2 \leq \tilde{x}_3 + \tilde{z}_1 - \tilde{z}_2 \leq \tilde{x}_1 - \tilde{x}_2 + \tilde{z}_1 - \tilde{z}_2 \leq \tilde{x}_1 + \tilde{z}_1 \leq 1, \\ 0 \leq \tilde{z}_3 \leq \tilde{z}_1 - \tilde{z}_2 \leq \tilde{x}_3 + \tilde{z}_1 - \tilde{z}_2 \leq \tilde{x}_1 - \tilde{x}_2 + \tilde{z}_1 - \tilde{z}_2 \leq \tilde{x}_1 + \tilde{z}_1 \leq 1. \end{aligned}$$

Introduction of a new set of variables $\omega \in \mathbb{R}^6$ matching the inequality chain:

$$\omega_1 := \tilde{x}_1 + \tilde{z}_1, \omega_2 := \tilde{x}_1 - \tilde{x}_2 + \tilde{z}_1 - \tilde{z}_2, \omega_3 := \tilde{x}_3 + \tilde{z}_1 - \tilde{z}_2, \omega_4 := \tilde{z}_1 - \tilde{z}_2, \omega_5 := \tilde{z}_3, \omega_6 := \tilde{z}_1,$$

$$\int_0^1 \int_0^{\omega_1} \int_0^{\omega_2} \int_0^{\omega_3} \int_0^{\omega_4} \int_0^{\omega_5} \tilde{k}_1 \left(\left[\begin{array}{c} 1 - \omega_1 + \omega_6 \\ \omega_1 - \omega_2 + \omega_4 - \omega_6 \\ \omega_3 - \omega_4 \end{array} \right], \left[\begin{array}{c} 1 - \omega_1 \\ \omega_1 - \omega_2 \\ \omega_3 - \omega_4 + \omega_5 \end{array} \right] \right) d\omega.$$

Sub-domain D_{12} Forking inequality chain:

$$0 \leq \tilde{z}_1 \leq \tilde{z}_1 - \tilde{z}_2 \leq \tilde{z}_3 \leq \tilde{x}_3 + \tilde{z}_3 \leq \tilde{x}_1 - \tilde{x}_2 + \tilde{z}_1 - \tilde{z}_2 \leq \tilde{x}_1 + \tilde{z}_1 \leq 1.$$

Introduction of a new set of variables $\omega \in \mathbb{R}^6$ matching the inequality chain:

$$\omega_1 := \tilde{x}_1 + \tilde{z}_1, \omega_2 := \tilde{x}_1 - \tilde{x}_2 + \tilde{z}_1 - \tilde{z}_2, \omega_3 := \tilde{x}_3 + \tilde{z}_3, \omega_4 := \tilde{z}_3, \omega_5 := \tilde{z}_1 - \tilde{z}_2, \omega_6 := \tilde{z}_1,$$

$$\int_0^1 \int_0^{\omega_1} \int_0^{\omega_2} \int_0^{\omega_3} \int_0^{\omega_4} \int_0^{\omega_5} \tilde{k}_1 \left(\left[\begin{array}{c} 1 - \omega_1 + \omega_6 \\ \omega_1 - \omega_2 + \omega_5 - \omega_6 \\ \omega_3 - \omega_4 \end{array} \right], \left[\begin{array}{c} 1 - \omega_1 \\ \omega_1 - \omega_2 \\ \omega_3 \end{array} \right] \right) d\omega.$$

Sub-domain D_{13} Forking inequality chain:

$$0 \leq \tilde{z}_2 \leq \tilde{z}_1 \leq \tilde{z}_1 - \tilde{z}_3 \leq \tilde{x}_3 + \tilde{z}_1 \leq \tilde{x}_1 - \tilde{x}_2 + \tilde{z}_1 \leq \tilde{x}_1 + \tilde{z}_1 \leq 1.$$

Introduction of a new set of variables $\omega \in \mathbb{R}^6$ matching the inequality chain:

$$\omega_1 := \tilde{x}_1 + \tilde{z}_1, \omega_2 := \tilde{x}_1 - \tilde{x}_2 + \tilde{z}_1, \omega_3 := \tilde{x}_3 + \tilde{z}_1, \omega_4 := \tilde{z}_1 - \tilde{z}_3, \omega_5 := \tilde{z}_1, \omega_6 := \tilde{z}_2,$$

$$\int_0^1 \int_0^{\omega_1} \int_0^{\omega_2} \int_0^{\omega_3} \int_0^{\omega_4} \int_0^{\omega_5} \tilde{k}_1 \left(\left[\begin{array}{c} 1 - \omega_1 + \omega_5 \\ \omega_1 - \omega_2 \\ \omega_3 - \omega_5 \end{array} \right], \left[\begin{array}{c} 1 - \omega_1 \\ \omega_1 - \omega_2 + \omega_6 \\ \omega_3 - \omega_4 \end{array} \right] \right) d\omega.$$

Sub-domain D_{14} Forking inequality chain:

$$0 \leq \tilde{z}_2 \leq \tilde{z}_2 + \tilde{z}_3 \leq \tilde{z}_1 \leq \tilde{x}_3 + \tilde{z}_1 \leq \tilde{x}_1 - \tilde{x}_2 + \tilde{z}_1 \leq \tilde{x}_1 + \tilde{z}_1 \leq 1.$$

Introduction of a new set of variables $\omega \in \mathbb{R}^6$ matching the inequality chain:

$$\omega_1 := \tilde{x}_1 + \tilde{z}_1, \omega_2 := \tilde{x}_1 - \tilde{x}_2 + \tilde{z}_1, \omega_3 := \tilde{x}_3 + \tilde{z}_1, \omega_4 := \tilde{z}_1, \omega_5 := \tilde{z}_2 + \tilde{z}_3, \omega_6 := \tilde{z}_2,$$

$$\int_0^1 \int_0^{\omega_1} \int_0^{\omega_2} \int_0^{\omega_3} \int_0^{\omega_4} \int_0^{\omega_5} \tilde{k}_1 \left(\left[\begin{array}{c} 1 - \omega_1 + \omega_4 \\ \omega_1 - \omega_2 \\ \omega_3 - \omega_4 \end{array} \right], \left[\begin{array}{c} 1 - \omega_1 \\ \omega_1 - \omega_2 + \omega_6 \\ \omega_3 - \omega_4 + \omega_5 - \omega_6 \end{array} \right] \right) d\omega.$$

A. Appendix: Duffy Transformation

Sub-domain D₁₅ Forking inequality chain:

$$0 \leq \tilde{z}_2 \leq \tilde{z}_1 \leq \tilde{z}_2 + \tilde{z}_3 \leq \tilde{x}_3 + \tilde{z}_2 + \tilde{z}_3 \leq \tilde{x}_1 - \tilde{x}_2 + \tilde{z}_1 \leq \tilde{x}_1 + \tilde{z}_1 \leq 1.$$

Introduction of a new set of variables $\omega \in \mathbb{R}^6$ matching the inequality chain:

$$\omega_1 := \tilde{x}_1 + \tilde{z}_1, \omega_2 := \tilde{x}_1 - \tilde{x}_2 + \tilde{z}_1, \omega_3 := \tilde{x}_3 + \tilde{z}_2 + \tilde{z}_3, \omega_4 := \tilde{z}_2 + \tilde{z}_3, \omega_5 := \tilde{z}_1, \omega_6 := \tilde{z}_2,$$

$$\int_0^1 \int_0^{\omega_1} \int_0^{\omega_2} \int_0^{\omega_3} \int_0^{\omega_4} \int_0^{\omega_5} \tilde{k}_1 \left(\begin{bmatrix} 1 - \omega_1 + \omega_5 \\ \omega_1 - \omega_2 \\ \omega_3 - \omega_4 \end{bmatrix}, \begin{bmatrix} 1 - \omega_1 \\ \omega_1 - \omega_2 + \omega_6 \\ \omega_3 - \omega_6 \end{bmatrix} \right) d\omega.$$

Sub-domain D₁₆ Forking inequality chain:

$$0 \leq \tilde{z}_1 \leq \tilde{z}_2 \leq \tilde{z}_1 - \tilde{z}_3 \leq \tilde{x}_3 + \tilde{z}_1 \leq \tilde{x}_1 - \tilde{x}_2 + \tilde{z}_1 \leq \tilde{x}_1 + \tilde{z}_1 \leq 1.$$

Introduction of a new set of variables $\omega \in \mathbb{R}^6$ matching the inequality chain:

$$\omega_1 := \tilde{x}_1 + \tilde{z}_1, \omega_2 := \tilde{x}_1 - \tilde{x}_2 + \tilde{z}_1, \omega_3 := \tilde{x}_3 + \tilde{z}_1, \omega_4 := \tilde{z}_1 - \tilde{z}_3, \omega_5 := \tilde{z}_2, \omega_6 := \tilde{z}_1,$$

$$\int_0^1 \int_0^{\omega_1} \int_0^{\omega_2} \int_0^{\omega_3} \int_0^{\omega_4} \int_0^{\omega_5} \tilde{k}_1 \left(\begin{bmatrix} 1 - \omega_1 + \omega_6 \\ \omega_1 - \omega_2 \\ \omega_3 - \omega_6 \end{bmatrix}, \begin{bmatrix} 1 - \omega_1 \\ \omega_1 - \omega_2 + \omega_5 \\ \omega_3 - \omega_4 \end{bmatrix} \right) d\omega.$$

Sub-domain D₁₇ Forking inequality chain:

$$0 \leq \tilde{z}_1 \leq \tilde{z}_1 - \tilde{z}_3 \leq \tilde{z}_2 \leq \tilde{x}_3 + \tilde{z}_2 + \tilde{z}_3 \leq \tilde{x}_1 - \tilde{x}_2 + \tilde{z}_1 \leq \tilde{x}_1 + \tilde{z}_1 \leq 1.$$

Introduction of a new set of variables $\omega \in \mathbb{R}^6$ matching the inequality chain:

$$\omega_1 := \tilde{x}_1 + \tilde{z}_1, \omega_2 := \tilde{x}_1 - \tilde{x}_2 + \tilde{z}_1, \omega_3 := \tilde{x}_3 + \tilde{z}_2 + \tilde{z}_3, \omega_4 := \tilde{z}_2, \omega_5 := \tilde{z}_1 - \tilde{z}_3, \omega_6 := \tilde{z}_1,$$

$$\int_0^1 \int_0^{\omega_1} \int_0^{\omega_2} \int_0^{\omega_3} \int_0^{\omega_4} \int_0^{\omega_5} \tilde{k}_1 \left(\begin{bmatrix} 1 - \omega_1 + \omega_6 \\ \omega_1 - \omega_2 \\ \omega_3 - \omega_4 + \omega_5 - \omega_6 \end{bmatrix}, \begin{bmatrix} 1 - \omega_1 \\ \omega_1 - \omega_2 + \omega_4 \\ \omega_3 - \omega_4 \end{bmatrix} \right) d\omega.$$

Sub-domain D₁₈ Forking inequality chain:

$$0 \leq \tilde{z}_1 \leq \tilde{z}_2 \leq \tilde{z}_2 + \tilde{z}_3 \leq \tilde{x}_3 + \tilde{z}_2 + \tilde{z}_3 \leq \tilde{x}_1 - \tilde{x}_2 + \tilde{z}_1 \leq \tilde{x}_1 + \tilde{z}_1 \leq 1.$$

Introduction of a new set of variables $\omega \in \mathbb{R}^6$ matching the inequality chain:

$$\omega_1 := \tilde{x}_1 + \tilde{z}_1, \omega_2 := \tilde{x}_1 - \tilde{x}_2 + \tilde{z}_1, \omega_3 := \tilde{x}_3 + \tilde{z}_2 + \tilde{z}_3, \omega_4 := \tilde{z}_2 + \tilde{z}_3, \omega_5 := \tilde{z}_2, \omega_6 := \tilde{z}_1,$$

$$\int_0^1 \int_0^{\omega_1} \int_0^{\omega_2} \int_0^{\omega_3} \int_0^{\omega_4} \int_0^{\omega_5} \tilde{k}_1 \left(\begin{bmatrix} 1 - \omega_1 + \omega_6 \\ \omega_1 - \omega_2 \\ \omega_3 - \omega_4 \end{bmatrix}, \begin{bmatrix} 1 - \omega_1 \\ \omega_1 - \omega_2 + \omega_5 \\ \omega_3 - \omega_5 \end{bmatrix} \right) d\omega.$$

A.2. Interaction between a tetrahedron and a panel

This section is dedicated to the singularity removal regarding the interaction between a tetrahedron and a panel. Similar to Section A.2.1 we explain the the missing steps of the Duffy transformation which were omitted in Section 3.3.

A.2.1. Point singularity

First, we start with the point singularity. Following the approach of Section 3.2.1, the integration domain is considered as a set of inequalities and rewriting:

$$\left\{ \begin{array}{l} 0 \leq \tilde{x}_1 \leq 1 \\ 0 \leq \tilde{x}_2 \leq 1 - \tilde{x}_1 \\ 0 \leq \tilde{x}_3 \leq 1 - \tilde{x}_1 - \tilde{x}_2 \\ 0 \leq \tilde{y}_1 \leq 1 \\ 0 \leq \tilde{z}_5 \leq 1 - \tilde{y}_1 \end{array} \right\} \Leftrightarrow \left\{ \begin{array}{l} 0 \leq \tilde{x}_1 \leq 1 \\ \tilde{x}_1 \leq \tilde{x}_1 + \tilde{x}_2 \leq 1 \\ \tilde{x}_1 + \tilde{x}_2 \leq \tilde{x}_1 + \tilde{x}_2 + \tilde{x}_3 \leq 1 \\ 0 \leq \tilde{y}_1 \leq 1 \\ \tilde{y}_1 \leq \tilde{y}_1 + \tilde{z}_5 \leq 1 \end{array} \right\}.$$

To guarantee a suitable forking inequality chain, the set is split up in the same way as (28):

$$\left\{ \begin{array}{l} 0 \leq \tilde{x}_1 \leq 1 \\ \tilde{x}_1 \leq \tilde{x}_1 + \tilde{x}_2 \leq 1 \\ \tilde{x}_1 + \tilde{x}_2 \leq \tilde{x}_1 + \tilde{x}_2 + \tilde{x}_3 \leq 1 \\ 0 \leq \tilde{y}_1 \leq 1 \\ \tilde{y}_1 \leq \tilde{y}_1 + \tilde{z}_5 \leq \tilde{x}_1 + \tilde{x}_2 + \tilde{x}_3 \end{array} \right\} \cup \left\{ \begin{array}{l} 0 \leq \tilde{y}_1 \leq 1 \\ \tilde{y}_1 \leq \tilde{y}_1 + \tilde{z}_5 \leq 1 \\ 0 \leq \tilde{x}_1 \leq 1 \\ \tilde{x}_1 \leq \tilde{x}_1 + \tilde{x}_2 \leq 1 \\ \tilde{x}_1 + \tilde{x}_2 \leq \tilde{x}_1 + \tilde{x}_2 + \tilde{x}_3 \leq \tilde{y}_1 + \tilde{z}_5 \end{array} \right\}.$$

Hence, we obtain two domains and for each of them a new set of variables $\omega \in \mathbb{R}^5$ is introduced satisfying a forking inequality chain:

- domain I:

$$\omega_1 := \tilde{z}_1 + \tilde{z}_2 + \tilde{z}_3, \omega_2 := \tilde{z}_1 + \tilde{z}_2, \omega_3 := \tilde{z}_1, \omega_4 := \tilde{z}_4 + \tilde{z}_5, \omega_5 := \tilde{z}_5,$$

$$\int_0^1 \int_0^{\omega_1} \int_0^{\omega_2} \int_0^{\omega_1} \int_0^{\omega_4} \tilde{k}_2 \left(\begin{array}{l} \omega_3 \\ \omega_2 - \omega_3 \\ \omega_1 - \omega_2 \end{array} \right), \begin{array}{l} \omega_5 \\ \omega_4 - \omega_5 \end{array} \right) d\omega.$$

- domain II:

$$\omega_1 := \tilde{z}_4 + \tilde{z}_5, \omega_2 := \tilde{z}_5, \omega_3 := \tilde{z}_1 + \tilde{z}_2 + \tilde{z}_3, \omega_4 := \tilde{z}_1 + \tilde{z}_2, \omega_5 := \tilde{z}_1,$$

$$\int_0^1 \int_0^{\omega_1} \int_0^{\omega_1} \int_0^{\omega_3} \int_0^{\omega_4} \tilde{k}_2 \left(\begin{array}{l} \omega_5 \\ \omega_4 - \omega_5 \\ \omega_3 - \omega_4 \end{array} \right), \begin{array}{l} \omega_2 \\ \omega_1 - \omega_2 \end{array} \right) d\omega.$$

A.2.2. Singularity along an edge

Next, the singularity along an edge is considered. As presented in Section 3.3.2 the integration domain is separated into two parts:

$$\left\{ \begin{array}{l} 0 \leq \tilde{x}_1 \leq 1 \\ 0 \leq \tilde{x}_2 \leq \tilde{x}_1 \\ 0 \leq \tilde{x}_3 \leq \tilde{x}_1 - \tilde{x}_2 \\ 0 \leq \tilde{y}_1 \leq \tilde{x}_1 \\ 0 \leq \tilde{y}_2 \leq \tilde{y}_1 \end{array} \right\} \cup \left\{ \begin{array}{l} 0 \leq \tilde{y}_1 \leq 1 \\ 0 \leq \tilde{y}_2 \leq \tilde{y}_1 \\ 0 \leq \tilde{x}_1 \leq \tilde{y}_1 \\ 0 \leq \tilde{x}_2 \leq \tilde{x}_1 \\ 0 \leq \tilde{x}_3 \leq \tilde{x}_1 - \tilde{x}_2 \end{array} \right\}.$$

For each part we introduce local coordinates $\tilde{z} \in \mathbb{R}^4$,

$$\begin{aligned} \tilde{z}_1 &= \tilde{y}_1 - \tilde{x}_1, & \tilde{z}_2 &= \tilde{y}_2, & \tilde{z}_3 &= \tilde{x}_2, & \tilde{z}_4 &= \tilde{x}_3 & \text{and} \\ \tilde{z}_1 &= \tilde{x}_1 - \tilde{y}_1, & \tilde{z}_2 &= \tilde{x}_2, & \tilde{z}_3 &= \tilde{x}_3, & \tilde{z}_4 &= \tilde{y}_2, \end{aligned}$$

to describe the singularity as point singularity at the origin:

$$\left\{ \begin{array}{l} 0 \leq \tilde{x}_1 \leq 1 \\ 0 \leq \tilde{z}_3 \leq \tilde{x}_1 \\ 0 \leq \tilde{z}_4 \leq \tilde{x}_1 - \tilde{z}_3 \\ -\tilde{x}_1 \leq \tilde{z}_1 \leq 0 \\ 0 \leq \tilde{z}_2 \leq \tilde{x}_1 + \tilde{z}_1 \end{array} \right\} \cup \left\{ \begin{array}{l} 0 \leq \tilde{y}_1 \leq 1 \\ 0 \leq \tilde{z}_4 \leq \tilde{y}_1 \\ -\tilde{y}_1 \leq \tilde{z}_1 \leq 0 \\ 0 \leq \tilde{z}_2 \leq \tilde{y}_1 + \tilde{z}_1 \\ 0 \leq \tilde{z}_3 \leq \tilde{y}_1 + \tilde{z}_1 - \tilde{z}_2 \end{array} \right\}.$$

The next step is to check for each sub-domain if it satisfies a forking inequality chain, which satisfies the requirements of our approach. Starting with the first one, we obtain:

$$0 \leq \tilde{z}_3 \leq \tilde{z}_3 + \tilde{z}_4 \leq \tilde{x}_1 \text{ und } 0 \leq -\tilde{z}_1 \leq -\tilde{z}_1 + \tilde{z}_2 \leq \tilde{x}_1.$$

Since the forking happens one link to early, the domain has to be split up:

$$\left\{ \begin{array}{l} 0 \leq \tilde{x}_1 \leq 1 \\ 0 \leq \tilde{z}_3 \leq \tilde{x}_1 \\ 0 \leq \tilde{z}_4 \leq \tilde{x}_1 - \tilde{z}_3 \\ -\tilde{x}_1 \leq \tilde{z}_1 \leq 0 \\ 0 \leq \tilde{z}_2 \leq \tilde{z}_1 + \tilde{z}_3 + \tilde{z}_4 \end{array} \right\} \cup \left\{ \begin{array}{l} 0 \leq \tilde{x}_1 \leq 1 \\ 0 \leq \tilde{z}_3 \leq \tilde{x}_1 \\ 0 \leq \tilde{z}_4 \leq -\tilde{z}_1 + \tilde{z}_2 - \tilde{z}_3 \\ -\tilde{x}_1 \leq \tilde{z}_1 \leq 0 \\ 0 \leq \tilde{z}_2 \leq \tilde{x}_1 + \tilde{z}_1 \end{array} \right\}.$$

These two domains satisfy each a suitable forking inequality chain. Therefore, we can introduce now a new set of variables $\omega \in \mathbb{R}^5$ corresponding to these inequality chains:

$$\omega_1 := \tilde{x}_1, \omega_2 := \tilde{z}_3 + \tilde{z}_4, \omega_3 := \tilde{z}_3, \omega_4 := -\tilde{z}_1 + \tilde{z}_2, \omega_5 := -\tilde{z}_1,$$

$$\int_0^1 \int_0^{\omega_1} \int_0^{\omega_2} \int_0^{\omega_2} \int_0^{\omega_4} \tilde{k}_2 \left(\begin{bmatrix} 1 - \omega_1 \\ \omega_3 \\ \omega_2 - \omega_3 \end{bmatrix}, \begin{bmatrix} 1 - \omega_1 + \omega_5 \\ \omega_4 - \omega_5 \end{bmatrix} \right) d\omega$$

and

$$\omega_1 := \tilde{x}_1, \omega_2 := \tilde{z}_1 - \tilde{z}_2, \omega_3 := -\tilde{z}_1, \omega_4 := \tilde{z}_3 + \tilde{z}_4, \omega_5 := \tilde{z}_3,$$

A. Appendix: Duffy Transformation

$$\int_0^1 \int_0^{\omega_1} \int_0^{\omega_2} \int_0^{\omega_2} \int_0^{\omega_4} \tilde{k}_2 \left(\begin{bmatrix} 1 - \omega_1 \\ \omega_5 \\ \omega_4 - \omega_5 \end{bmatrix}, \begin{bmatrix} 1 - \omega_1 + \omega_3 \\ \omega_2 - \omega_3 \end{bmatrix} \right) d\omega.$$

For the second domain the approach is analogous. First, we investigate whether the domain satisfies a suitable forking inequality chain or not:

$$0 \leq \tilde{z}_4 \leq \tilde{y}_1 \text{ und } 0 \leq -\tilde{z}_1 \leq -\tilde{z}_1 + \tilde{z}_2 \leq -\tilde{z}_1 + \tilde{z}_2 + \tilde{z}_3 \leq \tilde{y}_1.$$

Here, we have the same issue as with the first sub-domain, the chain splits up one link to early. In order to solve this, the domain gets subdivided:

$$\left\{ \begin{array}{l} 0 \leq \tilde{y}_1 \leq 1 \\ 0 \leq \tilde{z}_4 \leq \tilde{y}_1 \\ -\tilde{y}_1 \leq \tilde{z}_1 \leq 0 \\ 0 \leq \tilde{z}_2 \leq \tilde{y}_1 + \tilde{z}_1 \\ 0 \leq \tilde{z}_3 \leq \tilde{z}_4 + \tilde{z}_1 - \tilde{z}_2 \end{array} \right\} \cup \left\{ \begin{array}{l} 0 \leq \tilde{y}_1 \leq 1 \\ 0 \leq \tilde{z}_4 \leq -\tilde{z}_1 + \tilde{z}_2 + \tilde{z}_3 \\ -\tilde{y}_1 \leq \tilde{z}_1 \leq 0 \\ 0 \leq \tilde{z}_2 \leq \tilde{y}_1 + \tilde{z}_1 \\ 0 \leq \tilde{z}_3 \leq \tilde{y}_1 + \tilde{z}_1 - \tilde{z}_2 \end{array} \right\}.$$

Since these sub-domains satisfy a suitable forking inequality chain, a new set of variables $\omega \in \mathbb{R}^5$ corresponding to this inequality chains can be presented:

$$\omega_1 := \tilde{y}_1, \omega_2 := \tilde{z}_4, \omega_3 := -\tilde{z}_1 + \tilde{z}_2 + \tilde{z}_3, \omega_4 := -\tilde{z}_1 + \tilde{z}_2, \omega_5 := -\tilde{z}_1,$$

$$\int_0^1 \int_0^{\omega_1} \int_0^{\omega_2} \int_0^{\omega_3} \int_0^{\omega_4} \tilde{k}_2 \left(\begin{bmatrix} 1 - \omega_1 + \omega_5 \\ \omega_4 - \omega_5 \\ \omega_3 - \omega_4 \end{bmatrix}, \begin{bmatrix} 1 - \omega_1 \\ \omega_2 \end{bmatrix} \right) d\omega$$

$$\omega_1 := \tilde{y}_1, \omega_2 := -\tilde{z}_1 + \tilde{z}_2 + \tilde{z}_3, \omega_3 := \tilde{z}_4, \omega_4 := -\tilde{z}_1 + \tilde{z}_2, \omega_5 := -\tilde{z}_1,$$

$$\int_0^1 \int_0^{\omega_1} \int_0^{\omega_2} \int_0^{\omega_2} \int_0^{\omega_4} \tilde{k}_2 \left(\begin{bmatrix} 1 - \omega_1 + \omega_5 \\ \omega_4 - \omega_5 \\ \omega_2 - \omega_4 \end{bmatrix}, \begin{bmatrix} 1 - \omega_1 \\ \omega_3 \end{bmatrix} \right) d\omega.$$

A.2.3. Singularity on a face

A.2.3.1. Derivation of the integration domains The approach is similar as to the approaches in Appendices A.1.1 and A.1.2. The main difference is that here only five variables appear. After introducing local coordinates to describe the singularity as a three-dimensional point singularity and interchanging the integration order, we obtain the set

$$D := \left\{ \begin{array}{l} -1 \leq \tilde{z}_1 \leq 1 \\ -1 + \max\{0, \tilde{z}_1\} \leq \tilde{z}_2 \leq 1 + \min\{0, \tilde{z}_1\} \\ \max\{0, -\tilde{z}_1, -\tilde{z}_2, \tilde{z}_2 - \tilde{z}_1\} \leq \tilde{x}_1 \leq \min\{1, 1 - \tilde{z}_1\} \\ \max\{0, -\tilde{z}_2\} \leq \tilde{x}_2 \leq \tilde{x}_1 + \min\{0, \tilde{z}_1 - \tilde{z}_2\} \\ 0 \leq \tilde{z}_3 \leq \tilde{x}_1 - \tilde{x}_2 \end{array} \right\}.$$

The next steps are to solve the min and max conditions. We start with the case $-1 \leq \tilde{z}_1 \leq 0$ and choose \tilde{z}_2 so that the min and max conditions can be resolved. By doing so, we obtain three

A. Appendix: Duffy Transformation

sub-domains:

$$D_1 := \left\{ \begin{array}{l} -1 \leq \tilde{z}_1 \leq 0 \\ -1 \leq \tilde{z}_2 \leq \tilde{z}_1 \\ -\tilde{z}_2 \leq \tilde{x}_1 \leq 1 \\ -\tilde{z}_2 \leq \tilde{x}_2 \leq \tilde{x}_1 \\ 0 \leq \tilde{z}_3 \leq \tilde{x}_1 - \tilde{x}_2 \end{array} \right\}, \quad D_2 := \left\{ \begin{array}{l} -1 \leq \tilde{z}_1 \leq 0 \\ \tilde{z}_1 \leq \tilde{z}_2 \leq 0 \\ -\tilde{z}_1 \leq \tilde{x}_1 \leq 1 \\ -\tilde{z}_2 \leq \tilde{x}_2 \leq \tilde{x}_1 + \tilde{z}_1 - \tilde{z}_2 \\ 0 \leq \tilde{z}_3 \leq \tilde{x}_1 - \tilde{x}_2 \end{array} \right\}$$

$$\text{and } D_3 := \left\{ \begin{array}{l} -1 \leq \tilde{z}_1 \leq 0 \\ 0 \leq \tilde{z}_2 \leq 1 + \tilde{z}_1 \\ -z_1 + z_2 \leq \tilde{x}_1 \leq 1 \\ 0 \leq \tilde{x}_2 \leq \tilde{x}_1 + \tilde{z}_1 - \tilde{z}_2 \\ 0 \leq \tilde{z}_3 \leq \tilde{x}_1 - \tilde{x}_2 \end{array} \right\}.$$

The procedure is repeated for the case $0 \leq \tilde{z}_1 \leq 1$, which leads to:

$$D_4 := \left\{ \begin{array}{l} 0 \leq \tilde{z}_1 \leq 1 \\ -1 + \tilde{z}_1 \leq \tilde{z}_2 \leq 0 \\ -\tilde{z}_2 \leq \tilde{x}_1 \leq 1 - z_1 \\ -\tilde{z}_2 \leq \tilde{x}_2 \leq \tilde{x}_1 \\ 0 \leq \tilde{z}_3 \leq \tilde{x}_1 - \tilde{x}_2 \end{array} \right\}, \quad D_5 := \left\{ \begin{array}{l} 0 \leq \tilde{z}_1 \leq 1 \\ 0 \leq \tilde{z}_2 \leq \tilde{z}_1 \\ 0 \leq \tilde{x}_1 \leq 1 - \tilde{z}_1 \\ 0 \leq \tilde{x}_2 \leq \tilde{x}_1 \\ 0 \leq \tilde{z}_3 \leq \tilde{x}_1 - \tilde{x}_2 \end{array} \right\},$$

$$\text{and } D_6 := \left\{ \begin{array}{l} 0 \leq \tilde{z}_1 \leq 1 \\ \tilde{z}_1 \leq \tilde{z}_2 \leq 1 \\ -\tilde{z}_1 + \tilde{z}_2 \leq \tilde{x}_1 \leq 1 - \tilde{z}_1 \\ 0 \leq \tilde{x}_2 \leq \tilde{x}_1 + \tilde{z}_1 - \tilde{z}_2 \\ 0 \leq \tilde{z}_3 \leq \tilde{x}_1 - \tilde{x}_2 \end{array} \right\}.$$

All in all, the min and max conditions can be resolved, by splitting up D into six sub-domains:

$$D = \bigcup_{i=1}^6 D_i.$$

A.2.3.2. Preparations for the non-linear transformation The next step is to check, if each sub-domain satisfies a suitable forking inequality chain, i.e. the split up happens after the third link and only the first and second link may depend on the components of \tilde{x} . These are necessary requirements to lift the singularity.

Sub-domain D_1 For D_1 we even get only one inequality chain,

$$0 \leq -\tilde{z}_1 \leq -\tilde{z}_2 \leq -\tilde{z}_2 + \tilde{z}_3 \leq \tilde{x}_1 - \tilde{x}_2 - \tilde{z}_2 \leq \tilde{x}_1 \leq 1,$$

which is sufficient for our purpose. Then a new set of variables $\omega \in \mathbb{R}^5$ is introduced to represent this ordering:

$$\omega_1 := \tilde{x}_1, \quad \omega_2 := \tilde{x}_1 - \tilde{x}_2 - \tilde{z}_2, \quad \omega_3 := -\tilde{z}_2 + \tilde{z}_3, \quad \omega_4 := -\tilde{z}_2, \quad \omega_5 := -\tilde{z}_1,$$

$$\int_0^1 \int_0^{\omega_1} \int_0^{\omega_2} \int_0^{\omega_3} \int_0^{\omega_4} \tilde{k}_1 \left(\left[\begin{array}{c} 1 - \omega_1 \\ \omega_1 - \omega_2 + \omega_4 \\ \omega_3 - \omega_4 \end{array} \right], \left[\begin{array}{c} 1 - \omega_1 + \omega_5 \\ \omega_1 - \omega_2 \end{array} \right] \right) d\omega.$$

A. Appendix: Duffy Transformation

Sub-domain D_2 The treatment of D_2 is a little bit more elaborate, since the forking inequality chain,

$$\begin{aligned} 0 &\leq -\tilde{z}_2 \leq -\tilde{z}_1 \leq \tilde{x}_1 - \tilde{x}_2 - \tilde{z}_2 \leq \tilde{x}_1 \leq 1, \\ 0 &\leq -\tilde{z}_2 \leq -\tilde{z}_2 + \tilde{z}_3 \leq \tilde{x}_1 - \tilde{x}_2 - \tilde{z}_2 \leq \tilde{x}_1 \leq 1, \end{aligned}$$

does not fulfill our requirements. Therefore, an additional split up of this region is needed:

$$D_2 = \left\{ \begin{array}{l} -1 \leq \tilde{z}_1 \leq 0 \\ \tilde{z}_1 \leq \tilde{z}_2 \leq 0 \\ -\tilde{z}_1 \leq \tilde{x}_1 \leq 1 \\ -\tilde{z}_2 \leq \tilde{x}_2 \leq \tilde{x}_1 + \tilde{z}_1 - \tilde{z}_2 \\ 0 \leq \tilde{z}_3 \leq -\tilde{z}_1 + \tilde{z}_2 \end{array} \right\} \cup \left\{ \begin{array}{l} \tilde{z}_2 - \tilde{z}_3 \leq \tilde{z}_1 \leq 0 \\ \tilde{z}_1 \leq \tilde{z}_2 \leq 0 \\ -\tilde{z}_1 \leq \tilde{x}_1 \leq 1 \\ -\tilde{z}_2 \leq \tilde{x}_2 \leq \tilde{x}_1 + \tilde{z}_1 - \tilde{z}_2 \\ 0 \leq \tilde{z}_3 \leq \tilde{x}_1 - \tilde{x}_2 \end{array} \right\}.$$

This allows us to introduce a new set of variables $\omega \in \mathbb{R}^5$:

$$\begin{aligned} \omega_1 &:= \tilde{x}_1, \omega_2 := \tilde{x}_1 - \tilde{x}_2 - \tilde{z}_2, \omega_3 := -\tilde{z}_1, \omega_4 := -\tilde{z}_2 + \tilde{z}_3, \omega_5 := -\tilde{z}_2, \\ &\int_0^1 \int_0^{\omega_1} \int_0^{\omega_2} \int_0^{\omega_3} \int_0^{\omega_4} \tilde{k}_2 \left(\begin{bmatrix} 1 - \omega_1 \\ \omega_1 - \omega_2 + \omega_5 \\ \omega_4 - \omega_5 \end{bmatrix}, \begin{bmatrix} 1 - \omega_1 + \omega_3 \\ \omega_1 - \omega_2 \end{bmatrix} \right) d\omega, \\ \omega_1 &:= \tilde{x}_1, \omega_2 := \tilde{x}_1 - \tilde{x}_2 - \tilde{z}_2, \omega_3 := -\tilde{z}_2 + \tilde{z}_3, \omega_4 := -\tilde{z}_1, \omega_5 := -\tilde{z}_2, \\ &\int_0^1 \int_0^{\omega_1} \int_0^{\omega_2} \int_0^{\omega_3} \int_0^{\omega_4} \tilde{k}_2 \left(\begin{bmatrix} 1 - \omega_1 \\ \omega_1 - \omega_2 + \omega_5 \\ \omega_3 - \omega_5 \end{bmatrix}, \begin{bmatrix} 1 - \omega_1 + \omega_4 \\ \omega_1 - \omega_2 \end{bmatrix} \right) d\omega. \end{aligned}$$

Sub-domain D_3 By taking a closer look at D_3 ,

$$\begin{aligned} 0 &\leq -\tilde{z}_1 \leq -\tilde{z}_1 + \tilde{z}_2 \leq \tilde{x}_1 - \tilde{x}_2 \leq \tilde{x}_1 \leq 1 \\ 0 &\leq \tilde{z}_3 \leq \tilde{x}_1 - \tilde{x}_2 \leq \tilde{x}_1 \leq 1 \end{aligned}$$

we see that we have the same issue as with D_2 , which is solved in the same way:

$$D_3 = \left\{ \begin{array}{l} -1 \leq \tilde{z}_1 \leq 0 \\ 0 \leq \tilde{z}_2 \leq 1 + \tilde{z}_1 \\ -\tilde{z}_1 + \tilde{z}_2 \leq \tilde{x}_1 \leq 1 \\ 0 \leq \tilde{x}_2 \leq \tilde{x}_1 + \tilde{z}_1 - \tilde{z}_2 \\ 0 \leq \tilde{z}_3 \leq -\tilde{z}_1 + \tilde{z}_2 \end{array} \right\} \cup \left\{ \begin{array}{l} -1 \leq \tilde{z}_1 \leq 0 \\ 0 \leq \tilde{z}_2 \leq \tilde{z}_1 + \tilde{z}_3 \\ -\tilde{z}_1 + \tilde{z}_2 \leq \tilde{x}_1 \leq 1 \\ 0 \leq \tilde{x}_2 \leq \tilde{x}_1 + \tilde{z}_1 - \tilde{z}_2 \\ 0 \leq \tilde{z}_3 \leq \tilde{x}_1 - \tilde{x}_2 \end{array} \right\}.$$

The next step is to introduce a new set of variables $\omega \in \mathbb{R}^5$ corresponding to the forking inequality chains:

$$\begin{aligned} \omega_1 &:= \tilde{x}_1, \omega_2 := \tilde{x}_1 - \tilde{x}_2, \omega_3 := -\tilde{z}_1 + \tilde{z}_2, \omega_4 := -\tilde{z}_1, \omega_5 := \tilde{z}_3, \\ &\int_0^1 \int_0^{\omega_1} \int_0^{\omega_2} \int_0^{\omega_3} \int_0^{\omega_4} \tilde{k}_2 \left(\begin{bmatrix} 1 - \omega_1 \\ \omega_1 - \omega_2 \\ \omega_5 \end{bmatrix}, \begin{bmatrix} 1 - \omega_1 + \omega_4 \\ \omega_1 - \omega_2 + \omega_3 - \omega_4 \end{bmatrix} \right) d\omega, \\ \omega_1 &:= \tilde{x}_1, \omega_2 := \tilde{x}_1 - \tilde{x}_2, \omega_3 := \tilde{z}_3, \omega_4 := -\tilde{z}_1 + \tilde{z}_2, \omega_5 := -\tilde{z}_1, \\ &\int_0^1 \int_0^{\omega_1} \int_0^{\omega_2} \int_0^{\omega_3} \int_0^{\omega_4} \tilde{k}_2 \left(\begin{bmatrix} 1 - \omega_1 \\ \omega_1 - \omega_2 \\ \omega_3 \end{bmatrix}, \begin{bmatrix} 1 - \omega_1 + \omega_5 \\ \omega_1 - \omega_2 + \omega_4 - \omega_5 \end{bmatrix} \right) d\omega. \end{aligned}$$

A. Appendix: Duffy Transformation

Sub-domain D_4 For D_4 the approach is straight forward, since there already exists a suitable inequality chain:

$$0 \leq \tilde{z}_1 \leq \tilde{z}_1 - \tilde{z}_2 \leq \tilde{z}_1 - \tilde{z}_2 + \tilde{z}_3 \leq \tilde{x}_1 - \tilde{x}_2 + \tilde{z}_1 - \tilde{z}_2 \leq \tilde{x}_1 + \tilde{z}_1 \leq 1.$$

Therefore, we can introduce a new set of variables $\omega \in \mathbb{R}^5$ matching the inequality chain:

$$\omega_1 := \tilde{x}_1 + \tilde{z}_1, \omega_2 := \tilde{x}_1 - \tilde{x}_2 + \tilde{z}_1 - \tilde{z}_2, \omega_3 := \tilde{z}_1 - \tilde{z}_2 + \tilde{z}_3, \omega_4 := \tilde{z}_1 - \tilde{z}_2, \omega_5 := \tilde{z}_1,$$

$$\int_0^1 \int_0^{\omega_1} \int_0^{\omega_2} \int_0^{\omega_3} \int_0^{\omega_4} \tilde{k}_2 \left(\begin{bmatrix} 1 - \omega_1 + \omega_5 \\ \omega_1 - \omega_2 + \omega_4 - \omega_5 \\ \omega_3 - \omega_4 \end{bmatrix}, \begin{bmatrix} 1 - \omega_1 \\ \omega_1 - \omega_2 \end{bmatrix} \right) d\omega.$$

Sub-domain D_5 The treatment of D_5 is analog to the treatment of D_4 , since we have here one suitable inequality chain:

$$0 \leq \tilde{z}_2 \leq \tilde{z}_1 \leq \tilde{z}_1 + \tilde{z}_3 \leq \tilde{x}_1 - \tilde{x}_2 + \tilde{z}_1 \leq \tilde{x}_1 + \tilde{z}_1 \leq 1.$$

This one is used to introduce a new set of variables $\omega \in \mathbb{R}^5$:

$$\omega_1 := \tilde{x}_1 + \tilde{z}_1, \omega_2 := \tilde{x}_1 - \tilde{x}_2 + \tilde{z}_1, \omega_3 := \tilde{z}_1 + \tilde{z}_3, \omega_4 := \tilde{z}_1, \omega_5 := \tilde{z}_2,$$

$$\int_0^1 \int_0^{\omega_1} \int_0^{\omega_2} \int_0^{\omega_3} \int_0^{\omega_4} \tilde{k}_2 \left(\begin{bmatrix} 1 - \omega_1 + \omega_4 \\ \omega_1 - \omega_2 \\ \omega_3 - \omega_4 \end{bmatrix}, \begin{bmatrix} 1 - \omega_1 \\ \omega_1 - \omega_2 + \omega_5 \end{bmatrix} \right) d\omega.$$

Sub-domain D_6 The last sub-domain is similar to D_2 , since an additional split up of D_6 is necessary. This is, because the forking inequality chain is not suitable to our approach:

$$0 \leq \tilde{z}_1 \leq \tilde{z}_2 \leq \tilde{x}_1 - \tilde{x}_2 + \tilde{z}_1 \leq \tilde{x}_1 + \tilde{z}_1 \leq 1$$

$$0 \leq \tilde{z}_1 \leq \tilde{z}_1 + \tilde{z}_3 \leq \tilde{x}_1 - \tilde{x}_2 + \tilde{z}_1 \leq \tilde{x}_1 + \tilde{z}_1 \leq 1.$$

Resolve this issue, D_6 is subdivided:

$$D_6 = \left\{ \begin{array}{l} 0 \leq \tilde{z}_1 \leq 1 \\ \tilde{z}_1 \leq \tilde{z}_2 \leq 1 \\ -\tilde{z}_1 + \tilde{z}_2 \leq \tilde{x}_1 \leq 1 - \tilde{z}_1 \\ 0 \leq \tilde{x}_2 \leq \tilde{x}_1 + \tilde{z}_1 - \tilde{z}_2 \\ 0 \leq \tilde{z}_3 \leq -\tilde{z}_1 + \tilde{z}_2 \end{array} \right\} \cup \left\{ \begin{array}{l} 0 \leq \tilde{z}_1 \leq 1 \\ \tilde{z}_1 \leq \tilde{z}_2 \leq \tilde{z}_1 + \tilde{z}_3 \\ -\tilde{z}_1 + \tilde{z}_2 \leq \tilde{x}_1 \leq 1 - \tilde{z}_1 \\ 0 \leq \tilde{x}_2 \leq \tilde{x}_1 + \tilde{z}_1 - \tilde{z}_2 \\ 0 \leq \tilde{z}_3 \leq \tilde{x}_1 - \tilde{x}_2 \end{array} \right\}.$$

Following this new ordering we introduce a new set of variables $\omega \in \mathbb{R}^5$ for each sub-domain:

$$\omega_1 := \tilde{x}_1 + \tilde{z}_1, \omega_2 := \tilde{x}_1 - \tilde{x}_2 + \tilde{z}_1, \omega_3 := \tilde{z}_2, \omega_4 := \tilde{z}_1 + \tilde{z}_3, \omega_5 := \tilde{z}_1,$$

$$\int_0^1 \int_0^{\omega_1} \int_0^{\omega_2} \int_0^{\omega_3} \int_0^{\omega_4} \tilde{k}_2 \left(\begin{bmatrix} 1 - \omega_1 + \omega_5 \\ \omega_1 - \omega_2 \\ \omega_4 - \omega_5 \end{bmatrix}, \begin{bmatrix} 1 - \omega_1 \\ \omega_1 - \omega_2 + \omega_3 \end{bmatrix} \right) d\omega,$$

$$\omega_1 := \tilde{x}_1 + \tilde{z}_1, \omega_2 := \tilde{x}_1 - \tilde{x}_2 + \tilde{z}_1, \omega_3 := \tilde{z}_1 + \tilde{z}_3, \omega_4 := \tilde{z}_2, \omega_5 := \tilde{z}_1,$$

$$\int_0^1 \int_0^{\omega_1} \int_0^{\omega_2} \int_0^{\omega_3} \int_0^{\omega_4} \tilde{k}_2 \left(\begin{bmatrix} 1 - \omega_1 + \omega_5 \\ \omega_1 - \omega_2 \\ \omega_3 - \omega_5 \end{bmatrix}, \begin{bmatrix} 1 - \omega_1 \\ \omega_1 - \omega_2 + \omega_4 \end{bmatrix} \right) d\omega.$$

List of Figures

1.	Σ and the far-fields $\mathcal{F}_{2\rho}(X)$ and $\mathcal{F}_\rho(X)$	78
2.	Error versus k of the cross approximation (black), Chebyshev interpolation (blue), and sparse grid interpolation (red).	81
3.	Integration error for different values of h using tensor Gauss quadrature formulas . . .	93
4.	Integration error for different values of h using symmetric cubature formulas	93
5.	Comparison of the relative errors for $h = 0.0001$	94
6.	Exact solution u	96
7.	Absolute error between the analytic and numerical solution	96
8.	$A_{\mathcal{H}}$ for $N = 7\,100$	100
9.	$A_{\mathcal{H}^2}$ for $N = 7\,100$	100

List of Tables

1.	Costs of the Duffy transformation for volume-volume integrals	29
2.	Costs of Duffy transformation for volume-surface integrals	29
3.	Costs of the numerical integration	41
4.	Number of points for the symmetric cubature rules on the unit tetrahedron	42
5.	Number of points for the symmetric cubature rules on unit panel	42
6.	Approximation error of s_k and tensor Chebyshev interpolation polynomial of degree k	81
7.	Approximation error of s_k and sparse grid interpolation polynomial for k nodes.	81
8.	Number of evaluations of the kernel	95
9.	Storage requirements for the stiffness matrix in MB for two different values of s	97
10.	Computation time for the setting of the stiffness matrix for two different values of s	97
11.	Computation time for the setting of the stiffness matrix for two different values of s	98
12.	Number of steps for solving the system for two different values of s	98
13.	Comparison between the three different \mathcal{H} -matrix approximations	99
14.	Time comparison for setting up the stiffness matrix	100
15.	Memory comparison between \mathcal{H} -, uniform \mathcal{H} - and \mathcal{H}^2 -matrices	101
16.	Time comparison for solving the linear system	101

References

- [1] G. Acosta, F. M. Bersetche and J. P. Borthagaray. A short FE implementation for a 2d homogeneous Dirichlet problem of a fractional Laplacian. *Comput. Math. Appl.* 74(4), 784–916, 2017.
- [2] G. Acosta and J. P. Borthagaray. A Fractional Laplace Equation: Regularity of Solutions and Finite Element Approximations. *SIAM J. Numer. Anal.* 55(2), 472–495, 2017.
- [3] M. Ainsworth and C. Glusa. Aspects of an adaptive finite element method for the fractional Laplacian: A priori and posteriori error estimates, efficient implementation and multigrid solver. *Comput. Methods Appl. Mech. Eng.* 327, 4–35, 2017.
- [4] M. Ainsworth and C. Glusa. Towards an efficient finite element method for the integral fractional Laplacian on polygonal domains. In: *Contemporary Computational Mathematics - A Celebration of the 80th Birthday of Ian Sloan*, Vol. 1,2, Springer, Cham, 17–58, 2018.
- [5] M. Ainsworth, W. McLean and T. Tran. The conditioning of boundary element equations on locally refined meshes and preconditioning by diagonal scaling. *SIAM J. Num. Anal.* 36(6), 1901–1932, 1999.
- [6] S. Arya and D. M. Mount. Approximate nearest neighbor searching. In: *Proceedings of 4th Annual ACM-SIAM Symposium on Discrete Algorithms*, 271–280, ACM Press, New York, 1993.
- [7] S. Arya and D. M. Mount. Approximate range searching. In: *Proceedings of 11th Annual ACM Symposium on Computational Geometry*, 172–181. ACM Press, New York, 1995.
- [8] S. Arya, D. M. Mount, N. S. Netanyahu, R. Silverman and A. Y. Wu. An optimal algorithm for approximate nearest neighbor searching. *J. ACM* 45(6), 891–923, 1998.
- [9] J. Bäck, F. Nobile, L. Tamellini and R. Tempone. Stochastic spectral Galerkin and collocation methods for PDEs with random coefficients: a numerical comparison. In: *Spectral and High Order Methods for Partial Differential Equations*, LNCSE 76, 43–62, Springer, Berlin, Heidelberg, 2011.
- [10] M. Bauer. Neue Formen der Adaptivität bei der Kreuzapproximation nicht-lokaler Operatoren. Dissertation, Universität Bayreuth, 2023.
- [11] M. Bauer, M. Bebendorf and B. Feist. Kernel-independent adaptive construction of \mathcal{H}^2 -matrix approximations. *Numer. Math.* 150, 1–32, 2022.
- [12] M. Bebendorf. Approximation of boundary element matrices. *Numer. Math.* 86(4), 565–589, 2000.
- [13] M. Bebendorf. *Hierarchical Matrices: A Means to Efficiently Solve Elliptic Boundary Value Problems*, volume 63 of *Lect. Notes in Comput. Sci. Eng.* Springer, Berlin, 2008.
- [14] M. Bebendorf and R. Grzhibovskis. Accelerating Galerkin BEM for Linear Elasticity using Adaptive Cross Approximation. *Math. Methods Appl. Sci.* 29(14), 1721–1747, 2006.

References

- [15] M. Bebendorf, C. Kuske and R. Venn. Wideband nested cross approximation for Helmholtz problems. *Numer. Math.* 130, 1–34, 2015.
- [16] M. Bebendorf and S. Rjasanow. Adaptive low-rank approximation of collocation matrices. *Computing* 70(1), 1–24, 2003.
- [17] J. Bertoin. *Lévy Processes*. Cambridge University Press, 1996.
- [18] S. Börm. Efficient Numerical Methods for Non-local Operators. *Tracts in Mathematics* 14. EMS, 2010.
- [19] S. Börm, M. Löhndorf and J. M. Melenk. Approximation of integral operators by variable-order interpolation. *Numer. Math.* 99(4), 605–643, 2005.
- [20] J. Borthagaray, L. Del Pezzo and S. Martinez. Finite Element Approximation for the Fractional Eigenvalue Problem. *J. Sci. Comput.* 77, 308–329, 2018.
- [21] D. Braess. *Finite Elemente – Theorie, schnelle Löser und Anwendungen in der Elastizitätstheorie*. Springer-Verlag, Berlin, Heidelberg, 2013.
- [22] C. Bucur. Some observations on the Green function for the ball in the fractional Laplace framework. *Commun. Pure Appl. Anal.* 15(2), 657–699, 2016.
- [23] A. Bueno-Orovio, D. Kay, V. Grau, B. Rodriguez and K. Burrage. Fractional diffusion models of cardiac electrical propagation: role of structural heterogeneity in dispersion of repolarization. *J. R. Soc. Interface* 11 (2014).
- [24] M. Buhmann. *Radial Basis Functions: Theory and Implementations*. Cambridge Monographs on Applied and Computational Mathematics, Cambridge University Press, Cambridge, 2003.
- [25] L. A. Caffarelli and L. Silvestre. An Extension Problem Related to the Fractional Laplacian. *Commun. Partial. Differ. Equ.* 32(8), 1245–1260, 2007.
- [26] L. A. Carafelli and A. Vasseur. Drift diffusion equations with fractional diffusion and the quasi-geostrophic equation. *Ann. of Math.* 2, 171(3), 1903–1930, 2010.
- [27] Z. Chen and R. Song. Estimates in Green functions and Poisson kernels for symmetric stable processes. *Math. Ann.* 312, 465–501, 1998.
- [28] H. Cheng, L. Greengard and V. Rokhlin. A fast adaptive multipole algorithm in three dimensions. *J. Comput. Phys.* 155(2), 468–498, 1999.
- [29] A. Chernov, T. von Petersdorff and C. Schwab. Quadrature algorithms for high dimensional singular integrands on simplices. *Numer. Algor.* 70, 847–874, 2015.
- [30] B. A. Cipra. The best of the 20th century: Editors name top 10 algorithms. *SIAM News* 33(4), 2000.
- [31] M. Ciarlett, Jr. Analysis of the Scott-Zhang interpolation in the fractional order Sobolev spaces. *J. Numer. Math.*, 21(3), 173–180, 2013.

References

- [32] P. Constantin. Euler Equations, Navier-Stokes Equations and Turbulence. In: *Mathematical foundation of turbulent viscous flows*, Springer, Berlin, 1–43, 2006.
- [33] P. Constantin and M. Ignatova, Critical SQG in bounded domains. *Ann. of PDE* 2(8), 2016.
- [34] M. Cozzi. Interior regularity of solutions of non-local equations in Sobolev and Nikol'skii spaces. *Annali di Matematica Pura ed Applicata* 196, 555–578, 2017.
- [35] P. J. Davis. *Interpolation and Approximation*. Blaisdell, New York, 1963.
- [36] M. G. Duffy. Quadrature over a pyramid or cube of integrands with a singularity at a vertex. *SIAM J. Numer. Anal.* 19(6), 1260–1282, 1982.
- [37] D. A. Dunavant. High degree efficient symmetrical Gaussian quadrature rules for the triangle. *Int. J. Numer. Methods Eng.* 21(6), 1129–1148, 1985.
- [38] G. Dziuk. *Theorie und Numerik Partieller Differentialgleichungen*. Walter de Gruyter, Berlin, 2010.
- [39] A. Ern and J. L. Guermond. *Theory and Practice of Finite Elements*. Appl- Math. Sc. 159, Springer, New York, 2004.
- [40] L. C. Evans. *Partial Differential Equations Second Edition*. American Mathematical Society, 2010.
- [41] E. B. Fabes, C. E. Kenig and R. Serapioni. The local regularity of solutions of degenerate elliptic equations. *Commun. Partial Differ. Equ.* 7(1), 77–116, 1982.
- [42] M. Faustmann, J. M. Melenk and D. Praetorius. A new proof for the existence of \mathcal{H} -matrix approximants to the inverse of FEM matrices: the Dirichlet problem for the Laplacian. In: *Spectral and High Order Methods for Partial Differential Equations – ICOSAHOM 2012*, Springer Lect. Notes Comp. Sci. Eng. 95, 249–259, 2014.
- [43] M. Faustmann, J. M. Melenk and D. Praetorius. \mathcal{H} -matrix approximability of the inverse of FEM matrices. *Numer. Math.* 131, 615–642, 2015.
- [44] M. Faustmann, J. M. Melenk and D. Praetorius. Existence of \mathcal{H} -matrix approximants to the inverse of BEM matrices: the simple-layer operator. *Math. Comp.* 85(297), 119–152, 2016.
- [45] M. Faustmann, J. M. Melenk and D. Praetorius. Existence of \mathcal{H} -matrix approximants to the inverses of BEM matrices: the hyper singular integral operator. *IMA J. Numer. Anal.* 37(3), 1211–1244, 2017.
- [46] D. Gilbarg and N. S. Trudinger. *Elliptic Partial Differential Equations of Second Order*. Springer, Berlin Heidelberg, 2001.
- [47] G. H. Golub and Ch. F. Van Loan. *Matrix computations*. Johns Hopkins University Press, Baltimore, MD, third edition, 1996.

References

- [48] L. F. Greengard and V. Rokhlin. A fast algorithm for particle simulations. *J. Comput. Phys.* 73(2), 325–348, 1987.
- [49] L. F. Greengard and V. Rokhlin. A new version of the fast multipole method for the Laplace equation in three dimensions. *Acta Numer.* 6, 229–269, 1997.
- [50] W. Hackbusch. A sparse matrix arithmetic based on \mathcal{H} -matrices. Part I: introduction to \mathcal{H} -matrices. *Computing* 62(2), 89–108, 1999.
- [51] W. Hackbusch. *Hierarchical Matrices: Algorithms and Analysis*. Springer Series in Computational Mathematics, Springer, Berlin, Heidelberg, 2015.
- [52] W. Hackbusch. *Elliptic Differential Equations Theory and Numerical Treatment Second Edition*. Springer, Berlin, 2017.
- [53] W. Hackbusch and B. N. Khoromskij. A sparse \mathcal{H} -matrix arithmetic. Part II: Application to multi-dimensional problems. *Computing* 64(1):21–47, 2000.
- [54] W. Hackbusch, B. N. Khoromskij and R. Kriemann. Hierarchical matrices based on a weak admissibility criterion. *Computing* 73, 207–243, 2004.
- [55] W. Hackbusch, B. N. Khoromskij and S. A. Sauter. *On \mathcal{H}^2 -Matrices* In: Bungartz, H.-J., Hoppe, R.H.W., Zenger, Ch. (eds.) *Lectures on Applied Mathematics*, 9–29. Springer, Berlin, 2000.
- [56] P. C. Hammer, O. J. Marlowe and A. H. Stroud. Numerical integration over simplexes and cones. *Mathematical tables and other Aids to Computation* 10(55), 130–137, 1956.
- [57] H. Harbrecht and M. Peters. Comparison of fast boundary element methods on parametric surfaces. *Comput. Methods Appl. Mech. Eng.* 261, 39–55, 2013.
- [58] M. Ito. On α -harmonic functions. *Nagoya Math. J.* 26, 205–221, 1966.
- [59] A. Janicki and A. Weron. *Simulation and Chaotic Behavior of α -Stable Processes*. Marcel Dekker Inc, New York, 1994.
- [60] M. Karkulik and J. M. Melenk. \mathcal{H} -matrix approximability of inverses of discretisations of the fractional Laplacian. *Adv. Comput. Math.* 45, 2893–2919, 2019.
- [61] M. Kassmann. A new formulation of Harnack’s inequality for nonlocal operators. *Comptes Rendus Math.* 349, 637–640, 2011.
- [62] P. Keast. Moderate-degree tetrahedral quadrature formulas. *Comput. Methods Appl. Mech. Eng.* 55, 339–348.
- [63] J. Klafter, M. F. Shlesinger and G. Zumofen. Beyond Brownian motion. *Phys. Today* 49(2), 33-39, 1996.
- [64] M. Kwasnicki. Ten Equivalent Definitions Of The Fractional Laplace Operator. *Fract. Calc. Appl. Anal.* 20(1), 7–51, 2017.

References

- [65] N. S. Landkof. *Foundation of Modern Potential Theory*. Springer, Berlin Heidelberg, 1972.
- [66] N. Laskin. *Fractional quantum mechanics*. World Scientific, Hackensack, 2018.
- [67] N. Laskin. Fractional Schrödinger equation. *Phys. Rev. E* 66, 2002.
- [68] F. Leja. Sur certaines suites liées aux ensembles plans et leur application à la représentation conforme. *Ann. Polon. Math.* 4, 8–13, 1957.
- [69] A. Lischke, G. Pang, M. Gulian, F. Song, C. Glusa, X. Zheng, Z. Mao, W. Cai, M. M. Meerschaert, M. Ainsworth and G. E. Karniadakis. What Is the Fractional Laplacian? A Comparative Review with New Results. *J. Comp. Phys.* 404, 2020.
- [70] W. McLean. *Strongly Elliptic Systems and Boundary Integral Equations*. Cambridge University Press, Cambridge, 2000.
- [71] K. Pearson On lines and planes of closest fit to systems of points in space. *Philosophical Magazine* 2(6), 559–572, 1901.
- [72] G. Richardson. The Trigonometry of the Tetrahedron. *Math. Gazette* 2(32), 149–158, 1902.
- [73] M. Riesz. Integrales de Riemann-Liouville et potentiels. *Acta Sci. Math.* 9, 1–42, 1938.
- [74] V. Rokhlin. Rapid solution of integral equations of classical potential theory. *J. Comput. Phys.* 60(2), 187–207, 1985.
- [75] S. A. Sauter and C. Schwab. *Boundary Element Methods*. Springer, Berlin, Heidelberg, 2011.
- [76] L. R. Scott and S. Zhang. Finite Element Interpolation of Nonsmooth Functions Satisfying Boundary Conditions. *Math. Comput.* 54(190), 483–493, 1990.
- [77] P. Silvester. Symmetric quadrature formulae for simplexes. *Math. Comput.* 24, 95–100, 1970.
- [78] O. Steinbach. *Numerical Approximation Methods for Elliptic Boundary Value Problems: Finite and Boundary Elements*. Springer, LLC, 2008.
- [79] F. Stenger. *Numerical methods based on Sin and analytic functions*. Springer, Heidelberg, 1993.
- [80] P. Stinga. User’s guide to the fractional Laplacian and the method of semigroups. In: *Volume 2 Fractional Differential Equations*, 235–266, De Gruyter, 2019.
- [81] L. Ying, G. Biros, and D. Zorin. A kernel-independent adaptive fast multipole algorithm in two and three dimensions. *J. Comput. Phys.* 196(2), 591–626, 2004.
- [82] Y. Yinyun. Gaussian quadrature formulae for tetrahedral regions. *Comput. Methods Appl. Mech. Eng.* 43(3), 349–353, 1984.
- [83] K. Yosida. *Functional Analysis Sixth Edition*. Springer, Berlin, 1995.
- [84] H. Wendland. *Scattered Data Approximation. Cambridge Monographs on Applied and Computational Mathematics*. Cambridge University Press, Cambridge, 2005.

References

- [85] G. M. Zaslavsky. Chaos, fractional kinetics, and anomalous transport. *Phys. Rep.* 371(6), 461–580, 2002.
- [86] L. Zhang, T. Cui and H. Liu. A set of symmetric quadrature rules on triangles and tetrahedra. *J. Comput. Math.* 27(1), 89–96, 2009.

Publications

- [1] M. Bauer, M. Bebendorf and B. Feist. Kernel-independent adaptive construction of \mathcal{H}^2 -matrix approximations. *Numer. Math.* 150, 1–32, 2022.
- [2] B. Feist and M. Bebendorf. Fractional Laplacian – Quadrature rules for singular double integrals in 3D. *J. Comp. Methods Appl. Math*, <https://doi.org/10.1515/cmam-2022-0159>, 2023.

Eidesstattliche Versicherung

Hiermit versichere ich an Eides statt, dass ich die vorliegende Arbeit selbstständig verfasst und keine anderen als die von mir angegebenen Quellen und Hilfsmittel verwendet habe.

Weiterhin erkläre ich, dass ich die Hilfe von gewerblichen Promotionsberatern bzw. -vermittlern oder ähnlichen Dienstleistern weder bisher in Anspruch genommen habe, noch künftig in Anspruch nehmen werde.

Zusätzlich erkläre ich hiermit, dass ich keinerlei frühere Promotionsversuche unternommen habe.

Bayreuth, den 14.04.2023

Unterschrift